

Cloud Integration of Industrial IoT Systems. Architecture, Security Aspects and Sample Implementations

Katalin Ferencz^{1,2}, József Domokos², Levente Kovács³

¹Doctoral School of Applied Informatics and Applied Mathematics, Óbuda University, Bécsi út 96/b, 1034 Budapest, Hungary, ferenczkatalin@stud.uni-obuda.hu

²Faculty of Technical and Human Sciences, Târgu-Mureş, Sapientia Hungarian University of Transylvania, Sighişoarei road no. 2, 540485 Târgu-Mureş/Corunca, Romania, {ferenczkatalin, domi}@ms.sapientia.ro

³John von Neumann Faculty of Informatics, Óbuda University, Bécsi út 96/b, 1034 Budapest, Hungary, kovacs@uni-obuda.hu

Abstract: Today's industry is increasingly characterized by the integration of Internet of Things (IoT) devices and the rapidly spreading digitization trend, which are also known as the foundations of Industry 4.0. The industrial revolution characterizes our everyday life, as a result of which the integration of smart devices is gaining more and more space in industry as well. As a result of the introduction of Industry 4.0, the implementation of the automation of production processes also becomes an important issue, as well as the continuous collection of data and their storage in the cloud. As a result of these integration, the method of collecting data, the usability of cloud-based systems, the feasibility of artificial intelligence-based data analysis, the visualization of massive amounts of collected data, cybersecurity issues, etc. have become everyday issues. In this article, we provide a detailed overview of a general IIoT (Industrial IoT) system, its various cloud service-based implementations, and present our open-source alternative solution. At the same time, we present the study of the security aspects and the integration of SOC into an IIoT system. Taking these aspects into account, we present two sample applications that try to offer ready to use solutions to certain problems of today's industry.

Keywords: Industry 4.0; Internet of Things; Cloud Infrastructure; Cybersecurity; Sensor data collection, Data Processing

1 Introduction

In the last decade, the state of the industry's digital development and the impact of the fourth industrial revolution on real production processes have become central topics in the field of industry. But what does this actually mean for industry and factories? We can put it simply that we can be everyday observers of the "smartening" of industry, that is, the development of intelligent industry.

With the beginning of the fourth industrial revolution, it has become very important for industry to successfully compete with the rapid development of technology by adapting autonomous, self-organizing resources, cyber-physical manufacturing systems, and real-time communication. To achieve this, it became necessary to introduce industrial IoT (Industrial Internet of Things - IIoT) devices, artificial intelligence (AI) based software, cloud-based systems (for example, databases), large amounts of data (Big Data) and the use of cybersecurity and automation. With the beginning of the fourth industrial revolution, industry is undergoing a major transformation. The main feature of the industry we have known so far was the use of rigid standards and rules, which provided companies with a high degree of security. The new industrial revolution is trying to transform these rigid norms and reform the existing production methods, thereby providing new opportunities for the integration of intelligent devices and innovative solutions. The fundamental element of the fourth industrial revolution is the intertwining of information technology, data and automation, that is, digitization [22].

The digitized industry, which can also be called a smart factory, is characterized by the fact that it uses intelligent devices in the processes of production, warehousing, and transport, through which it is able to collect large amounts of data in a short time (using various sensors or entire sensor networks), store and process. Emphasis must be placed on the fact that the storage of large amounts of data has concrete value if it is utilized, if this data is also processed and analysed, which can be realized by machine learning and artificial intelligence. Using the analysed data, we are able to create user interfaces and dashboards where we can continuously display and monitor, even in real-time, all the processes in the factory. It is possible to model and optimize the correct operation of the system, and at the same time, by analysing the data, system anomalies can be detected and even unwanted failures can be predicted. All of these have an impact on correct decision making, optimization of production processes, the utilization of machines can be increased, or we can even predict the service life of parts, which results in predictive maintenance [16].

Due to the IIoT, an important feature of today's smart factories is that the equipment continuously sends data to databases, communicates with controllers, software systems, and data analysis applications. This continuous multi-directional communication makes units compatible with industrial IoT devices an

integral part of intelligent processes. By using various IoT hubs, any type of device can transmit data to the cloud, database or any other unit connected for use. We can store, manage and process the locally collected data using private or public cloud systems in the fastest and most cost-effective way [15]. There are many providers on the market who can provide these services for a fee, such as Amazon, Microsoft, Google, etc., or it is possible to use a self-hosted system. Their architecture is usually very similar, but it can be implemented by using various technologies and software [5].

It is important to consider that the increasing spread of the digital development of the industry does not only generate positive results, so it is necessary to examine its negative side as well. Increased digitization also results in problems that have not been emphasized in the industry so far, specifically in the area of cybersecurity. System security topics need to be treated as a priority, because of smart devices built into industrial systems can appear as attack points, and the use of cloud services and remote access can also be treated as potential vulnerabilities. When designing traditional industrial systems (for example, communication network), cybersecurity was mostly not a priority, as they were closed systems, the system was only available on the site, in the factory area, and was not available from the outside. With the spread of the industrial integration of IoT devices, the consideration of the appropriate security aspects must also play a role during planning, but for this the industrial cyber security teams must have the appropriate knowledge, which was not needed in the industry until now.

In the remaining parts of the paper, a general architecture is presented, which takes the collected data through the stages of storage, processing, analysis and display through 4 different technological implementations. We will present the three best-known and most used services on the market (Amazon Web Services, Microsoft Azure and Google Cloud Platform) as well as our own, open-source system, which also results in a system that conforms to the general architecture. Then, the security issues caused by the integration of IIoT devices will come into focus, as it will receive special attention for the industry to properly know its own devices, their parameters and behaviour, as well as to have a cybersecurity protocol or strategy to protect its entire system. In order to present such a system, we created and present a descriptive architecture that takes into account the basic security regulations. Finally, in order to prove the viability of the system, two sample applications using open-source implementations are also presented.

We would like to give a comprehensive picture of how the use of IIoT devices can be implemented and utilized for industry, and how it will be a key player in Industry 4.0.

2 Application of Cloud Systems in Industry

The IoT systems integrated in the industry we are examining can generally be described with the following self-architecture (Figure 1) and contain four important parts: data collection, data storage, data processing and execution.

Data collection consists of environmental data measured by various sensors, or by using data provided by other industrial machines through SCADA (Supervisory Control and Data Acquisition) Systems, PLCs (Programmable Logic Controller), DCSs (Distributed Control System) etc.

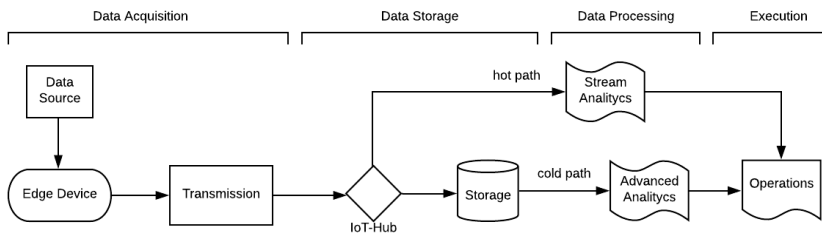


Figure 1

End-to-end data flow architecture in IIoT

The collected data is transmitted from the device to a higher-order unit using various network protocols, such as FieldBus, ControlBus, OPC (Open Platform Communications), Message Queue Telemetry Transport (MQTT), Advanced MQTT (AMQTT), HTTP, HTTPS, Constrained Application Protocol (CoAP), etc. Through network protocols, the data is transmitted to an IoT-Hub, which acts as a gateway between the device and the cloud.

Due to the versatile operation of the IoT-Hub, the incoming data is forwarded in several directions in accordance with the system requirements. The most common solution is to transfer these data to the database for immediate storage. It is possible to analyse these stored data at a later date using an algorithm based on artificial intelligence. This type of data processing is called the cold path. But as another solution, an IoT-Hub also provides the possibility of immediate data processing, which can provide real-time results, this is known as process analysis, that is, the hot path of data processing. As a result of, this type of analysis, the collected data can be used with the help of the obtained calculated data, for example, these data can provide valuable information. Based on these calculated data, it is possible to visualize data, create reports and alerts, and detect anomalies using various algorithms [2].

In the following, we will examine the general architecture described above in the case of Microsoft Azure, Amazon Web Services and Google Cloud Platform, as well as in the case of a system developed by us that uses open-source technologies. In each case, the system is built on the basis of the same

architecture, but with the help of technological equivalents provided by the given service provider.

2.1 Microsoft Azure

The figure below (Figure 2) shows the technological components provided by the Microsoft Azure service provider for the creation and deployment of an IIoT system.

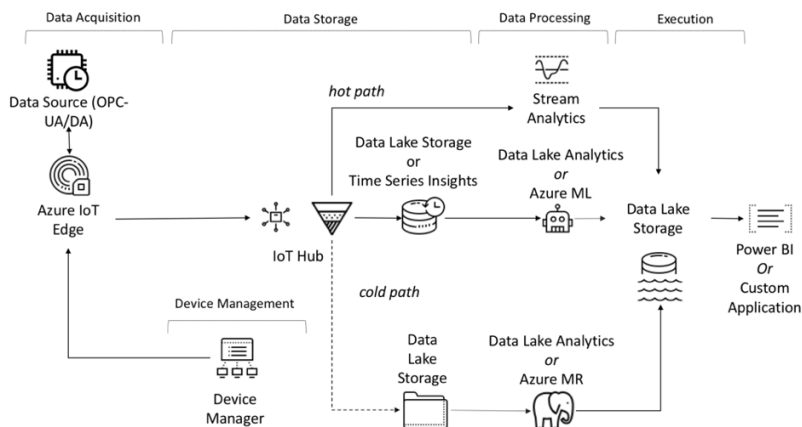


Figure 2

Azure IIoT architecture [20]

Data is collected from sensors and other industrial devices through Azure IoT Edge using various protocols such as, HTTP, AMQP, MQTT, OPC UA, etc. This forwards the data to Azure IoT Hub. The IoT-Hub is an intermediate layer used for device registration and management. From there, the data is processed by Stream Analytics, which forms the hot path of the analysis. Azure Stream Analytics is a real-time analytics and complex event processing engine designed to analyse and process large volumes of fast data streams simultaneously from multiple sources. The result of the analysis is stored in Data Lake Storage. It is possible to store this data in two types of databases, one is Time Series Insight and the other is Azure Data Lake Storage. Time Series Insight is suitable for storing, visualizing and querying large-scale time series data. Azure Data Lake Storage is a highly scalable data store that you can use to store data for later analysis and visualization. The stored data is cold path analysed by Data Lake Analytics or Azure ML (Machine Learning). Data Lake Analytics is a big data service for processing huge amounts of data. ML Analytics is an environment in which we can conduct advanced machine learning-based analytics for predictive modelling. Finally, Power BI or other custom applications can be used to display the data.

Power BI is a business analytics service that provides insights and tracks viewing real-world data.

2.2 Amazon Web Service (AWS)

Using the services provided by Amazon, the collected data is sent by Greengrass to the unit corresponding to the IoT-Hub, as shown in Figure 3. GreenGrass is software that extends the capabilities of the cloud to the local device and allows the device to collect and analyze data closer to the source of information.

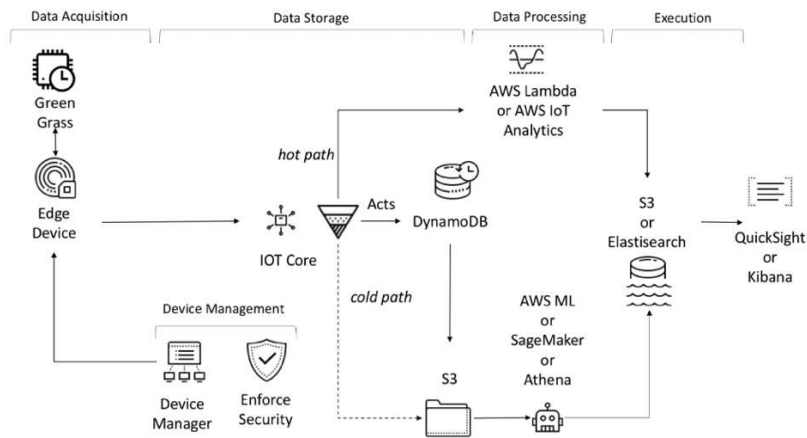


Figure 3
AWS IIoT architecture [30]

AWS IoT Core corresponds to the IoT-Hub, to which the devices send the collected data using various protocols, such as MQTT. There are several options for storing data here as well, depending on the type of data we want to store. DynamoDB can be used to store time series, or the S3 database can be used to store object data. In order to process the data quickly, we can use AWS Lambda serverless platform or AWS IoT Analytics. For more advanced analysis, AWS provides the user with several options: AWS ML, SageMaker, Athena. The results of the analyzes of fast and advanced algorithms are usually stored in S3 or Elasticsearch type database storage. It is also possible to establish a direct connection to the QuickSight or Kibana visualization services that provide immediate visualization.

2.3 Google Cloud Platform (GCP)

The services provided by Google Cloud Platform allow the implementation of the architecture shown in the following figure (Figure 4). Google IoT Core supports

the MQTT and HTTPS protocols, so data can only be transmitted to the processing system via these protocols.

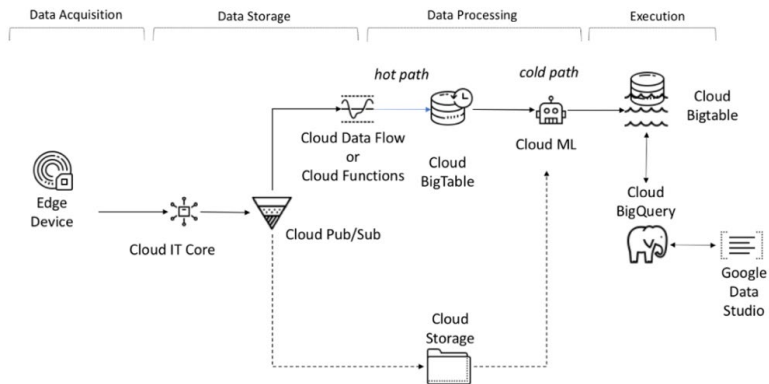


Figure 4
GCP IIoT architecture [20]

Google IoT Core corresponds to IoT-Hub, which acts as a central hub for connecting remote devices and uses the Google Pub/Sub service for data transfer. Cloud Data Flow or Cloud Functions service can be used to quickly process data and create Stream Analytics. Cloud Bigtable can be used to store time series or event type data, and Cloud Storage can be used to store object type data. Cloud BigQuery and Cloud ML services can be used for batch analysis of data. Google Data Studio is responsible for data visualization.

2.4 Open-Source Implementations

Considering that in many cases we are unable to subscribe to the above-mentioned service providers, or it is simply not allowed for the data to be managed by an external service provider, we also need systems that are built from our own components. In the following, we will examine the IIoT system designed and implemented by us using open-source components, which implements similar functionality to the systems presented above with a similar architecture. Figure 5 shows that the sensor data is provided, that is, in our case generated, by a Python program, which in reality can be replaced by any sensors. In this case, the generated sensor data (relative humidity, ambient pressure and temperature, pressure, and electrical energy) are generated based on the analysis of an existing data set, which is presented in detail in a previous article [12].

The data transfer was realized by an open-source implementation of the MQTT protocol called Mosquitto [9], which transmits the data to the Node-RED [21] framework. The Mosquitto implementation we use is only one of the many MQTT protocol implementations, as it is possible to choose from several options and

implementations as needed [32]. Node-RED acts as an open source IoT edge, which can fulfill several roles due to its versatile functionality. The data received by Node-RED can be analyzed and displayed immediately with the help of the Dashboard (User Interface) module using various built-in node diagrams (charts). This forms the so-called hot path of data processing.

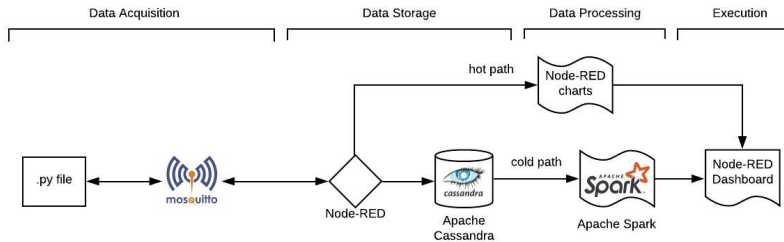


Figure 5

The architecture of the IIoT system developed by us using open-source components

The data is stored in a cluster built in the NoSQL type Apache Cassandra [3] open-source database system for post-processing and data analysis. In addition to the Apache Cassandra database, we can also choose MongoDB, Hbase, Redis, Couchbase or other database systems deemed suitable for the purpose [1]. The data processing can be realized by the open-source Apache Spark framework developed for analysis, which uses the Spark Machine Learning (ML) library [8], [10], [23]. A detailed description of the implemented system can be found in previously published conference papers [11], [12], [13]. Using the possibilities provided by the Spark Machine Learning libraries, we also performed data analysis using some ML Python-based libraries (pyspark.ml.features, pyspark.ml.regression, pyspark.ml.evaluation, etc.).

Node-RED and its accompanying Dashboard offer powerful tools for developing IoT solutions, but they do come with some limitations. One limitation is that Node-RED may require additional configuration and setup to work with certain hardware or protocols, which can be challenging for users with limited technical expertise. Additionally, while Node-RED provides a visual programming interface, complex applications may require extensive flows and can become difficult to manage and debug. As the Node-RED Dashboard offers basic data visualization capabilities it is possible that may not meet the advanced data visualization requirements of more complex industrial applications. Despite these limitations, Node-RED has found utility in industrial environments, where its ease of use, extensibility, and versatility make it a valuable tool for process automation, data acquisition and monitoring, predictive maintenance, and remote control of industrial systems [26], [4]. In this way Node-RED is being utilized in industrial settings to streamline operations, enable innovation in IoT solutions, and enhance productivity and automation [18].

2.5 Other Options for Implementation of Similar Systems

In addition to the globally widespread and well-known platforms (Azure, AWS, GCP) and open-source solutions presented above, many other targeted platforms and systems are available on the market.

Kuzzle, thethings.io, and Thinger.io are three notable platforms that offer Internet of Things (IoT) solutions for developers, businesses, and industries. Kuzzle provides a flexible, open-source backend solution for building IoT applications with real-time communication and data synchronization features. Kuzzle's advantages include high scalability, real-time communication, and advanced security features, while its disadvantages may include a steeper learning curve and limited community support [20]. Thethings.io offers a cloud-based Enterprise IoT platform for managing and visualizing data from connected devices, while Thinger.io provides an end-to-end IoT platform with cloud-based data management, device connectivity, and application development tools. Thethings.io's (free and paid plans) advantages include easy integration with IoT devices, a user-friendly dashboard, and comprehensive analytics, while its disadvantages may include limited customization options and potential scalability challenges for large-scale deployments [27]. Thinger.io (free and paid plans) offers benefits such as robust security measures, comprehensive support for diverse IoT protocols, and a thriving user community, but it may pose challenges in terms of user onboarding and scalability for extensive IoT deployments [28].

In terms of data visualization, we already have many options and solutions on the market. Grafana [6] is a popular and versatile data visualization and monitoring platform that empowers users to create dynamic and interactive dashboards for real-time data analysis. With its rich set of features and customizable options, Grafana offers a powerful solution for visualizing complex data from various sources. However, like any other software tool, Grafana also has limitations, including a potential learning curve for beginners and the possibility of lacking some enterprise-grade features or support that certain organizations may require. Nevertheless, Grafana's strengths lie in its flexibility, ease of use, and ability to deliver actionable insights through visually appealing dashboards.

These platforms are widely used in various industries for developing IoT solutions, ranging from smart home and healthcare to logistics and industrial automation, offering powerful tools and features for building modern IoT applications.

3 Security Issues of IIoT Systems

In general, the industrial systems presented above must always be operational and in a constantly active, working state, so minor or major shutdowns caused by unexpected attacks are not allowed and should definitely be avoided. Taking all these into account, industrial companies integrating intelligent manufacturing methods realize that the proper knowledge and protection of their systems, as well as the analysis of their data, must be an area to be treated as an important priority [24].

In order to manage or even prevent the various attacks arising from the integration of the technological innovations of Industry 4.0, a cyber-security protocol or strategy and the development of a new kind of security approach are needed. In the management of these threats, the Security Operations Center (SOC) plays a prominent role, which monitors the devices around the clock and centralizes the security supervision and control of the devices. The application of SOC enables real-time threat detection and response to security incidents. In addition, with the help of SOC, we can provide rapid security detection in order to identify, investigate, prioritize and solve security problems. As a result, it is possible to detect threats early and alert the relevant security teams, who can fix security problems in a short time without interrupting production processes, thus reducing the impact of a future attack.

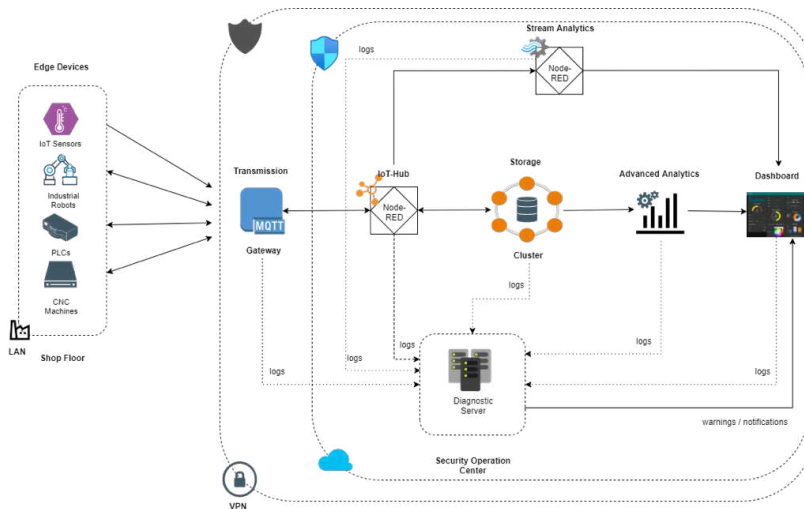


Figure 6

Proposed secure industrial system architecture (with SOC included)

An industrial environment can use a variety of devices such as IoT devices, microcontrollers, sensors, enterprise computers, internal networks, virtual environments, manufacturing equipment, etc. (Figure 6). An important operational

parameter of all these devices is that these can generate and transmit various type of data to a central unit. These data can be structured data and unstructured data, which can be analysed to obtain up-to-date system information about the state and operation of the entire system, which is essential to protect the system operation. The processing of the collected data is essential, since based on them, a model of the system's normal operation can be prepared, and based on this model, it is possible to filter out abnormalities and anomalies that can be detected in the system, as these can even result in system failure or be signs of unwanted interventions.

At the lowest (shop floor) of industrial systems are operational technologies, that is, OT (Operational Technology), whose role is to monitor and manage the tools of industrial processes. OT includes HMI (Human-Machine Interface), SCADA, PLC, pumps, sensors, robots, etc. Based on the operating principle of these devices integrated into the system, they can connect to the internal network of the factory environment. All kinds of communication are then carried out through these networks, that is, these devices can receive or transmit data and commands to higher decision making levels. From the shop floor, the data is transmitted to a more protected network (for example, using a Virtual Private Network) by several protocols (for example, MQTT, Fieldbus, Modbus, DNP3, Ethernet, Profinet,). Here, a unit serving as a gateway transmits this data to a hub, such as Node-RED can act as such an IoT-hub, or AWS IoT, or Azure IoT Hub, etc. This particular hub is able to transmit data in specified directions, so at this architectural level the data is transmitted to the database, which could be a SQL (for example, MSSQL - Microsoft SQL) or a NoSQL type of database built as a split cluster, such as the Apache Cassandra database system, which can be on-premises or can be rented as Software-as-a-Service. Depending on the quality and characteristics of the chosen storage method, it is possible to create advanced analytics by using algorithms based on artificial intelligence (the cold path of data processing). The IoT-Hub provides the opportunity to implement a real-time data processing, which is called Stream Analytics (the hot route of data processing). This analysis mode can provide results describing the current state of the system and useable information can be obtained based on the results of the analyses [17], [19].

3.1 Vulnerabilities of Industrial Systems

It is critical for any industrial system to know what features and vulnerabilities the integrated devices have. The importance of this lies in the fact that an attack in the absence of this knowledge can make the entire production or part of the production lines inoperable, which, depending on the industry, can even cause personal injury or property damage.

Systems designed before the spread of the fourth industrial revolution were designed in such a way that the entire system would be isolated from the “outside

world” (not connected to internet or any public network), so external attacks were not possible. It should be mentioned here that a prominent part of the devices in the OT now have a certain level of their own security system or protocol (blocking of ports, username-password, etc.), but most of them are switched off during commissioning in order to ensure that the system is put into operation and its operation should be implemented as soon as possible, such as not having to constantly use passwords when configuring the machines. Thus, as a result, these devices can become easy targets for malicious attackers, due to the aforementioned "negligence". Taking this into account, the appearance of smart devices in the field of industry may question the security of the system, due to the fact that IoT devices are devices that can be easily connected to the Internet, thus creating a critical vulnerable interface on the internal network (in many cases inadequately protected). Another possible point of vulnerability is incomplete testing or code review during the design of various software, which can also generate new risk factors, such as forgotten authentication data (username and password) in the source code.

Due to some of the previously presented incomplete security protections typical of OT devices, the IT team is responsible for ensuring adequate protection of the communication network, thus guaranteeing the protection of the entire system. Communication protocols link endpoints back to the shop floor or controller, making them the most vulnerable parts of industrial systems. As an additional attack surface, we can also consider the insecure Internet connection, which also entails unsafe remote access. These enable easy hacking of industrial systems, in the event that unsafe and protected protocols are used. Besides that, the appropriate behaviour of employees is also a critical and at the same time a very common safety issue. It is also important to treat this factor with high priority, since they can be connected to the machines in the factory with USB, laptops and other portable devices, and in the event that these devices were previously infected in an outside, insecure network, and then connected to the industrial system can cause serious damage to your machines.

3.2 Types of Attacks

In the field of industry, it is increasingly seen that the transformed manufacturing technologies increase the attack surfaces, the purpose of which is usually industrial espionage or sabotage. Typically, these targeted attacks can have complex consequences, such as economic loss, production loss, downtime, and machine damage or in the worst case, human injury. With these in mind, we must prepare risk management, so we can build a proactive protection system.

Systems using smart devices are most often hit by denial of service (DoS) attacks, access control attacks, authentication attacks, protocol and application integrity attacks [25].

Several categories of threats can be distinguished [31]:

- **Data Leakage:** Smart devices capture large amounts of data for analysis, monitoring, and logging purposes. In "closed" industrial systems, these data are transmitted without encryption via the internal network to the database designated for storage. If packet capture devices are placed in the immediate vicinity of these routes for malicious purposes, valuable operational information, usernames or even passwords can fall into unauthorized hands.
- **Unauthorized access:** If the default usernames and passwords of the software and machines are not changed (typically not), then as soon as the IoT device is connected to the Internet, it becomes an easily attacked device. In order to avoid this, the best protection protocol can be the use of strong authentication, even two-step settings.
- **Denial of Service (DoS):** This is one of the most common types of attacks in the digital world. However, a particular form of it is Distributed Denial of Services (DDoS), which works by essentially observing IoT endpoints that have been compromised and are easily accessible for some reason, and then creates a "botnet". It will receive and forward commands to the specified endpoints. As a result, an attacker can easily overload the internal network, causing the device intended to be used by the real user to become unresponsive or a complete network crash.
- **Faked data output:** In this category, the attacker managed to get into the system and, with the aim of creating a vulnerability, places foreign code in the software of a specific device so that the device (for example, a sensor) transmits false, manipulated data to the center, that is, implements false data entry. Furthermore, the attacker can create a "backdoor" that allows him to communicate remotely, so he can transmit additional commands to the selected devices.

Since the spread of the fourth industrial revolution, there have been many attacks on large industrial companies and plants, which should serve as a warning to everyone that special attention must be paid to the cybersecurity of our systems.

4 IoT Device Integration Solutions

Through two sample practical examples, we will show how, thanks to today's advanced technology (smart, IoT devices), we have the options to store the collected data on demand, to use different IIoT communication protocols (in our case MQTT), as well as to incorporate the functionalities provided by the increasingly widespread Node-RED (IBM development). We will provide insight into how, through innovative IT developments, the data of certain industrial systems can be stored, displayed and analysed with simple implementations.

The architecture of both systems is structured similarly, just like the general architecture presented in Chapter 2, and the "real-time" sensor data is provided by a Python code, the logic of which tries to simulate the operating principles of some sensors of the Combined Cycle Power Plant (CCPP) [7]. The data describing the operation will communicate with the Node-RED development environment by using the Mosquitto MQTT broker, which will act as an IoT-Hub. From there, the data continues its journey in two directions: it is entered into the Apache Cassandra database cluster and displayed in real-time using the Node-RED Dashboard. Also, on the Node-RED Dashboard, we provide the possibility to read, display and modify the values of the sensors, thus resulting in the use of two-way communication of the MQTT broker.

4.1 Sensor Data (Generic Plant Equipment) Collection and Monitoring Application

We created an application for monitoring a general factory machine and its environment, the architecture of which is shown in Figure 7. Using various simulated sensors, we record the data measured during operation of a generic machine (speed, revolutions, status, working hours, etc.) and the changes affecting its environment parameters (temperature, light conditions and humidity).

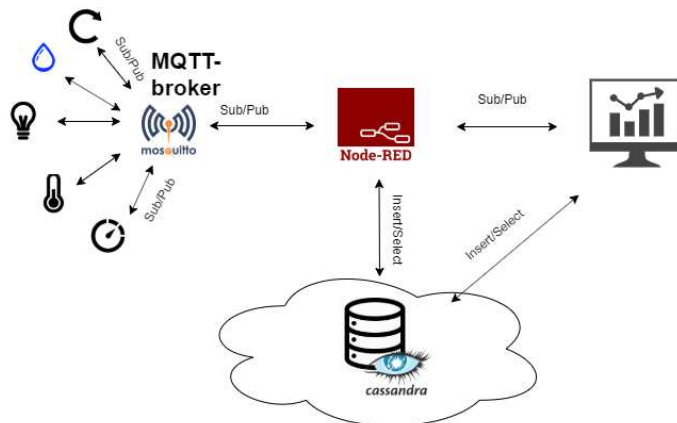


Figure 7

Block diagram of the sample system

These data are transmitted to Node-RED in real-time by a Mosquitto MQTT broker and displayed on a graphical interface, as well as stored in a Cassandra NoSQL database. Considering the possibilities offered by the Node-RED Dashboard, we created an easy-to-understand user interface (Figure 8), as well as an associated logic, where we use the data, we consider it important in real-time, and we can also manipulate some selected parameters on the interface.

The possibility of changing the parameters is implemented on the Dashboard so that we can intervene in real-time, thereby simulating the real operation at some level. Reading and writing to the database is also done using the Node-RED platform.

With the help of a Python code, we create a simulation describing the operation of a general industrial machine and its environment, thus creating a sufficient amount of sensor data. Using this code, we can generate sensors and put them in a JSON (JavaScript Object Notation) object, as well as give each of them an initial value. Due to the data provided by the MQTT broker and the possibility that the code generating the sensor data not only transmits the data to the broker, but can also receive it, we can override the value as desired. We want to store this generated data and display it on the interface in real-time.

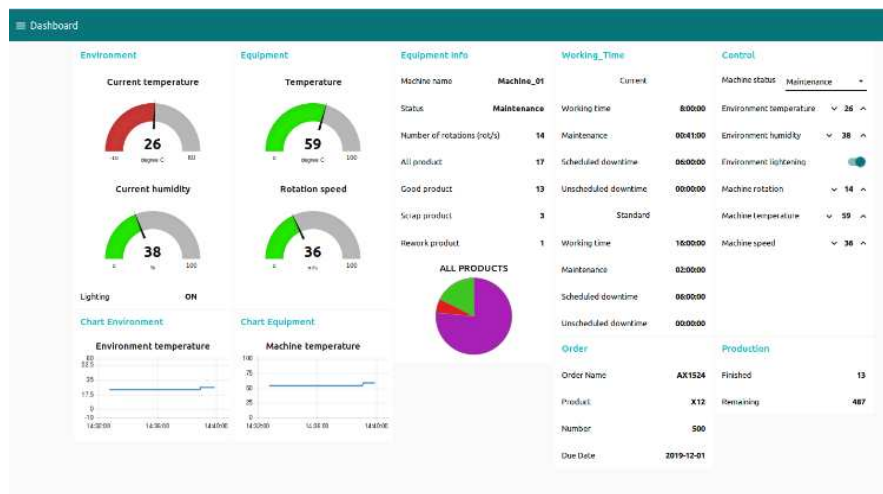


Figure 8

User Interface created using Node Red Dashboard

In the basic case, the sensors created by the simulation act as data senders that register on the MQTT broker. The interested parties will be the Apache Cassandra NoSQL database node and the Node-RED dashboard elements, so these will subscribe to the broker. These interested parties tell the MQTT broker exactly what data these are interested in. When we change the value of a parameter on the interface, it will already behave as a data sender. The above-mentioned Node-RED Dashboard can be created with the help of the dashboard elements in the node panel, which can be displayed on the interface by placing them in the flow panel. We have to configure these elements based on the information that defines the operation of the system, and if the operation of these elements is related to each other, we can connect them, so that they receive the previous output value as an input parameter. Writing program code is necessary if we want to process the

data of the Dashboard elements in the background (function node), or if we want to write them to a database, or if we want to perform any other operation with the data managed by the given element.

We use the NoSQL Apache Cassandra database to store all kinds of data. We chose Apache Cassandra because it is important for data from IoT devices that the storage system is scalable, always available and fault-tolerant. Also, with Cassandra, it is easy to implement storage and access in the cloud. Cassandra can store data on multiple nodes to provide enhanced security and high availability. Taking this into account, we built a 3-node system, ensuring that our data is not lost even in the event of a more critical shutdown. We were then able to display statistical information using the stored data.

In order to simulate real production, a simple Node-RED process can be used to create products with different ratings at regular intervals (every 10 minutes): defective, recyclable and good; thereby modelling a real production process.

4.2 Partial Simulation of the CCPP Operation

By analyzing the historical data of the previously mentioned CCPP database and using them, we created a partial simulation of the operation of the power plant (Figure 9).

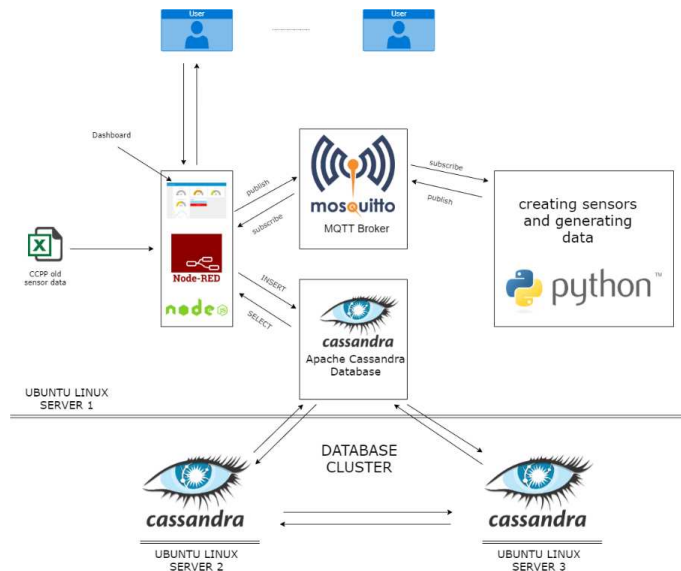


Figure 9

Block diagram of the system built to simulate CCPP

Starting from the data describing the most important system presented in Tüfekci's article [19], we wrote the historical data set into the Apache Cassandra and then using an application created in Python, we created sensor values similar to the historical data by simulation. Due to the efficiency of the simulation, there is no need for physical devices, it reduces the time interval for its reproduction, and enables simulation. We generated the simulated sensor data using the Python code, and using the Mosquito MQTT broker, we transmitted the data to the database via Node-RED and, if necessary, we can modify the values of the sensors on the user interface. In addition to storing the created data, using Node-RED's user interface (dashboard), we can continuously display and even modify the current values of sensors. Figure 10 shows the user interface displaying the sensor data and the possibility to modify the data.

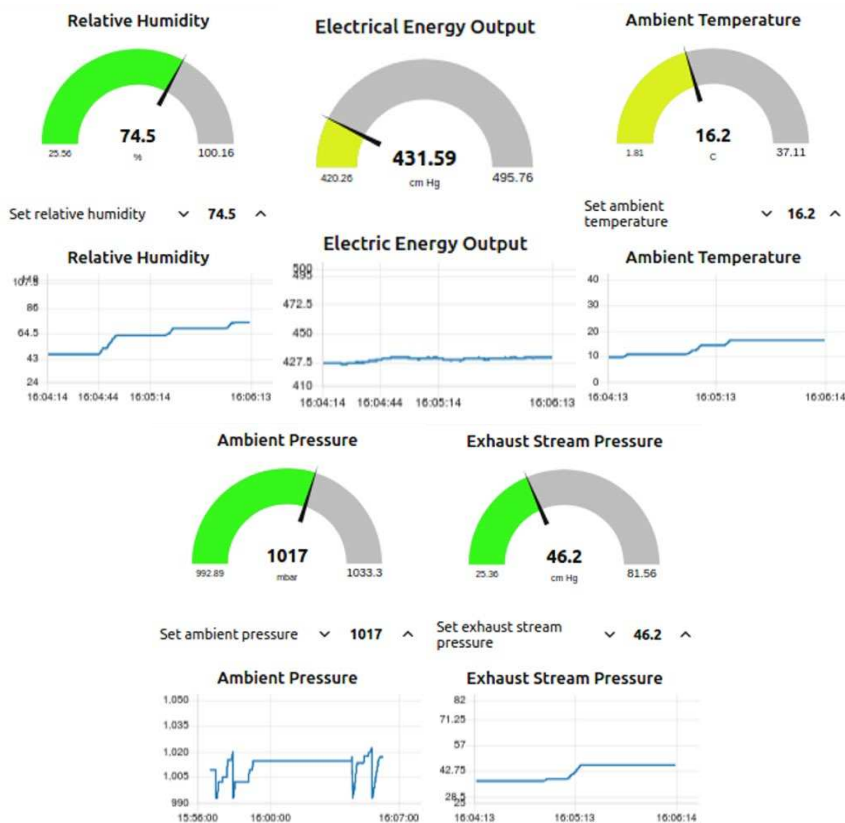


Figure 10

Generated sensor data on the dashboard

To import the historical data set (9568 data points from 5 sensors) into the database, we created a data flow in Node-RED, with the help of which the system can simply write the contents of the excel file into the database. Then, we were

able to display these data using the Node-RED Dashboard module. As a result, we can interpret 6 years of sensor data changes.

An important part of our work is that we were able to create a model in Node-RED by analysing the historical data and with the help of the correlations provided by Tüfekci, thus creating real data describing the operation of our plant system.

4.3 Application of Apache Spark for Statistical Processing of Collected Data

With the built-in functionality of Apache Spark, we can examine basic descriptive statistical analyses by running a few commands. The following descriptive statistics were examined during the research:

- Mean, Standard deviation, minimum and maximum values:
 - count – number of items in that column;
 - mean – arithmetic mean (sample mean), undistorted;
 - estimate of expected value;
 - stddev – standard deviation, the mean squared deviation from the arithmetic mean - how much our values deviate from the average;
 - min. and max. – determination of minimum and maximum value;
 - 25%, 50%, 75% – approximate percentage of quartiles;
- Median – the mean value of the data set, gives a robust estimate and is not sensitive to extreme values.
- Variance: it is used to describe the fluctuation of the data around the mean, that is, the value of the variance is small when our data move around the mean. The variance corresponds to the square of the standard deviation.
- Skewness: determines the offset of the peak of the distribution from the center position.
- Kurtosis: an indicator that describes the shape of the data set vertically.
- Covariance: gives the co-movement of two different variables.
- Correlation: it gives the magnitude and direction of the linear relationship between two values, that is it defines their relationship to each other.

Furthermore, we were able to perform outlier detection with the help of some functions and commands with the functionality of Apache Spark. With this architecture system, we performed the various descriptive data processing statistics indicated above, which were presented in the [14] article.

Conclusions

Based on the various solutions of the presented IIoT systems, it can be seen that we can "easily" implement the same system using cloud-based components developed by various service providers (Azure, AWS, GCP) for varying fees. The preparation of these implementations in the given field requires appropriate professional (industrial) and technical knowledge.

In the case of Microsoft, Amazon and Google, the services used are included in the product family they distributions are included, in most cases without compatibility problems. Using the products of multinational companies, all data and analysis logic end up in the cloud, on the service provider's servers,

The system was created as an in-house implementation: however it uses open-source, free services, and implements the same system as the previous three. In this case, we also need the right knowledge, but it is not so clear how to use one or another service, since these are not from the same service provider. Creating your own system open-source requires the creation and administration of your own hardware infrastructure.

Even new algorithms can be developed and tested in the own data analysis section. In order to achieve this, however, considerable human resources are also required.

The industrial integration of IoT or industrial IoT devices is unavoidable for any industrial representative who wants to stay competitive in today's digitized industry. On the other hand, it is a serious challenge to continuously maintain security without risking availability. Industry representatives create ever more connected small worlds around them, so it is necessary to prepare for protection against the threats and vulnerabilities associated with digitization. Companies integrating the principles of Industry 4.0 must be up to date in the field of cybersecurity and must make it possible to quickly detect and respond to threats. The proven SOC systems and software (for example, SIEM) provide a solution for this, but it is also important to educate human resources on security awareness.

It should also be taken into account that no tool can fully protect against all cyber-attacks, but it is possible to prepare for them by taking precautions, and in the event of an attack, reduce possible negative effects and minimize system downtime.

The presented implementations properly reflect that with the help of the open-source Node-RED development environment, it is easy to implement the communication of different IoT technologies with each other. In this way, it can provide cost- and time-efficient solution options for those representatives of the industry who wants to test the effectiveness of a new smart system. At the same time, Node-RED has a distinct advantage in the field of data visualization, as well as the MQTT protocol over traditionally used industrial solutions, since spectacular results can be achieved by applying simple logic, so it proves to be

much more efficient in terms of cost and time. Thanks to this, the interface can be easily expanded as needed, in order to be able to monitor all sensor or machine data that we deem important.

In industry, the use of IoT devices mostly receives special attention due to the optimization of processes, the detection of errors and the implementation of predictive maintenance, since cost reduction can be achieved with the help of their integration, and by analysing and using the collected data, we can get to know our systems better.

Based on the above implementations, we can evaluate the development and integrability of today's technology in such a way that it is properly applied for use in the industrial field, for the use of IIoT. But it is not necessary to limit yourself to the use of just one of these services, even if they are paid large open source, but they can be integrated and used together, and in many cases their combined use is recommended, depending on what task we want to use them for.

Acknowledgement

This work was supported by the Collegium Talentum Programme of Hungary.

References

- [1] Amghar, Souad, Safae Cherdal, and Salma Mouline. "Which NoSQL database for IoT applications?." 2018 international conference on selected topics in mobile and wireless networking (mow'net). IEEE, 2018
- [2] Andreeski, Cvetko, and Daniela Mechkaroska. "Modelling, Forecasting and Testing Decisions for Seasonal Time Series in Tourism." *Acta Polytechnica Hungarica* 17.10 (2020): 149-171
- [3] Apache Cassandra, Open Source NoSQL Database, Accessed on: Aug. 17, 2022 [Online] Available: <https://cassandra.apache.org/>
- [4] Badii, Claudio, et al. "Industry 4.0 synoptics controlled by IoT applications in Node-RED." 2020 International Conferences on Internet of Things (iThings) and IEEE Green Computing and Communications (GreenCom) and IEEE Cyber, Physical and Social Computing (CPSCom) and IEEE Smart Data (SmartData) and IEEE Congress on Cybermatics (Cybermatics). IEEE, 2020
- [5] Chaczko, Zenon, et al. "Biomimetic middleware design principles for IoT infrastructures." *Acta Polytechnica Hungarica* (2020)
- [6] Chakraborty, Mainak, and Ajit Pratap Kundan. "Grafana." *Monitoring Cloud-Native Applications: Lead Agile Operations Confidently Using Open Source Software*. Berkeley, CA: Apress, 2021, 187-240
- [7] Combined Cycle Power Plant Data Set, Accessed on: Aug. 17, 2022 [Online] Available: <https://archive.ics.uci.edu/ml/datasets/Combined+Cycle+>

- [8] Díaz, Manuel, Cristian Martín, and Bartolomé Rubio. "State-of-the-art, challenges, and open issues in the integration of Internet of things and cloud computing." *Journal of Network and Computer applications* 67 (2016): 99-117
- [9] Eclipse Mosquitto, An open source MQTT broker, Accessed on: Aug. 17, 2022 [Online] Available: <https://mosquitto.org/>
- [10] Ed-daoudy, Abderrahmane, and Khalil Maalmi. "A new Internet of Things architecture for real-time prediction of various diseases using machine learning on big data environment." *Journal of Big Data* 6.1 (2019): 1-25
- [11] Ferencz, Katalin, and József Domokos. "IoT Sensor Data Acquisition and Storage System Using Raspberry Pi and Apache Cassandra." 2018 International IEEE Conference and Workshop in Óbuda on Electrical and Power Engineering (CANDO-EPE). IEEE, 2018
- [12] Ferencz, Katalin, and József Domokos. "Rapid prototyping of IoT applications for the industry." 2020 IEEE International Conference on Automation, Quality and Testing, Robotics (AQTR). IEEE, 2020
- [13] Ferencz, Katalin, and József Domokos. "Using Node-RED platform in an industrial environment." XXXV. Jubileumi Kandó Konferencia, Budapest (2019): 52-63
- [14] Ferencz, Katalin, József Domokos, and Levente Kovács. "A statistical approach to time series sensor data evaluation using Apache Spark modules." 2022 IEEE 16th International Symposium on Applied Computational Intelligence and Informatics (SACI) IEEE, 2022
- [15] Galambos, Péter. "Cloud, fog, and mist computing: Advanced robot applications." *IEEE Systems, Man, and Cybernetics Magazine* 6.1 (2020): 41-45
- [16] Galambos, Péter, et al. "Design, programming and orchestration of heterogeneous manufacturing systems through VR-powered remote collaboration." *Robotics and Computer-Integrated Manufacturing* 33 (2015): 68-77
- [17] Jelacic, Bojan, et al. "Security risk assessment-based cloud migration methodology for smart grid OT services." *Acta Polytechnica Hungarica* 17.5 (2020): 113-134
- [18] Kanagachidambaresan, G. R. "Node-Red Programming and Page GUI Builder for Industry 4.0 Dashboard Design." *Role of Single Board Computers (SBCs) in Rapid IoT Prototyping*. Cham: Springer International Publishing, 2021, 121-140
- [19] Katalin, Ferencz, and Domokos József. "Ipari IoT szolgáltatások és nyílt forráskódú rendszerek áttekintése: Overview of Industrial IoT services and

- open source systems.", *Energetika-Elektrotechnika– Számítástechnika és Oktatás Multi-konferencia* (2020): 69-74
- [20] Kuzzle Documentation. Accessed on: April 23, 2023 [Online] Available: <https://docs.kuzzle.io/core/2/guides/introduction/what-is-kuzzle/>
- [21] Node-RED, Low-code programming for event/driven applications, Accessed on: Aug. 17, 2022 [Online] Available: <https://nodered.org/>
- [22] Okanović, Andrea, et al. "Innovating a model for measuring competitiveness in accordance with the challenges of industry 4.0." *Acta Polytechnica Hungarica* 17.7 (2020): 67-88
- [23] Pääkkönen, Pekka. "Feasibility analysis of AsterixDB and Spark streaming with Cassandra for stream-based processing." *Journal of Big Data* 3.1 (2016): 1-25
- [24] R. Peters, "Securing the Industrial Internet of Things in OT Networks", Fortinet, Dec. 18, 2018. Accessed on: Apr. 24, 2021. [Online] Available: <https://www.fortinet.com/blog/industry-trends/securing-the-industrial-internet-of-things-in-ot-networks>
- [25] Russell, Brian, and Drew Van Duren. *Practical internet of things security*. Packt Publishing Ltd, 2016
- [26] Tabaa, Mohamed, et al. "Industrial communication based on modbus and node-RED." *Procedia computer science* 130 (2018): 583-588
- [27] thethings.io Documentation. Accessed on: April 23, 2023 [Online] Available: <https://developers.thethings.io/docs/getting-started>
- [28] Thinger.io Documentation. Accessed on: April 23, 2023 [Online] Available: <https://docs.thinger.io/>
- [29] Tüfekci, Pinar. "Prediction of full load electrical power output of a base load operated combined cycle power plant using machine learning methods." *International Journal of Electrical Power & Energy Systems* 60 (2014): 126-140
- [30] Veneri, Giacomo, and Antonio Capasso. *Hands-on industrial Internet of Things: create a powerful industrial IoT infrastructure using industry 4.0*. Packt Publishing Ltd, 2018
- [31] Weissman, David, and Anura Jayasumana. "Integrating IoT monitoring for security operation center." *2020 Global Internet of Things Summit (GloTS) IEEE*, 2020
- [32] Wukkadada, Bharati, et al. "Comparison with HTTP and MQTT in Internet of Things (IoT)." *2018 International Conference on Inventive Research in Computing Applications (ICIRCA)*. IEEE, 2018

Q-sort Evaluation of Risk Factors by Automotive Experts

Tamás Bence Venczel¹, László Berényi² and Krisztián Hriczó³

¹ Institute of Mathematics, University of Miskolc, 3515 Miskolc-Egyetemváros, e-mail: bence.venczel.tamas@uni-miskolc.hu

² Institute of Management Science, University of Miskolc, 3515 Miskolc-Egyetemváros, e-mail: laszlo.berenyi@uni-miskolc.hu

³ Institute of Mathematics, University of Miskolc, 3515 Miskolc-Egyetemváros, e-mail: krisztian.hriczo@uni-miskolc.hu

Abstract: The high level of standardization within the automotive industry may support avoiding the occurrence of common and unforeseen risks. There are several risk management methods available, but effective actions need to understand current challenges. Automotive risk management requires a comprehensive measure and evaluation approach. The research aims to map the risk factors of managing the automotive industry for preparing a decision support model through a pilot study. The analysis used a list of risk factors based on the literature and idiographic data collection among 22 experts in 2023. The study used the Q-methodology to create characteristic patterns of opinions. Three factors were separated and entitled based on their expressed opinions Factor 1 “Follow Standards!”, Factor 2 “Take Control!” and Factor 3 “Be Flexible!”. Factor 1 respects mostly the automotive standards (e.g., IATF, VDA, and FMEA). Factor 2 consists of opinions to support actions that can increase overall control. Factor 3 supports every aspect to increase flexibility. There is consensus among the three factors on the high importance of Total Productive Maintenance (TPM) and proper supplier selection among the respondents. Relative opinions in the field may contribute to developing company-level risk mitigation strategies and understanding supply chain-level challenges. The study confirms the applicability of Q-methodology to discover opinion groups and, therefore, can be considered a novel contribution to the research field, from a methodological perspective.

Keywords: Automotive industry; Q-sort, Risk management

1 Introduction

Happenings in the automotive industry have an extensive impact on the economy since it is one of the most globalized industries [1] [2]. The Global, European and Hungarian vehicle industry has recovered after the COVID-19 pandemic and

lockdowns, and the growth has continued in 2022 [3] [4]. A lesson learned from the situation is rethinking risk management in the field. Due to the complexity of the automotive supply chain, important measures have been taken to organize necessary activities on the topic of Supply Chain Risk Management (SCRM) [5]. There is a growing consumer expectation for vehicles, including product quality [6], sustainability [7], and technological innovation [8]. The competition and the increasing pressure of legal regulations result in a challenging entrepreneurial and technological environment. The changing environment raises new forms and sources of risks that require updated solutions. Automotive supply chains are changing rapidly and becoming more complex over time. As a result, the emphasis on the proper approach to risk management is valued. The study deals with the practical opportunities of the Q-methodology, for this purpose and contributes to renewing the knowledge base of automotive risk management by exploring the relative importance of risk factors, by expert opinions. The analysis uses the Q-methodology to establish a ranking. The fundamental goal of this study is to exploit possibilities, in order to support risk management actions, within the industry, to foster financial growth and the secure, safe introduction of new products.

2 Literature Review

2.1 Automotive Supply Chain Risks

A wide range of information is available regarding the definition of risks, risk management, and its relation to project management [9]. The early studies on risk management started in the 1980s and continued to develop in the past decades. A database from the 1980s showed that “many projects met their time-target - the average slippage was 17% - but there was a clear over-run on costs - the average over-spend was 88%”. Williams’ article [10] shows a comprehensive review of the topic.

Brustbauer [11] analyzed the risk management practices of SMEs, based on a questionnaire in 2014. He suggests that companies should apply a passive (defensive strategy) or active (offensive strategy) risk management method [11]. The chosen method should be based mainly on company size, sector affiliation, and ownership structure. Risk management is a major issue for SMEs, mostly because of the lack of resources for this activity, and about two-thirds of the analyzed companies have a passive risk management approach. The author interprets that applying risk management increases competitiveness and success. A key factor for effective risk management is the awareness of the company regarding possible risks. If a company is not able to define the risk in itself and its

surroundings, it is not possible to create an effective action plan for risk mitigation [11].

A study across Brazil [12] in 2017 was performed in two stages (first: face-to-face interviews, second: online survey) regarding the risk management behavior of startups. Pearson's correlation was used to explore patterns of risk management at the companies. ISO31000 procedure is recommended by the author, which standard offers a simple and easy-to-implement procedure.

Automotive risk management has extensive literature, including supply chain risks. Regardless of the qualitative or quantitative nature of the suggested procedures, there is an agreement on the main knowledge areas covering risk classification, risk factor analysis, risk management methods, and risk gap identification [13]. The researchers emphasize the importance of supply chain risk management (SCRM) [14].

The general approach to the risk management process consists of four steps, even for supply chains [14]:

1. Risk identification
2. Risk assessment
3. Risk management decision and implementation
4. Risk monitoring

There are competing models and approaches to risk management. Some authors focused on empirical analysis; others argued in favor of literature-based, theoretical model creation followed by empirical confirmation [15-19]. A case study investigated two Hungarian supply chains in 2006 to understand the dynamics of cooperation where the connection between corporate strategy and supply chain management has been confirmed [20]. Considering the effects of the 2008 economic crisis, a study proposed policy recommendations to support risk mitigation of suppliers [21]. A comprehensive review of the Hungarian automotive industry compared to the V4 countries was performed in 2017 with historical intent. The study proposed two possible future development paths for V4 countries with recommendations to support the intensive development of the vehicle industry [22]. A current case study from 2022 categorized the risks according to their effect on the company into five groups, entitled Operational, Process, Suppliers, Security, and Labor Rights, and provided a probability-impact matrix for the investigated companies. The broadly accepted Analytic Hierarchy Process (AHP) was used for a systematic weight calculation; the results highlighted the bad quality of the final product as the most significant risk [23].

Huang et al. [24] focused on the disruptions of automotive supply chains based on the literature review of 866 journal articles. According to the results, automotive supply chain risk management has attracted increasingly more attention from society and scholars over the past decades.

KPMG [25] also stated that supply chains are highly vulnerable. 78% of global automotive executives rated that recent volatility in commodity prices would impact their business, and 80% believed that labor shortages would impact their business. Material shortages, demand uncertainties, increasing environmental regulations, labor market scarcity, disruptions due to the globalized nature of the automotive industry, and increasing complexity of tariffs and trade regulations are considered the main vulnerability factors. To ease the effect of such risks, it is recommended to regionalize the supply chain, ensure supply chain diversity, establish a task force to manage critical commodities, establish strategic partnerships or joint ventures and ensure the appropriate level of transparency [25].

The risk mitigation activities in automotive supply chains tend toward technical and financial risk management actions; however, the studies in the field emphasize more attention to the strategic and methodological tools for risk mitigation. The ultimate goal is to develop effective risk mitigation strategies. Methodological development suggests considering multi-criteria decision-making (MCDM), multi-objective decision-making (MODM) [26] and ISO 31000 [27], and probability and impact analysis [28]. The experience of the German automotive industry [29] provides professional support to the efforts. The categorization of risks has been investigated, and it is the basis of the initial concept for grouping, as presented in Table 1 [30].

Table 1
Input data for risk mitigation actions and statement list

Risk mitigation category	Risk mitigation action
<i>Financial risk management</i>	Insurance
	Forward of futures contracts
	Real options approach
<i>Avoidance</i>	Dropping specific products/ geographical markets/supplier or customer organizations
	Delay new market entry
	Vendor selection methodologies
	Vertical integration
	Horizontal mergers and acquisitions
<i>Control</i>	Inventory system: Increased stockpiling and the use of buffer inventory
	Maintaining excess capacity in production, storage, handling and/or transport
	Imposing contractual obligations on suppliers and customers
	Gain market power
	Long-term contractual agreements and commitments with suppliers and customers

<i>Cooperation</i>	Collaborative relationship management (e.g., partnerships, alliances, or joint ventures)
	Joint efforts to improve visibility, transparency, information transmission/sharing, and understanding within supply chain
	Risk sharing
	Aligning incentives and revenue sharing policies in a supply chain
<i>Imitation</i>	Joint efforts to prepare supply chain continuity plans
	Imitation of product and process technologies
<i>Flexibility</i>	Follow other firms in moving into new markets
	Product diversification
	Geographic diversification
	Increase overall flexibility
	Flexible input sourcing (e.g., Dual sourcing and multiple sourcing)
	Back-up supplier
	Localized sourcing
	Flexible workforce size and skills, plants, and equipment
	Multinational production
	Postponement
	Flexible supply contracts
Flexible manufacturing	
Flexible distribution	

2.2 Q-methodology

Evaluation of the relative importance of risk factors cannot be uniform by the activity, size, or other company and supply chain characteristics. Individual evaluations may be available, and exploring opinion patterns may promote establishing effective risk-mitigation strategies. Due to the subjective aspects of the topic, it is necessary to apply a method that can objectify opinions. Although using a set of questions evaluated on a Likert scale offers results that are easy to interpret, distortions of the evaluation can be misleading [31]. A direct or paired ranking method is relatively more expedient; however, the huge number of considerable risk factors makes the workload unreasonably difficult for the respondents. Q-methodology offers an optimal solution to rank a higher number of factors and effectively create opinion groups by statistical evaluation. The method was developed by physicist and psychologist William Stephenson in the 1930s and widely used in several areas like marketing, psychology, or any study which analyzes subjective opinions [32].

Q-methodology is a combination of qualitative and quantitative analysis. The respondents are asked to express their opinions by sorting a set of statements, whether they agree or disagree, according to a specified question. Data processing can be performed manually onsite, but online support is available. The traditional process uses prepared cards with the statements, which must be placed on a board to represent the ordered opinions individually. After gathering data, a wide range of software is available for evaluation [33]. The main steps of Q-methodology can be summarized as follows (based on [34-36]):

- Making the initial data matrix of the evaluations
- Calculating the correlations
- Selecting the number of factors
- Calculating rotated factors loadings
- Determining factor weights and scores
- Analysis of distinguishing statements
- Presenting patterns of opinions by the final factors

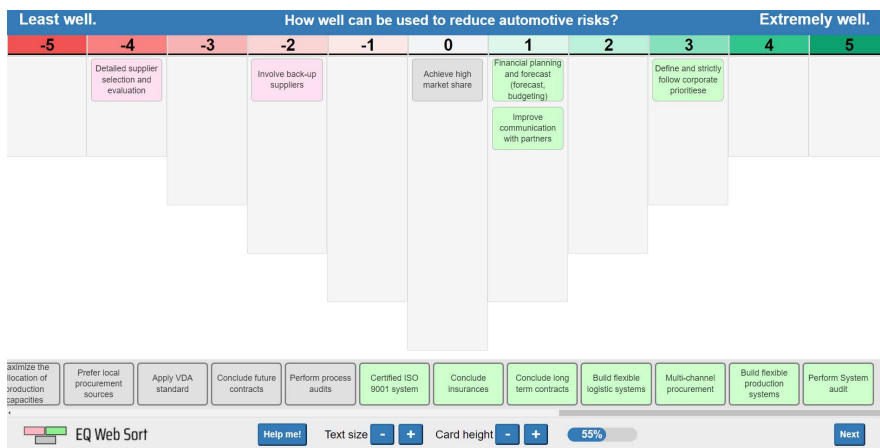


Figure 1
Q-sort pattern

The question for evaluation asked the respondents to sort the items by their importance in their opinion. The forced sort pattern assures normal distribution of the evaluations of the participants [32]. Figure 1, shows the design for evaluations in the original language. A supplementary questionnaire is proposed for collecting additional data for further groupings and evaluations.

3 Research Design

3.1 Research Goal

The need for effective risk mitigation strategies raises the question of what risk factors are remarkable in the automotive industry. However, considering that the individual challenges of the companies are inevitable, a core set of factors must be identified to support supply chains. The study aims to explore the characteristic patterns of expert opinion to contribute to a common understanding of automotive risks. Moreover, based on experts' opinions offer an initial point for developing risk mitigation strategies. We consider the results a pilot study, regardless of the opportunities of the methods.

3.2 Research Method

A preliminary list of risk factors based on an international literature review was refined and supplemented by interviews with Hungarian automotive industry experts for the analysis. The next step was preparing the statements for evaluation by the Q-methodology [37]. The process configuration is summarized in Table 2, including support tools and steps.

Table 2
Data collection and analysis process

Main Activity		Steps & tools				
1.	<i>Topic selection</i>	Interview with industry experts	Risk factors from the literature	Confirmation of risk factors (Google Forms)		
2.	<i>Survey development and data collection</i>	Programming (EQ Web Configurator)	Survey publishing (Netlify)	Data Collection (link via e-mail)	Data management (Firebase)	Data output (JSON format)
3.	<i>Q-sort analysis</i>	KADE input	Calculate correlations	Principal component analysis	Varimax rotation for a selected number of factors based on scree-plot	Output tables: Factor loadings, Z-scores, Factor visualizations
4.	<i>Further analysis and presentation of results</i>	Factor presentation	Cross-tabulation Rank orders	Developing new surveys		

The statement list of the questionnaire used an item collection by Ceryno [17], and additional categories were defined, including common automotive tools and standards (Table 1). The study was designed for a voluntary online survey managed by the software EQ Web Sort version 2.0.0, and data processing was performed with the free Ken-Q Analysis Desktop Edition (KADE) software

version 1.2.1. The factors were defined by considering the scree plot by eigenvalues, and principal component analysis with Varimax rotation was for maximizing the sum of the variances of the squared correlations between variables and factors. The software also allows centroid factors and other types of analysis, but this explorative solution was selected since preliminary knowledge of the possible factor numbers and contents was missing.

3.3 Sample Characteristics

Data was collected online from respondents between 20th January 2023 and 27th January 2023. An invitation was sent to 38 automotive experts at three different international Tier-1 supplier-level automotive companies located in Hungary. The research sample consists of 22 evaluations. Sample characteristics are summarized in Table 3.

Table 3
Sample composition

	Grouping factors	Number	% sample
	< 5 years	2	9.1%
Total work experience in the automotive industry	5 years – 10 years	10	45.5%
	11 years – 15 years	6	27.3%
	16 years – 20 years	4	18.2%
	HR, administration	3	13.6%
	Engineering I (production, maintenance, facility, IT)	4	18.2%
	Engineering II (development, testing, project management)	4	18.2%
Area of current job	Quality, supplier quality assurance	5	22.7%
	Production	3	13.6%
	Supply chain (logistics, procurement)	3	13.6%

Furthermore, respondents were asked after completion of Q-sort to rate six questions related to current challenges of automotive risks on a five-point scale (higher values mean higher risk). They were asked to judge how much they think automotive depends on these factors. The highest average rating was received for supply issues related to microchips, while the lowest average rating was received for local political decisions (Figure 2).

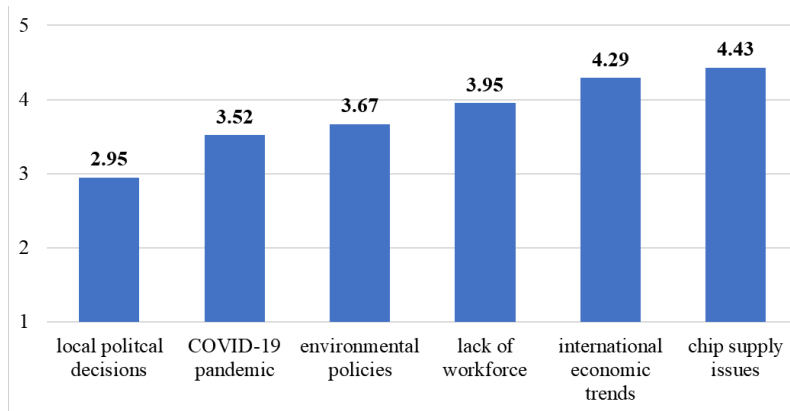


Figure 2
Average ratings of risk factors

4 Results

4.1 Demarcation of the Factors

The principal component analysis offered a maximum of eight factors based on the 22 responses, seven of which were at a greater eigenvalue than 1 (Figure 3). The variance explained is 32% for the first factor, and the total variance explained is 43% for two factors and 52% for three factors. The scree plot (Figure 3) suggested establishing three factors. It is worth noting that the total variance explained is a maximum of 77% with eight factors, but the differences between the further factors are not remarkable. Factor characteristics are summarized in Table 4.

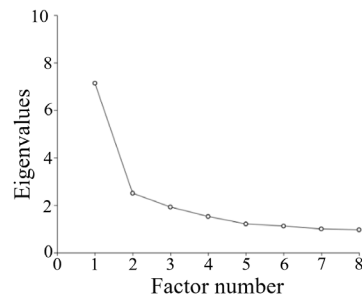


Figure 3
Scree plot (KADE output)

Table 4
Factor characteristics

	Factor 1	Factor 2	Factor 3
Eigenvalues	7.1415	2.5047	1.9244
% explained variance	32	11	9
Total % explained variance	32	43	52
% explained variance after VARIMAX rotation	21	19	12
Number of members (% of total respondents)	8 (40%)	8 (40%)	4 (20%)
The ratio of flagged within the factor	88.89%	100.00%	80.00%
Correlation with Factor 1	1	0.5255	0.2201
Correlation with Factor 2	0.5255	1	0.3347
Correlation with Factor 3	0.2201	0.3347	1

4.2 Factor Scores

The z-score is a weighted average of the values that the Q-sorts most closely related to the factor given to a statement, and it is continuous [38]. It is calculated as a mathematical expression of the distance between a particular absolute score and the mean average score of the measured sample [36]. Based on the z-core analysis, significant similarities and differences can be found between the factors (Table 5). Most significant differences in z-scores were discovered with statements in “Flexible and well-trained employees”, “Apply IATF standard” and “Use FMEA method”. Most significant similarities of z-scores were discovered with statements in “Total Productive Maintenance (TPM)” and “Budget planning and forecast”. The analysis of z-cores mainly supports the recognition of patterns of opinions in Factors.

Table 5
Factor scores filtered on threshold level $P < 0.0001$

Factor	Threshold	Q Sort Value	Statement
Factor 1	$P < 0.0001$	4	Use FMEA method
	$P < 0.0001$	5	Apply IATF standard
	$P < 0.0001$	3	Apply ISO 9001 standard
	$P < 0.0001$	4	Apply LEAN principles
	$P < 0.0001$	1	Flexible production systems
	$P < 0.0001$	5	Apply VDA standard
	$P < 0.0001$	4	Process audit
Factor 2	$P < 0.0001$	-5	Aim for high market share
	$P < 0.0001$	-2	Flexible production systems
	$P < 0.0001$	5	Standardized production
	$P < 0.0001$	-4	Build wide range of product-portfolio
	$P < 0.0001$	4	Maximize allocation of production capacities

Factor 3	P < 0.0001	5	Flexible and well-trained employees
	P < 0.0001	5	Flexible production systems
	P < 0.0001	3	Flexible logistics systems
	P < 0.0001	2	Avoid too much expansion by rejecting new projects
	P < 0.0001	-3	System audit

4.3 Patterns of Opinions in Factors

The ranking orders by the three factors are represented in Figures 4-6. Based on the results, there are several consensus statements (marked with blue background), like “Total Productive Maintenance (TMP)”, “Strong cooperation with customers and suppliers”, and “Copy technologies and processes of competitors”. The distinguishing statements are displayed in the figures at a maximum p=0.05 threshold value. These statements show the items of the evaluation that draw the idiographic patterns. According to Factor 1, 23 of 38 statements are listed; in the cases of Factor 2 and Factor 3, 18 and 20 items are listed. The figures suggest characteristic opinion patterns. It is to note that the distinguishing statements are focused on the leftmost and rightmost sides of the evaluations.

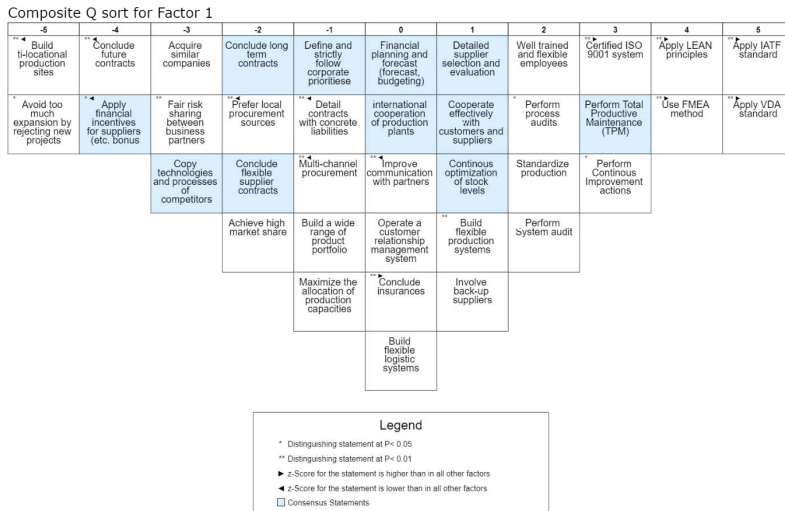


Figure 4
Factor 1 ranking order

Composite Q sort for Factor 2

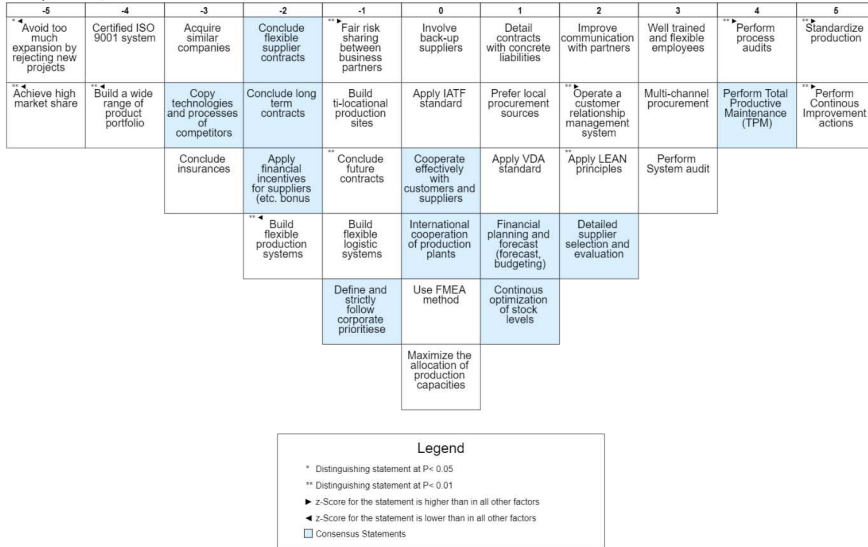


Figure 5

Factor 2 ranking order

Composite Q sort for Factor 3

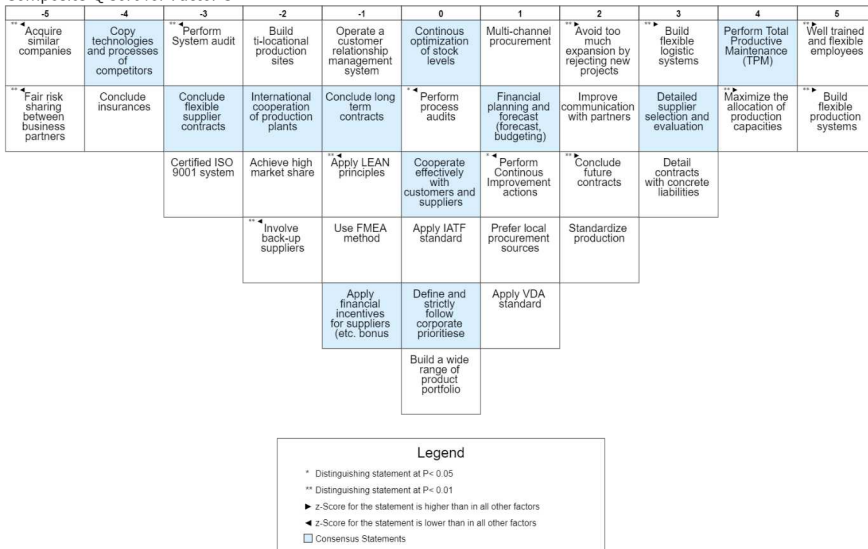


Figure 6

Factor 3 ranking order

4.4 Dependency of the Automotive Industry on some Issues

An additional question in the survey asked to evaluate the dependence of the automotive industry on some issues. The respondents were asked to mark their opinion on a five-point scale (1: not dependent on it, 5: extremely dependent on it). Figure 8 shows the issues and the mean values of the evaluations by factors as a simplified visualization.

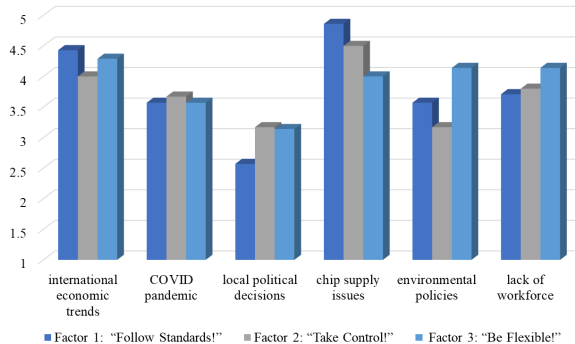


Figure 7
Cross-tabulation results

The COVID-19 pandemic and local political decisions were not considered the most relevant issues regarding the dependence of the automotive industry. The impact of environmental policies is high among the respondents of Factor 3. Chip supply and international trends are at the top of the list, but visible differences exist between the factors. The lack of a workforce is considered a more serious issue than the COVID-19 pandemic or local politics.

The non-parametric Kruskal-Wallis H test was used to check the significance of the differences (Table 6).

Table 6
Kruskal-Wallis H-test results by factors

Survey item	Kruskal-Wallis H	df	Asymp. Sig.
international economic trends	1.683	2	0.431
COVID pandemic	0.132	2	0.936
local political decisions	1.446	2	0.485
chip supply issues	2.341	2	0.310
environmental policies	3.341	2	0.188
lack of workforce	0.726	2	0.696

Despite the visual differences, the variance analysis test did not find statistically significant differences between the factors. The detailed analysis confirmed a

significant difference between Factor 2 and Factor 3 regarding the role of environmental policies (Kruskal-Wallis $H=4.158$, $d_f=1$, $\text{sig.}=0.041$).

5 Discussion

The main target of the study is to discover opinions in the field that may contribute to developing company-level risk mitigation strategies and understanding supply chain-level challenges. To define mitigation strategies, we need to show and understand the differences between the discovered opinion groups. According to the most and least preferred items of the survey statements (Table 7), the three opinion groups about the relative importance of risk factors can be entitled as follows:

- Factor 1 – “Follow Standards!”
- Factor 2 – “Take Control!”
- Factor 3 – “Be Flexible!”

Table 7
Summary table of factor statements with mitigation categories

	Factor 1 “Follow Standards!”	Factor 2 “Take Control!”	Factor 3 “Be Flexible!”
<i>Most significant statements</i>	Apply IATF standard (AUT)	Standardized production (CTRL)	Flexible and well-trained employees (FLEX)
	Apply VDA standard (AUT)	Continuous Improvement actions (AUT)	Flexible production systems (FLEX)
	Apply LEAN principles (AUT)	Process audit (CTRL)	Total Productive Maintenance (TPM) (AUT)
	Use FMEA method (AUT)	Total Productive Maintenance (TPM) (AUT)	Maximize allocation of production capabilities (FLEX)
<i>Least significant statements</i>	Multi-locational production (FLEX)	Avoid too much expansion by rejecting new projects (AVOID)	Acquisition of similar companies (CTRL)
	Avoid too much expansion by rejecting new projects (AVOID)	Aim for high market share (CTRL)	Fair risk sharing between customers and suppliers (COOP)
	Conclude futures contracts (FIN)	Apply ISO 9001 standard (AUT)	Copy technologies and processes of competitors (IMIT)
	Financial incentives for suppliers (FIN)	Build wide range of product portfolio (CTRL)	Insurance (FIN)

The Q-methodology suggests asking for reasoning about the most and least preferred selection. Taking the qualitative information and the responses into consideration, we can define the most significant characteristics of the groups. Risk mitigation categories (based on Table 1) have been added to Table 7 for better visualization.

Factor 1 “Follow Standards!” can be described as a group of individuals with a strong belief in well-established automotive standards and tools. They think that avoiding most of the risks is possible by following the rules and strongly reject anything related to expansion as they see high risk in any expansion activities. They do not prefer local suppliers or even multi-channel procurement; probably, they believe that if we apply the right standards in the supply chain, we can avoid risks. They rate low the efficiency of financial risk mitigation actions. This group rated lowest the importance of communication (but still on a neutral level).

Factor 2 “Take Control!” can be described as a group of individuals with a strong belief in self-driven standardization activities. They rate the importance of general automotive standards rather low/neutral. They would like to have risks in “their own hands” rather than rely on systems. Conscious prevention and control are key factors for them. They refuse high market share and wide product portfolio as it increases the uncontrollable activities. Flexibility is rated low, except for employee flexibility, which is rated higher than Factor 1, which shows they rely on people’s capabilities rather than general standards.

Factor 3 “Be Flexible!” can be described as a group of individuals with a strong belief in actions to increase overall flexibility, especially regarding production and employee flexibility. They think people, production, and logistics should all be as flexible as possible. Maximized allocation of available capacities preferred by them. They prefer future contracts, which are also a form to support financial flexibility. The highest rejection rate towards company acquisitions was observed within this group. Only this opinion group rated the application of LEAN principles lower than neutral. Continuous Improvement (CI) actions were rated lower than those rated by Factor 1 or Factor 2 groups.

Consensus statements show that the experts agree about the statement’s rating and therefore represent the opinion of all respondents statistically. The high-rated statements mean that most respondents agree on the greater efficiency of the item in reducing risks compared to lower-rated ones. Neutral-rated statements cover a medium level. Consensus statements represent the items with a high agreement among the respondents regardless of which they belong. An interesting future research question is the reason for the consensus statement ratings and their possible effect on risk mitigation. Maybe an increase in the usage of some actions from neutral statements could increase the efficiency of an organization to mitigate risks, but it can be judged after objectively understanding the effect of the applied actions.

The highest-rated consensus statements:

- Total Productive Maintenance (TPM)
- Detailed supplier selection and evaluation

Neutral consensus statements:

- Budget planning and forecast
- Continuous optimization of stocks
- Strong cooperation with customers and suppliers
- Define enterprise priorities and strictly follow them
- International cooperation of production plants
- Long term contracts

The lowest-rated consensus statements:

- Copy technologies and processes of competitors
- Financial incentives for suppliers
- Flexible supplier contracts

Although the mean values of the evaluation of the impact of some general topics affecting the economy and society show visible patterns by the factors, the Kruskal-Wallis analysis of variance test could not confirm those. The high variance of the evaluations can be in line with the variety of the companies in products or the level of contribution. The result suggests the need for company-level risk evaluations, but the common trends can provide valuable input.

Conclusions

This study aimed to explore the characteristic patterns of expert opinion on risk factors in the automotive industry for a current understanding. A Q-sort evaluation separated three distinct opinion groups as factors. Factor 1, called “Follow Standards!”, respects mostly, the automotive standards (e.g., IATF, VDA, and FMEA) and rejects flexible reactions. Factor 2, called “Take Control”, consists of opinions to support actions that can increase overall control. Factor 3, called “Be Flexible!”, supports every aspect to increase flexibility, including people, production, and logistics, but the effectiveness of conscious development activities at a lower rate.

Although there are three opinion groups explored, some remarkable similarities are reflected in consensus statements. There is consensus on the high importance of Total Productive Maintenance (TPM) and proper supplier selection among the respondents. Budget planning and customer-supplier relationship management activities were rated neutral, which might raise attention to these areas as the

literature highlights their importance [12][16][19]. Financial risk management and competitor imitation actions were rated least efficient, suggesting that experts prefer actions and systems that give them the power to handle risks internally.

The analysis of general risk factors in the automotive industry shows differences in the perception of the respondents regarding the disruption in chip supply, environmental policies, and the lack of workforce. The experts agreed on the moderate impact level of the COVID-19 pandemic on automotive supply chains, compared to other issues.

A theoretical implication is the applicability of Q-methodology to discover characteristic patterns of expert opinion in the automotive industry; therefore, it is recommended to continue further research in the field. However, supply chain integration has been measured by Q-sort, but it is not directly relevant to risk management [32][33]. The measurement of opinions about the risk factors in the automotive industry by the Q-methodology can be considered a theoretical contribution to the field.

The findings can be used to enhance risk management tools and provide input for more effective risk management. Based on the weighted opinions, it is intended to provide input to establish complex risk mitigation strategies. As an output, organizations can define actions for their risk management practice and discover areas that could require strategic management attention and resources. Despite the thorough design of the survey and the combination of various methods during the research, there are some limitations to the generalization of the results.

The study is limited to Hungary; future research could consist of a broader range of respondents, including experts from various European countries and a more focused approach, based on the opinion groups revealed in this study, concentrating on a systematic selection of samples.

References

- [1] T. J. Sturgeon, O. Memedovic, J. V. Biesebroeck, and G. Gereffi, 'Globalisation of the automotive industry: main features and trends', *Int. J. Technol. Learn. Innov. Dev.*, Vol. 2, No. 1/2, p. 7, 2009, doi: 10.1504/IJTLID.2009.021954
- [2] T. Sturgeon, J. Van Biesebroeck, and G. Gereffi, 'Value chains, networks and clusters: reframing the global automotive industry', *J. Econ. Geogr.*, Vol. 8, No. 3, pp. 297-321, Feb. 2008, doi: 10.1093/jeg/lbn007
- [3] 'The Automobile Industry Pocket Guide 2022-2023'. ACEA - European Automobile Manufacturers' Association, 2022
- [4] 'Western European Passenger Car Sales Update', *São Paulo*, p. 10, 2022
- [5] G. C. Dias, C. T. Hernandez, and U. R. de Oliveira, 'Supply chain risk management and risk ranking in the automotive industry', *Gest. Produção*, Vol. 27, No. 1, p. e3800, 2020, doi: 10.1590/0104-530x3800-20

-
- [6] L.-H. Lin and I.-Y. Lu, 'Product quality as a determinant of product innovation: an empirical analysis of the global automotive industry', *Total Qual. Manag. Bus. Excell.*, Vol. 17, No. 2, pp. 141-147, Mar. 2006, doi: 10.1080/14783360500450434
- [7] W. Wellbrock, D. Ludin, L. Röhrle, and W. Gerstlberger, 'Sustainability in the automotive industry, importance of and impact on automobile interior – insights from an empirical survey', *Int. J. Corp. Soc. Responsib.*, Vol. 5, No. 1, p. 10, Dec. 2020, doi: 10.1186/s40991-020-00057-z
- [8] T. B. Venczel, L. Berényi, and K. Hriczó, 'Evolution of Startups in Automotive Supply Chain', in *Vehicle and Automotive Engineering 4*, K. Jármai and Á. Cservenák, Eds., in *Lecture Notes in Mechanical Engineering*. Cham: Springer International Publishing, 2023, pp. 412-420, doi: 10.1007/978-3-031-15211-5_34
- [9] Fekete I., 'Integrated risk management in practice', *Vezetud. Bp. Manag. Rev.*, pp. 33-46, Jan. 2015, doi: 10.14267/VEZTUD.2015.01.03
- [10] T. Williams, 'A classified bibliography of recent research relating to project risk management', *Eur. J. Oper. Res.*, Vol. 85, pp. 18-38
- [11] J. Brustbauer, 'Enterprise risk management in SMEs: Towards a structural model', *Int. Small Bus. J. Res. Entrep.*, Vol. 34, No. 1, pp. 70-85, Feb. 2016, doi: 10.1177/0266242614542853
- [12] M. F. Blos, M. Quaddus, H. M. Wee, and K. Watanabe, 'Supply chain risk management (SCRM): a case study on the automotive and electronic industries in Brazil', *Supply Chain Manag. Int. J.*, Vol. 14, No. 4, pp. 247-252, Jun. 2009, doi: 10.1108/13598540910970072
- [13] W. Ho, T. Zheng, H. Yildiz, and S. Talluri, 'Supply chain risk management: a literature review', *Int. J. Prod. Res.*, Vol. 53, No. 16, pp. 5031-5069, Aug. 2015, doi: 10.1080/00207543.2015.1030467
- [14] J. V. Blackhurst, K. P. Scheibe, and D. J. Johnson, 'Supplier risk assessment and monitoring for the automotive industry', *Int. J. Phys. Distrib. Logist. Manag.*, Vol. 38, No. 2, pp. 143-165, Mar. 2008, doi: 10.1108/09600030810861215
- [15] D. Kern, R. Moser, E. Hartmann, and M. Moder, 'Supply risk management: model development and empirical analysis', *Int. J. Phys. Distrib. Logist. Manag.*, Vol. 42, No. 1, pp. 60-82, Jan. 2012, doi: 10.1108/09600031211202472
- [16] J.-H. Thun, M. Drüke, and D. Hoenig, 'Managing uncertainty – an empirical analysis of supply chain risk management in small and medium-sized enterprises', *Int. J. Prod. Res.*, Vol. 49, No. 18, pp. 5511-5525, Sep. 2011, doi: 10.1080/00207543.2011.563901

- [17] P. S. Ceryno, L. F. Scavarda, and K. Klingebiel, 'Supply chain risk: empirical research in the automotive industry', *J. Risk Res.*, Vol. 18, No. 9, pp. 1145-1164, Oct. 2015, doi: 10.1080/13669877.2014.913662
- [18] G. Macher, E. Armengaud, E. Brenner, and C. Kreiner, 'A Review of Threat Analysis and Risk Assessment Methods in the Automotive Context', in *Computer Safety, Reliability, and Security*, A. Skavhaug, J. Guiochet, and F. Bitsch, Eds., in Lecture Notes in Computer Science, Vol. 9922. Cham: Springer International Publishing, 2016, pp. 130-141, doi: 10.1007/978-3-319-45477-1_11
- [19] N. Yoga Irsyadillah and S. Dadang, 'A LITERATURE REVIEW OF SUPPLY CHAIN RISK MANAGEMENT IN AUTOMOTIVE INDUSTRY', *J. Mod. Manuf. Syst. Technol.*, Vol. 4, No. 2, pp. 12-22, Sep. 2020, doi: 10.15282/jmmst.v4i2.5020
- [20] K. Demeter, A. Gelei, and I. Jenei, 'The effect of strategy on supply chain configuration and management practices on the basis of two supply chains in the Hungarian automotive industry', *Int. J. Prod. Econ.*, Vol. 104, No. 2, pp. 555-570, Dec. 2006, doi: 10.1016/j.ijpe.2006.05.002
- [21] K. Antalóczy and M. Sass, 'The impact of the crisis on the Hungarian automotive industry', 2011
- [22] J. Rechnitzer, R. Hausmann, and T. Tóth, 'Insight into the Hungarian Automotive Industry in International Comparison'
- [23] M. J. Hermoso-Orzáez and J. Garzón-Moreno, 'Risk management methodology in the supply chain: a case study applied', *Ann. Oper. Res.*, Vol. 313, No. 2, pp. 1051-1075, Jun. 2022, doi: 10.1007/s10479-021-04220-y
- [24] K. Huang, J. Wang, and J. Zhang, 'Automotive Supply Chain Disruption Risk Management: A Visualization Analysis Based on Bibliometric', *Processes*, Vol. 11, No. 3, p. 710, Feb. 2023, doi: 10.3390/pr11030710
- [25] 'Vulnerable Supply', KPMG, 2022
- [26] S. Kamran and Y. Hossein, 'MODM-MCDM Approach to Partner Selection in Auto Industry A Case Study on Mazda of Iran', *Int. J. Bus. Manag.*, Vol. 5, Oct. 2010, doi: 10.5539/ijbm.v5n11p183
- [27] E. Dehdar, A. Azizi, and S. Aghabeigi, 'Supply Chain Risk Mitigation Strategies in Automotive Industry: A Review', in *2018 IEEE International Conference on Industrial Engineering and Engineering Management (IEEM)*, Bangkok: IEEE, Dec. 2018, pp. 84-88, doi: 10.1109/IEEM.2018.8607626
- [28] D. Simchi-Levi *et al.*, 'Identifying Risks and Mitigating Disruptions in the Automotive Supply Chain', *Interfaces*, Vol. 45, No. 5, pp. 375-390, Oct. 2015, doi: 10.1287/inte.2015.0804

- [29] J.-H. Thun and D. Hoenig, 'An empirical analysis of supply chain risk management in the German automotive industry', *Int. J. Prod. Econ.*, Vol. 131, No. 1, pp. 242-249, May 2011, doi: 10.1016/j.ijpe.2009.10.010
- [30] M. Junaid, Y. Xue, and M. W. Syed, 'Construction of Index System for Risk Assessment in Supply Chains of Automotive Industry', Vol. 9, No. 4, 2020
- [31] S. E. Asch, 'Effects of group pressure upon the modification and distortion of judgments.', in *Groups, leadership and men; research in human relations.*, Oxford, England: Carnegie Press, 1951, pp. 177-190
- [32] W. STEPHENSON, 'CORRELATING PERSONS INSTEAD OF TESTS', *J. Pers.*, Vol. 4, No. 1, pp. 17-24, Sep. 1935, doi: 10.1111/j.1467-6494.1935.tb02022.x
- [33] B. Lee, 'Tools for Collecting a Concourse and Selecting a Q Sample', *Operant Subj.*, Vol. 41, May 2020, doi: 10.22488/okstate.20.100579
- [34] S. R. Brown, 'A Primer on Q Methodology', *Operant Subj.*, Vol. 16, No. 3/4, 1993, doi: 10.22488/okstate.93.100504
- [35] B. S. Lee, 'THE FUNDAMENTALS OF Q METHODOLOGY', *J. Res. Methodol.*, Vol. 2, No. 2, pp. 57-95, Nov. 2017, doi: 10.21487/jrm.2017.11.2.2.57
- [36] S. Watts and P. Stenner, *Doing Q Methodological Research: Theory, Method and Interpretation*. London, 2023. doi: 10.4135/9781446251911
- [37] A. Rahma, D. Mardiatno, and D. Rahmawati Hizbaron, 'Q methodology to determine distinguishing and consensus factors (a case study of university students' ecoliteracy on disaster risk reduction)', *E3S Web Conf.*, Vol. 200, p. 01003, 2020, doi: 10.1051/e3sconf/202020001003
- [38] A. Zabala and U. Pascual, 'Bootstrapping Q Methodology to Improve the Understanding of Human Perspectives', *PLOS ONE*, Vol. 11, No. 2, p. e0148087, Feb. 2016, doi: 10.1371/journal.pone.0148087

Study on Information Security Awareness using the Behavioral-Cognitive Internet Security Questionnaire

Kresimir Solic

Josip Juraj Strossmayer University of Osijek, Faculty of Medicine Osijek, Josipa Huttlera 4, 31000 Osijek, Croatia, kresimir@mefos.hr

Tena Velki

Josip Juraj Strossmayer University of Osijek, Faculty of Education Osijek, Cara Hadrijana 10, pp 330, 31000 Osijek, Croatia, tvelki@foozos.hr

Igor Fosic

HEP-Telekomunikacije, Martina Divalta 199, 31000 Osijek, Croatia, Igor.Fosic@hep.hr

Marin Vukovic

University of Zagreb, Faculty of Electrical Engineering and Computing, Unska 3, 10000 Zagreb, Croatia, Marin.Vukovic@fer.hr

Abstract: As technical security solutions are far from being enough to protect different kinds of information and communication systems, due to the human element, it was necessary to involve psychologists and define this problem as an interdisciplinary one. A validated questionnaire can be a good instrument for measuring users' information security awareness, knowledge on privacy issues and risk involved in online behavior, so conclusions gathered through empirical studies based on those kinds of questionnaires should be helpful in designing educative training programs. The aim of this paper was both to present the validated Behavioral-Cognitive Internet Security Questionnaire and prove its suitability for international usage as well as to present general conclusions regarding information and communication system users gathered through its development process. In this study, were included participants from 41 different countries, while English, Croatian, Slovenian and Hungarian language versions of questionnaire were used. Results have shown that developed questionnaire can be used internationally and the sum of the

conclusions is that users believe themselves to act more safely than they actually do; awareness has been rising over the years, but risk in online behavior has not been mitigated. Consequently, many users will still reveal their password, mostly under the influence of friendship or authority. Therefore, seeing as existing solutions are not good enough to resolve this global problem further studies should focus on developing some kind of an interactive platform that will be based on the results of empirical studies. It should not be based on restrictions, but rather on educational training, preferably personalized, and expanded with real-time warning solutions in order to keep up with constant changes in this field.

Keywords: ICT users; information security; security awareness; BCISQ questionnaire

1 Introduction

Nowadays there is finally a consensus among engineers and information security managers that technical security solutions are far from being enough to protect various ICT systems, due to the human element. This is because however good security procedures and hardware and software are, the impact of the user on the overall system security remains significant [1-4]. Once this problem was identified, it was necessary to include psychologists and define the problem as an interdisciplinary one [5], focusing on (miss) behavior and cross-cultural research with data collection and measurement issues [6].

Authors of this paper began their research into the users' impact back in 2009 [7, 8] and published their first validated questionnaire in 2014. The first published questionnaire was the UISAQ (Users' Information Security Awareness Questionnaire), which was validated in the Croatian language [9] and then translated into English [10] in order to reach a broader audience. After that first questionnaire, other scientifically validated security awareness (and risky online behavior, knowledge) questionnaires followed. The SeBIS (Security Behavior Intentions Scale) was developed in the USA and published in 2016 [11]. In the same year, the FMS (Four Measurements Scales) was designed and validated in Turkey [12]. The HAIS Q (Human Aspects of Information Security) was developed in Australia, with a validated version published in 2017 [13] and some preliminary results published earlier, in 2014 [14]. Further development of the UISAQ questionnaire ensued, based on an international, short and efficient version of the questionnaire. To the best of our knowledge, there are currently those four scientifically validated questionnaires for users' knowledge, (information security) awareness and online behavior examination. In scientific literature there have been many other attempts to test and partly measure online users' behavior regarding security and privacy issues, but through statistical process of validation, a questionnaire becomes a measurement instrument with defined reliability [15, 16]. So, it is of great importance to first undergo the

scientific validation process or to use other already validated questionnaires. Today's version of the Behavior Cognitive Information Security Questionnaire (BCISQ) presented in this paper has been validated in several languages, but primarily in English, and has been used internationally [17, 18].

The aim of this paper is both to present the validated BCISQ questionnaire and prove its suitability for international usage as well as to present general conclusions regarding online ICT system users' information security awareness, knowledge on privacy issues and risk of online behavior based on data gathered through its development process. The rest of the paper is organized as follows: next section describes the questionnaire, examinees and some properties of the statistical data analysis, then the following section presents a detailed theoretical background and history of the BCISQ's development. After results combined with discussion, the paper ends with the most important conclusions of this paper.

2 Overview of the Development of Constructs, Participants and Applied Data Analyses

The validated part of the BCISQ questionnaire comprises 17 items grouped into four scales, where two scales make a subgroup of the Behavioral Elements and two other scales make a subgroup of the Cognitive Elements. Under the Additional Questions there are two subgroups: Demographic Questions and Questions about Experience (Figure 1).

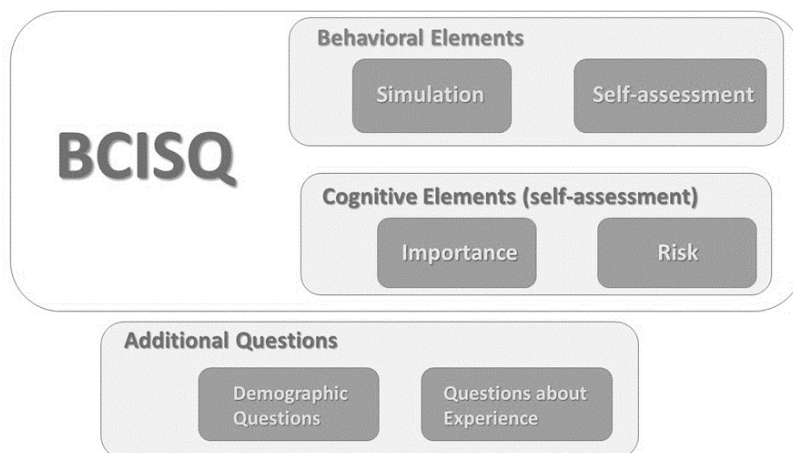


Figure 1
Schema of the BCISQ questionnaire

Demographic questions examine age, gender, level of education, field of expertise and current country of residence. Three questions examine the level of knowledge and experience regarding security and privacy on the Internet and two questions examine time spent online (Table 1).

Table 1
Questions regarding security, privacy and time spent online

Questions	Possible answers
<i>Level of knowledge and experience regarding security and privacy</i>	
How would you rate your knowledge about information security and privacy?	Poor/ Good/ Excellent
How would you rate your general technical knowledge about computers and the Internet?	Poor/ Good/ Excellent
Have you ever had some training or other experience(s) regarding security and privacy on the Internet?	Yes/ No
<i>Consumption of time on the Internet</i>	
How long have you been using the Internet?	A couple of years/ Half of life/ As long as I remember
On a daily basis, how often do you use Internet?	Less than 1 hour/ 2 to 3 hours daily/ 4 to 5 hours daily/ between 6 to 10 hours daily/ more than 10 hours daily

The 17 questions of the validated section referring to BS, BA, CI and CR are explained in the table (Table 2). Answers to the questions in the Behavioral Simulation scale are actually participant's action or lack of action in giving particular information, while answers to the questions in other three scales that are based on the self-assessment process represent scoring answers on the Likert scale from zero to four (Table 2).

In the Behavior Simulation scale participants can score up to 4 points (either based on answering Yes or filling in e-mail address or password), where a higher score means riskier behavior. In the Behavior Self-assessment scale each of the four questions has answers scored up to 4 points (answer Not very important gives zero, and answer Very important gives 4 points) and the arithmetic mean of those four answers gives the total score of the scale, where a higher score also means riskier behavior.

In the Cognitive Elements scale, subscale of Importance, each of the four questions has answers scored up to 4 points (answer Never gives zero, and answer Always gives 4 points) and the arithmetic mean of those four answers gives the total score of the scale, where a higher score means a higher level of awareness. While in the Cognitive Elements scale, subscale of Risk.

Table 2
List of items constructing each of the four scales of the BCISQ questionnaire

Items (questions)	Proposed answers
<i>Behavior scale (BS): risky behavior Simulation</i>	
Would you like to receive notifications from third-party partners about studies that investigate human behaviors, marketing, Internet security or other related topics?	Yes/ No
Would you like to receive free anti-virus software from third-party partners on your e-mail?	
If you would like to receive notifications and our free promotion material, please leave your e-mail:	<i>empty space for writing in (can be left empty)</i>
For checking the quality of your password security please write down your most used password:	
<i>Behavior scale (BA): risky behavior Self-assessment (Frequency of your behavior:)</i>	
How often do you lend your e-mail login and password to your friends or relatives?	Never/ Rarely/ Sometimes/ Often/ Always
How often do you lend your private debit or credit card(s) and associated PIN(s) to anyone?	
How often do you reveal your PIN (by non-concealment or saying it out loud) when you pay by card?	
How often do you reveal the password of your e-mail account to others?	
<i>Cognitive scale (CI): Importance</i>	
How would you rate the importance of maintaining protection of your computer equipment, laptop, smartphone (e.g. periodic updates of antispyware and antivirus software)?	Not very important/ Rather important/ Not sure/ Important/ Very important/
How would you rate the importance of logging off from different information systems when you finish your work (e.g. from social network, e-mail system, your laptop, etc.)?	
How would you rate the importance of checking removable media for viruses before usage?	
How would you rate the importance of periodical changing of your passwords with new ones, at least for frequently used services?	
<i>Cognitive scale (CR): Risk</i>	
How would you rate the risk of someone stealing your identity on the Internet (e-banking, Facebook, e-mail)?	Not very risky/ Somewhat risky/ Not sure/ Risky/ Very risky/
How would you rate the risk of someone stealing the money from your bank account when using mobile or Internet banking?	
How would you rate the risk of someone hacking your personal computer, laptop or smart phone?	
How would you rate the risk of losing your private photos and videos?	
How would you rate the risk of someone misusing your debit or credit card?	

Each of the five questions has answers scored up to 4 points (answer Not very risky gives zero, and answer Very risky gives 4 points) and the arithmetic mean of those five answers gives the total score of the scale, where a higher score means also a higher level of awareness. After submitting their answers, participants get a short explanation with some recommendations for more secure behavior on the Internet.

There were in total 960 examinees included in the study, with median age of 22 years (with interquartile range from 20 to 28, and total range from 18 to 72 years of age). More than two-thirds (71.2%) were female examinees and most were examined during year 2000 (42.6%). Most examinees were from Croatia (614, 64.0%) and Slovenia (192, 20.0%), then from Hungary (18, 1.9%), Czech Republic (15, 1.6%), Germany (12, 1.3%), Portugal (10, 1.0%) and USA (8, 0.8%). In total, the examinees were from 41 different countries around the globe.

Model fit has been analyzed during validation of different versions of the questionnaire, and it did turn out to be good, including the previous version in German [17]. As a result, in this analysis, answers to all translated versions were included [19, 20], in which context the English language version was considered the original version [21]. Moreover, participant groups overlapped because many examinees filled in the English version even though they had a version in their own language available.

Standard statistical methods were used for data analysis, specifically nonparametric Mann-Whitney U test for two and Kruskal-Wallis H test for three or more independent samples of numerical data. The significance level was set at 0.05 and all P values were two-tailed, while the snowball sampling method was used for data collection [16]. The online version that was used in this research is available on the following url: <http://security.o-i.hr/>.

3 Theoretical Background and History of Development

Earlier studies on the subject of ICT system users' awareness, online behavior and knowledge regarding information security issues mostly examined password quality and frequency of revealing passwords among users. Results showed that around 50% of the examined users reveal their passwords in some way [10, 11] while the proportion among children and adolescents is much higher, reaching approximately 77% [22]. With some simpler technical methods (e.g. dictionary attack) it is possible to break around 25% of used passwords [23-25] and more than 50% of the ICT system users prefer to use the same password for different systems [26]. On the other hand, 78% of ICT system users assess their information security skills as good [27].

When determining ICT system users' significant influence on the information security as an interdisciplinary problem, scientists integrated knowledge from behavioral and computer science fields. Maybe most important solutions existing nowadays for measuring that significant influence are statistically/scientifically validated questionnaires as measurement instruments. A validated questionnaire is a much more serious measurement instrument than a simple list of questions in a poll, because validity implies the degree to which a questionnaire actually measures what it is supposed to measure. A valid questionnaire, as any measurement instrument, involves a specific development procedure. The first step is establishing content validity, i.e. choosing items adequate for the problem intended for measurement. In other words, content validity reflects the experts' view of whether the questionnaire contains items which cover all aspects of the construct being measured. The second step is conducting a pilot study using a sample questionnaire, which is at least 5 to 8 times bigger than the initial questionnaire. The third step is a test of construct validity, done by using principal component analysis on underlying components that are being measured by questionnaire items. This way it is possible to identify items that have low factor loadings and should be removed. In step four, the goal is to analyze reliability using the Cronbach's Alpha test for internal consistency and remove items that violate overall reliability. In step five, a new study is conducted in order to check again for construct validity and reliability, confirm overall construct validity of the new questionnaire and additionally check for external validity. External validity shows the extent to which the results of a study can be generalized to and across other situations and people, i.e. age and gender differences [15, 28]. In order to test the BCISQ questionnaire internationally, the snowball sampling method for recruiting participants has been used. Existing subjects from different countries, authors' acquaintances and colleagues, provided referrals to recruit samples required for this research study [16].

To the best of the authors' knowledge, there are four validated questionnaires that have been developed for this purpose so far, even though there are many empirical studies trying to examine and measure ICT users' online behavior and their information security awareness and knowledge.

The Users' Information Security Awareness Questionnaire (UISAQ) was first developed and validated in the Croatian language and later translated into English language [10]. Validation was published in year 2015, with the final version consisting of 33 items grouped into two scales: Scale of Computer users' potentially risky behavior ($k=17$) and Scale of Information security knowledge ($k=16$). Both of the two scales are divided into three subscales, which makes six scales in total. The questionnaire has demographic questions and two control questions [9].

A year later, scientists from the USA developed and validated a questionnaire titled Security Behavior Intentions Scale (SeBIS) [11]. The SeBIS comprises 24

items and measures the computer security attitudes of end-users. It has four scales measuring awareness and relevant computer security behaviors.

The same year, scientists from Turkey developed a more elaborate questionnaire called the Four Measurements Scales (FMS). It has a total of 89 items measuring risky and conservative behavior, exposure to violation and risk perception of ICT system's users [12].

The Human Aspects of Information Security (HAIS Q) is the most recently validated questionnaire [13]. It was developed by Australian scientists and the final version comprises a total of 63 items. Those questions are grouped into seven large domains (password management, email use, Internet use, social media use, use of mobile devices, information management and reporting about incidents). Each of the seven domains is divided into 3 smaller domains (knowledge, attitudes and behavior), which in the end means that the questionnaire consists of 21 subscales.

Other related work is a study presenting development of an instrument that measures the security and privacy habits/practices of end users, specifically students. It seems that it is still in the development phase [29].

Some drawbacks of the existing questionnaires are as follows: the UISAQ has not been validated in the English language, all questionnaires have too many items/questions (except the SeBIS), they are based only on the self-assessment process and do not measure the level of actual behavior. All of those questionnaires were used only in their countries of origin, but not abroad or internationally.

All those drawbacks are confronted with the proposed new international questionnaire presented in this paper. The BCISQ has been developed and validated primarily in the English language, it has only 17 items/questions grouped into four scales, measures actual behavior with simulation and has very good statistical parameters [21]. In the development phases, the BCISQ questionnaire even had a version in German, while now it has validated versions in Croatian and Slovenian and an additional version in the Hungarian language. The BCISQ questionnaire was used abroad with intention to be used globally [17, 18].

Some general conclusions gathered so far measuring ICT users' knowledge, awareness and risk of their behavior are:

- Children with the average age of less than 8 are starting to use Internet in EU countries. They are the most vulnerable group of the Internet users [30, 31]
- Female users are slightly more cautious on the Internet [22, 32]
- In developing countries with both a large sample size and large age span, gender differences were not significant [9, 22, 33]

- Older and less experienced users are also more cautious and more careful when using Internet [31, 34]
- Electrical engineers (generally more technically experienced users) are unexpectedly less cautious and their behavior is riskier [22, 31, 35].
- Some users tend to note that privacy protection is important, but are behaving risky. This is also known as the privacy paradox [36-38].
- Over the last decade, users have generally shown higher knowledge (i.e. higher level of risk awareness), but behaved in a way that was riskier [35]
- We did not get any correlation between real and self-assessed risk behavior among ICT users [21].

Those conclusions listed above have been confirmed, but also expanded, by the results gained in this study. Results that are gained in this study are explained and discussed in the next section.

4 Questionnaire's Reliability and Current Results by Countries and Total Results

Perhaps the most interesting and most intriguing result was connected with revealing one's password. Almost half of the participants (439, 45.7%) seemed to have provided their real password. Although this field, which represented a trick question about the supposed examination of quality of the password could have been left unfilled, some participants provided passwords that were clearly fake, or wrote "I will not" or "I do not give my password," and those passwords were left out. But, if only half were the real passwords, they are still too many. From experience, it has been observed that in workshops or presentations dealing with this topic, students, but also colleagues, give away their passwords out of a sense of collegiality, trust or authority. Interestingly, in workshops where they received post-its and were asked to reveal their password, purportedly to check their strength, more than 70% of the participants revealed it. Also, during conferences, when the online version of the questionnaire was used and participants answered by mobile phones, again almost 70% provided their password [39]. As already indicated, these proportions are very high. However, it is not possible to verify with great certainty whether the answers are correct, because it is possible that the password provided could be false, outdated or changed immediately after the filling in of the questionnaire because the participants got some cautionary information and additional advice at the end of the questionnaire.

Also, this question regarding the password affects the reliability of the scale in the last validated version, the one in Slovenian. When this question is excluded, Cronbach's alpha improves significantly ($\alpha = 0.706$; Table 3). Consequently,

owing to the inability to verify the accuracy of the answers to this question, the plan is to substitute it by a new question in the next version of the questionnaire.

A part of this study applied in Slovenia has shown that users from that country exhibit somewhat worse behavior compared to other users (Kruskal-Wallis H test, $p = 0.002$), but they also give themselves worse scores in the self-assessment regarding the risk of their behavior (Kruskal-Wallis H test, $p < 0.001$). Nevertheless, the overall results of this study give no correlation between real and self-assessed risk behavior among ICT users (Table 6). There was no correlation between real and self-assessed risk behavior among ICT users in the previous study either [21]. This group of users (the Slovenian sample) is somewhat unusual, as they also reduce the Cronbach's alpha for those two scales, but the authors have not managed to identify the reason.

Overall mean values of scoring answers are not (yet) reference values for the BCISQ questionnaire, but in the future, once an upgraded version is made, with the unstable question regarding password eliminated, the authors plan to define normed reference values, as it was done for the earlier UISAQ questionnaire. However, those mean values can be used for comparison between some specific group of users and the sample of users analyzed in this study (Table 3).

It seems that ICT users using Unix OS, which represents mostly Android on mobile phones, give themselves better scores regarding risk in their behavior (Kruskal-Wallis H test, $p = 0.003$). However, they are not better in real behavior, so this may mean that they have an unjustified higher opinion of their online behavior (Table 3). Better self-assessment of risk in ICT users' online behavior does not have any correlation with any of the other three scales (Table 6).

When examining scores over the four-year period it is possible to conclude that ICT users were significantly more careful (Kruskal-Wallis H test, $p < 0.001$) during the period of the Covid-19 pandemic. Examinees self-assessed their online behavior better and better identified risky behavior presented in some risky online situations (Table 3). However, results collected during the first six months of 2022 are showing that there is no promising trend, especially not in ICT users' real online behavior (Table 3). One previous study did show increased knowledge and security awareness among middle aged ICT users, but also a tendency toward risky online behavior that increases with age [35].

Female users are significantly more cautious (Mann-Whitney U test, $p < 0.007$) than male ICT users (Table 4). This result is in line with previous studies [22, 31] However, in developing countries with both a large sample size and large age span, gender differences were not significant [33].

Table 3
Comparisons by versions and years

	BS‡	p*	BA‡	p*	CI	p*	CR	p*
<i>Cronbach's Alpha per version for each scale</i>								
English /n=159	0.615		0.725		0.791		0.901	
Croatian /n=594	0.685		0.640		0.729		0.925	
Slovenian /n=173	0.582†		0.396		0.727		0.880	
Hungarian /n=34	0.717		0.677		0.836		0.929	
Overall	0.654		0.620		0.750		0.917	
<i>Mean (SD) values of scoring answers per version for each scale</i>								
English /n=159	0.90 (1.11)	0.002	0.27 (0.42)	<0.001	2.81 (0.93)	0.17	2.16 (1.21)	<0.001
Croatian /n=594	1.12 (1.23)		0.22 (0.40)		2.99 (0.74)		2.81 (1.11)	
Slovenian /n=173	1.36 (1.23)		0.31 (0.37)		2.94 (0.77)		2.61 (0.99)	
Hngarian /n=34	0.88 (1.23)		0.26 (0.40)		2.71 (0.97)		2.64 (1.18)	
Overall /n=960	1.12 (1.22)		0.25 (0.40)		2.94 (0.79)		2.66 (1.13)	
<i>Mean (SD) values of scoring answers regarding used OS when accessing questionnaire</i>								
Unix /n=482	1.17 (1.25)	0.08	0.22 (0.37)	0.003	2.99 (0.76)	0.07	2.72 (1.08)	0.44
Windows /n=317	0.98 (1.14)		0.27 (0.46)		2.94 (0.78)		2.62 (1.14)	
Macintosh /n=161	1.21 (1.25)		0.29 (0.37)		2.81 (0.86)		2.57 (1.25)	
<i>Differences in mean (SD) values of scoring answers regarding years</i>								
2019 /n=202	1.18 (1.31)	0.54	0.27 (0.40)	<0.001	2.89 (0.85)	0.39	2.35 (1.11)	<0.001
2020 /n=409	1.03 (1.17)		0.22 (0.42)		3.00 (0.74)		2.80 (1.13)	
2021 /n=222	1.18 (1.21)		0.24 (0.39)		2.94 (0.79)		2.76 (1.13)	
2022 /n=127	1.18 (1.25)		0.32 (0.37)		2.86 (0.83)		2.54 (1.06)	

*Kruskal-Wallis H test; †after removing the question regarding the password, Cronbach's Alpha becomes much better ($\alpha=0.71$); ‡lower mean values represent less risky behavior

Used abbreviations are BS: Behavior scale of Simulation, BA: Behavior scale of Self-assessment, CI: Cognitive scale of Importance, CR: Cognitive scale of Risk

Table 4
Comparison by demographic elements

	BS _‡	p*	BA _‡	p*	CI	p*	CR	p*
<i>Differences in mean (SD) values of scoring answers regarding gender</i>								
Male /n=276	1.01 (1.15)	0.11	0.23 (0.37)	0.69	2.84 (0.81)	0.007	2.35 (1.19)	<0.001
Female /n=684	1.16 (1.24)		0.25 (0.41)		2.98 (0.78)		2.79 (1.08)	
<i>Differences in mean (SD) values of scoring answers regarding education</i>								
Secondary school only /n=179	1.29 (1.27)	0.07	0.28 (0.47)	0.12	2.88 (0.79)	0.003	2.87 (1.07)	<0.001
High school /n=426	1.00 (1.12)		0.22 (0.39)		2.91 (0.77)		2.74 (1.16)	
Bachelor's degree (BSc) /n=136	1.23 (1.22)		0.27 (0.41)		3.08 (0.80)		2.52 (1.12)	
Master's degree (MSc) /n=164	1.16 (1.37)		0.25 (0.35)		3.07 (0.70)		2.46 (1.11)	
Postgraduate (PhD) /n=55	1.09 (1.25)		0.28 (0.35)		2.63 (1.02)		2.36 (0.98)	
<i>Differences in mean (SD) values of scoring answers regarding participants' profile</i>								
Students /n=670	1.10 (1.18)	0.84	0.24 (0.40)	0.11	2.95 (0.74)	0.51	2.75 (1.13)	<0.001
Others /n=290	1.14 (1.30)		0.27 (0.40)		2.92 (0.89)		2.46 (1.10)	
<i>Differences in mean (SD) values of scoring answers regarding area of expertise</i>								
Natural sciences /n=51	1.20 (1.22)	0.43	0.25 (0.43)	0.43	2.81 (0.87)	0.13	2.55 (1.13)	0.03
Technical /n=87	0.98 (1.16)		0.30 (0.41)		2.83 (0.86)		2.31 (1.17)	
Biomedicine and Health /n=407	1.14 (1.17)		0.22 (0.36)		2.98 (0.74)		2.75 (1.09)	
Biotechnical /n=7	0.57 (0.79)		0.14 (0.24)		3.18 (0.51)		2.86 (0.93)	
Social sciences /n=270	1.17 (1.28)		0.27 (0.43)		2.91 (0.77)		2.68 (1.14)	
Humanities /n=75	1.13 (1.36)		0.24 (0.41)		3.05 (0.78)		2.74 (1.18)	
Art /n=14	0.57 (0.76)		0.38 (0.56)		2.34 (1.20)		1.99 (1.21)	

Interdisciplinary /n=49	1.02 (1.25)		0.22 (0.38)		3.03 (0.90)		2.64 (1.15)	
----------------------------	----------------	--	----------------	--	----------------	--	----------------	--

*Mann-Whitney U test for two, and Kruskal-Wallis H test for more than two groups; ‡lower mean values represent less risky behavior

Used abbreviations are BS: Behavior scale of Simulation, BA: Behavior scale of Self-assessment, CI: Cognitive scale of Importance, CR: Cognitive scale of Risk

Regarding results there is a certain connection between education and awareness, but not between the level of education and risk involved in online behavior (Table 4). This result is in line with the results of a previous study which showed that more knowledgeable users behave more casually, with a higher level of risk when online. For example, electrical engineers, who are generally more technically experienced users, are unexpectedly less cautious and behave in a way that is riskier [22, 31, 35]. Generally, some users tend to note that privacy protection is important, but are behaving riskily, in line with the so-called privacy paradox phenomenon [36-38].

It also seems that students are more aware (Mann-Whitney U test, $p < 0.001$) of online risks (Table 4), but there is also low but significant negative correlation of awareness with age of the ICT user (Table 6), implying the reason for this result. Also, in some previous studies, older and less experienced users were also more cautious and more careful when online [31, 34].

Generally, ICT system users with higher level of knowledge about information security and privacy are significantly better in both real and self-assessed online behavior and have significantly higher awareness regarding the importance of behaving carefully while online (Kruskal-Wallis H test, $p < 0.007$). However, users that had some kind of training regarding security and privacy on the Internet are significantly better (Mann-Whitney U test, $p < 0.001$) only in terms of the awareness regarding the importance to behave carefully while online (Table 5). It seems that existing training programs only effect awareness of importance and are not enough to correct user behavior. Existing training programs require evaluation of their effectiveness and adaptation in order to transform new knowledge into practical behavior [41, 42]. Also, personalized user training programs can be one possible solution [43, 44]. Training programs are only part of the education process which should start as early as possible in a person's life [45], because children of no more than eight years of age are starting to use the Internet in EU countries. And the young are the most vulnerable group of ICT users [30].

Users that have excellent general technical knowledge about computers and Internet score their own behavior as better compared to others, to a statistically significant extent (Kruskal-Wallis H test, $p < 0.001$) (Table 5). They also have somewhat better scores regarding real behavior, which is in line with another empirical study on self-assessing information security skills [27].

Again, a more experienced ICT user is more nonchalant in the assessment of risky online situations, probably thinking that such a situation cannot happen to them (Table 5).

Table 5
Questions regarding security, privacy and f time spent online

	BS‡	p*	BA‡	p*	CI	p*	CR	p*
<i>Differences in mean (SD) values of scoring answers regarding knowledge about information security and privacy issues</i>								
Poor 154	1.33 (1.30)	0.004	0.33 (0.45)	0.003	2.73 (0.85)	<0.001	2.63 (1.09)	0.48
Good 667	1.12 (1.21)		0.24 (0.39)		2.94 (0.77)		2.70 (1.09)	
Excellent 139	0.88 (1.12)		0.19 (0.37)		3.19 (0.77)		2.52 (1.32)	
<i>Differences in mean (SD) values of scoring answers regarding general technical knowledge about computers and the Internet</i>								
Poor	1.19 (1.26)	0.52	0.36 (0.49)	<0.001	2.87 (0.89)	0.20	2.72 (1.09)	0.23
Good	1.12 (1.22)		0.24 (0.39)		2.94 (0.76)		2.69 (1.11)	
Excellent	1.04 (1.18)		0.19 (0.31)		3.01 (0.82)		2.50 (1.23)	
<i>Differences in mean (SD) values of scoring answers regarding some training in security</i>								
No 587	1.13 (1.19)	0.26	0.25 (0.40)	0.87	2.87 (0.80)	<0.001	2.67 (1.12)	0.99
Yes 373	1.10 (1.27)		0.24 (0.40)		3.05 (0.76)		2.65 (1.14)	
<i>Differences in mean (SD) values of scoring answers regarding period of using Internet</i>								
A couple of years /n=120	1.26 (1.29)	0.20	0.31 (0.55)	0.79	2.91 (0.88)	0.93	2.94 (1.01)	<0.001
Half of my life /n=655	1.13 (1.23)		0.24 (0.39)		2.95 (0.77)		2.68 (1.11)	
As long as I remember /n=185	0.97 (1.12)		0.21 (0.30)		2.92 (0.82)		2.41 (1.22)	
<i>Differences in mean (SD) values of scoring answers regarding frequency of Internet usage</i>								
Less than 1 hour /n=29	1.24 (1.41)	0.48	0.34 (0.55)	0.32	2.94 (0.92)	0.96	2.66 (1.19)	0.44
1 to 3 hours daily /n=243	1.18 (1.25)		0.25 (0.40)		2.97 (0.76)		2.72 (1.06)	
4 to 5 hours daily /n=370	1.15 (1.23)		0.26 (0.39)		2.94 (0.78)		2.70 (1.13)	
Between 6 and 10 /n=253	1.04 (1.18)		0.23 (0.42)		2.95 (0.78)		2.60 (1.18)	
More than	0.94		0.19		2.84		2.48	

10 hours /n=65	(1.10)		(0.33)		(0.92)		(1.14)	
-------------------	--------	--	--------	--	--------	--	--------	--

*Mann-Whitney U test for two, and Kruskal-Wallis H test for more than two groups; ‡ lower mean values represent less risky behavior

Used abbreviations are BS: Behavior scale of Simulation, BA: Behavior scale of Self-assessment, CI: Cognitive scale of Importance, CR: Cognitive scale of Risk

As already discussed earlier in this chapter, the main result of correlation analysis between each scale is that there is no correlation ($\rho = 0.036$) between real and self-assessed risk involved in online behavior (between BS and BA, Table 6), as users think they behave more securely than they do (e.g. means of overall scoring values in Table 3). Even though there is statistically significant correlation for some pairs of the examined variables, the coefficient of correlation is very low and close to value zero (one is the highest correlation coefficient). There is low positive correlation ($\rho = 0.244$) between the importance of online security and back up, including the rating of risky online situations (CI and CR scales), as these two scales basically measure two related elements of user' awareness (Table 6). There is also significant negative, but very small correlation ($\rho = -0.118$) between users' age and users' rating of risky situations, possibly connected to knowledge about security issues, as older users have somewhat less experience in these situations (Table 6).

Table 6
Correlations between age and individual scale

Correlation between variables		coefficient of correlation: rho	95% Confidence interval of rho	p*
Age	BS‡	-0.013	-0.076 to 0.050	0.68
	BA‡	0.044	-0.020 to 0.107	0.18
	CI	0.070	0.006 to 0.132	0.03
	CR	-0.118	-0.180 to -0.055	<0.001
BS‡	BA‡	0.036	-0.028 to 0.099	0.27
	CI	-0.018	-0.081 to 0.046	0.59
	CR	0.086	0.023 to 0.148	0.008
BA‡	CI	-0.135	-0.197 to -0.073	<0.001
	CR	-0.084	-0.146 to -0.021	0.009
CI	CR	0.244	0.184 to 0.303	<0.001

*Spearman's correlation test; ‡ lower mean values represent less risky behavior

Used abbreviations are BS: Behavior scale of Simulation, BA: Behavior scale of Self-assessment, CI: Cognitive scale of Importance, CR: Cognitive scale of Risk

Conclusions

Results presented here show that previously validated BCISQ is a good measurement instrument and can be used worldwide to examine any particular group of users or to make comparisons among different groups in order to test differences between, for example, countries and cultures or to analyze employees

of a company or some government institution [21]. Previous research has shown how important it is to analyze ICT user behavior and their impact on overall security [6].

There have been several key conclusions so far. Specifically, there is no correlation between real and self-assessed behavior [21]. There is also significant, but surprisingly negative correlation between the level of knowledge and safe behavior [31, 35]. Moreover, risky behavior in real life is mirrored in the digital world, with women, for example, behaving more cautiously compared to men, both in digital and real world [22, 32]. Also, a higher level of knowledge and awareness does not imply less risky online behavior, and even though it seems that awareness has been rising over the years, riskiness of online behavior has not been improved [35]. More than two thirds of users will reveal their password, mostly under the influence of friendship or authority, and at the same time a similar percentage assess their information security skills as good.

Therefore, future studies should answer the question of how to educate the users, how to make them more cautious and how to increase their awareness of these highly important issues [36, 37]. Restrictions and controls over ICT system users should not be among the solutions for this major problem, on the other hand, education alone is clearly not enough. The scientific community, in cooperation with professionals from the real sector, the practitioners, should find models that could lead to some new solutions that will succeed in influencing risky user behavior by raising their awareness of this problem [39, 40].

Changes in the field of information security, in particular protection of privacy, are happening constantly and daily (“Change is the only constant in life”). Because of that, solutions regarding security awareness need to be adjusted frequently through time in order to improve usability and sustainability [41]. In this sense, by the time the process of validation of the questionnaire is completed, the final version becomes outdated very soon, requiring corrections.

The authors' main goal was to develop a global and short questionnaire that will measure both real and self-assessed behavior and the level of knowledge and awareness among all kinds of ICT users. But, much more challenging is to develop a model or a platform that will be of help to ICT users in terms of teaching them about online threats, to raise their awareness, and to inform about risky behavior in real-time, but not to restrict the users' use of Internet services.

One of the limitations of our study is that proposed BCISQ questionnaire focuses on the general worldwide population, but does not include specific ICT users. Also, we had majority of examinees from Croatia and only several examinees from some of the 41 included country. In that way, although the sample size is relatively large ($n = 960$), it should be significantly larger in the future studies.

So regarding pointed limitations, potential future work could involve the use of the proposed BCISQ in different countries in order to examine differences

between cultures. Furthermore, some more detailed comparison between existing and new questionnaires could result in a new, better and more universal international questionnaire. Additionally, focusing on specific groups of users would be a great benefit to development of new versions of this questionnaire. As the ICT field is rapidly growing and evolving, encompassing the rapid development of new technologies and applications, new research will require the inclusion of additional items in the questionnaire to cover the entire scope of applications. Certainly some self-educational solutions should be developed based on the mentioned questionnaires, like the one developed based on the UISAQ [46]. All future scientific efforts and educational attempts should focus on increasing information security awareness among ICT system users in order to reduce risky online activities.

Acknowledgement

This research did not receive any specific grant from funding agencies in the public, commercial, or not-for-profit sectors.

References

- [1] R Diesch, M Pfaff, H Kremer. Prerequisite to Measure Information Security - A State of the Art Literature Review. In: Proceedings of the 4th International Conference on Information Systems Security and Privacy. SCITEPRESS, 2018
- [2] R von Solms, J van Niekerk. From information security to cyber security. *Comput Secur*, 38:97-102, 2013
- [3] MA Sasse, S Brostoff, D Weirich. Transforming the “Weakest Link” - a Human/Computer Interaction Approach to Usable and Effective Security. *BT Technol J*, 19(3):122-131, 2001
- [4] SJ Lukasik. Protecting users of the cyber commons. *Commun ACM*, 54(9):54-61, 2011
- [5] K Solic, K Nenadic, D Galic. Empirical Study on the Correlation between User Awareness and Information Security. *International Journal of Electrical and Computer Engineering*, 3(2):47-51, 2012
- [6] RE Crossler, et. al. Future directions for behavioral information security research. *Comput Secur*, 2013;32:90-101. 2013
- [7] K Solic, K Grgic. Usage of Unsecured Free Web-based E-mail Services among Biomedical Researchers. In: Proceedings of the 31st International Conference on Information Technology Interfaces (ITI). Cavtat/Dubrovnik, Croatia: IEEE; 2009
- [8] K Solic, V Ilakovac. Security Perception of a Portable PC User (The Difference Between Medical Doctors and Engineers): A Pilot Study. *Med Glas*, 6(2):261-264, 2009

- [9] T Velki, K Solic, K Nenadic. Development and Validation of Users' Information Security Awareness Questionnaire (UISAQ) *Psihologijske teme*, 24(3):401-424, 2015
- [10] T Velki, K Solic, H Ocevcic. Development of users' information security awareness questionnaire (UISAQ) - Ongoing work. In: *Proceedings of the 37th International Convention on Information and Communication Technology, Electronics and Microelectronics (MIPRO) Opatija, Croatia: IEEE; 2014*
- [11] S Egelman, M Harbach, E Peer. Behavior ever follows intention?: A validation of the security behavior intentions scale (SeBIS) In: *Proceedings of the 2016 CHI Conference on Human Factors in Computing Systems. New York, NY, USA: ACM; 2016*
- [12] G Ögütçü, ÖM Testik, O Chouseinoglou. Analysis of personal information security behavior and awareness. *Comput Secur*, 56:83-93, 2016
- [13] K Parsons, D Calic, M Pattinson, M Butavicius, A McCormac, T Zwaans. The Human Aspects of Information Security Questionnaire (HAIS-Q): Two further validation studies. *Comput Secur*, 66:40-51, 2017
- [14] K Parsons, A McCormac, M Butavicius, M Pattinson, C Jerram. Determining employee awareness using the Human Aspects of Information Security Questionnaire (HAIS-Q) *Comput Secur*, 42:165-176, 2014
- [15] MJG Yébenes Prous, FR Salvanés, LC Ortells. Validation of questionnaires. *Reumatol Clín (Engl Ed)*, 5(4):171-177, 2009
- [16] A Field. *Discovering statistics using IBM SPSS statistics*. 4th ed. London, England: SAGE Publications; 2013
- [17] T Velki, A Mayer, J Norget. Development of a new international behavioral-cognitive internet security questionnaire: Preliminary results from Croatian and German samples. In: *Proceedings of the 42nd International Convention on Information and Communication Technology, Electronics and Microelectronics (MIPRO) Opatija, Croatia: IEEE; 2019*
- [18] K Solic, T Velki, P Pucer, B Zvanut. Translation and validation of the BCISQ onto Slovenian language - preliminary results. In: *Proceedings of the 14th Croatian Society for Medical Informatics Symposium (HDMI) Zagreb, Croatia; 2019*
- [19] T Velki, K Solic. Development of Social Engineering Research Tool on College Student Population: Behavioural Cognitive Internet Security Questionnaire (BCISQ) *Polic. sigur*, 29(4/2020):341-355, 2020
- [20] T Velki, K Solic, B Zvanu. Cross-cultural validation and psychometric testing of the Slovenian version of the Behavioral-Cognitive Internet Security Questionnaire (BCISQ) *Elektrotehniški Vestnik*, 89(3):103-108, 2022

- [21] T Velki, K Solic. Development and validation of a new measurement instrument: The Behavioral-Cognitive Internet Security Questionnaire (BCISQ). *Int j electr comput eng syst*, 10(1):19-24, 2019
- [22] T Velki, K Solic, V Gorjanac, K Nenadic. Empirical study on the risky behavior and security awareness among secondary school pupils - validation and preliminary results. In: *Proceedings of the 40th International Convention on Information and Communication Technology, Electronics and Microelectronics (MIPRO)*. Opatija, Croatia: IEEE; 2017
- [23] AG Voyiatzis, CA Fidas, DN Serpanos, NM Avouris. An empirical study on the web password strength in Greece. In: *Proceedings of the 15th Panhellenic Conference on Informatics*. USA: IEEE; 2011
- [24] M Dell' Amico, P Michiardi, Y Roudier. Password strength: An empirical analysis. In: *Proceedings of the IEEE INFOCOM*. San Diego, California, USA: IEEE; 2010
- [25] PG Kelley, et al. Guess again (and again and again): Measuring password strength by simulating password-cracking algorithms. In: *Proceedings of the IEEE Symposium on Security and Privacy*. San Francisco, California, USA: IEEE, 2012
- [26] K Solic, H Ocevcic, D Blazevic. Survey on password quality and confidentiality. *Automatika*, 56(1):69-75, 2015
- [27] M Kyytsönen, J Ikonen, A-M Aalto, T Vehko. The self-assessed information security skills of the Finnish population: A regression analysis. *Comput Secur*, 118(102732), 2022
- [28] H Taherdoost. Validity and reliability of the research instrument; How to test the validation of a questionnaire/survey in a research. *SSRN Electron J*, 5(3):28-36, 2016
- [29] NF Khan, N Ikram. Development of students' security and privacy habits scale. In: *Lecture Notes in Networks and Systems*. Cham: Springer International Publishing, 951-963, 2020
- [30] S Livingstone, L Haddon, A Görzig, K Ólafsson. Risks and safety on the internet: the perspective of European children: full findings and policy implications from the EU Kids Online survey of 9-16 year olds and their parents in 25 countries. *EU Kids Online Network*, Lse.ac.uk. 2012
- [31] K Solic, T Velki, T Galba. Empirical study on ICT system's users' risky behavior and security awareness. In: *Proceedings of the 38th International Convention on Information and Communication Technology, Electronics and Microelectronics (MIPRO)* Opatija, Croatia: IEEE; 2015
- [32] M Sharples, R Graber, C Harrison, K Logan. E-safety and Web 2.0 for children aged 11-16. *J Comput Assist Learn*, 25(1):70-84, 2009

- [33] EJ Helsper. Gendered Internet use across generations and life stages. *Communic Res*, 37(3):352-374, 2010
- [34] K Solic, M Plesa, T Velki, K Nenadic. Awareness About Information Security and Privacy Among Healthcare Employees. *SEEMEDJ*, 3(1):21-28, 2019
- [35] T Velki, K Romstein. User risky behavior and security awareness through lifespan. *Int j electr comput eng syst*, 9(2):53-63, 2019
- [36] N Gerber, P Gerber, M Volkamer. Explaining the privacy paradox: A systematic review of literature investigating privacy attitude and behavior. *Comput Secur*, 77:226-261, 2018
- [37] S Kokolakis. Privacy attitudes and privacy behaviour: A review of current research on the privacy paradox phenomenon. *Comput Secur*, 64:122-134, 2017
- [38] DP Snyman, H Kruger, WD Kearney. I shall, we shall, and all others will: paradoxical information security behaviour. *Inf Comput Secur*, 26(3):290-305, 2018
- [39] T Velki. Psychologists as information-communication system users: Is this bridge between information-communication and behavioral science enough to prevent risky online behaviors? In: *Proceedings of the 45th Jubilee International Convention on Information, Communication and Electronic Technology (MIPRO) Opatija, Croatia: IEEE; 2022*
- [40] T Velki, K Solic. *Handbook for Information Security and Privacy*. Faculty of Education, Josip Juraj Strossmayer University of Osijek, 2018
- [41] S Chaudhary, V Gkioulos, S Katsikas, Developing metrics to assess the effectiveness of cybersecurity awareness program, *Journal of Cybersecurity*, 8(1):1-19, 2022
- [42] W He, Z Zhang. Enterprise cybersecurity training and awareness programs: Recommendations for success. *J Organ Comput*, 29(4):249-257, 2019
- [43] D Fujs, S Vrhovec, D Vavpotic. Towards personalized user training for secure use of information Systems. *int Arab j inf technol*, 19(3):307-313, 2022
- [44] H Aldawood, G Skinner. Reviewing cyber security social engineering training and awareness programs-pitfalls and ongoing issues. *Future internet*, 11(3):73, 2019
- [45] AA Al Shamsi. Effectiveness of Cyber Security Awareness Program for young children: A Case Study in UAE. *International Journal of Information Technology and Language Studies*, 3(2):8-29, 2019
- [46] T Galba, K Solic, I Lukic. An information security and privacy self-assessment (ISPSA) tool for internet users. *Acta Polytechnica Hungarica*, 12(7):149-162, 2015

A Complex Comparatrive Study of Two Dissimilar Engine Valve Constructions, for the In-Cylinder Flow Behaviour of a High Speed, IC Engine

László Kovács, Betti Bolló, Szilárd Szabó

University of Miskolc, Institute of Energy Engineering and Chemical Machinery,
Miskolc-Egyetemváros, 3515 Miskolc, Hungary, aramkola@uni-miskolc.hu,
betti.bollo@uni-miskolc.hu, szilard.szabo@uni-miskolc.hu

Abstract: In our research we investigated the possibility of offering a viable alternative for internal combustion engines' poppet valves. After examining in-cylinder flow characterization methods, we derived a computer model of the base concept and a special swinging valve arrangement. The flow characterization of both arrangements has been completed using numerical fluid dynamics software. To minimize numerical errors different mesh scenarios were investigated and evaluated. From our research activity a clear picture has been drawn on the qualities of the proposed system. The swinging valve arrangement improves the efficiency of the gas exchange process. Also, the flow during the intake process is more structured and has less local vorticity. The results have also shown a very favourable charge movement pattern that is ideal for GDI engines. All of these findings produce an appropriate platform for a stratified charging, extra lean burning engine concept. The construction concept lends itself to be flawlessly integrated in a throttle-less engine control environment as well. With these qualities the new valve arrangement may be the ideal solution to produce fuel efficient, high specific output engines, for those transportation systems that will still need to rely on fossil fuels in the future.

Keywords: IC engine; swinging valve; poppet valve; flow test; 0D/1D engine simulation

1 Introduction

In the case of gasoline, diesel or gas-powered internal combustion engines currently in series production, almost without exception, a straight-line valve located in the cylinder head is used. In valve timing systems with alternating movement, it is a difficult task to reduce the energy required for its operation (reduction of mechanical losses), provide good gas exchange process and design a reliable, less service-demanding construction. The volumetric efficiency an engine can achieve with traditional poppet valves is limited. The valve heads block the

flow of gases and their choking effect decreases the efficiency of the gas exchange process. This present research concentrates on the examination of the possibilities of a novel design of a valve using swaying motion to better utilize the possibilities in engine downsizing, as shown in [1].

1.1 Introducing the Novel Valve Concept

In engines equipped with poppet valves, the incoming fresh mixture needs to get around the valve head which can be seen in Figure 1. This hinders flow capabilities of the intake port. Mass flow is reduced that in turn limits the power delivery in general. On the exhaust side, the situation is about the same. In this case, the spent gases face a flow condition that delays the emptying of the cylinder that results in greater pumping loss and fuel consumption.

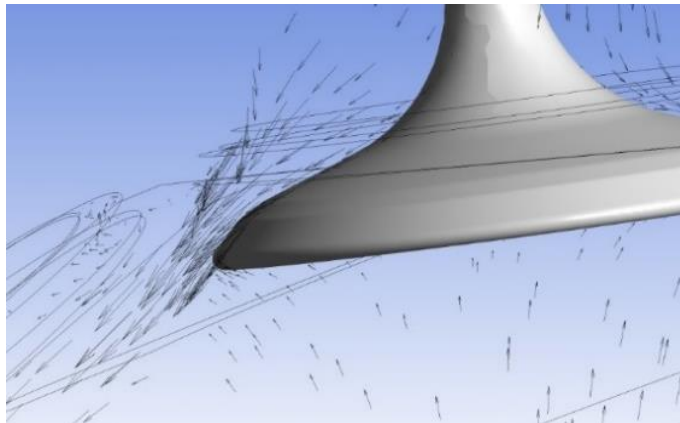


Figure 1

Flow vectors around the valve head

The devised solution uses a pivoting valve element for both the intake and exhaust ports to quickly open large cross-sections for the flowing gases, without making them to change direction. The familiar valves, cams, rockers, valve springs, etc. from the previously used control systems are eliminated. An important aspect of the construction is that the parts could be manufactured using known and widespread technology, so that the production problems and costs are as small as possible. The layout of the swinging valve system is shown in Figure 2, and the details of the valve system are discussed in [1] [3].

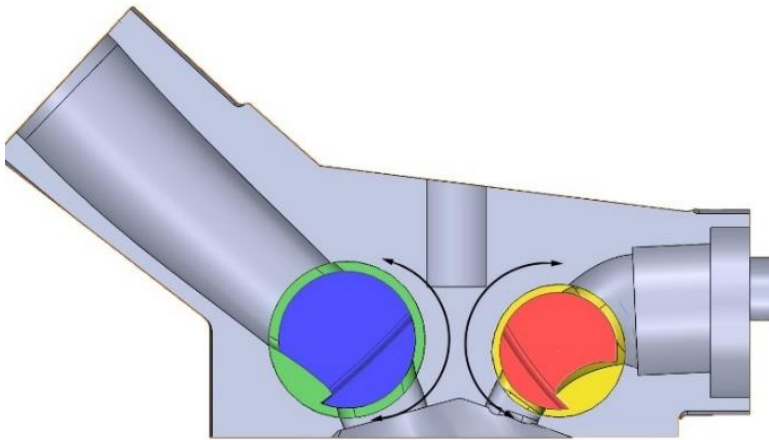


Figure 2
Swinging valve arrangement

2 Objectives of the Project

Thermodynamically the poppet valve engines must make a compromise between efficient combustion chamber shape and suitably sized valves with adequate flow capability. To reach a given performance level, the four-valve arrangement is the best compromise but the space required by the valves in the cylinder head reduces the squish area. Increasing squish area would otherwise improve combustion efficiency and fuel consumption but on the contrary, valve size or in worst case the number of valves should be decreased. With the new swinging valve design high compression ratio can be reached and the squish area can be maximized to increase the speed of combustion and decrease the danger of detonation. In comparison to poppet valve designs an engine equipped with the new valve system may have the following features:

- Reduced flow losses
- Reduced power requirement to operate valves and valve gear
- The value of the force to open the exhaust valve is independent of the combustion chamber pressure
- A more complete purging of combustion chamber
- Possibility to apply greater ports
- Improved volumetric efficiency
- Better power, ideally over a wider range of engine speeds
- Higher possible maximum engine rpm

- Greater squish area
- Piston face without valve pockets to improve combustion efficiency and reduce the formation of HC emission
- Higher possible compression ratio because of the absence of the hot exhaust valve heads
- Better burning characteristics and lower emissions due to improved combustion
- Higher tumble ratio due to the positioning and flow pattern of the valve
- Higher combustion speed due to increased squish and tumbling action
- Due to increased tumble, burn rates are improved therefore less pre-ignition is required
- Enhanced stratified combustion
- With electronic valve drive Miller and Atkinson cycles can be applied in different speed regimes of the engine
- Better power-to-weight ratio due to the improved volumetric efficiency and lighter valve system

3 Literature Review: Historical Background of Non-Conventional Engine Valves

As described in [4], the most important development from the early days of motor industry until the era just after WW II. Lot of detail information can be gathered from [5] and [6] as well. The common feature of all is that they rotate continuously at a speed directly proportional to the crankshaft rotation speed. These can be divided into four groups:

Mixed (radial/axial) flow rotary valves:

In these designs there is a single valve that contains both the intake and exhaust passages. The flow must have an approximately 90 degrees change of direction within the valve body. Most recent practical development was the Bishop Rotary Valve designed and tested to operate in a Formula 1 engine [7] [8].

Side ported valves:

There may be a single common valve for both the intake and exhaust flow control. The flow path is formed by the cutaways machined into the side of the valves. Constructors have been using this solution since the 19th Century and this kind of assembly even reached Formula 1 beside other car applications [8] [9].

Radial cross flow rotary valves:

The cutaway breaks through the valve body forming a symmetrical part. The flow of gases passes through the valve body. Due to the constant rotation, there are strong vortices at the opening and closing edges limiting its flow capability. Information on examples can be found in [10], though a working sample of this principle was created in Obuda University in 2002 by Z. Boruzs.

Rotating cylinder head type valves:

In these systems the cylinder head had one or two channels that lined up with their respective ports during its rotation. The timing of the rotation exactly matched the requirements of the four-stroke working principle. This concept was proved to be successful earlier in a torpedo engine and in a world speed record motorcycle. [5] [6].

4 Materials and Methods

4.1 Research Completed so far

In previous stages of our research a cylinder head fitted with the novel pivoting valves had been designed and manufactured to establish its flow parameters. The information gathered had been compared to the relevant data obtained from the same engine's original cylinder head that used poppet valves. The engine data used for the research can be found in Table 1.

Table 1
Parameters of the base engine

Configuration:	4-stroke, 4 valve, 90-degree V2,
Bore x Stroke:	81 x 62.6 mm
Swept volume:	0.645 litre
Maximum Power:	60.5 kW / 9000 rpm
Maximum Torque:	68.2 Nm/ 7500 rpm
Highest engine speed:	11000 rpm

The previously mentioned flow test had been carried out using a Superflow SF600 flow test bench. Swinging valves produced better flow rates: 14.5% improvement for the intake valve and 11.36% improvement for the exhaust valve over the poppet valves with the same flow cross sectional areas. Description of the flow test and the equipment used can be found in [11]. The results were then further processed in a 0D/1D engine modelling environment where both engines were recreated and the base engine had been validated against performance measurements obtained using a dynamometer (Figure 3).



Figure 3

Dynamometer test of the base engine

Results from the engine simulation exposed engine performance improvements beyond expectation. This is best illustrated by the performance curve shown in Figure 4 in [12].

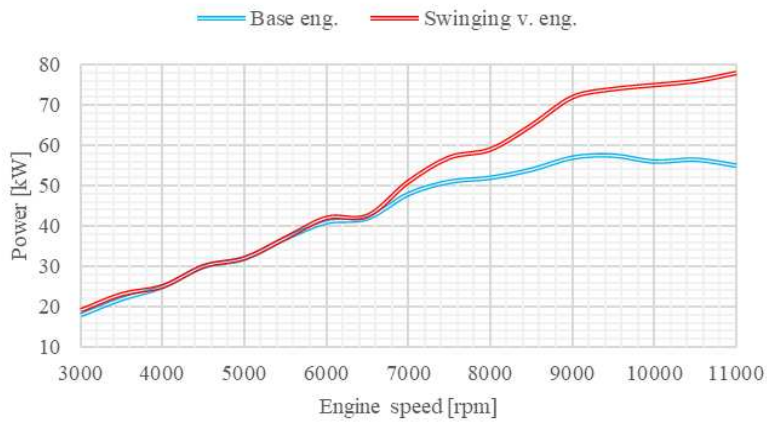


Figure 4

Comparison of simulated engine power obtained using pivoting valve system and the poppet valve base engine

4.2 Core Idea behind the Research: Stratified Charging and the Swinging Valve

Before combustion is started by the spark plug a suitable air-fuel mixture has to be produced in the combustion chamber. In the past carburetors served this purpose but with advancements in technology Direct Fuel Injection (DFI) has been developed. In this latter case the fuel injector is placed in the cylinder and injects fuel during the compression stroke where it evaporates. The specific position of the injector and the in-cylinder air movement prevents the formation of a homogenous cylinder charge and assists that most of the injected fuel reaches the spark gap by the end of compression stroke. By the time ignition takes place a cloud of easily ignitable fuel rich mixture surrounds the spark plug. The remaining combustion chamber volume consist much less, if any, fuel. The average fuel content across the combustion chamber is far from stoichiometric, resulting in lambda values in the range of 1.6-2. This improves fuel efficiency and decreases CO₂ emission. To facilitate the uneven distribution of fuel in the combustion chamber, the tumbling motion of the fresh mixture within the cylinder needs to be improved. Tumble is a rotational motion of the fresh charge around the axis that is perpendicular to the cylinder symmetry plane and normally parallel with the crank shaft (Figure 5). It is also enhanced by the inclination of the intake port. In poppet valve engines shallower port angles, produce greater tumble effect but sacrifice volumetric efficiency.

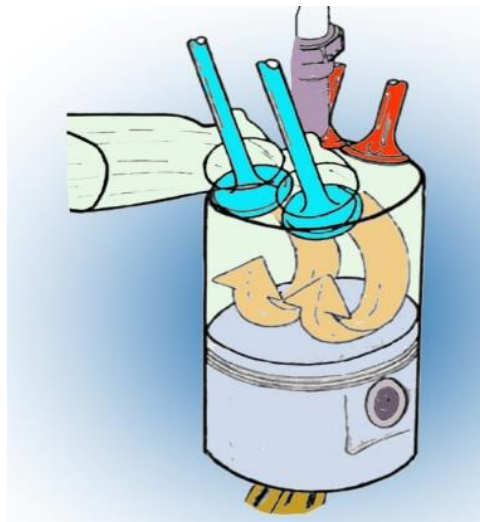


Figure 5

Formation of in-cylinder tumble vortex flow

The swaying valve, that our research is focused on addresses this problem since it directs the incoming intake flow in a path that enhances tumble while keeping volumetric efficiency high. So far, vortices required for tumble have been

generated by intake port flow deflectors. As is stated in [13] these devices constrain engine efficiency and add to structural complexity that in turn increases system failure possibility.

5 Numerical Simulation

Since the intake process has a substantial effect on the complete working cycle of the engine, we made a comparative test regarding the original and the newly devised valve systems. To follow the process with dedicated measuring equipment would have required an apparatus that is very difficult to obtain and is beyond our technical possibilities. Hence, we used CFD technique for the examination of the delicate flow structures within the cylinder of a working engine. This solution yielded more accurate results than could have been achieved by measurements. In the current phase of preliminary design, the CFD simulation proved to be of suitable accuracy to pinpoint the significant differences between engines equipped with swinging valves and poppet valves while also appropriately identifies the strengths of our construction even without validation. Certainly, it is going to be inevitable to use high tech measuring techniques in the upcoming phases of development.

5.1 Creating the Flow Space

Therefore, the purpose of the numerical model was to simulate the intake flow entering the cylinder in the case of both valve systems therefore, a CAD model of the poppet valve cylinder head was generated. In order to get the exact shape of the ducts to be modelled in the cylinder head, moulds of the intake and exhaust ports were modelled in a two-component silicone rubber. The detailed description of the process can be found in [14].

5.2 Model Refinement and Meshing

Using the above methods, the CAD model was transferred to the Ansys SpaceClaim software, where it was prepared for the flow simulation. This included eliminating any model errors in the created 3D geometry that arise due to data transfer irregularities between the two program packages. These errors are not visible to the naked eye and cause "leakage" of the model and fail to create the closed flow space required for numerical simulation. This task was completed with a built-in function of the software.

In order to simplify the geometry small surface elements, that are difficult to mesh, were eliminated and a vertical plane of symmetry was created. This way the size of the model was halved, and the time required for the simulation was also

significantly reduced, although it still took several days. It is important that the model was not only simplified by using the plane of symmetry, but was divided into suitable volumes in preparation for meshing. This was necessary due to the flow modelling [14].

From the refined poppet valve model, volumes consisting of tetrahedral and hexahedral cells were created. The yellow-coloured part in Figure 6 must consist of hexagonal elements, because this is the only way to properly model the piston movement. Since the cylinder, the combustion chamber and the intake pipe can be considered static, we used the traditional tetrahedral mesh in these volumes.

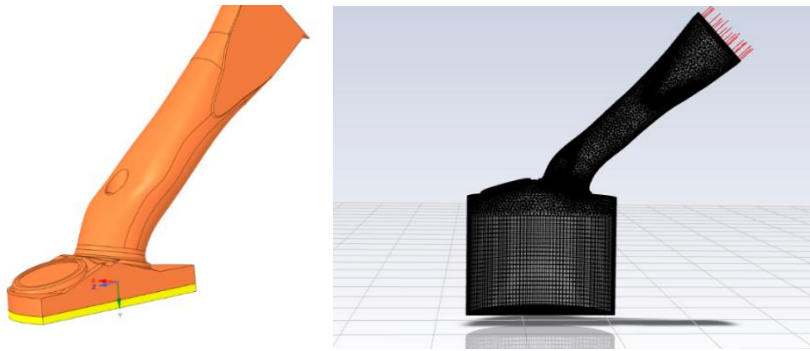


Figure 6

Poppet valve flow space divided into sub-volumes for simulation (left) and the resulting grid (right)

The same procedure was utilised with the swinging valve cylinder head. The flow volume was divided into several separate parts, in which the most suitable method could be used for the calculations (Figure 7). Tetragonal mesh was applied in the intake pipe and valve body, while predominantly hexagonal mesh in the combustion chamber, and swept hexagonal mesh in the cylinder. Near the piston only swept cells, could be used as only this solution enables the piston to be simulated as a moving wall.

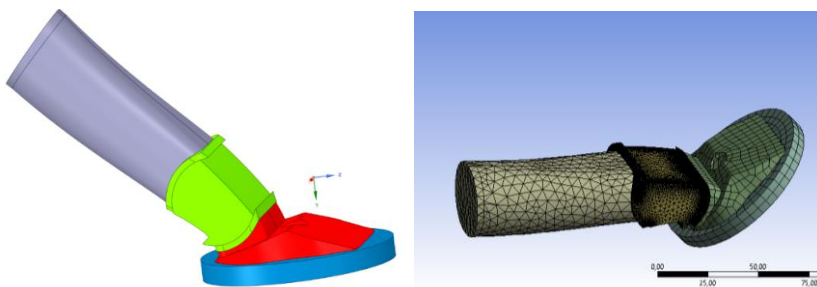


Figure 7

Sub-volumes created for the swinging valve simulation (left) and the resulting grid (right)

5.3 Grid Independence Test

Finding the right grid spacing presented the greatest challenge: it took considerable time to achieve a stable simulation. The difficulty was caused by the edges of the poppet valves that prevented a uniform cell size to be formed on the moving face symbolizing the piston. Based on data found in [16], the quality of meshing has a significant impact on the results obtained, therefore several cell sizes were tested during meshing. For this purpose, we used the swinging valve 3D model. By refining the mesh beyond the cell size absolutely necessary for the stability of the calculation, the flow values changed only in the vicinity of the walls and only the location of the stagnant gas mass changed. It was observed that the cell size needed to be smaller than a critical value to avoid the distorting effect of the valve edges, and enable stable simulation. Further reducing the mesh cell size over the necessary minimum dimension resulted in unchanged flow values (Figure 8). Based on this observation, the poppet valve cylinder head model was created using 0.5 mm cell size. On the grounds of keeping every possible detail identical between the different models, the same mesh sizing had been adopted for the simulation of the swinging valve system. The meshing parameters, as well as the time characteristics of calculations for different mesh densities, are included in Table 2.

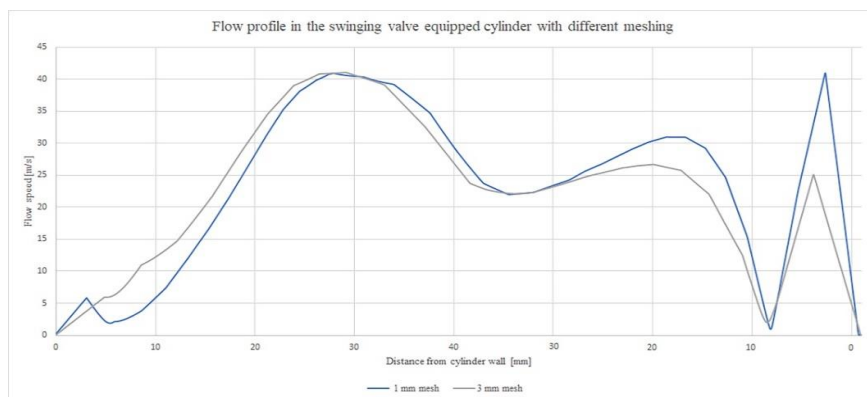


Figure 8

Flow results obtained using different mesh sizes

Table 2

The main characteristics of the mesh types used in different valve arrangements

Cell size on the piston surface	Number of nodes	Number of cells	Calculation time:	Number of time steps:	Length of time steps:
3 mm (swinging valve)	169580	563825	4.85 h	500	1.33×10^{-5} sec

1 mm (swinging valve)	602538	2224769	20.21 h	500	1.33×10^{-5} sec
0.5 mm (poppet valve/swinging valve)	473182/ 415367	1517665/ 1460337	64.7 h	1000	6.66×10^{-6} sec

6 Results

6.1 Simulation Set up

The calculations were targeted at an engine speed of 7000 rpm. The choice of this specific engine speed was made using the results presented in [3], [12] where it was demonstrated, using extensive 0D/1D simulation, that this was the speed that corresponded to the highest delivery ratio. Parameters used for the calculations can be found in Table 3.

Table 3
Parameters used in the 0D/1D engine simulation

Engine speed of the greatest delivery ratio	7000 rpm
Crank angle for the greatest piston speed	75 ATDC
Value of greatest piston speed	23.5 m/s

Ansys Fluent was utilized to complete the simulation. Dynamic meshing was exploited and user defined functions (UDF) were created for both valve systems to model the poppet valve and swinging valve motions. The only opening to the atmosphere was a pressure outlet where flow direction was kept undefined. This way in-cylinder pressure variations could determine the actual particle movement, while in the same time, a more robust solution stability could be achieved. The piston movement was replicated by implementing the layering technique. All moving boundaries were treated as “rigid bodies” and remeshing technique was used around the valves, plus surfaces adjacent to the pivoting valve body were treated as “deforming walls”. The simulation was set-up as transient with details already mentioned in Table 2. Turbulence was modelled by using shear stress transport (SST) using the $k-\omega$ scenario that is able to capture wall turbulence as well as flow phenomenon in the free stream [15]. Second Order Upwind solver was used whereas relaxation factors needed to be decreased appr. 20% to achieve converging results during subsequent time steps.

6.2 Calculation Results

To analyse the results of the calculation, it was necessary to display the rotating gas masses. This could be done by representing the flow vectors and the unidirectionally moving surfaces together (Figure 14). This image shows that by the end of the induction stroke, several centres of rotation have formed in the flow space. Their location is chaotic, which does not help directing the fuel in such a way that it is focused in the vicinity of the spark plug at the end of the compression stroke.

To get numerical values on the degree of vorticity in the poppet valve equipped cylinder head, a plane passing through the axis of the valve was created. With the combined use of vector and contour representation, the rotating gas masses and the stationary portions could be identified. As can be clearly seen in Figure 9, despite the closing valve and the piston stopping at the bottom dead centre, the inflow into the cylinder takes place at a speed of 0.5M. Using a graphical representation of the obtained results, it could be deduced that the flow with the traditional valve is chaotic. The centres of rotation producing the most intense vorticity were selected to lay measuring lines across them. Using 1000 measurement points per line numerical results were obtained, which were represented in a diagram shown in Figure 10.

The same procedure was repeated using the swinging valve system. From the graphical results a more coherent flow structure emerged. In contrary to the chaotic streams of the poppet valve, a very orderly flow pattern was observed, which resembled a curved torus. The direction of the swirl pointed towards the spark plug, which would be ideal for a stratified charge engine to be developed in the future. The rotating ring of air is directed towards the cylinder head which is really beneficial in the context of stratified charging, lean burning engines (Figure 11).

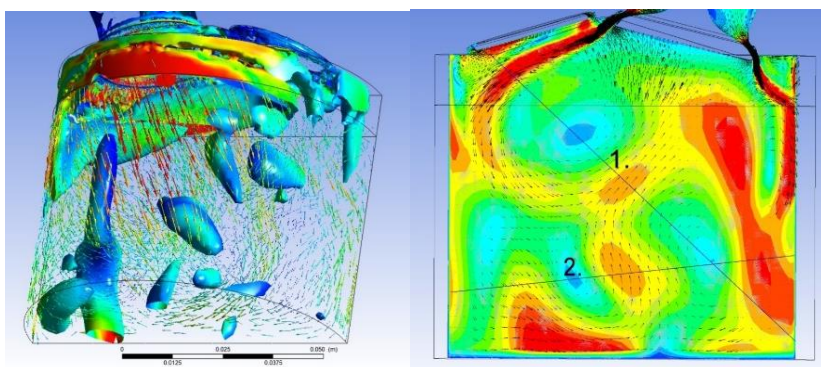


Figure 9

Representation of chaotic flow structures (left) and the measuring lines used to determine numerical values in the plane of the valve stem (right)

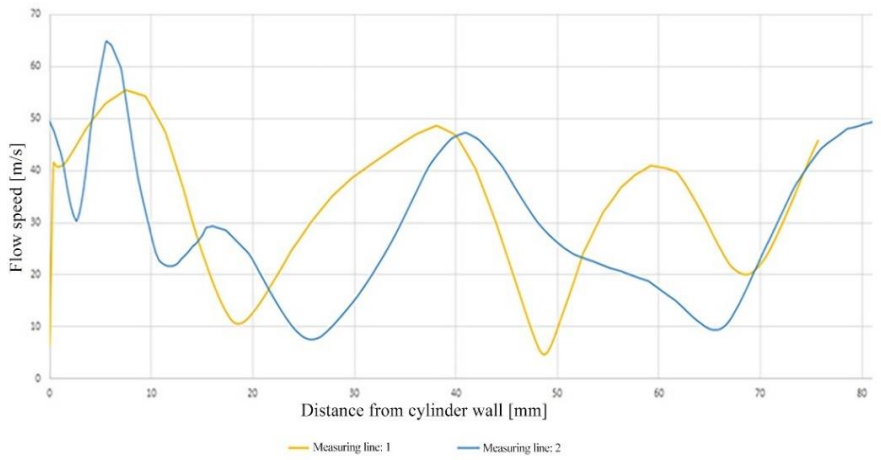


Figure 10

Flow profiles along different measuring lines in the poppet valves equipped cylinder model

In order to extract numerical results from the swinging valve model, a display plane was created that coincided with the symmetry plane of the cylinder (Figure 11). Then, as was shown at the poppet valve system, a measuring line consisting of 1000 data points, was laid across the centers of the vortices that, in this case, could be easily identified. The results were displayed in a graph showing a distinctly different flow distribution than the one obtained in the poppet valve model (Figure 12).

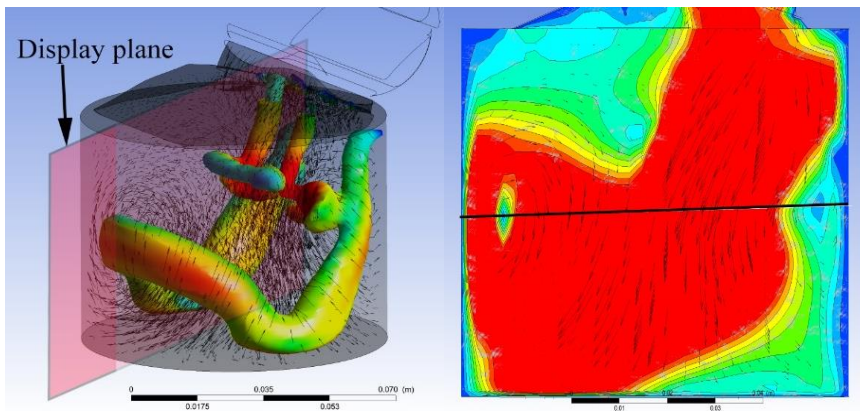


Figure 11

Torus like flow structure is formed in the swinging valve equipped cylinder model (left) and the measuring line used to determine numerical values in the display plane (right)

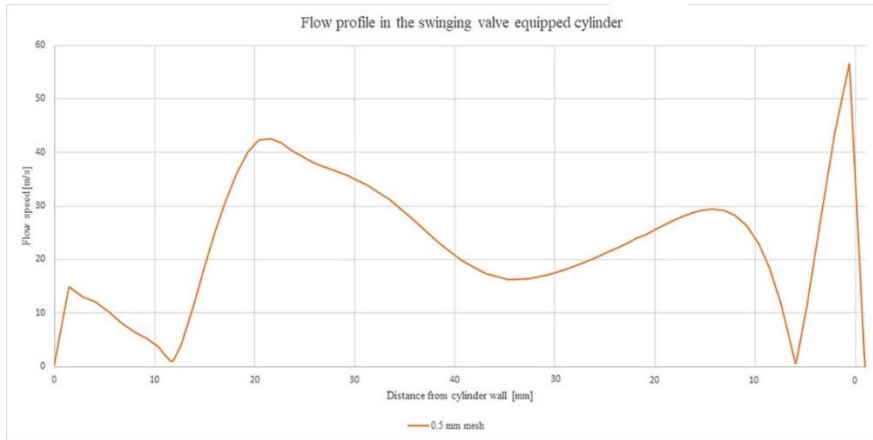


Figure 12

Flow profile along in the display plane along the measuring line in the swinging valve equipped cylinder model with 0.5 mm mesh size

7 Discussion

As can be found in [17], the flow field in the cylinder can be examined as a rotating solid body which centre of rotation is the stationary mass in the centre of the vortex. Using this reasoning, the rotation speed of the vortices can be determined according to the well-known calculation:

$$n_{TR} = \frac{30v}{r\pi} \quad (1)$$

Where:

n_{TR} : tumble rotational speed [rpm]

v : vortex peripheral speed [m/s]

r : vortex radius [m]

With the help of equation No. 1, the Tumble Ratio (TR) can be determined in relation to the engine speed according to [18][1]:

$$TR = \frac{n_{TR}}{n_{ck}} \quad (2)$$

Where:

TR: Tumble Ratio

n_{TR} : Tumble rotational speed [rpm]

n_{ck} : Engine crank shaft rotational speed [rpm]

As is stated in [1], tumble is defined by the tangential component of the incoming charge. Since all possible steps were taken to keep the swaying valve parameters identical to the poppet valve specifications both valve systems share the same inclination angle of 12 degrees measured from the symmetry axis of the cylinder. Therefore, the calculation methods presented in the aforementioned literature would not produce meaningful results in our case.

Since the primary goal of our research is to determine the differences between the traditional valve system and the rocker valve system, we have therefore introduced the Relative Tumble Rate, with which we could get information not only about the ratio of the vortex spaces and the crankshaft speed, but also about the size of the gas mass involved in the movement:

$$RTR = \frac{TR}{R_{RF}} \quad (3)$$

Where:

RTR : Relative Tumble Rate

R_{RF} : Relative Flow Radius

The relative flow radius can be expressed as the ratio between the instantaneous tumble radius and a characteristic size of the cylinder space, which in this case is ideally the radius of the bore. The instantaneous radius can be calculated from the graphical analysis of the numerical data (Figure 8), while the radius of the cylinder is obvious.

$$R_{RF} = \frac{R_{instl}}{R_H} \quad (4)$$

Where:

R_{instl} : Instantaneous Tumble Radius [m]

R_H : Radius of cylinder bore [m]

Using the above relationships, we determined the Relative Tumble Rate for both valve systems. The calculations showed that in the swinging valve cylinder head, the Relative Tumble Rate is 36.69% higher on the side above the exhaust valve, and 10.45% on the side closer to the cylinder wall. The detailed results of the calculations are summarized in Tables 5 and 6.

Table 5
Flow parameters of poppet valve equipped cylinder head

Parameter	Tumble direction: right	Tumble direction: left
R_{inst} [mm]	6.288	9.759
v [m/s]	114.114	134.191
n_{TR} [rpm]	173283.5	131304.7
RTR	3.751	4.411

Table 6
Flow parameters of swinging valve equipped cylinder head

Parameter	Tumble direction: right	Tumble direction: left
R_{inst} [mm]	51.047	19.192
v [m/s]	155.991	148.25
n_{TR} [rpm]	29180.857	73766
RTR	5.127	4.873

Conclusions

From the outcomes of our research, it is obvious that the swinging valve concept provides more favorable tumble properties, that may be ideal for stratified mixture formation, in GDI engines. The slower rotating greater mass of fresh gas, that revolves opposite to the crank shaft rotation, creates a situation where the fuel being injected, will not be broken up by the fast spinning vortices, shed off from the valve edges. Therefore, fuel can be concentrated around the spark plug with more ease and that may assist the production of more sophisticated lean burn engines. It has been demonstrated that engines employing valves performing swaying motions, surpass poppet valve cylinder head equipped engines. Swinging valves offer simpler solutions, to achieve the required performance characteristics, with a reduced engine displacement, thus, perfectly fitting into current engine downsizing concepts.

References

- [1] Kovacs, L., Szabo, Sz.: Challenges of Engine Downsizing, The Publications of the XXVII. microCAD International Scientific Conference, University of Miskolc, 21-22 March, 2013, Miskolc
- [2] Kovacs, L.: Analytical examination of the valve control system of a high-speed internal combustion engine, GÉP 2014/1, 2014, LXV. évfolyam, pp. 28-33
- [3] Kovacs, L., Szabo, Sz.: Comparative study on the improvement of the gas exchange process efficiency of a high-speed IC engine using swinging valve. *Analecta Technica Szegedinensia*, 2019, 13(2), pp. 28-37

-
- [4] Hunter, M. C. I.: Rotary Valve Engines, London, UK, Hutchinson's Scientific and Technical Publications, 1946
- [5] Douglas, S.: Museum of Retro Technology: Power Generation, Unusual Internal Combustion Engines: Rotary Valve IC Engines, Available at: <http://www.douglas-self.com/MUSEUM/POWER/unusualICeng/RotaryValveIC/RotaryValveIC.htm>, Accessed on: 24.01.2023
- [6] Wood, J.: Aspin Rotary Valve Engines, Available at: <http://www.aspin.info>, Accessed on: 09.01.2023
- [7] Wallis, T.: The Bishop Rotary Valve, AutoTechnology, Motorsport Technology Special 2007, pp. 2-5, FISITA, 2007
- [8] Horrocks, G.: A Numerical Study of Rotary Valve Internal Combustion Engine, Unpublished PhD Dissertation, The University of Technology, Sydney, 2001
- [9] Grimonprez, D.: The story of Guy Nègre and MDI, Available at: <https://sites.google.com/site/rijdenopperslucht/home/menu-en/mdi-en/mdi-bedrijf-en/guy-negre-en?tmpl=%2Fsystem%2Fapp%2Ftemplates%2Fprint%2F&showPrintDialog=1>, Accessed on 11.01.2023
- [10] Coates International, Ltd. The Coates Spherical Rotary Valve (CSRV) System, Available at: <http://www.coatesengine.com>, Accessed on: 09.04.2023
- [11] Kovacs, L., Szabo, Sz.: Improving the power characteristics of an Internal Combustion Engine with the help of a 0D/1D engine model, ANNALS of Faculty Engineering Hunedoara– International Journal of Engineering, 2015, Tome XIII – Fascicule 2, 83-88
- [12] Kovacs, L., Szabo, Sz.: Test validated 0D/1D engine model of a Swinging Valve internal combustion engine, Multidisciplinary sciences, Vol. 11, 2021, 4 sz, pp. 266-277
- [13] Kaplan, M.: Influence of swirl, tumble and squish flows on combustion characteristics and emissions in internal combustion engine-review, Amasya University Technology Faculty, Mechanical Engineering Department, Published by Editorial Board Members of IJAET, 2019, e-ISSN: 2146-9067
- [14] Kovacs, L., Szabo, Sz.: Examination of tumble rate with two dissimilar engine valve systems, GÉP (0016-8572): LXXIII 2 pp. 5-10, 2022
- [15] Andrych-Zalewska, M.: Simulation tests of selected gas flow parameters through combustion engine valves, Combustion Engines, 183(4), pp. 21-28, 2020, <https://doi.org/10.19206/CE-2020-404>

- [16] Hamid, M. F., Idroas, M. Y., Sa'ad, S., Teoh Yew Heng, T. Y., Mat, S. C., Alimuddin, Z., Shamsuddin, K. A., Shuib., R. K., and Abdullah, M. K.: Numerical Investigation of Fluid Flow and In-Cylinder Air flow Characteristics for Higher Viscosity Fuel Applications Processes 2020, 8, 439; doi:10.3390/pr8040439, ISSN 2227-9717
- [17] Falfari, S., Brusiani, F., Pelloni, P.: 3D CFD analysis of the influence of some geometrical engine parameters on small PFI engine performances – the effects on the tumble motion and the mean turbulent intensity distribution, 68th Conference of the Italian Thermal Machines Engineering Association, ATI2013, 11-13 September 2013, Bologna, Italy, 2014, Energy Procedia 45, 701-710
- [18] Bozza, R., De Bellis, V., Fantoni, S. and Colangelo, D.: CFD 3D Analysis of Charge Motion and Combustion in a Spark-Ignition Internal Combustion Engine under Close-to-Idle Condition, E3S Web of Conferences 197, 75° National ATI Congress – #7 Clean Energy for all (ATI 2020) 2020, Rome, Italy, September 15-16, 2020
- [19] Falfari, S., Brusiani, F., Bianchi, G. M.: Numerical analysis of in-cylinder tumble flow structures –parametric 0D model development, 68th Conference of the Italian Thermal Machines Engineering Association, ATI2013, 2014, Energy Procedia 45, 987-996

Application of the Theory of Absorbing Markov Processes, for Estimating the Load of Road Sections and Charging Stations, for Electric Car Transport

László Hanka

Óbuda University, Bánki Donát Faculty of Mechanical and Safety Engineering,
Institute of Natural Science and Basic Subjects, Népszínház u. 8, H-1081
Budapest, Hungary, hanka.laszlo@bkg.uni-obuda.hu

University of Public Service, Faculty of Military Science and Officer Training,
Department of Natural Science hanka.laszlo@uni-nke.hu

Abstract: Due to the short range of pure electric vehicles, considering a long trip, the number and the locations of electric charging stations, especially the distance between consecutive charging stations, is a basic question, because the discharged battery must be recharged quite frequently. Today, the network of electric charging stations is unsatisfactory. During the construction of new and expansion of existing networks, the load of roads and the utilization of existing or imagined charging stations must be taken into account. For the estimation of these features, a perfect mathematical tool, is the theory of absorbing Markov-chains. In this article a possible mathematical model, using Markov-chains, extended by the logit regression model will be presented.

Keywords: electric car; charging station; absorbing Markov process; logistic model

1 Introduction

The long-distance route for an electric vehicle requires lots of possibilities for recharging its battery, because, considering recent technology, the range of an electric car is not satisfactory for long-distance transport. The battery must be recharged frequently, therefore along roads, for example at road junctions lots of new charging stations must be built. The location, the number, the density, and the capacity of these charging stations are basic questions, because on the one hand, there is an expectation from the perspective of the drivers, on the other hand providing charging service for vehicles is a business enterprise for providers. These characteristic values and the utilization of charging stations strongly depend on the load of road sections in a road network.

In this article a mathematical model will be proposed, that can be applied to estimating the above-mentioned characteristic values. The point is, that this problem can be characterized by probabilities since in this process there are lots of random variables, for example, how does a driver select a new road section at a road junction, how many charging stations must be used for reaching the destination, etc.

Two mathematical tools, will be presented for examining the above-mentioned problem. On one hand, the logistic regression/decision-making model will be applied for giving probabilities that are associated with the road sections and on the other hand, it will be proven, that for estimating some fundamental quantity, the theory of absorbing Markov-chains can be used efficiently.

In the literature several concepts can be found related this question. First, this problem is considered as an optimization problem [1] [2]. For optimization authors propose for example the very efficient genetic algorithm. Second, several other perspectives can be emphasized, like topography of the road network, and the battery lifetime [3]. Modelling the traffic of vehicles by graphs is commonly applied tool in the literature [4-6]. And finally, the probabilistic point of view is also arises, the Monte-Carlo simulation process can be a possible mathematical tool too [7].

In this paper the author proposes a different procedure for modelling the traffic. Instead of handling it as an optimization problem a probabilistic model is presented, which is based on the very efficient and widely applied theory of Markov-process, that is combined with a probabilistic model. The advantage of this procedure is that the Markov chain is basically independent to the specific probabilistic model. In the article one probabilistic approach is presented but any other method can be chosen by the user, it doesn't affect the structure of the Markov process. Furthermore this method requires a small amount of calculations, even if the network is great, only powers of matrices and some eigenvectors must be determined.

The rest of the paper is organised as follows: In Section 2, a simple example is examined, illustrating basic problems and challenges, in Section 3, one possible probabilistic model is proposed for choosing road sections, in Sections 4-6, the proposed application of the theory of absorbing Markov-chains is demonstrated, in these sections the construction procedure of Markov matrices and numerical results also can be found. In Section 7, the proposed algorithm is applied for a more general road network which has more terminal points. Finally, in Section 8, conclusions are summarized.

2 A Case Study

As an introduction, the road network, depicted in figure 1. will be studied in detail. As it can be seen, there is one initial point, node $\{1\}$, and one terminal point/destination, which is node $\{6\}$. This graph illustrates the road network by

edges, which can be considered as road sections, and nodes that illustrate road junctions. This graph is called transition diagram in the theory of Markov-chains. Changing stations can be at road junctions, or along any road sections.

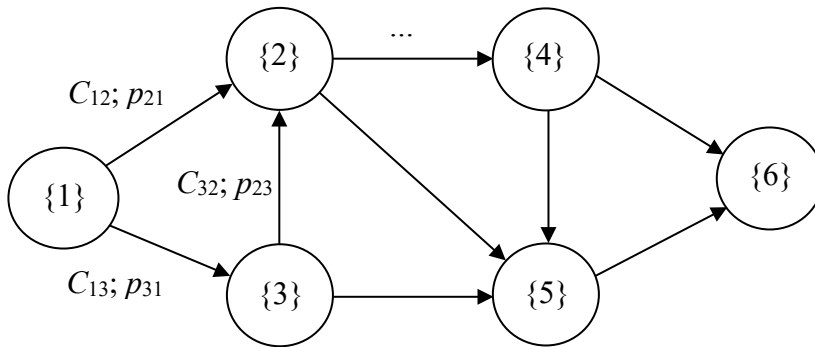


Figure 1

Transition diagram: The graph of a road network, with edges between nodes $\{j\} \rightarrow \{i\}$ that are possible routes, the cost of the road sections (C_{ij}) and transition probabilities (p_{ij})

The point is that at some nodes in this example at nodes {2}, {3} and {4}, there is more than one possibility for the further route, the driver has to select one following road section, by some probability, therefore, from the initial point {1} to destination {6} there are several possibilities for choosing a route. The list below gives every possible route:

- R₁: {1} → {2} → {4} → {6}
- R₂: {1} → {2} → {5} → {6}
- R₃: {1} → {3} → {5} → {6}
- R₄: {1} → {2} → {4} → {5} → {6}
- R₅: {1} → {3} → {2} → {4} → {6}
- R₆: {1} → {3} → {2} → {5} → {6}
- R₇: {1} → {3} → {2} → {4} → {5} → {6}

Considering the choice of possible routes, several questions arise. Since a probability model will be presented, the most important and basic problem is the probability that can be attached to one specific route, if at one node in the road network, there is a possibility for choosing a further road section, because it is a fundamental decision-making process for the driver. In other words, if from the node $\{j\}$ there is a direct route to node $\{i\}$, these are consecutive nodes in the network, then the transition probability p_{ij} must be determined by a plausible and reasonable method.

In the following section, it will be demonstrated in detail, that the first reasonable assumption is that this transition probability depends on the "cost" of the road section, which is denoted by C_{ji} költségtől. Several different definitions can be given for this "cost" it depends on expectations, demands, drivers, etc. In this article, we assume that the cost C_{ji} is proportional to the time that is required for the travel along the road $\{j\} \rightarrow \{i\}$, but instead of time that quantity could be the fuel consumption too. If the length of the road section is S_{ji} , then the cost of the road section can be defined by the following formula

$$C_{ji} = \frac{S_{ji}}{v} + T \quad (1)$$

where v is the average velocity of the vehicle considering the whole route, and T is the average charging time of the accumulator. This quantity is naturally taken into account only in nodes $\{2,3,4,5\}$ and we assume that at node $\{1\}$ the vehicle starts with a fully charged battery. This cost must be used if the probability of the choice of the road section is determined. The cost is the basis of the definition of the probability distribution which is defined by the logistic decision-making model. This model will be presented in Section 2 in detail.

3 The Logistic Model of Transition Probabilities

The logistic probability model [8] [9] first of all defines the ratio of two probabilities, the quantity that is called "odds", and not the probability itself. This model is widely used in decision-making processes, like the process that is being studied in this article. This model can also be used for giving a probability distribution, the method is as follows.

First of all assume, that there are only two choices. The probability of choosing option one is p , and naturally in this case the probability of option two is $1 - p$. According to the logistic model, the natural logarithm of the ratio of these probabilities "the odds", are approximated by a first-order polynomial by the following formula:

$$\ln\left(\frac{p}{1-p}\right) = a + bx =: \beta(x) \quad (2)$$

where x can be an "explanatory variable" in a linear regression model. This definition is the reason for the "logistic regression" name. For simplicity, we introduce a notation β for the right-hand side, which is, by assumption, a linear function of the cost, defined in formula (1). Solving this equation for p , the following probability distribution is obtained for the two option case

$$p = p(\beta) = \frac{e^\beta}{1 + e^\beta}; \quad 1 - p = \frac{1}{1 + e^\beta}; \quad (3)$$

Thanks to the shape of the graph of the function defined by (3) the obtained curve is called a sigmoid curve (Figure 2).

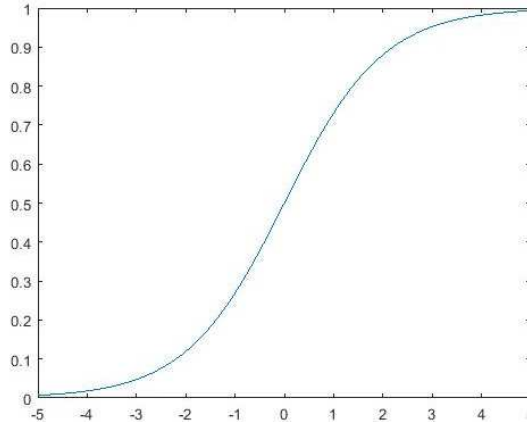


Figure 2

The graph of the function defined by (3), the "sigmoid curve"

The obvious and clear advantage of the application of formula (3) is that independent of the value of β , the codomain of the function is always the interval $[0,1]$ therefore, for any β the value of the function can be considered as a probability.

In practice, in real life generally, there are not only two options for choice but more than two. Consequently, the probability distribution that is defined by formula (3) must be given in a more general form. Assume that there are K options, and one option must be selected. The question is, how can be modified the previously presented simple procedure?

The process is the following [8]. One specific option is chosen as a reference, it can be any, for example, let it be the choice K , and every odds is defined as a ratio of option p_r and p_K , for every possible $r = 1, 2, 3, \dots, K - 1$, similarly to (2):

$$\ln\left(\frac{p_1}{p_K}\right) = \beta_1; \quad \ln\left(\frac{p_2}{p_K}\right) = \beta_2; \quad \dots \quad \ln\left(\frac{p_{K-1}}{p_K}\right) = \beta_{K-1}; \quad (4)$$

from which it follows that,

$$p_1 = p_K e^{\beta_1}; \quad p_2 = p_K e^{\beta_2}; \quad \dots \quad p_{K-1} = p_K e^{\beta_{K-1}}; \quad (5)$$

and naturally,

$$p_K = 1 - \sum_{r=1}^{K-1} p_r = 1 - \sum_{r=1}^{K-1} p_K e^{\beta_r} = 1 - p_K \sum_{r=1}^{K-1} e^{\beta_r}; \quad (6)$$

from where by some rearrangement, the following probability distribution is obtained,

$$p_K = \frac{1}{1 + \sum_{r=1}^{K-1} e^{\beta_r}}; \quad p_k = \frac{e^{\beta_k}}{1 + \sum_{r=1}^{K-1} e^{\beta_r}}; \quad k = 1, 2, \dots, K-1. \quad (7)$$

Formula (7) defines the probability distribution of a decision-making process for K options. The only disadvantage of this result is that the distribution in this form seems pretty strange because for option K it provides a different formula as if option K would be specific. Since in general there is no discrimination between options, giving this distribution in a symmetric form would be expedient. Using a linear parameter transformation, the distribution can be modified. Introducing parameters γ_r according to formulas as follows:

$$\beta_r = \gamma_r - \gamma_K; \quad r = 1, 2, \dots, K-1; \quad \beta_K = \gamma_K - \gamma_K = 0; \quad (8)$$

instead of parameters β_r the distribution can be given using "new" parameters. On the one hand

$$\begin{aligned} p_k &= \frac{e^{\beta_k}}{1 + \sum_{r=1}^{K-1} e^{\beta_r}} = \frac{e^{\gamma_k - \gamma_K}}{1 + \sum_{r=1}^{K-1} e^{\gamma_r - \gamma_K}} = \frac{e^{-\gamma_K} e^{\gamma_k}}{1 + e^{-\gamma_K} \sum_{r=1}^{K-1} e^{\gamma_r}} = \\ &= \frac{e^{\gamma_k}}{e^{\gamma_K} + \sum_{r=1}^{K-1} e^{\gamma_r}} = \frac{e^{\gamma_k}}{\sum_{r=1}^K e^{\gamma_r}}; \quad k = 1, 2, \dots, K-1. \end{aligned} \quad (9)$$

and on the other hand,

$$\begin{aligned} p_K &= \frac{1}{1 + \sum_{r=1}^{K-1} e^{\beta_r}} = \frac{1}{1 + \sum_{r=1}^{K-1} e^{\gamma_r - \gamma_K}} = \frac{1}{1 + e^{-\gamma_K} \sum_{r=1}^{K-1} e^{\gamma_r}} = \\ &= \frac{e^{\gamma_K}}{e^{\gamma_K} + \sum_{r=1}^{K-1} e^{\gamma_r}} = \frac{e^{\gamma_K}}{\sum_{r=1}^K e^{\gamma_r}}; \end{aligned} \quad (10)$$

Consequently, a symmetric form of the probability distribution in a decision-making model is obtained for K choices, according to the logistic probability model. Summarizing results, the distribution is as follows

$$p_k = \frac{e^{\gamma_k}}{\sum_{r=1}^K e^{\gamma_r}}; \quad k = 1, 2, \dots, K. \quad (11)$$

This distribution will be applied when the traffic of electric vehicles will be examined. Naturally, the basic question is the definition of parameters γ_r . A plausible and reasonable definition can be the following

$$\gamma_r = -C_r; \quad r = 1, 2, \dots, K. \quad (12)$$

where C_r is the cost of route r . Using this definition, the probability distribution for the problem, that is being examined in this article, is the following [8] [9]:

$$p_k = \frac{e^{-C_k}}{\sum_{r=1}^K e^{-C_r}}; \quad k = 1, 2, \dots, K. \quad (13)$$

The obvious benefit of the application of this model is that thanks to the negative exponent, the exponential function is strictly decreasing, the probability of the choice of "expensive" routes is highly, "exponentially" reduced, and conversely, the probability of the choice of "cheap" routes are highlighted, emphasizing the chance of inexpensive road sections. In the following section, this probability model will be used for modeling the traffic using Markov-chains.

4 Modelling the Traffic by Markov-Chains

Considering the road network, depicted in Figure 1, basically two problems must be examined. The first and basic question is the probability of the event that a vehicle is at one specific node (road junction). In mathematics, in the theory of Markov-chains these are "states" ($p_i, i = 1, 2, \dots, 6$). These probabilities that form a discrete distribution are usually summarized in a state vector

$$\boldsymbol{\pi}_n = \left[p_1^{(n)}, p_2^{(n)}, p_3^{(n)}, p_4^{(n)}, p_5^{(n)}, p_6^{(n)} \right]^T; \quad n = 0, 1, 2, \dots \quad (14)$$

The notation " $\boldsymbol{\pi}$ " is commonly used in the theory. The superscript n refers to the fact, that in every junction/node, there is a challenge for the driver, a new road section must be selected, and after every step, the probability distribution changes.

In formula (14) N highlights that the given distribution is valid after n steps. Finally T superscript stands for the transpose of the vector because the vector must be a column vector.

The initial state vector, the initial probability distribution in case, depicted in Figure 1. is obviously the following:

$$\boldsymbol{\pi}_0 = [1, 0, 0, 0, 0, 0]^T ; \quad (15)$$

The second fundamental question is the probability of the choice of the route $\{j\} \rightarrow \{i\}$ which is p_{ij} if $\{j\}$ and $\{i\}$ are consecutive nodes along the route in this order. Considering the order of subscripts, the explanation of the notation is the following. This probability, p_{ij} is a conditional probability, the probability of the event that the vehicle is at the node $\{i\}$, using the language of the theory of Markov-chains [10-13], it is in the state $\{i\}$ now, assuming that its previous state was the node $\{j\}$. This probability, which is called transition probability, is denoted by the symbol $P(i | j)$ in probability theory, for which the notation p_{ij} is only a simplification.

The matrix, that contains every transition probability for the road network, depicted in Figure 1., which is called the "transition probability matrix" [10, 13], is the following:

$$\mathbf{A} = \begin{array}{c} \text{From} \\ \left[\begin{array}{cccc|cc} 0 & 0 & 0 & 0 & 0 & 0 \\ p_{21} & 0 & p_{23} & 0 & 0 & 0 \\ p_{31} & 0 & 0 & 0 & 0 & 0 \\ 0 & p_{42} & 0 & 0 & 0 & 0 \\ 0 & p_{52} & p_{53} & p_{54} & 0 & 0 \\ \hline 0 & 0 & 0 & p_{64} & 1 & 1 \end{array} \right] ; \quad \text{to} \end{array} \quad (16)$$

Considering the structure of the matrix the role of rows and columns must be clarified. Column (j) is the former state the "old" node/junction/position of the vehicle, where the vehicle comes from, and row (i) is the latter state, the "new" node/junction/position where the vehicle goes to. Every transition probability p_{ij} is obviously zero if there is no immediate connection between junctions $\{j\}$ and $\{i\}$, in other words, there is no edge in the graph between nodes $\{j\}$ and $\{i\}$. Furthermore, it is also obvious that $p_{65} = 1$ since from state $\{5\}$ there is only one route to state $\{6\}$, there is no possibility for choice between nodes $\{5\}$ and $\{6\}$, therefore, the probability of selecting route $\{5\} \rightarrow \{6\}$ is 1. Finally, since the goal is reaching node $\{6\}$ the vehicle remains in this state by probability $p_{66} = 1$. This state plays a particular role because this state can be accessed from every other state, but from this state, no other nodes can be accessed. If a vehicle reaches this state it remains in that state. This kind of state is called an "absorbing state". It must be emphasized that despite that $p_{65} = 1$ state $\{5\}$ is not absorbing, because there is a

transition from the state {5} to state {6}. According to this observation, the examined stochastic process is an absorbing Markov-chain. The commonly applied partition [11] [12] can be seen in the transition probability matrix (16).

The matrix \mathbf{A} , defined by the formula (16) is a column-stochastic Markov-matrix, which means that the sum of entries in every column sum up to one

$$\sum_{i=1}^6 p_{ij} = 1; \quad j = 1, 2, \dots, 6. \quad (17)$$

According to the theory of Markov-chains [10-13], the state vectors after some steps can be calculated by the following matrix-vector products

$$\boldsymbol{\pi}_1 = \mathbf{A}\boldsymbol{\pi}_0; \quad \boldsymbol{\pi}_2 = \mathbf{A}\boldsymbol{\pi}_1 = \mathbf{A}^2\boldsymbol{\pi}_0; \quad \boldsymbol{\pi}_3 = \mathbf{A}\boldsymbol{\pi}_2 = \mathbf{A}^3\boldsymbol{\pi}_0; \dots; \boldsymbol{\pi}_n = \mathbf{A}\boldsymbol{\pi}_{n-1} = \mathbf{A}^n\boldsymbol{\pi}_0; \dots \quad (18)$$

Considering (18) it is clear, that state vectors basically depend on transition probabilities. Our goal in the following section, using the logistic probability model presented in section 2., determining transition probabilities so that answers can be given to the questions asked in the introduction.

(In some literature the role of rows and columns are interchanged in the matrix (16). In this case, the state vector (14) must be a row vector, the state transition matrix is row-stochastic and multiplications in (18) are in the opposite order $\boldsymbol{\pi}_n = \boldsymbol{\pi}_{n-1}\mathbf{A}$, etc. We use the above-given definition and consequences exclusively in this article.)

5 Determination of Transition Probabilities

In this section transition probabilities will be calculated [1] [2], which are entries of matrix \mathbf{A} in (16), using the logistic decision-making model presented in Section 2, for the road network, illustrated in Figure 1. Probabilities will be calculated using the formula (13) for every node, considering reasonable modifications. The most important consequence of Section 2. is that for a route $\{j\} \rightarrow \{i\}$ the transition probability is proportional to $\exp(-C_{ij})$, so the only remaining problem is finding the normalizing factor such that (17) would be fulfilled. If the question is the transition probability p_{ij} from the state $\{j\}$ to state $\{i\}$ then the answer will be the following:

$$p_{ij} = e^{-C_{ji}} \frac{\sum_{R \in \Omega_{i6}} e^{-C_{i6}^R}}{\sum_{R \in \Omega_{j6}} e^{-C_{j6}^R}}; \quad (19)$$

where Ω_{i6} denotes the set of every possible route from the state $\{i\}$ to state $\{6\}$.

Simply to say, the transition probability is computed by multiplying the exponential factor by a normalization factor. This normalization factor is simply a ratio of the sum of weight factors considering every route from the node $\{i\}$ to the node $\{6\}$ and the sum of weight factors considering every route from the node $\{j\}$ to node $\{6\}$. It will be clear, that these probabilities form a discrete distribution in every column.

Illustrating the procedure, we determine the distribution in the first column of matrix **A** in detail. Using the formula (19) the following is obtained

$$p_{21} = e^{-C_{12}} \frac{\sum_{R \in \Omega_{26}} e^{-C_{26}^R}}{\sum_{R \in \Omega_{16}} e^{-C_{16}^R}} = \quad (20)$$

$$= e^{-C_{12}} \frac{e^{-C_{246}} + e^{-C_{256}} + e^{-C_{2456}}}{e^{-C_{1246}} + e^{-C_{1256}} + e^{-C_{12456}} + e^{-C_{1356}} + e^{-C_{13246}} + e^{-C_{13256}} + e^{-C_{132456}}};$$

where the cost $C_{j...6}$ in the exponent of the exponential function denotes the total cost of the route $\{j\} \rightarrow \dots \rightarrow \{6\}$ no matter how long it is. To make it clear assume first, that for every route $\{j\} \rightarrow \{i\}$ the cost C_{ji} is one unit. In this case, it is clear, that the total cost is proportional to the length of the route. For example for the route $\{2\} \rightarrow \{4\} \rightarrow \{6\}$ the cost is 2 units, for the route $\{1\} \rightarrow \{3\} \rightarrow \{2\} \rightarrow \{4\} \rightarrow \{6\}$ the total cost is 4 units, etc.

For the sake of simpler formulas, the notation $\alpha = \exp(-1)$ is introduced. In this case, the formula (20) is equivalent to the following

$$p_{21} = \alpha \frac{\alpha^2 + \alpha^2 + \alpha^3}{\alpha^3 + \alpha^3 + \alpha^4 + \alpha^3 + \alpha^4 + \alpha^4 + \alpha^5} = \frac{2\alpha^3 + \alpha^4}{3\alpha^3 + 3\alpha^4 + \alpha^5}; \quad (21)$$

The other non-zero probability in the first column can be obtained by a similar procedure

$$p_{31} = \alpha \frac{\alpha^3 + \alpha^3 + \alpha^4 + \alpha^2}{\alpha^3 + \alpha^3 + \alpha^4 + \alpha^3 + \alpha^4 + \alpha^4 + \alpha^5} = \frac{\alpha^3 + 2\alpha^4 + \alpha^5}{3\alpha^3 + 3\alpha^4 + \alpha^5}; \quad (22)$$

It is clear that the requirement $p_{21} + p_{31} = 1$ is fulfilled, so a probability distribution is obtained.

Repeating the previous process, every probability distribution can be computed in columns of matrix **A**. The results are as follows

$$\begin{aligned}
 p_{42} &= \frac{\alpha^2 + \alpha^3}{2\alpha^2 + \alpha^3}; & p_{23} &= \frac{2\alpha^3 + \alpha^4}{\alpha^2 + 2\alpha^3 + \alpha^4}; & p_{54} &= \frac{\alpha^2}{\alpha + \alpha^2}; \\
 p_{52} &= \frac{\alpha^2}{2\alpha^2 + \alpha^3}; & p_{53} &= \frac{\alpha^2}{\alpha^2 + 2\alpha^3 + \alpha^4}; & p_{64} &= \frac{\alpha}{\alpha + \alpha^2};
 \end{aligned} \tag{23}$$

It is clear that in every column a discrete distribution is obtained, in other words, the matrix \mathbf{A} is column-stochastic. Therefore the Markov-matrix \mathbf{A} has been constructed. Using the above-given definition of α , the Markov-matrix, filled up with numerical data is the following

$$\mathbf{A} = \left[\begin{array}{cccccc|c}
 0 & 0 & 0 & 0 & 0 & 0 & 0 \\
 0.5586 & 0 & 0.4656 & 0 & 0 & 0 & 0 \\
 0.4414 & 0 & 0 & 0 & 0 & 0 & 0 \\
 0 & 0.5777 & 0 & 0 & 0 & 0 & 0 \\
 0 & 0.4223 & 0.5344 & 0.2689 & 0 & 0 & 0 \\
 \hline
 0 & 0 & 0 & 0.7311 & 1 & 1 & 1
 \end{array} \right]; \tag{24}$$

The commonly applied and suitable partition of matrix \mathbf{A} has been preserved. Compare matrix (16) and (24). The benefit of this partition will be clarified in the following section. In Section 5 the application of Markov-matrix will be presented, and it will be demonstrated that the theory can be efficiently applied to the examination of public transport.

6 Properties of Absorbing Markov-Chains

Considering (18) and (24) the probability of any state can be calculated for every integer n . The probability distribution of states can be seen below for $n = 1, 2, 3$, etc.

$$\pi_1 = \mathbf{A}\pi_0 = \begin{bmatrix} 0 \\ 0.5586 \\ 0.4414 \\ 0 \\ 0 \\ 0 \end{bmatrix}; \quad \pi_2 = \mathbf{A}^2\pi_0 = \begin{bmatrix} 0 \\ 0.2055 \\ 0 \\ 0.3227 \\ 0.4718 \\ 0 \end{bmatrix}; \quad \pi_3 = \mathbf{A}^3\pi_0 = \begin{bmatrix} 0 \\ 0 \\ 0 \\ 0.1187 \\ 0.1736 \\ 0.7077 \end{bmatrix}; \dots; \text{etc.} \tag{25}$$

A bit more interesting question is what the powers of matrix \mathbf{A} look like. The powers of \mathbf{A} can be seen below for every positive integer exponent.

$$\begin{aligned}
\mathbf{A}^2 &= \begin{bmatrix} 0 & 0 & 0 & 0 & 0 & 0 \\ 0.2055 & 0 & 0 & 0 & 0 & 0 \\ 0 & 0 & 0 & 0 & 0 & 0 \\ 0.3227 & 0 & 0.2689 & 0 & 0 & 0 \\ 0.4718 & 0.1554 & 0.1966 & 0 & 0 & 0 \\ 0 & 0.8446 & 0.5344 & 1 & 1 & 1 \end{bmatrix}; \quad \mathbf{A}^3 = \begin{bmatrix} 0 & 0 & 0 & 0 & 0 & 0 \\ 0 & 0 & 0 & 0 & 0 & 0 \\ 0 & 0 & 0 & 0 & 0 & 0 \\ 0.1187 & 0 & 0 & 0 & 0 & 0 \\ 0.1736 & 0 & 0.0723 & 0 & 0 & 0 \\ 0.7077 & 1 & 0.9277 & 1 & 1 & 1 \end{bmatrix}; \\
\mathbf{A}^4 &= \begin{bmatrix} 0 & 0 & 0 & 0 & 0 & 0 \\ 0 & 0 & 0 & 0 & 0 & 0 \\ 0 & 0 & 0 & 0 & 0 & 0 \\ 0 & 0 & 0 & 0 & 0 & 0 \\ 0.0319 & 0 & 0 & 0 & 0 & 0 \\ 0.9681 & 1 & 1 & 1 & 1 & 1 \end{bmatrix}; \quad \mathbf{A}^5 = \begin{bmatrix} 0 & 0 & 0 & 0 & 0 & 0 \\ 0 & 0 & 0 & 0 & 0 & 0 \\ 0 & 0 & 0 & 0 & 0 & 0 \\ 0 & 0 & 0 & 0 & 0 & 0 \\ 0 & 0 & 0 & 0 & 0 & 0 \\ 1 & 1 & 1 & 1 & 1 & 1 \end{bmatrix} = \mathbf{A}^n, \quad n > 5;
\end{aligned} \tag{26}$$

The result must be underlined, that for $n \geq 5$ the n th power of \mathbf{A} stays the same, in other words, it becomes stable, and it won't change if the exponent increases. A "stable matrix" or a "limit matrix" [3-6] is obtained, which is generally defined by the following limit:

$$\lim_{n \rightarrow \infty} \mathbf{A}^n \tag{27}$$

In this specific illustrating example the limit is reached if $n = 5$. This value depends on the shape and structure of the transition diagram, it can be less and also greater. This stable matrix can be computed in general, the form of the limit matrix can be given by the suitable partition that has already been applied earlier in (16) and (24). In general, the partitioned form of \mathbf{A} is the following:

$$\mathbf{A} = \begin{bmatrix} \mathbf{Q}_{(n-k) \times (n-k)} & \mathbf{0}_{(n-k) \times k} \\ \mathbf{R}_{k \times (n-k)} & \mathbf{I}_{k \times k} \end{bmatrix} \tag{28}$$

in which the meaning of partitions is clear according to (16) és (24), but we emphasize that $\mathbf{0}$ is the zero matrix, and \mathbf{I} is the identity matrix, k is the number of absorbing states (in the examined example $k = 1$), and n is the total number of states (in this case $n = 6$). Using this partition calculations that are necessary for powers of \mathbf{A} and the stable matrix can be carried out easily. For some specific exponents, and for any n integer exponent the power of \mathbf{A} can be found below:

$$\begin{aligned}
\mathbf{A}^2 &= \begin{bmatrix} \mathbf{Q} & \mathbf{0} \\ \mathbf{R} & \mathbf{I} \end{bmatrix} \begin{bmatrix} \mathbf{Q} & \mathbf{0} \\ \mathbf{R} & \mathbf{I} \end{bmatrix} = \begin{bmatrix} \mathbf{Q}^2 & \mathbf{0} \\ \mathbf{RQ} + \mathbf{R} & \mathbf{I} \end{bmatrix} \\
\mathbf{A}^3 &= \begin{bmatrix} \mathbf{Q}^2 & \mathbf{0} \\ \mathbf{RQ} + \mathbf{R} & \mathbf{I} \end{bmatrix} \begin{bmatrix} \mathbf{Q} & \mathbf{0} \\ \mathbf{R} & \mathbf{I} \end{bmatrix} = \begin{bmatrix} \mathbf{Q}^3 & \mathbf{0} \\ \mathbf{RQ}^2 + \mathbf{RQ} + \mathbf{R} & \mathbf{I} \end{bmatrix} \\
\mathbf{A}^4 &= \begin{bmatrix} \mathbf{Q}^3 & \mathbf{0} \\ \mathbf{RQ}^2 + \mathbf{RQ} + \mathbf{R} & \mathbf{I} \end{bmatrix} \begin{bmatrix} \mathbf{Q} & \mathbf{0} \\ \mathbf{R} & \mathbf{I} \end{bmatrix} = \begin{bmatrix} \mathbf{Q}^4 & \mathbf{0} \\ \mathbf{RQ}^3 + \mathbf{RQ}^2 + \mathbf{RQ} + \mathbf{R} & \mathbf{I} \end{bmatrix} \\
&\dots
\end{aligned}$$

$$\begin{aligned}
 A^n &= \begin{bmatrix} Q^n & \mathbf{0} \\ RQ^{n-1} + \dots + RQ^3 + RQ^2 + RQ + R & I \end{bmatrix} \\
 &= \begin{bmatrix} Q^n & \mathbf{0} \\ R(Q^{n-1} + \dots + Q^3 + Q^2 + Q + I) & I \end{bmatrix}
 \end{aligned} \tag{29}$$

The stable matrix is obtained if $n \rightarrow \infty$. Since matrix \mathbf{Q} is one partition of the Markov-matrix, every entry is less than 1 (see 24), therefore the sequence of powers of matrix \mathbf{Q} tends to the zero matrix, according to the properties of the geometric sequence. The sum in the lower left corner, using again the properties of the geometric series, can be given in the following simple form:

$$I + Q + Q^2 + Q^3 + \dots + Q^{n-1} + \dots = (I - Q)^{-1} \tag{30}$$

which sum exists if in some positive integer power of \mathbf{Q} , every entry is less than 1 [10, 11, 13]. In this example, it is valid for \mathbf{Q} itself. Summarizing observations, the stable matrix can be given in a general form:

$$\lim_{n \rightarrow \infty} A^n = \begin{bmatrix} \mathbf{0} & \mathbf{0} \\ R(I - Q)^{-1} & I \end{bmatrix} \tag{31}$$

Using this limit matrix, on the basis of the theory of Markov-chains, the traffic, the public transport can be characterized numerically. The load of road sections and the utility of charging stations can be estimated by probabilities.

The justification of this statement is, that some parts and partitions of the limit matrix have fundamental meaning [10-13].

- 1) The entry in the i th row and j th column of the matrix $(\mathbf{I} - \mathbf{Q})^{-1}$ is the expected value of the random variable that the node $\{i\}$ is reached exactly from the node $\{j\}$, in other words, the average number of vehicles along the road section $\{j\} \rightarrow \{i\}$.
- 2) The sum of columns of the matrix $(\mathbf{I} - \mathbf{Q})^{-1}$ which is the row vector $\mathbf{1}^T(\mathbf{I} - \mathbf{Q})^{-1}$ has also fundamental meaning. The j th coordinate of this vector is the average number of steps, in other words, the expected value of steps from the state $\{j\}$ to the absorbing state, the average number of road sections for a vehicle from the node $\{j\}$ to the destination.
- 3) The (i, j) entry in the matrix $R(\mathbf{I} - \mathbf{Q})^{-1}$ is the probability of the event, that the absorbing state $\{i\}$ is reached through the state $\{j\}$. In other words, the probability of the event that the vehicle reaches the destination $\{i\}$ and before it attains node $\{j\}$, for example, charges its battery at that road junction.

For the road network, depicted in Figure 1, and for the transition probability matrix that is given by (24) these matrices are as follows:

$$(\mathbf{I} - \mathbf{Q})^{-1} = \begin{bmatrix} 1 & 0 & 0 & 0 & 0 \\ 0.7641 & 1 & 0.4656 & 0 & 0 \\ 0.4414 & 0 & 1 & 0 & 0 \\ 0.4414 & 0.5777 & 0.2689 & 1 & 0 \\ 0.6773 & 0.5777 & 0.8034 & 0.2689 & 1 \end{bmatrix} \quad (32)$$

In this matrix for example the entry (2,3) is 0.4656, which means that from the node {3} to node {2} the expected number of selecting the road section is 0.4656, etc. These numbers characterize the whole road network, and the load of various road sections can be compared. The indirect consequence of these data is that the utilization of charging stations at the nodes can be concluded. Summing columns of the previous matrix, the following row vector is obtained:

$$\mathbf{1}^T(\mathbf{I} - \mathbf{Q})^{-1} = [3.3242 \quad 2.1554 \quad 2.5379 \quad 1.2689 \quad 1.0000] \quad (33)$$

As we described earlier, the meaning of these vector components is the average number of steps from a specific node to the destination. For example, it is obviously 1 at the node {5} because from this node a vehicle can only go to node {6} and the "distance" is only one step. But the from the node {2} the average number of steps to node {6} is 2.1554.

Finally the result:

$$\mathbf{R}(\mathbf{I} - \mathbf{Q})^{-1} = [1.0000 \quad 1.0000 \quad 1.0000 \quad 1.0000 \quad 1.0000] \quad (34)$$

is trivial in this case, because there is only one destination/target in this network, therefore independent of nodes, the vehicle reaches node {6} by probability 1.

7 A Case Study for Two Absorbing States

Illustrating the proposed method, we present one more example, which is a bit more general than the previously studied example. Let the road network be the graph depicted in Figure 3:

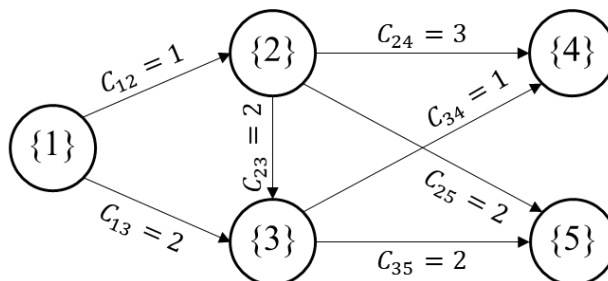


Figure 3

Transition diagram: The graph of a road network, with one initial point, two absorbing states and different road costs

The obvious difference between this second illustrating example and the previous one, on the one hand is that in this road network there are two terminal nodes, in other word two absorbing states $\{4\}$ and $\{5\}$, and on the other hand, road costs are not units and are not the same. In this section the application of the proposed mathematical tools will be presented for this more general case.

The column stochastic Markov-matrix for this case, is as follows and the necessary partition is also marked:

$$\mathbf{A} = \begin{bmatrix} \mathbf{Q}_{3 \times 3} & \mathbf{0}_{3 \times 2} \\ \mathbf{R}_{2 \times 3} & \mathbf{I}_{2 \times 2} \end{bmatrix} = \left[\begin{array}{ccc|cc} 0 & 0 & 0 & 0 & 0 \\ p_{21} & 0 & 0 & 0 & 0 \\ p_{31} & p_{32} & 0 & 0 & 0 \\ \hline 0 & p_{42} & p_{43} & 1 & 0 \\ 0 & p_{52} & p_{53} & 0 & 1 \end{array} \right] \quad (35)$$

Due to the fact that in this network there are 5 nodes, the transition probability matrix is a 5×5 matrix. Furthermore, since in this network there are two absorbing states, $k = 2$, in the partition of the matrix the identity matrix in the lower right corner is a 2×2 matrix, therefore matrix \mathbf{Q} in the upper left corner is a 3×3 matrix.

The probability distributions in the columns of \mathbf{A} can be given by following the same logic. Using the same α notation for $\exp(-1)$, columns of \mathbf{A} are as follows:

$$\left\{ \begin{array}{l} p_{21} = \frac{\alpha^5 + 2\alpha^4 + \alpha^3}{\alpha^5 + 3\alpha^4 + 2\alpha^3}; \\ p_{31} = \frac{\alpha^4 + \alpha^3}{\alpha^5 + 3\alpha^4 + 2\alpha^3}; \end{array} \right. \left\{ \begin{array}{l} p_{32} = \frac{\alpha^4 + \alpha^3}{\alpha^4 + 2\alpha^3 + \alpha^2}; \\ p_{42} = \frac{\alpha^3}{\alpha^4 + 2\alpha^3 + \alpha^2}; \\ p_{52} = \frac{\alpha^2}{\alpha^4 + 2\alpha^3 + \alpha^2}; \end{array} \right. \left\{ \begin{array}{l} p_{43} = \frac{\alpha}{\alpha + \alpha^2}; \\ p_{53} = \frac{\alpha^2}{\alpha + \alpha^2}; \end{array} \right. \quad (36)$$

since for example,

$$\begin{aligned} p_{21} &= e^{-C_{12}} \frac{\sum_{R \in \Omega_{2v}} e^{-C_{2v}^R}}{\sum_{R \in \Omega_{1v}} e^{-C_{1v}^R}} = \\ &= e^{-C_{12}} \frac{e^{-C_{24}} + e^{-C_{234}} + e^{-C_{25}} + e^{-C_{235}}}{e^{-C_{124}} + e^{-C_{125}} + e^{-C_{1234}} + e^{-C_{1235}} + e^{-C_{134}} + e^{-C_{135}}} = \frac{\alpha^5 + 2\alpha^4 + \alpha^3}{\alpha^5 + 3\alpha^4 + 2\alpha^3}; \end{aligned} \quad (37)$$

because $C_{1235} = 1 + 2 + 2 = 5$, etc. It is clear that these columns sum up to one, so the matrix is indeed column-stochastic. Markov-matrix filled up with numerical values can be seen below

$$A = \begin{bmatrix} 0 & 0 & 0 & | & 0 & 0 \\ 0.5777 & 0 & 0 & | & 0 & 0 \\ 0.4223 & 0.2689 & 0 & | & 0 & 0 \\ \hline 0 & 0.1966 & 0.7311 & | & 1.0000 & 0 \\ 0 & 0.5344 & 0.2689 & | & 0 & 1.0000 \end{bmatrix} \quad (38)$$

State vectors,

$$\begin{aligned} \pi_0 &= \begin{bmatrix} 1 \\ 0 \\ 0 \\ 0 \\ 0 \end{bmatrix}; \quad \pi_1 = A\pi_0 = \begin{bmatrix} 0 \\ 0.5777 \\ 0.4223 \\ 0 \\ 0 \end{bmatrix}; \quad \pi_2 = A\pi_1 = A^2\pi_0 = \begin{bmatrix} 0 \\ 0 \\ 0.1554 \\ 0.4223 \\ 0.4223 \end{bmatrix}; \\ \pi_3 &= A\pi_2 = A^3\pi_0 = \begin{bmatrix} 0 \\ 0 \\ 0 \\ 0.5359 \\ 0.4641 \end{bmatrix}; \text{ etc.} \end{aligned} \quad (39)$$

and powers of A for different exponents are illustrated below,

$$\begin{aligned} A &= \begin{bmatrix} 0 & 0 & 0 & 0 & 0 \\ 0.5777 & 0 & 0 & 0 & 0 \\ 0.4223 & 0.2689 & 0 & 0 & 0 \\ 0 & 0.1966 & 0.7311 & 1 & 0 \\ 0 & 0.5344 & 0.2689 & 0 & 1 \end{bmatrix}; \\ A^2 &= \begin{bmatrix} 0 & 0 & 0 & 0 & 0 \\ 0 & 0 & 0 & 0 & 0 \\ 0.1544 & 0 & 0 & 0 & 0 \\ 0.4223 & 0.3932 & 0.7311 & 1 & 0 \\ 0.4223 & 0.6068 & 0.2689 & 0 & 1 \end{bmatrix}; \\ A^3 &= \begin{bmatrix} 0 & 0 & 0 & 0 & 0 \\ 0 & 0 & 0 & 0 & 0 \\ 0 & 0 & 0 & 0 & 0 \\ 0.5359 & 0.3932 & 0.7311 & 1 & 0 \\ 0.4641 & 0.6068 & 0.2689 & 0 & 1 \end{bmatrix} = A^4 = A^5 \dots = \lim_{n \rightarrow \infty} A^n \end{aligned} \quad (40)$$

The first observation is that the stable matrix is reached for $n = 3$. Finally, the partitions of the stable matrix must be examined.

1) The expected number of "road section choices" can be seen in the matrix $(I - Q)^{-1}$:

$$(I - Q)^{-1} = \begin{bmatrix} 1 & 0 & 0 \\ 0.5777 & 1 & 0 \\ 0.5777 & 0.2689 & 1 \end{bmatrix} \quad (41)$$

2) The average number of steps to absorbing states are provided by the row vector $\mathbf{1}^T(I - Q)^{-1}$:

$$\mathbf{1}^T(I - Q)^{-1} = [2.1554 \quad 1.2689 \quad 1] \quad (42)$$

3) The probability of the event that one absorbing state is reached from a specific node, is given by the matrix $\mathbf{R}(\mathbf{I} - \mathbf{Q})^{-1}$:

$$\mathbf{R}(\mathbf{I} - \mathbf{Q})^{-1} = \begin{bmatrix} 0.5359 & 0.3932 & 0.7311 \\ 0.4641 & 0.6068 & 0.2689 \end{bmatrix} \quad (43)$$

In this case, a great and basic difference can be realized between the first and the second example. In this matrix there are two rows, and the reason is clear, there are two absorbing states, so from any state both absorbing states can be reached, there are two options for any intermediate state, the probability for reaching one or the other absorbing state can be found in the matrix. It must be emphasised, that in all columns, probabilities form a distribution!

Conclusions

In this work, a method has been presented on how the theory of absorbing Markov-chains can be used for modeling the traffic of vehicles along a given road network. The basis of this mathematical model is the logistic regression model, which is a sophisticated method for giving a probability of any decision in a decision-making process. The possible application of this logistic model is reasonable, because along a road network in every road junction, there is an expectation against the driver for choosing a following road section, so in every node, there is a decision-making process.

It has been shown that the combination of these two theories can be used for estimating the load of road sections, and the utilization of charging stations, because these quantities can be characterized by data that can be found in the limit of the Markov-matrix. The process was illustrated by two examples. The first example, contained only one initial point and one destination with the same and unit road costs. In the second example, there is more than one destination in the road network, the road costs are different and not units.

Further study will possibly include modifying the number of initial points and for a greater network/graph, an efficient and simpler method must be developed for giving the Markov-matrix.

Calculations have been performed using the software MATLAB.

References

- [1] Lech-Nikonczuk: The method of route optimization of electric vehicle, *Procedia Computer Science* Volume 207, 2022, pp. 4454-4462
- [2] Luque at al.: Optimization of the powertrain of electric vehicles for a given route, *Transportation Research Procedia* Volume 58, 2021, pp. 246-253
- [3] Perger-Auer: Energy efficient route planning for electric vehicles with special consideration of the topography and battery lifetime, *Energy Efficiency* volume 13, 2020, pp. 1705-1726

- [4] Pokorádi: Graph model-based analysis of technical systems, IOP Conf. Ser.: Mater. Sci. Eng. 393 012007, 2018
- [5] Péter-Szabó: A new network model for the analysis of air traffic network, Periodica Polytechnica Transportation Engineering, 40(1), pp. 39-44
- [6] Péter-Szauter-Rozsás-Lakatos: Integrated application of network traffic and intelligent driver models in the test laboratory analysis of autonomous vehicles and electric vehicles, International Journal of Heavy Vehicle Systems Vol. 27, Nos. 1-2, 2020, pp. 227-245
- [7] Pokorádi: Monte-Carlo Simulation-Based Accessibility Analysis of Temporal Systems, Symmetry 2022, 14(5), p. 983
- [8] Wackerly: Mathematical Statistics with Applications, Brooks/Cole, USA, 2008
- [9] Bijma: An Introduction to Mathematical Statistics, Amsterdam University Press, 2017
- [10] Karlin - Taylor: An introduction to stochastic modeling, Academic Press, London, 1998
- [11] Ross: Stochastic processes, John Wiley and sons, USA, 1996
- [12] Knill: Probability and Stochastic Processes with Applications, Overseas Press, India, 2006
- [13] Hillier - Lieberman: Introduction to Operations Research, McGraw-Hill, USA, 2001

Geometric and Tooth Contact Analysis of the Areas and Perimeters, on the Archimedean Worm Wheels depending on the Modification of the Axial Module

Sándor Bodzás¹, Gyöngyi Szanyi²

¹Department of Mechanical Engineering, University of Debrecen

²Department of Basic Technical Studies, University of Debrecen

4031 Debrecen, Ótemető u. 2-4, Hungary

*E-mail: ¹bodzassandor@eng.unideb.hu, ²szanyi.gyongyi@science.unideb.hu

Abstract: The goal of this study is to determine the correlation between the modification of the axial module and the received mechanical parameters on the teeth, of the worm gear. We analyze the areas and perimeters of the impressions on the teeth of the worm gear comparing the module changing. Six types of Archimedean worm gear drives are designed by the modification of the axial module to analyze the mechanical parameters between the connecting teeth of the pinion and the gear. After that, computer aided models are generated. These pairs are loaded with the same torque, to analyze the mechanical parameters on the tooth contact zone. Due to the geometric establishment, three teeth of the worm wheels are connected with the worm surface, at the same time, that is why these teeth are analyzed continuously. We approach the kinematic impressions on the surface of the worm wheel, by polygon method, to get percentage ratios between the areas and perimeters of the overall profile and the tooth contact zone, on the worm wheel, for each connecting tooth. We also determine the correlation between the axial module and the analyzed mechanical parameters, assuming average values, on the contact surfaces.

Keywords: worm; worm wheel; module; teeth; stress; deformation

1 Introduction

Worm gear drives are widely used for different engineering constructions, they provide high transmission ratios and perpendicular shaft positions, between the elements. More teeth are connected at the same time, this is why higher torque can be transferred, than in the case of spur gears and bevel gears [1, 2, 4-9, 20-22, 24].

The aim of the TCA is to analyze the mechanical parameters of the gear pairs in the tooth connection based on different loads. It is a part of finite element analysis where the tooth connection can be analyzed. Consequently, it is possible to simulate

the working conditions of the gear pairs. If we get non-required results, it is possible to mediate the design process, before the real manufacturing and the industrial working begins [7] [23].

Although the manufacturing process of the worm wheel is complicated, it can be generated by direct motion mapping. It means the geometry of the worm defines the cutting tool, which is called hob, which manufactures the teeth of the worm wheel [1, 4, 25-27]. Geometrically, the worm and the hob are the same. The difference between them are the addendum and the tooth width. We should provide clearances during the tooth connection to avoid heat deformations [1, 4, 25-27].

F. L. Litvin found the mathematical processes needed to determine and optimize the tooth contact areas in case of different gears. He designed special drives for different companies. His research group developed computer aided software for the geometrical designing and the localization of the contact area on toothed gears [6, 7, 23].

A. Fuentes Aznar and his research group deal with TCA which contains geometric design, CAD and FEM for standardized gear drives and special connecting elements [7]. The aim of the TCA is to determine the mechanical parameters on the tooth contact zone by different load forces and torques depending on the material type [7] [23].

I. Dudás researches the manufacturing development of the different worm gear drives. He also analyzes these elements by mathematical way to provide the correct connection and manufacturing process for them. The development stages of the grinding processes are important for the assurance of the better connection and the reduction of the wearing between the kinematic pairs [4].

T. Bercey analyzed the connection of the globoid worm and hyperbolic gear. On the other hand, he proved the application of the kinematic method in case of toroidal gears [2] [3].

I. Sz. Krivenko invented the cylindrical worm gear drives having an arched profile in the axial section. Based on his experience, he recommended a certain design process for this construction. The advantage of this geometry is the convex-concave teeth connection, which results in better contact lines and areas, than in case of linear profile [8].

V. Goldfarb works on the geometrical development of spiroid- and cylindrical worm gears by mathematical and constructional way. He analyzes the contact mechanical parameters by FEM for the geometrical localization [13] [14].

Paper [9] presents the matrix - vectorial mathematical model of the double worm-face gear with cylindrical worm and a graphical modelling which is based on the specific geometrical characteristics accomplished by means of the Autodesk Inventor 3D modelling program.

Paper [10] presents a computation method of worm gears with Archimedean and involute worms when engagement correction is presented, based on the contact pressures and wear of tooth of the wheel, as well as the gear life and the sliding speed in the engagement.

Paper [11] illustrates a machining method of large-sized cylindrical worm gears with Niemann profiles using a computer numerical control (CNC) machining center is introduced. The tooth contact pattern and transmission errors of large-sized worm gear pair with Niemann profiles are analyzed before machining of the worm and worm wheel. After that, the machining conditions of the worm is determined by calculating each offset distance between the worm axis and the center axis of the end mill, and then the worm is machined by swarf cutting. That means machining by the side surface of the end mill.

Paper [12] describes the results of the machine tool setting errors of the worm gear hobbing and its effects of the shaft misalignments of the worm gear set on the interference.

Paper [15] presents the investigation of the meshing theory for the mismatched ZC1 worm drive. The contact endpoints, the datum point, and the internal instantaneous contact points are all determined by solving their corresponding nonlinear equation sets iteratively. The numerical results of the relative principal curvature, the transmission error, and the drive ratio error of the worm drive are all obtained.

Paper [16] presents the geometric and kinematic design of spur gears, bevel gears, worm gears, planetary gears and face gear drives. It contains formulas for the geometric design and recommends manufacturing strategies for these gear pairs.

Paper [17] presents the geometric interference of cylindrical worm gear drives using an oversized hob to cut the worm gear. The instantaneous line contact of a fully conjugated gear set becomes an instantaneous point contact when an oversized hob is used.

Paper [18] presents the increasing requirements of high-precision and high bearing capacity in industrial robot and aerospace technology, a novel point-contact hourglass worm drive consisting of an involute helical beveloid (IHB) gear and an oblique planar enveloping (OPE) hourglass worm.

Paper [29] presents a methodology for precisely calculating the tooth thickness of cylindrical worm gear, which is expounded in great detail, with the worm gear in the toroidal surface enveloping cylindrical worm pair, as a sample. This method can calculate the tooth thickness in any cross section of cylindrical worm gear, and it is universal for cylindrical worm gears.

Paper [30] presents an overall process of worm gear drives where all the steps from the idea to the final product are performed integrated on the computer. It is also important to reduce the dynamic loads by different methods. Dynamic Simulation in Autodesk Inventor Professional was chosen to analyze the dynamic operating

conditions of a project in a complete operating cycle. This simulation provides analysis tools that allow the evaluation of product performance in a 3D environment.

Paper [31] presents a meshing performance analysis which makes it possible to use the plane meshing theory and the space enveloping principle to analyze involute worm and helical gear drive. The meshing relationship between the involute worm and the counterpart rack, as well as the counterpart rack and the helical gear are shown, and the computational model of contact ratio and contact ellipse are obtained through the counterpart rack.

2 Mathematical Approach of Archimedean Worm

The worm surface is generated by such cutting tool which has straight-lined blade. This cutting edge is situated in the axial section of the worm [4, 6, 7, 20, 26-28]. The generating lines are in coordinate system C_p , which is connected to the edge of the tool. This coordinate system does rotational and linear motion at the same time, which generates the helical surface of the worm [4, 6, 7, 20, 26-28] on the C_{IR} coordinate system (Figure 1). The transformation matrix between the C_P and C_{IR} systems is:

$$M_{1R,p} = \begin{bmatrix} \cos\theta & -\sin\theta & 0 & 0 \\ \sin\theta & \cos\theta & 0 & 0 \\ 0 & 0 & 1 & \pm p \cdot \theta \\ 0 & 0 & 0 & 1 \end{bmatrix} \quad (1)$$

In case of right-hand worm, Surface side I can be calculated (Figure 1.a):

$$\left. \begin{aligned} x_{1RI} &= \eta \cdot \cos\alpha_{ax} \cdot \cos\theta \\ y_{1RI} &= \eta \cdot \cos\alpha_{ax} \cdot \sin\theta \\ z_{1RI} &= -\eta \cdot \sin\alpha_{ax} + \left(r_0 \cdot \tan\alpha_{ax} - \frac{p_x - s_{ax1}}{2} \right) + p \cdot \theta \end{aligned} \right\} \quad (2)$$

The generated surface on the C_{IR} coordinate system is after giving a helical motion for the C_P coordinate system (Figure 1.b.):

$$\vec{r}_{1R}(\eta, \theta) = M_{1R,p}(\theta) \cdot \vec{r}_p(\eta) \quad (3)$$

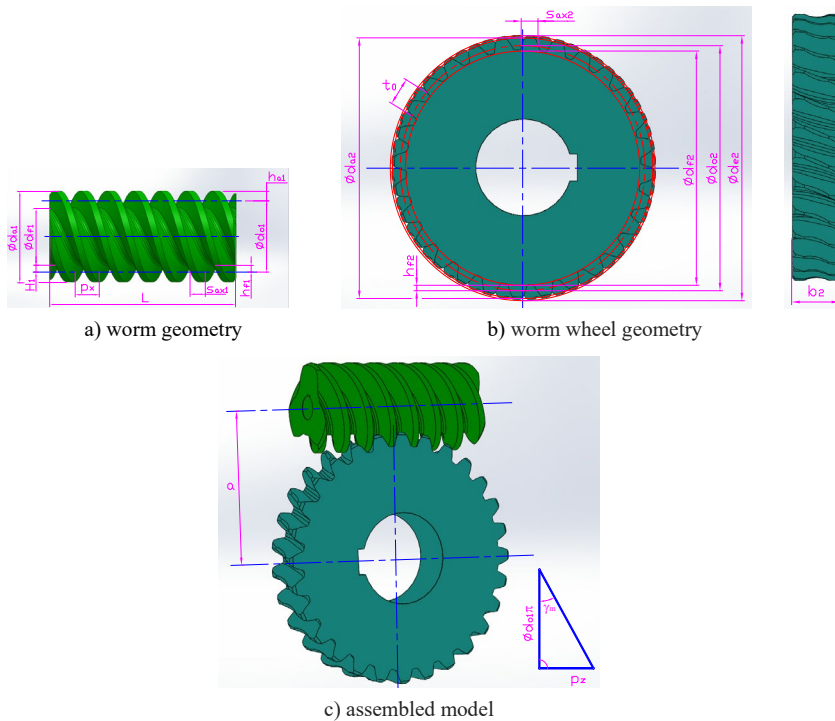
Based on Figure 1. the unit normal vector is [7]:

$$\vec{n}_{1R}(\eta, \theta) = \frac{\partial \vec{r}_{1R}}{\partial \eta} \times \frac{\partial \vec{r}_{1R}}{\partial \theta} \quad (4)$$

process. Using of the detailed formulas an own developed software can be made on an arbitrary programming language to prepare the CAD models of the worm and the worm wheel.

3 Design and Modelling Process

Based on the recommendations of the references [4-8, 13, 14, 16, 20, 21, 27] six types of Archimedean worm gear drives are designed by different axial modules. All the other input parameters are unchanged (f' , c^* , r' , z_1 , z_2 , L , b_2 , α_n , j).



The geometrical parameters of the worm and the worm wheel

Table 1
The calculated parameters of the designed worm gear drives

The parameters of the worm gear drive	I.	II.	III.	IV.	V.	VI.
Axial module (m_{ax}) [mm]	6.5	7	8	9	10	11
Diametral pitch (p_d) [mm]	3.907	3.628	3.175	2.822	2.54	2.309
Normal diametral pitch (p_{dn}) [mm]	4.022	3.751	3.314	2.978	2.712	2.497
Normal module (m_n) [mm]	6.315	6.77	7.662	8.527	9.363	10.168
Worm lead of thread (p_x) [mm]	61.3	66	75.4	84.8	94.2	103.7
Circular pitch of the worm-wheel (t_0) [mm]	20.4	22	25.1	28.3	31.4	34.6
Lead angle (γ_m) [mm]	13.7	14.7	16.7	18.6	20.6	22.4
Addendum coefficient (f')	1					
Clearance coefficient (c^*)	0.2					
Fillet coefficient (r')	0.3					
Number of threads (z_1)	3					
Number of teeth of the worm-wheel (z_2)	28					
Direction of the wheel	right hand					
Pitch diameter of the worm (d_{01}) [mm]	80					
Pitch diameter of the worm-wheel (d_{02}) [mm]	182	196	224	252	280	308
Outside diameter of the worm (d_{a1}) [mm]	93	94	96	98	100	102
Outside diameter of the worm-wheel (d_{a2}) [mm]	199.8	214.9	245.1	275.3	305.5	335.7
Center distance (a) [mm]	131	138	152	166	180	194
Face width of the worm-wheel (b_2) [mm]	50					
Worm length (L) [mm]	200					
Pressure angle (α_{ax}) [°]	20.5	20.6	20.8	21	21.2	21.5
Normal pressure angle (α_n) [°]	20					
Addendum of the worm (h_{a1}) [mm]	6.5	7	8	9	10	11
Addendum of the worm-wheel (h_{a2}) [mm]	6.5	7	8	9	10	11
Dedendum of the worm (h_{f1}) [mm]	7.6	8.2	9.3	10	11.7	12.8
Dedendum of the worm-wheel (h_{f2}) [mm]	7.6	8.2	9.3	10.5	11.7	12.8

Tooth thickness of the worm (S_{ax1}) [mm]	10.2	11	12.6	14.1	15.7	17.3
Tooth thickness of the worm-wheel (S_{ax2}) [mm]	9.2	10	11.6	13.1	14.7	16.3
Fillet radius (r) [mm]	1.9	2.1	2.4	2.7	3	3.3
Backlash (j) [mm]	1					
Transmission ratio (i)	3/28					
Diameter ratio (q)	10					11

4 Analysis of the Contact Surfaces of the Worm Wheel by TCA

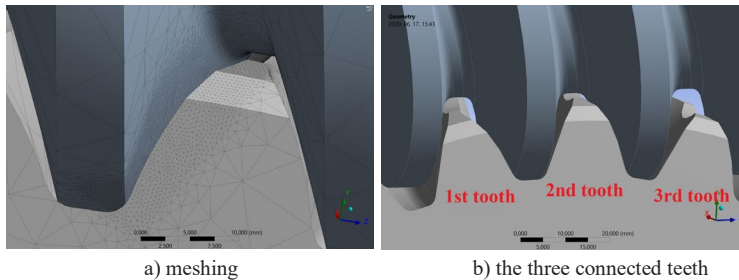


Figure 3

Tooth connection of the elements

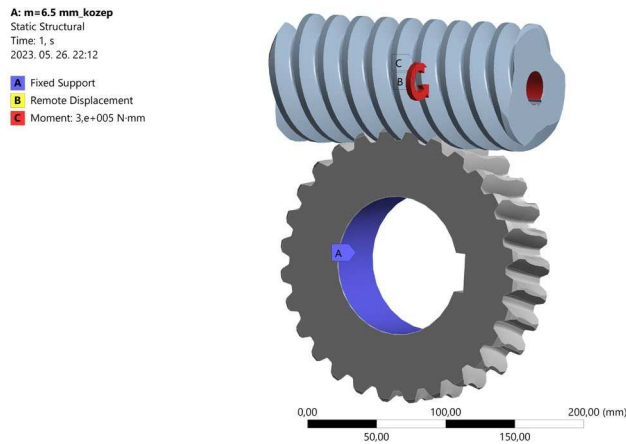


Figure 4

Tooth connection of the elements

Based on the geometrical facts, three worm wheel teeth are connected with the worm at the same time. Each connected tooth is analyzed. The material type of the elements is structural steel [28]. Dense meshing is applied on the analyzed contact

area (Figure 3). The dimension of the element is 0.4 mm. The method is tetrahedrons. Automatic meshing is selected on the outside area. The number of the nodes is 1133014. The number of the elements is 821968. The friction coefficient is $\mu=0.01$ on the contact zone. We suppose low friction between the contact surfaces (worm and worm gear). All degrees of freedom are fixed on the worm wheel. The rotation around the axis of rotation of the worm is permitted, other degrees of freedom are also fixed. The worm is loaded by 300 Nm torque around the axis of rotation. The same load is used for all of the drives (Figure 4).

4.1 Normal Stress Analysis

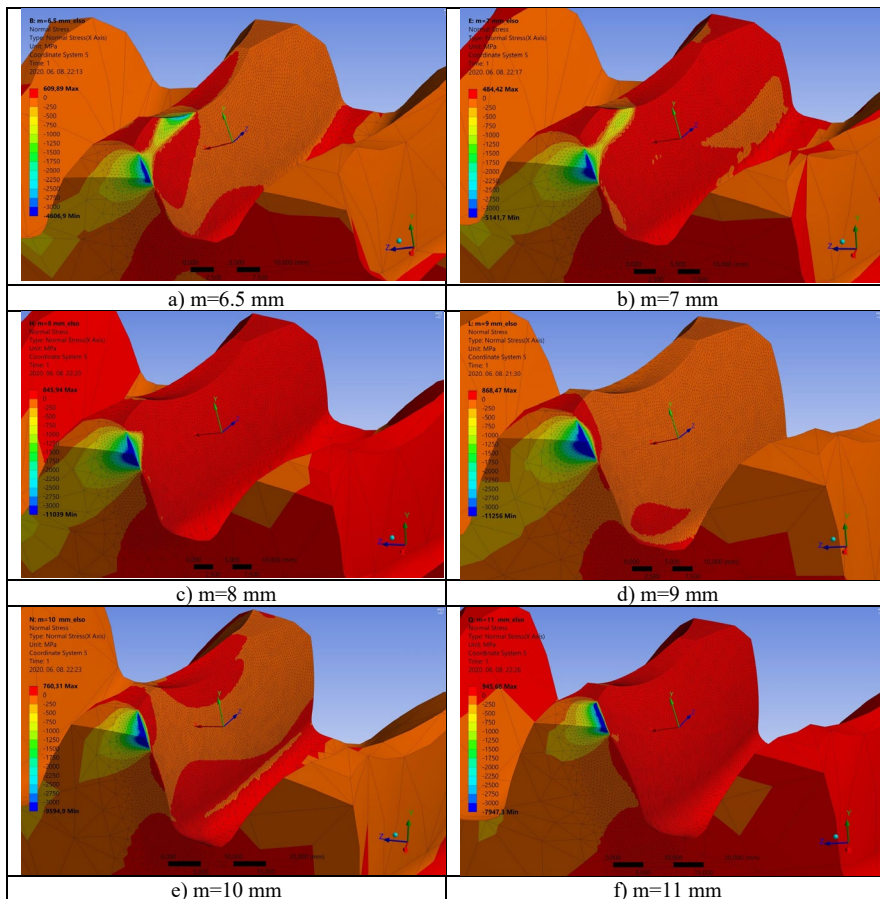


Figure 5

Normal stress results on the 1st tooth

The normal stress is interpreted perpendicularly for the surface of the worm wheel [19] [28]. We analyze the average stress results and the geometrical shape of the impressions on the surfaces of the worm wheels for each connected tooth. The result

on the 1st tooth can be seen on Figure 5. The received contact impressions on the teeth of the worm gears are approached by a lot of peripheral points which are imported to the GeoGebra mathematical software which is a complex mathematical software having a lot of operation possibilities. Using of this software, polygons were inserted at the imported peripheral points. As a result, we attained planar figures, that have areas and perimeters. They can be then calculated, for the comparisons. Figure 6 shows these polygons.

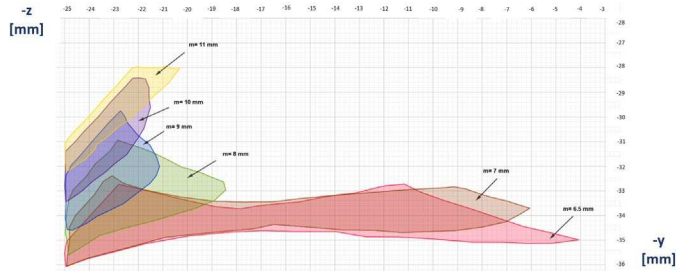


Figure 6

The structure of the stress impressions on the 1st tooth

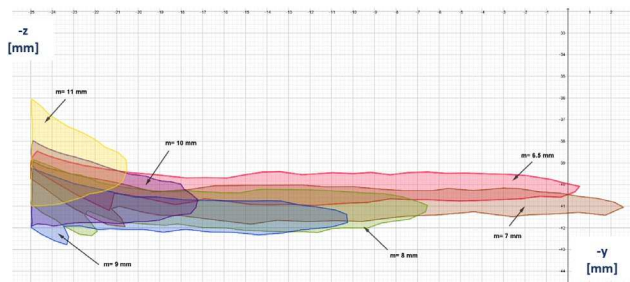


Figure 7

The structure of the stress impressions on the 2nd tooth

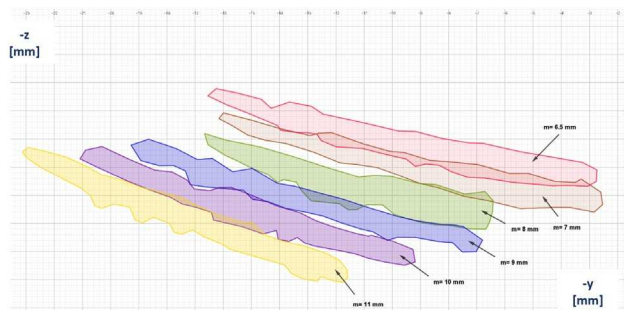


Figure 8

The structure of the stress impressions on the 3rd tooth

Result of the normal stress on the 2nd tooth can be seen on Figure 7. Figure 8 shows the results of normal stress on the 3rd tooth.

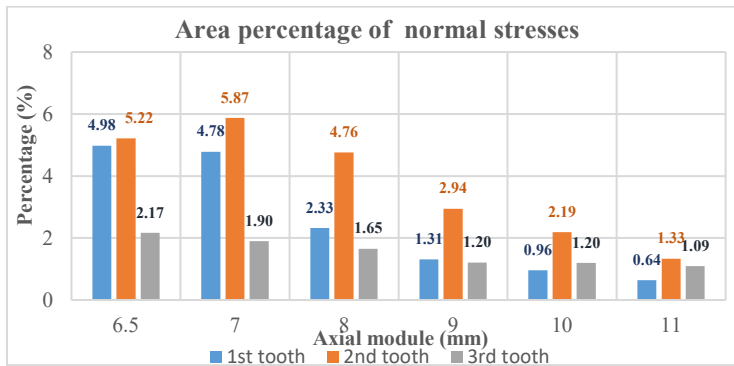


Figure 9

The area percentages of the impressions of the normal stress

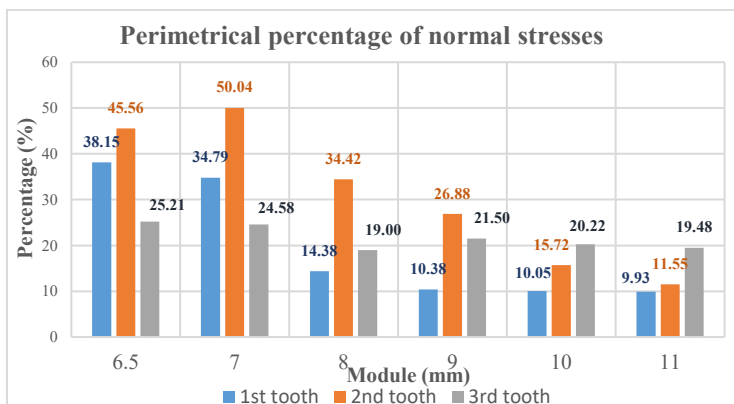


Figure 10

The perimetrical percentages as a result of the normal stress

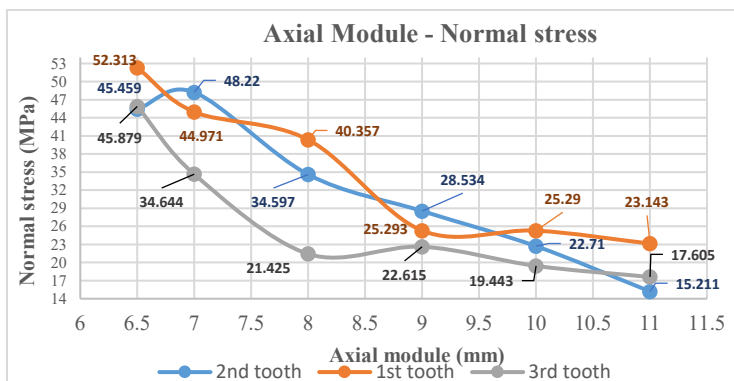


Figure 11

The average normal stress results in the function of the axial module

The geometrical areas of the surfaces of the worm wheels are determined by polygon method. Figure 9 shows the comparison of the contact impressions and the areas of the surfaces of the worm wheels in percentage.

Figure 10 shows the perimetrical percentages for the three teeth on each worm wheels as a result of the normal stress. The correlation between the average normal stress and the axial module can be seen in Figure 11.

4.2 Normal Deformation Analysis

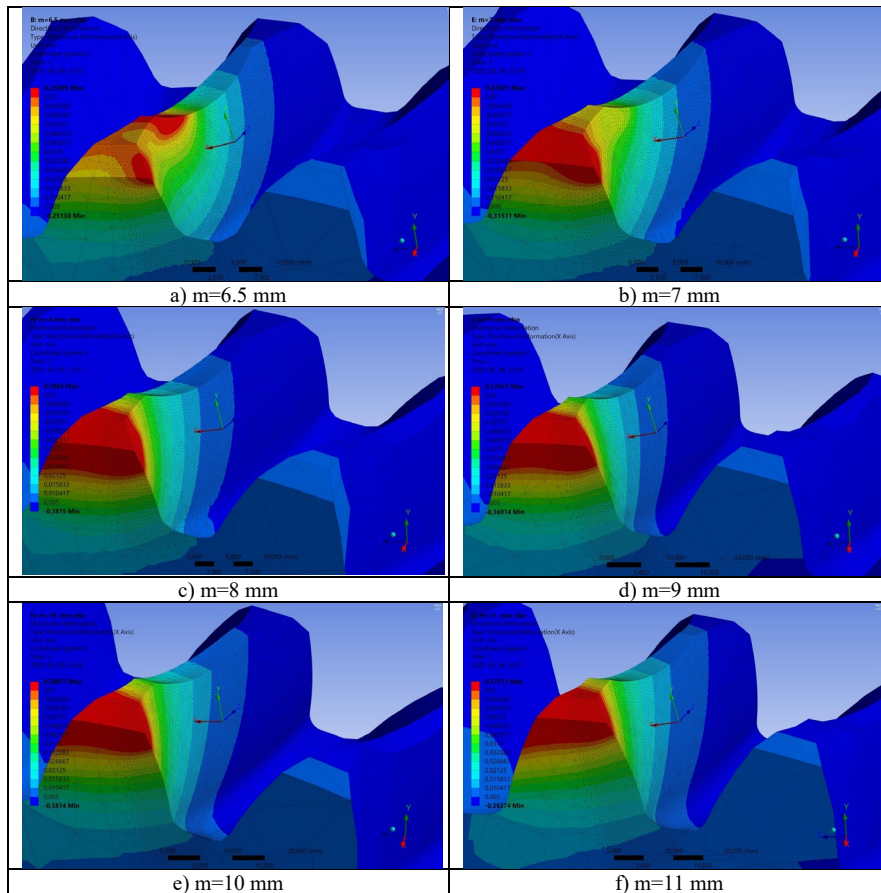


Figure 12

Results of normal deformation on the 1st tooth

The normal deformation is analyzed perpendicularly to the surface of the worm wheel [19] [28]. It was also analyzed for each connecting tooth of the worm wheel. The effects of the deformation zones are saved into the GeoGebra software. We approach the shape of the zones by lines which connect the border points of the

deformation zones (Polygon method). Similarly, to the stress analysis, we receive polygons, of which area and perimeter can be calculated. Figures 12 and 13, show the results for the case of the 1st tooth.

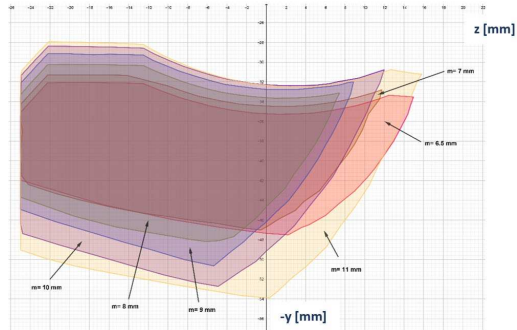


Figure 13

The resulted structure of deformation in case of the 1st tooth

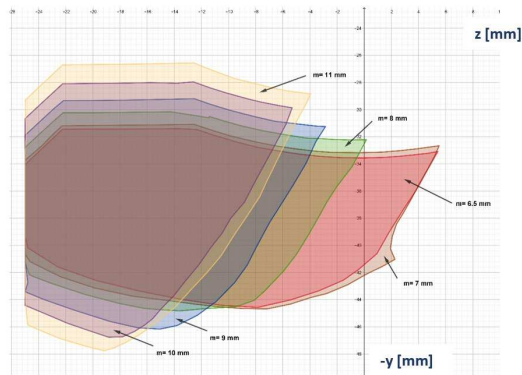


Figure 14

The structure of the deformation impressions on the 2nd tooth

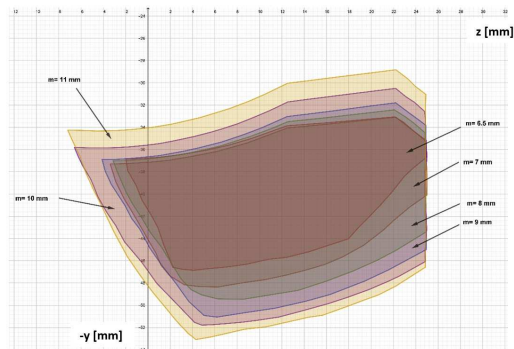


Figure 15

The scheme of the deformation impressions on the 3rd tooth

Figure 14 shows the result of the normal deformation in the 2nd tooth. Figure 15 shows the result of normal deformation in the 3rd tooth.

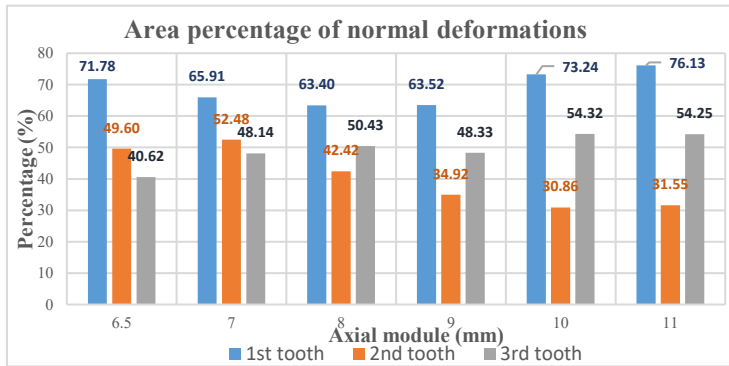


Figure 16

The resulted area percentages due to normal deformation

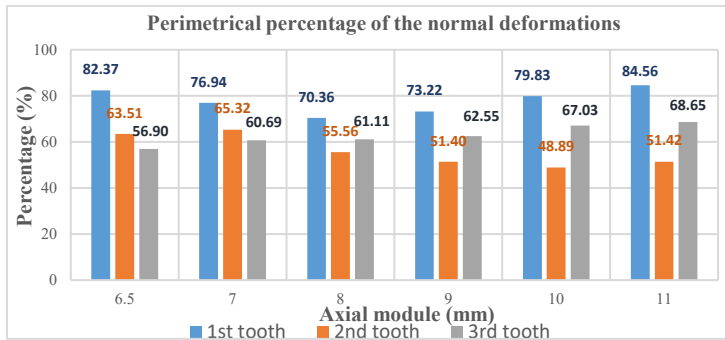


Figure 17

The resulted perimetrical percentages due to normal deformation

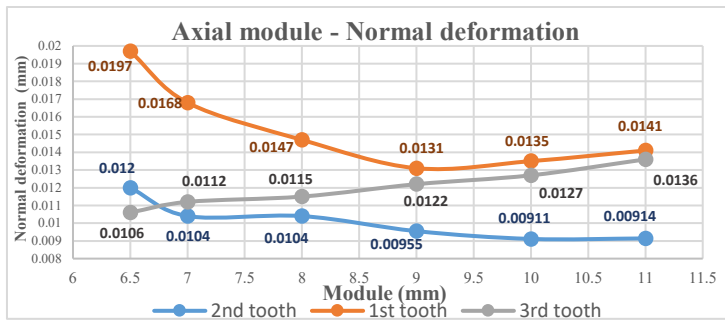


Figure 18

The average result due to normal deformation depending on the axial module

With the knowledge of the resultant areas, due to normal deformation and the whole surfaces of the teeth of the worm wheels, the area percentages can be determined (Figure 16).

Figure 17 shows the perimetrical percentages between the impressions of the normal deformations on the whole surfaces of the worm wheels.

The average normal deformation results in the function of the axial module, for each worm wheel, can be seen on Figure 18.

4.3 Axial- and Radial Deformation Analysis

The average deformations on the connecting teeth are also determined into axial and radial directions on the surfaces of the worm wheels (Figures 19 and 20).

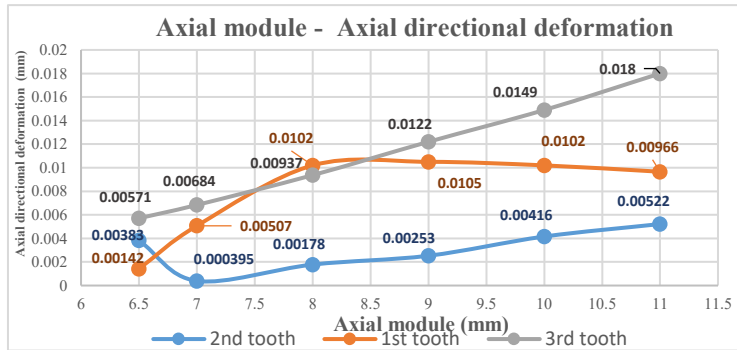


Figure 19

Axial module – axial directional deformation chart

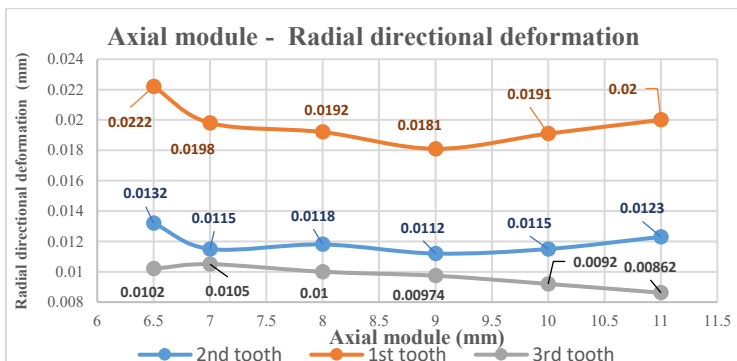


Figure 20

Axial module – radial directional deformation chart

Conclusions

The main property of the Archimedean worm is the linear profile, which is generated on the axial section of the worm, by a straight-lined blade. This geometry is widely used for different gear boxes providing good load transmission and high transmission ratio. That is why the TCA research is important, especially for their geometrical analysis. The mechanical parameters can be defined before the manufacturing and the real application.

The worm is loaded by 300 Nm torque around the axis of rotation in both cases. Analyzing the area percentages of the impressions (Figure 9) of the normal stress the following conclusions can be determined:

- The area percentages are continuously decreasing in the function of the enhancement of the axial module from $m=7$ mm axial module
- The highest percentages are on the 2nd tooth since it is totally in contact
- The results on the 3rd tooth are the lowest until the $m=9$ mm axial module
- After $m=9$ mm axial module the results on the 3rd tooth are higher than on the 1st tooth ($m=10$ mm and $m=11$ mm)

Analyzing the perimetrical percentages of the normal stress (Figure 10) the following conclusions can be determined:

- The results are constantly decreasing as a function of the increase of the axial module
- The highest percentages are on the 2nd tooth until $m=9$ mm axial module
- After $m=9$ mm axial module that the highest results are on the 3rd teeth,
- The lowest results are on the 3rd tooth until $m=7$ mm axial module
- After $m=7$ mm axial module the lowest results are on the 1st teeth

Based on Figure 11, the average normal stress results are fluctuating and increasing depending on the increasing of the axial module. The lowest results are approximately on the 3rd tooth. The highest results on the 1st and 2nd teeth are always fluctuating depending on the axial module.

Analyzing the area percentages of the impressions (Figure 16) of the normal deformations the following conclusions can be determined:

- The highest results are received on the 1st tooth due to the maximum loads. This result decreases until the $m=8$ mm axial module. After that, it starts increasing
- The results for the 2nd and 3rd teeth are continuously fluctuating, depending on the axial module
- The percentage areas of the $m=6.5$ mm and $m=7$ mm axial module are higher on the 2nd tooth than on the 3rd tooth. After that, the results on the 3rd tooth are the second highest

Analyzing the perimetrical percentages of the impressions (Figure 17) of the normal deformations the following conclusions can be determined:

- The highest results are on the 1st tooth, which decreases until $m=8$ mm axial module. After that, the parameter of this tooth starts increasing
- The perimeter percentages of the $m=6.5$ mm and $m=7$ mm axial module of worm wheels are higher on the 2nd tooth, than on the 3rd tooth. After that, the results on the 3rd tooth are the 2nd highest
- The results on the 2nd tooth are continuously fluctuating depending on the axial module
- The results on the 3rd tooth are increasing depending on the axial module

The average normal deformation values are also calculated (Figure 18). The following conclusions can be determined:

- The highest results are received on the 1st tooth, which decreases until $m=9$ mm axial module. After that, this parameter starts increasing. The highest result on the 1st tooth is in case of $m=6.5$ mm axial module
- The results on the 2nd tooth fluctuates and is continuously increasing. It is lower than the results on the 3rd tooth except in case of $m=6.5$ axial module
- The results on the 3rd tooth are continuously increasing depending on the axial module but it is always lower than the results on the 1st tooth

Based on the axial module – axial directional deformation chart (Figure 19) the following conclusions can be determined:

- The lowest results are on the 2nd tooth. It is continuously increasing from $m=7$ mm axial module
- The results on the 1st tooth are increasing until $m=8$ mm axial module. After that, they are decreasing. The highest result is in case of $m=8$ mm axial module
- The results on the 3rd tooth are continuously increasing depending on the axial module
- The results on the 3rd tooth are always higher than on the 2nd tooth

Based on the axial module – radial directional deformation chart (Figure 20) the following conclusions can be determined:

- The highest results are on the 1st tooth. This function is fluctuating. The highest result is in case of $m=6.5$ mm axial module
- The results of the 2nd tooth are also fluctuating. The highest results are in case of $m=6.5$ mm axial module
- The results of the 3rd tooth are continuously decreasing from $m=7$ mm axial module
- The lowest results are on the 3rd tooth

After the evaluation of the results, the geometric design of an Archimedean worm gear drive, is a very complex task. In this study, we analyzed the effects of the modification of the axial module, for the mechanical parameters, on the teeth of the worm wheels. We also shown the area and perimetrical percentages, for each tooth of the worm gear, in the function of the axial module. Our aim was to investigate the modification of the axial module, for the tooth contact zone and determine the dimensions of the tooth contact zone on the teeth of the worm gear. The wider the tooth connection zone, the better the power transmission at the teeth.

Acknowledgements

This research was supported by the **János Bolyai Research Scholarship of the Hungarian Academy of Sciences.**

Dr. Sándor Bodzás one of the authors of this publication, would like to express his great respect to **Prof. Illés Dudás † (2021)** (University of Miskolc, Miskolc, Hungary) who encouraged him and provided many consultations on the reasearch topic of worm gear drives. Prof. Dudás had several publications, scientific books and broad experience in this topic. He was the research leader of Dr. Sándor Bodzás' Ph.D. dissertation that was written in the field of geometric design and manufacturing analysis of conical worm gear drives and supported his work by useful remarks.

Dr. Sándor Bodzás, one of the authors of this publication, would like to express his great respect to **Prof. Tibor Bercsey † (2020)** (Budapest University of Technology and Economics, Budapest, Hungary) who provided many consultations on the reasearch topic of worm gear drives. Prof. Bercsey had several publications and broad experience in this topic. He was one of the reviewers of Dr. Sándor Bodzás' Ph.D. dissertation and supported his work by useful remarks.

References

- [1] Zs. Balajti: *Development of production geometry of kinematical gear drives*, Ph.D. dissertation, Miskolc, University of Miskolc, 2007
- [2] T. Bercsey: *Connection analysis of globoid worm and cylindrical gear having planar tooth surface*, University doctoral dissertation, Budapest, 1971
- [3] T. Bercsey: *Theorem of toroidal drives*, Candidate dissertation, Budapest, 1977
- [4] I. Dudás: *The Theory and Practice of Worm Gear Drives*, Kogan Page US., USA, 2004
- [5] P. Horák: *Tribology analysis of worm gear drives having circular profile*, PhD dissertation, BME, Budapest, 2003
- [6] F. L. Litvin: *Gear geometry and applied theory*, Englewood Cliffs, Prentice Hall, NJ., 1994

- [7] F. L. Litvin, A. Fuentes: *Gear Geometry and Applied Theory*, Cambridge University Press, 2004, ISBN 978 0 521 81517 8
- [8] I. Sz. Krivenko: *New Types of Worm Gears on Ships*, Sudostroenie, Leningrad, 1967
- [9] C. Bolos, M. Ciotea, B. Bucur, V. Bolos: *Modeling the double worm-face gears*, Journal of Industrial Design and Engineering Graphics, Volume 10, 2015
- [10] M. V. Chernets: *Prediction Method of Contact Pressures, Wear and Life of Worm Gears with Archimedean and Involute Worm, Taking Tooth Correction into Account*, Journal of Friction and Wear, 2019, Vol. 40, No. 4, pp. 342-348, ISSN 1068-3666, DOI: 10.3103/S1068366619040032
- [11] K. Kawasaki, I. Tsuji: *Machining method of large-sized cylindrical worm gears with Niemann profiles using CNC machining center*, the International Journal of Advanced Manufacturing Technology, 2019, 104:3717-3729, <https://doi.org/10.1007/s00170-019-04076-4>
- [12] J. Shon, N. Park: *Study on the influence of gear hobbing and shaft misalignments on the geometric interference of cylindrical worm gear set*, Journal of Mechanical Engineering Science, 2016, DOI: 10.1177/0954406216671543
- [13] V. Goldfarb, N. Barmina: *Theory and Practice of Gearing and Transmissions*, Springer, 2016, p. 450, ISBN 978-3-319-19740-1, DOI 10.1007/978-3-319-19740-1
- [14] V. Goldfarb, E. Trubachev, N. Barmina: *Advanced Gear Engineering*, Springer, 2018, p. 497, ISBN 978-3-319-60398-8, DOI 10.1007/978-3-319-60399-5
- [15] Q. Meng, Y. Zhao, J. Cui, Z. Yang: *Meshing theory of mismatched ZC1 worm drive*, Mechanism and Machine Theory, Elsevier, 2020, <https://doi.org/10.1016/j.mechmachtheory.2020.103869>
- [16] V. Vullo: *Gears, Volume 1: Geometric and Kinematic Design*, Springer, 2020, p. 880, ISBN 978-3-030-36501-1, <https://doi.org/10.1007/978-3-030-36502-8>
- [17] J. Sohn, N. Park: *Geometric interference in cylindrical worm gear drives using oversized hob to cut worm gears*, Mechanism and Machine Theory, Elsevier, 2016, <http://dx.doi.org/10.1016/j.mechmachtheory.2016.02.002>
- [18] Z. Zeng, Y. Chen, B. Chen, X. Du, C. Li: *Meshing performance investigations on a novel point-contact hourglass worm drive with backlash-adjustable*, Mechanism and Machine Theory, Elsevier, 2020, <https://doi.org/10.1016/j.mechmachtheory.2020.103841>
- [19] S. Moaveni: *Finite Element Analysis, Theory and Application with ANSYS*, Pearson Education Limited, 2015, ISBN 10: 0-273-77430-1, p. 928

- [20] Z. Terplán: *Machine elements IV.*, manuscript, Tankönyvkiadó, Budapest, 1975, p. 220
- [21] S. P. Radzevich: *Dudley's Handbook of Practical Gear Design and Manufacture*, Third edition, CRC Press, 2016, p. 656, ISBN 9781498753104
- [22] L. Dudás: *Modelling and simulation of a new worm gear drive having point-like contact*, *Engineering with Computers*, 2012, *Engineering with Computers: Volume 29, Issue 3*, 2013, pp. 251-272, ISSN 0177-0667
- [23] F. L. Litvin, I. Gonzalez-Perez, K. Yukishima, A. Fuentes, K. Hayasaka: *Design, simulation of meshing, and contact stresses for an improved worm gear drive*, *Mechanism and Machine Theory*, Elsevier, Volume 42, Issue 8, 2007, pp. 940-959, <https://doi.org/10.1016/j.mechmachtheory.2006.08.005>
- [24] T. Nieszporek, R. Gołębski, L. Soos: *Analysis of the worm-wheel toothing accuracy*, *Technical Gazette*, 24(4), 2017, 993-1000, <https://doi.org/10.17559/TV-20160422094400>
- [25] S. Bodzás: *Connection analysis of conical worm-, face gear- and tool surfaces*, PhD dissertation, University of Miskolc, 2014, p. 154
- [26] K. Bányai: *Inspection and production geometry of cylindrical worm gears*, University Doctoral Dissertation, Miskolc, 1977
- [27] D. Maros, V. Killman, V. Rohonyi: *Worm gear drives*, Műszaki Könyvkiadó, Budapest, 1970
- [28] S. Bodzás: *Computer-aided design and loaded tooth contact analyses of bevel gear pair having straight teeth by different loaded torques*, *Mechanics & Industry* 21 : 1 Paper: 109, 2020, <https://doi.org/10.1051/meca/2019076>
- [29] J. Cui, Y. Zhao, Q. Meng, G. Li: *Calculation method for tooth thickness of cylindrical worm gear*, *Forsch Ingenieurwes*, 2021 <https://doi.org/10.1007/s10010-021-00539-x>
- [30] A. B. Pop, A. M. Țițu: *Dynamic Simulation of Worm Gears Using CAD Applications*. In: Karabegović I. (eds) *New Technologies, Development and Application IV*. NT 2021. *Lecture Notes in Networks and Systems*, Vol. 233, Springer, Cham. https://doi.org/10.1007/978-3-030-75275-0_32
- [31] B. Lu, Y. Chen, L. Shixuan, C. Bingkui: *Meshing performance investigations of involute worm and helical gear drive based on counterpart rack*, 2021, *J Mech Sci Technol* 35, 3533-3548, <https://doi.org/10.1007/s12206-021-0725-7>

Nomenclature

$\vec{v}_{1R}^{(12)}$	(mm/min ⁻¹)	Relative velocity vector
\vec{n}_{1R}		Normal vector of the surface in C_{1R} coordinate system
\vec{r}_{1R}		Placement vector of the moving points of the profile curve
\vec{r}_P		Position vector of the generating curve of the tool surface

$M_{1R,P}$		Coordinate transformation matrix (transforms C_P to C_{1R})
O_{1R}, O_P		Origins of the appropriate coordinate systems
$C_{1R} (X_{1R}, Y_{1R}, Z_{1R})$		Rotational coordinate system related to the worm
$C_P (X_P, Y_P, Z_P)$		Tool coordinate system of generating curve
x, y, z	(mm)	Coordinates
η, θ		Internal parameters of the helicoidal surface
m_{ax}	(mm)	Axial module
p_d	(mm)	Diametral pitch
p_{dn}	(mm)	Normal diametral pitch
m_n	(mm)	Normal module
p_x	(mm)	Worm lead of thread
t_0	(mm)	Circular pitch of the worm-wheel
γ_m	(mm)	Lead angle
f^*		Addendum coefficient
c^*		Clearance coefficient
r^*		Fillet coefficient
Z_1		Number of threads
Z_2		Number of teeth of the worm-wheel
d_{01}	(mm)	Pitch diameter of the worm
d_{02}	(mm)	Pitch diameter of the worm-wheel
d_{a1}	(mm)	Outside diameter of the worm
d_{a2}	(mm)	Outside diameter of the worm-wheel
a	(mm)	Center distance
b_2	(mm)	Face width of the worm-wheel
L	(mm)	Worm length
α_{ax}	(°)	Pressure angle
α_n	(°)	Normal pressure angle
h_{a1}	(mm)	Addendum of the worm
h_{a2}	(mm)	Addendum of the worm-wheel
h_{f1}	(mm)	Dedendum of the worm
h_{f2}	(mm)	Dedendum of the worm-wheel
S_{ax1}	(mm)	Tooth thickness of the worm
S_{ax2}	(mm)	Tooth thickness of the worm-wheel
r	(mm)	Fillet radius
j	(mm)	Backlash
i		Transmission ratio
q		Diameter ratio
M	(Nm)	Load torque
μ		Friction coefficient
TCA		Tooth Contact Analysis
CAD		Computer Aided Design

A Network Management Solution for Pre-Alarm Detection in EPU Telecommunications Network

Mihailo Stanić, Aleksandar Lebl, Dragan Mitić, Žarko Markov

Institute for Telecommunications and Electronics, IRITEL A.D. BELGRADE
Batajnički put 23, 11080 Belgrade, Serbia
E-mails: mihailo@iritel.com; lebl@iritel.com; mita@iritel.com;
zmarkov@iritel.com

Abstract: The pre-alarm detection is a novel method for ensuring high availability of operational traffic in corporate telephone network of Electric Power Utility, beside usage of redundant elements and alternate routing. In this paper, is examined software solution for pre-alarm detection in network management domain. After the analysis of the domain characteristics was proposed solution based on analysis of traffic on direct links between telephone exchanges. In order to find when high priority Integrated Service Digital Network (ISDN) or Internet Protocol (IP) links are faulty, calls over high voltage power lines are analysed in two step process, using data retrieved from Call Detail Records of telephone exchanges. Increased accuracy of detection characterizes this solution compared with the previously proposed, because there are no false negatives in the detection process. In this research was verified that proposed solution can be implemented as an additional layer in network management hierarchy without change of existing network management system software or infrastructure.

Keywords: Electric power utility; High availability; Network management; Telephone network; Call detail record

1 Introduction

Telecommunications network in Electric Power Utility (EPU) is used to enable communication between its employees [1]. The role of telephone network in telecommunications network of EPU is to enable communication between Power Grid operators, and even in some countries its design is required by the government regulations, as explained in [2]. Frequency bands and power levels for communications over power line systems are defined in international recommendations [3]. The main objective of building separate network is achieving high availability because on emergency on power facility information

exchange between operators must be possible. The reliable and prolonged life is the subject of analysis for each implemented network type. For example, the same problem as in the case of telecommunications network in EPU may be also found in wireless sensor network implementation [4].

The telephone network in EPU differs from the public telephone network by introduction of prioritized traffic (operator traffic is with priority), usage of high voltage power lines like communications resources and solutions for maintaining high availability. It is demonstrated [5] that these methods can be improved, by using so-called pre-alarm detection, which is based on telephone traffic statistics. In the previous research was analyzed call statistics, defined efficiency parameters and proposed hardware implementation of detector as solution. In this paper, we are examining software solution in network management domain, as an extension of our research presented in [5-7].

After this introduction, in the Section 2 are summarized known methods for achieving high availability in telephone network of EPU, and process of occurrence of pre-alarm state. In the Section 3 is presented previous research on parameters used to measure detection efficiency.

In the Section 4 are analysed required characteristics of solution in network management domain, as well as their influence on detection process. In the Section 5 is provided detailed proposal of the pre-alarm detection software using information stored in Call Detail Record (CDR) of telephone exchange. The proposed algorithm is described, as well as its Impact on efficiency parameters. In Section 6 is described verification of the proposal. Behaviour of implemented pre-alarm detection software is described together with symbolic presentation of the traffic process. At the end, the conclusion is in the Section 7.

2 Known Methods for Achieving High Availability in the Telephone Network of EPU

Availability of telephone network of EPU represents the portion of time when it is working correctly. By high availability is considered availability of at least 99,999%.

Methods for increasing availability of the telephone network in EPU are alternate routing and redundant elements usage. In contrast to public telephone network, which is hierarchically organized, telephone network of EPU is built in one layer to enable usage of alternate routing. This procedure enables usage of another path when the first order route is not available. Alternate routing is used in two occasions: link failure (when the link is not available) and congestion on priority link. When the network operates without failures, calls are established according to the routing plan, using direct or shortest paths, and best quality links.

Redundant resources are used to improve the system availability, and emphasis is on redundant links.

Telephone network of EPU may be represented by nodes (telephone exchanges) and links. Despite electrical grid is built for electrical energy delivery, its complex interconnected structure can be used in communication network [1], [8]. Power Line Carrier Communication (PLCC) is a technology used for voice and data communication over high voltage power lines (over 50 kV) [9]. This technology operates using modulated carrier signals on the power lines [10], and it is used in the design of telephone network in EPU. Priority of links between two nodes is based on their characteristics (connection set-up time, speech quality. etc.) and therefore PLCC link is with the lowest priority. Since existing power lines make alternative networking infrastructure [10-11], PLCC links are widely used as telephone network of EPU.

The nodes, which are telephone exchanges when considering EPU telephone network, are in fact huge transformer stations with its engaged personnel. The primary personnel duty is to keep reliable electric power delivery and high telephone network availability. In order to achieve it, the personnel presence in network nodes is mandatory, which allows prompt reaction to each incident situation related to telephone network operation. The solution presented in this paper is based on software analysis. It is relatively simple procedure used to detect locally, on each node, system behaviour for traffic sources seizure and release. Since it is performed locally, the local personnel can provide immediate reaction in order to repair the network. Summary information if the pre-alarm exists on local link can be transferred to the network operations center. This can be achieved in different ways, of which one is explained in [12].

Since it is performed locally, time for network repair is shorter or same as if centralized management system is applied as the one presented in [13] for mobile operator networks supervision. Besides the possibility for faster reaction, the advantages of such a concept of local supervision are that there is no need for complex data mining over the numerous often non-useful alarms to detect root cause using specifically developed algorithms as in [14]. High accuracy of detection and quick response of local personnel are reason why it is also not necessary to use build complex software systems based on machine learning for analysis of data in order to enhance responsiveness in managing a large set of alarms [15].

Simplified model of links between two nodes in the network of EPU is presented in Figure 1. It was demonstrated [5], [7] that detection on one direct connection between two nodes is possible, without the need for information of call routing in the network. Since pre-alarm detection is performed locally, detection is not affected neither by network topology nor number of nodes in the network.

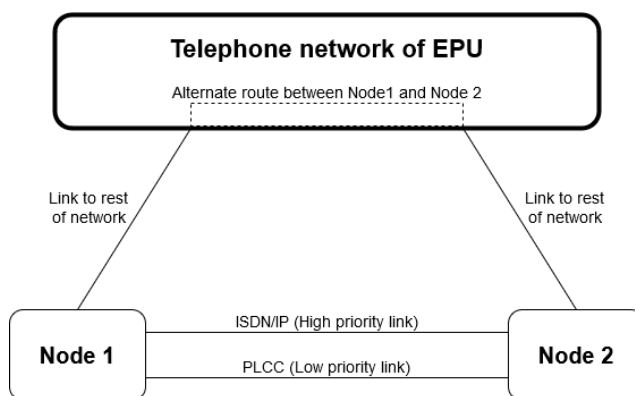


Figure 1

Model with two network nodes connected with one ISDN or IP link, and one PLCC link between two nodes

In this model, there are two direct links between nodes. Link of high priority may be Internet Protocol (IP) or Integrated Service Digital Network (ISDN) realized on optical cables, and PLCC link is of low priority.

The low priority link can be used in two cases [16]:

- 1) traffic is increased over the capacity of the other direct link (traffic overflow);
- 2) there is a failure on high priority link, therefore, the only direct link without failure between two nodes is low priority link.

The pre-alarm state means that high priority link is with failure and that lower priority link is used [5-7]. Direct traffic between two nodes still exist during pre-alarm state because decreased amount of traffic is carried over lower priority link, and availability is not affected. Such unwanted situation, which may precede alarm situation and complete link failure, is possible to be detected during initiated call by using statistically determined time duration of its dialing phase. There is a difference in the called party number selection on the old PLCC links and on more modern ISDN or IP links: the slowest pulse dialing is applied on PLCC link, while faster address messages are used in two other cases. This difference is used in the solution presented in [6] to implement test calls generation from a central point and to measure the time to ring-back tone. The problem solved in [7] is the same as in this paper, but in this paper are used different specific parameters of telephone call. As a conclusion, it may be said that detection is localized on single link in [7] and in this paper, i.e., test is performed separately for each link.

Since telephone traffic is still carried during pre-alarm state between two nodes, pre-alarm state is not detected in telephone network of EPU, nor it can be recognized by degradation of telephone service [5]. If the pre-alarm is not recognized, the failure might affect low priority link, and alarm state might become.

Alarm state in the network occurs when all links between two nodes are with failure, and there is no direct traffic between them. If the alternate routes are used for direct traffic, there is no traffic between two nodes which is not acceptable. It means that during alarm state the availability is affected.

3 Detector Efficiency Parameters

This chapter summarize results on research on efficiency parameters definition and provides formulas for multiple steps detection [5], [7].

It is demonstrated [5] that in telephone network of an EPU the analysis of telephone traffic can be used for pre-alarm detection using so-called detector. The detector is hardware system that locally monitors state of PLCC link. In detection is used characteristic of PLCC link that its state can be found using simple algorithms based on short seizures that are undetected by the detector [5]. It is more complex to determine state of high priority link, especially if the problem is in the switching systems (for example, in the signalization protocol). The principles of faulty link detection, presented in this paper, are universal and may be implemented in various types of networks [17].

The detection process can be performed in multiple steps. In the first step of detection, it is recognized that PLCC is seized (start of the call). After its release (end of the call), the timer is turned and it ticks during so-called detection interval. If the PLCC is used during that interval (the next call starts), the system goes to the next step. In the last step, upon the seizure of PLCC, pre-alarm is declared.

Possible detection results and their corresponding probabilities are presented in Table 1 for detector with K steps. As indicated, detection can be wrong in two cases: when non-existent pre-alarm is detected (false pre-alarm, false positive) and when the existent pre-alarm is not detected (miss in detection, false negative).

The state of traffic in whole network can affect the behaviour of the monitored link, which is still operational, if serious accident happens in distant part of the network. It would be the case when multiple links are not functional (or PLCC is used for traffic) and it is not possible to use alternate routing. In this hypothetical situation the observed link will be used to transit large number of connections and then it would be possible that pre-alarm or alarm state occurs on this link, although the locally generated traffic is not increased. As in normal operation false pre-alarm state is extremely rare, practically impossible, experimental verification of the developed solution in praxis is only possible by the test procedure which would include artificially stopping the data flow over the great number of carefully selected links in the network and thus causing the great traffic over the observed link.

Table 1
Detection results and their probabilities

link state (ISDN/IP link)	pre- alarm state (ISDN/IP link)	pre-alarm state (Detector)	result	characte- ristic	probability
Correct	Inactive	Inactive	Correct	-	-
		Active	<i>Wrong</i>	<i>False pre- alarm</i>	P_{fpaK}
Failure	Active	Inactive	<i>Wrong</i>	<i>Miss in detection</i>	P_{mK}
		Active	Correct	-	-

The probability of false pre-alarm P_{fpaK} is the product of two probabilities:

- 1) For first step probability that call arrives on PLCC (P_{onPLCC}) due to the overflow traffic;
- 2) From steps 2 to K probability that at least one new call arrives on PLCC during timer interval T_K . This implies that call from previous step must be finished, in order that PLCC can accept new call. The value of this probability for single step is $P_{call}(T_K)$, so for $K-1$ steps it is $P_{call}^{K-1}(T_K)$. The probability $P_{call}(T_K)$ presents excluded probability of interval without call arrivals from probability of all possible call arrivals:

$$P_{fpaK} = P_{onPLCC} \cdot P_{call}^{K-1}(T_K) \approx E_{n+1}(A) \cdot \left(1 - e^{-\frac{T_K}{T_{ia}} E_n(A)} \right)^{K-1} \quad (1)$$

where $E_n(A)$ is Erlang formula - the blocking probability (call congestion) in the group with n channels on ISDN or IP link with offered traffic A , $E_{n+1}(A)$ is the blocking probability in the group with n channels on ISDN or IP link and one channel that exists on the PLCC, T_{ia} is the mean inter-arrival time between calls, and T_K is detection interval. This is our original equation and it follows from [7].

The probability of miss in detection P_{m2} is calculated in system with failure on link with priority. It is the probability that after the end of call, during the timer interval next call doesn't arrive on PLCC:

$$P_{mK} = P_{m2} \cdot \sum_{i=0}^{K-2} (1 - P_{m2})^i \quad (2)$$

where P_{m2} is probability of miss in detection for two steps detector and it is:

$$P_{m2} \approx e^{-\frac{T_2}{T_{ia}}} \quad (3)$$

The third important parameter is meantime from failure to detection of pre-alarm state, T_{dpaK} . It is the sum of mean inter-arrival time after the failure occurs and mean call duration t_m and mean inter-arrival time before next call arrives for each step:

$$T_{dpaK} = T_{ia} + (t_m + T_{ia}) \cdot (K - 1) = K \cdot T_{ia} + (K - 1) \cdot t_m \quad (4)$$

It is concluded [5] that in most cases two steps detector can be used because the increased number of test steps provide small improvement of detection miss and false pre-alarm probability, but gradually degrades detection time.

4 Analysis of Network Management Domain for Pre-Alarm Detection

The network management is used for the establishment of services in the telecommunication network of EPU. The operation includes interaction of software system used for network management with software systems on the network element. Full specification of those management systems doesn't exist, and their implementations can be proprietary or based on various standards [18].

Management of telephone network of EPU is complex due to the diversification of vendors and adding new generation of equipment without discarding existing one. When the equipment of various vendors is used, various information models and even various communication protocols are used, which are mostly proprietary in the older generations of equipment. Previously telephone exchanges were designed specifically for EPU, but now the equipment used in Public Switched Telephone Network (PSTN) is the first choice for network upgrade. There are two reasons for this change: increased availability compared with the previous generations of devices [19] and economic benefit of using solutions from PSTN.

As mentioned in Section 2, there is no specification of pre-alarm detection, but using management systems some of its side-effects can be recognized. In the network management systems single link is not treated as network element. Its monitoring is performed by collecting information from network elements on both sides of the link. These network elements can be transmission systems or switching systems. Failures on the transmission system can be detected, but not all the failures on the switching system.

The objective of this paper is the design of a solution for pre-alarm detection using management information from one network element. To apply the proposed solution necessary information must exist on the network element, and management system must have access to that information, which shall include:

- 1) identification of used link for the call, and

- 2) start of the call time
- 3) end of the call time

One example of a record which contains call parameters may be found in [20]. In this example is necessary to include source (“channel”) or destination channel (“dstchannel”) to determine the used calling party or called party link (channel), “start” or “answer” to determine the time of the call beginning and “end” to determine the time of call end.

In the case when described necessary information does not exist on the network element, the modification of the software system on element is needed, which is unwanted consequence. Reason for this is that usually vendors don’t deliver programming code of software systems, so only they can make modifications on existed systems, which makes price of this operation higher. There are further problems: various hardware and software versions make maintenance difficult, sometime vendor doesn’t exist anymore, etc. Principally, adding non-existing features on the delivered network elements shouldn’t be considered.

Another important consideration is the organisation of data access to necessary information. Instead of direct access to network element, this paper proposes use of Northbound (integration) interface of the network management systems. This can localize the knowledge of information models and network protocols on the existing network management systems. Further, this proposal leads to one more important characteristic: it can be implemented as the additional layer in the network management hierarchy.

5 Pre-Alarm Detection Software Solution Proposal

Recently there were various efforts for usage of data stored in CDR for analysis of users behaviour in mobile communications network [21-22] and in this paper is accepted the same approach. In mentioned papers are analysed systems with generated large amount of data, which is collected during long period. In this system, the small portions of data should be collected in short intervals.

In classic telephony, CDR information is used for accounting, and it is produced by telephone exchanges. Since the objective of the telephone network of EPU is to provide telephone calls between dispatchers, presence of accounting information is not mandatory in telephone exchanges. Therefore, major of telephone exchanges specialized for telephone network of EPU is not storing accounting data. When telephone exchanges from PSTN are used, accounting information is stored on them, including CDR.

Format and structure of CDR are not standardized, and therefore their implementation is vendor specific. This paper uses assumption that information

that should be stored in CDR contains information on used channels and of the start of the call, because it is mandatory for determining rates between operators. It is also considered that this information can be accessed immediately after the start of the call.

Collecting information from any network element can be performed in two possible ways: by sending events or by polling. Call arrival is not treated as event in the existing system specification. Changes on software system of network element would be needed for the event-based mechanism, which is not an acceptable option (Section 4). Therefore, polling principle was selected.

The system performs in two steps, presented in Figure 2. The solution is based on the concept of two step detector [5]. The principal difference from the solution in [5] is that in this solution is used timer that is active during the whole program execution and that system behaviour is initiated by timer ticks. The pre-alarm is detected if the second call arrives on PLCC during the detection interval. Step 1 begins after the system is initialized and timer is started. After timer tick, information from CDR between two successive polls is processed. If the information of the start of the call on PLCC is found in processed data, system goes to step 2. Otherwise, system waits next timer tick to repeat the same steps.

Step 2 starts with the timer tick, and the end of call (started in step 1) is awaited. After this event information about calls between two consequent timer ticks is polled from CDR and processed. The arrival of the first call is awaited. When the call arrives, the route of the call is analysed. If no call arrived on PLCC, it is assumed that the first call arrived due to the increased traffic, and the detector returns to the first step. If the call arrived on PLCC, pre-alarm state is detected.

System presents pre-alarm detection until the user's action (acknowledgement of pre-alarm), and then returns to step 1.

It is enough to have single detection software on any of two nodes to detect pre-alarm in the model with two directly connected nodes, presented in Figure 1. The traffic doesn't stop during pre-alarm, therefore, it can be detected on any node.

There are changes in the efficiency parameters of this solution, compared to those of two steps detector [5]. Software timer interval T_T is used as detection interval length.

The probability of the occurrence of false pre-alarm upon (1) is:

$$P_{fpa} = E_{n+1}(A) \cdot \left(1 - e^{-\left(\frac{T_T}{T_{ia}} \cdot E_n(A)\right)} \right) \quad (5)$$

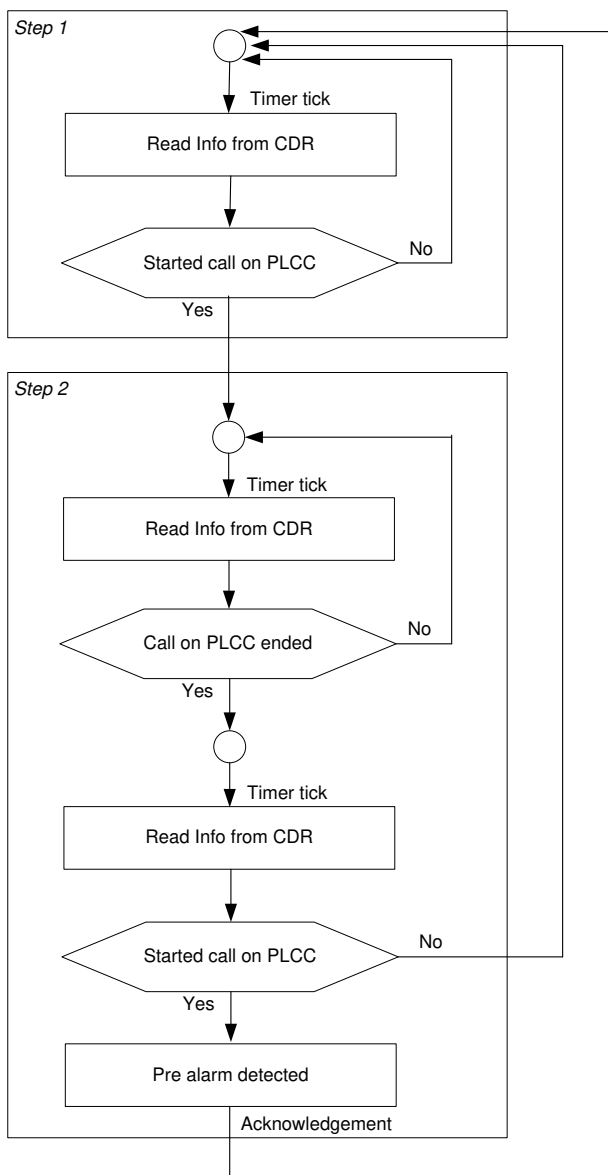


Figure 2
Algorithm of system behavior

The important improvement is that described solution cannot create the miss in detection because the second step is extended until the call arrives, and its probability P_m is:

$$P_m = 0 \tag{6}$$

Since detection is executed in discrete intervals of the length T_T , mean detection time T_{dpa} can be presented as integer number of those intervals. It is assumed that length of timer interval is at least equal to inter-arrival time between two calls (T_{ia}). The mean call duration t_m can be presented as the integer number of timer intervals increased by one. The resulting formula is:

$$T_{dpa} = 2 \cdot T_T + t_m = 2 \cdot T_T + \left(\left\lceil \frac{t_m}{T_T} \right\rceil + 1 \right) \cdot T_T = \left(\left\lceil \frac{t_m}{T_T} \right\rceil + 3 \right) \cdot T_T \quad (7)$$

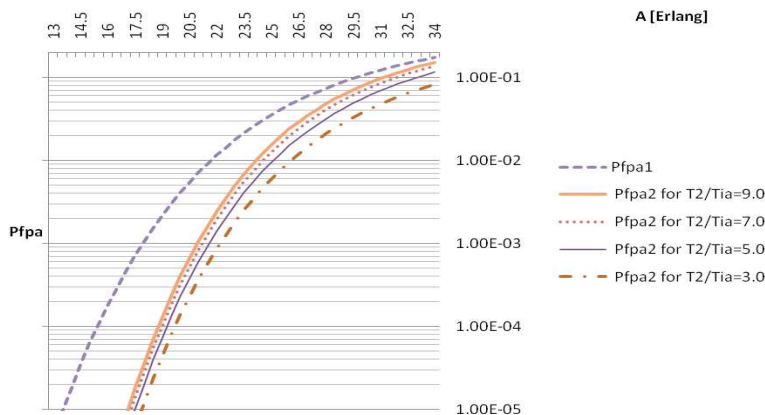


Figure 3

Probability of false pre-alarm (P_{fpa}) as the function of offered traffic (A) for two-step detector in the system with 30-channel ISDN link [23]

Figure 3 presents the values of false pre-alarm probability (P_{fpa}) as the function of offered traffic (A) calculated according to formula (1). These values are presented for two-step detector ($K=2$ in (1)) and for the 30-channel ISDN system (primary ISDN interface) as the link of the first choice. The graphs are presented for 4 various ratios of detection time and mean calls inter-arrival time (T_2/T_{ia}). The fifth graph for probability of false pre-alarm for one-step detector (P_{fpa1}) is presented for the comparison. It is important to emphasize which traffic values are real in EPU network. As transformer station personnel is not huge (surely not more than 10 people), it is not possible to have more than 10 simultaneous local connections. This means that the locally generated traffic may not be over 10E. It is possible to have also several transit connections due to the specific structure of EPU telephone network which is not hierarchical, but the number of these connections is not more than 5. Therefore, the total traffic in EPU network nodes is less than 15E. It means that the typical values of P_{fpa} are lower than 10^{-5} according to the graph from the Figure 3, or in other words practical values of P_{fpa} are very small. Even more important is that detection algorithm is adjusted to reach the probability of detection miss equal to 0 according to (6).

The improvement in detector performances compared with other solutions is related first to [7]. In [7] P_{fpa} has been determined in the same way as in this paper, but the second step in the detection period has not been spread until the next call arrival. This is the significant improvement because P_m according to the detection procedure in [7] has a low value, but typically higher than it is the value of P_{fpa} .

The second comparison is made to the solution from [6]. When considering the values of P_{fpa} and P_m obtained according to the algorithm presented in this paper and the solution from [6], it can be concluded that the presented results are better. It is possible to reach the value $P_m=0$ according to [6], but the corresponding P_{fpa} may be higher than 10^{-5} . It is possible to decrease P_{fpa} , but then it becomes $P_{fpa}>0$. The other difference is that it is necessary to generate test calls to realize the analysis according to [6]. For the procedure realization according to this paper it is enough to keep track of the existing traffic flow.

6 Proposal Verification

Verification of the proposed solution is made by implementing a Java application as the pre-alarm detection software. The diagram on Figure 4 presents the organization of the implemented system.

Existing system includes Telephone exchange and its Network Management System. Both systems were developed by IRITEL [24].

Pre-alarm detection software creates new layer in the system. It was added on top of the existing system (Figure 4), without influence on Telephone Exchange, and without modification in network management system software organization or in its infrastructure. In order to detect the pre-alarm, information from CDR of network management system was analysed. The application was accessing it in eXtensible Markup Language (XML) data format, which can encapsulate any other format - including proprietary one.

List of events from CDR are analysed in each timer tick. Timer tick initiates collection of events list between two successive ticks. Events in the list are analysed, and detection is made upon information on: time of occurrence, is this call on PLCC, and if this is start or end of the call.

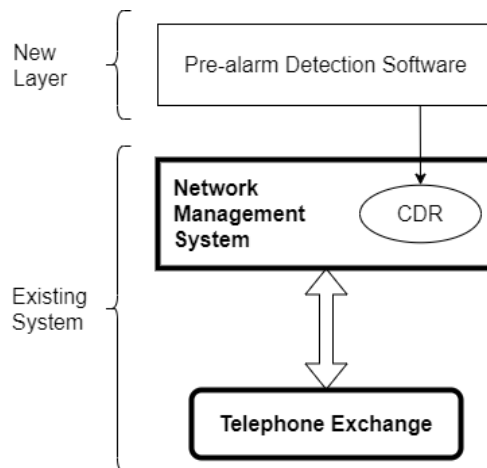


Figure 4
Organization of the implemented system

The state transition diagram of the detector is presented in the Figure 5:

- 1) Detector is in the inactive state in the start.
On each timer tick is collected data from CDR generated between last two ticks.
- 2) Detector remains in this state until the call arrives on PLCC, when it starts waiting the end of this call.
Pre-alarm detection software needs to discover which new calls arrived in the collected events list, and to recognize link where the call is routed. When the call is routed on PLCC, its end is awaited.
- 3) After the call ended, detector waits start of the next call.
On timer tick, data generated between last two ticks is collected from CDR, and then analysed if new call arrives.
- 4) If the call arrived, but not on PLCC, the system goes to Inactive state,
This means that in collected data between last two ticks from CDR call is recognized on high priority link. Detector concluded that previous call on PLCC was due to the overflow traffic.
- 5) If the call arrived on PLCC, the system goes to the pre-alarm detected state, where it remains until the user acknowledges pre-alarm.
This means that pre-alarm is detected by finding next call on PLCC, in data collected from CDR between last two ticks.

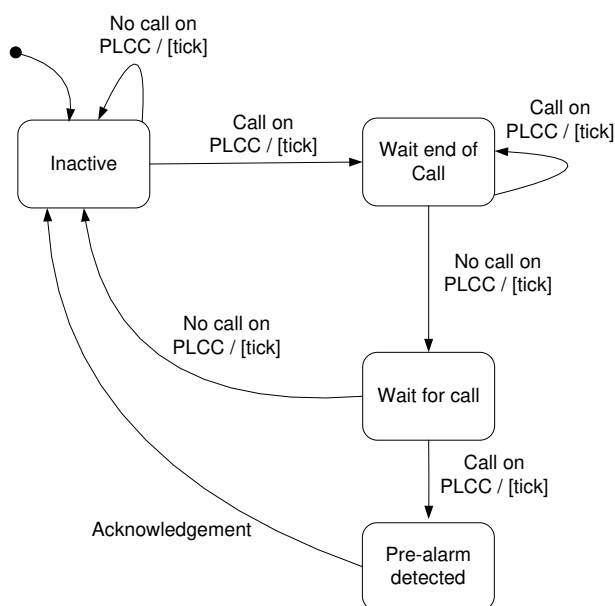


Figure 5
Pre-alarm detector state transition

Correct system behaviour is illustrated in Figure 6. Symbolic presentation of the traffic process on PLCC is based on detection diagrams introduced for two step detector [5] which consist of: *a)* carried traffic of the system, *b)* call arrival in the system, *c)* call arrivals on ISDN or IP link, *d)* call arrivals on PLCC link and *e)* traffic process on PLCC. Timer ticks are presented using dashed lines, and each timer interval is numbered. Moments of the occurrence of failure t_0 and detection t_d are presented.

In illustrative example in Figure 6, during interval 1, calls arrive only on priority link, and system resides in the step one. In interval 2 there is a call on PLCC, which will cause end of step 1 of detection. During interval 3, detector is in step two, but there are calls on priority link, and therefore system returns to step one. Interval 4 is analogue to interval 1, and system resides in step 1. During the interval 5, failure on priority links occurs. The next call arrives on PLCC, and step 1 of the detection ends. Since there are no calls in the system in the interval 6, system resides in step two, waiting for next call arrival. In the interval 7 calls arrive on PLCC, and pre-alarm is detected.

It is interesting to consider what pre-alarm detector efficiency depends on. According to the Figure 6, the time between a failure on ISDN/IP link and failure detection depends on the time between successive calls on PLCC link. This time is shorter with the increase of the offered traffic.

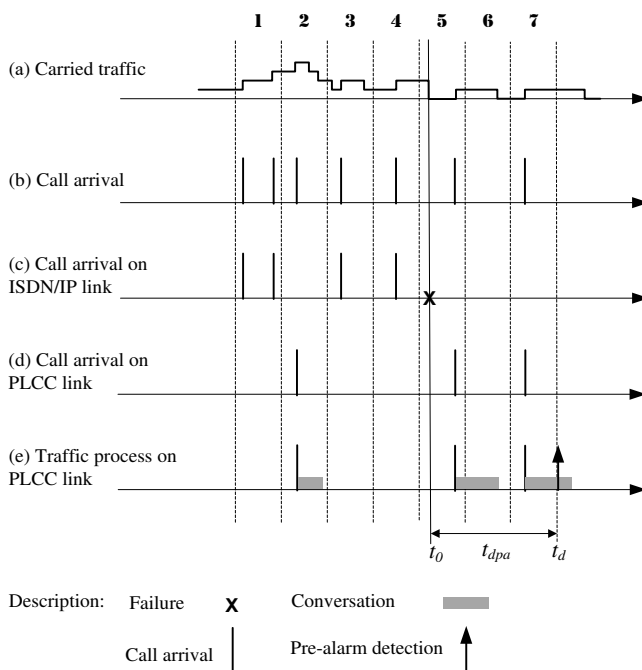


Figure 6
Detection diagrams for pre-alarm

Therefore, it may be concluded that detection rate is as higher when the offered traffic is greater. Unfortunately, too large increase of the offered traffic also leads to the false alarm probability increase. Let us consider one correct ISDN link in the intervals of great offered traffic. Let us, further, suppose that higher priority ISDN link is completely busy in time intervals t_B . There is a (low) probability that two successive calls are generated on PLCC link during this time interval t_B . These two calls may cause the state of detected pre-alarm, i.e. faulty ISDN link, which is incorrect information. The probability that all ISDN links are busy is very low. That's why the probability of false pre-alarm may be neglected.

Generally, there is a small number of solutions dealing with supervision of telecommunication network of EPU and these solutions are cited throughout this paper. Especially there are no solutions satisfying two important advantages over usual solutions: 1) only software based solution without need of additional specific hardware and 2) solution where software management is realized completely independently, without need to change existing software. That's why it would be hard to perform some additional efficiency parameters comparison besides the ones presented in this paper.

Conclusions

Telephone network of EPU primary objective is to provide high availability. Two standard methods for achieving high availability are: adding redundant elements and usage of alternate routing. In this paper, is proposed software solution for usage of network management in pre-alarm detection, a novel method for achieving high availability in telephone network of EPU. The solution is realized in two steps for collection and analysis of data stored in CDR. Steps in the process are invoked on timer tick. In the first step is awaited call on PLCC. In the second step, after the end of the call started in the first step, pre-alarm is detected if a call arrives on PLCC during the detection interval.

Description of the system behaviour is provided, and an example of call arrival process is demonstrated. Efficiency parameters of the proposed solution are compared with those previously defined in the literature. It is concluded that there is no miss in detection in the proposed solution. The probability of false pre-alarm is not changed compared with the solution in [5]. The exact values of the probability of false alarm in the EPU network are significantly lower than 10^{-5} due to low offered traffic. That's why it is difficult to test the solution in real conditions. It is necessary for testing purposes to artificially stop the traffic over the ISDN (IP) part of the considered link to verify detector behaviour in pre-alarm conditions. The character of discrete domain influences that the meantime to detection is slightly longer in the existing solution.

Solution can be implemented without changes in existing network infrastructure if existing management systems have stored data in CDR and if they have integration (Northbound) interface. The detection procedure is performed locally, and local personel can make necessary equipment repairment. If the telecommunications network management is centralized, only the summary information about pre-alarm should be transferred, and there is no need to transfer large amount of data for analysis, nor is required complex root cause analysis software in network operations center.

In literature is described pre-alarm detector usage to locally monitor PLCC link between two telephone exchanges. Additional hardware system for each link was required in detector implementation. In this paper, is proposed solution based on network management, and which implementation doesn't require additional hardware. It was demonstrated during verification that the described solution can be implemented as additional network management layer in the system, without change in existing network management system software or infrastructure.

Acknowledgement

This work is partially supported by the Ministry of Education, Science and Technological Development of the Republic of Serbia under Grant TR32007.

References

- [1] Lehpamer, H.: Introduction to Power Utility Communications, Artech House, ISBN-13: 978-1-63081-006-1, 2016
- [2] Ferreira, H. C., Lampe, L., Newburz, J., Swart T. G.: Power Line Communications Theory and Applications for Narrowband and Broadband Communications over Power Lines, A John Wiley and Sons, Ltd, Publication, July 2011
- [3] Cenelec – EN 50065-1: Signalling on low-voltage electrical installations in the frequency range 3 kHz to 148,5 kHz – Part 1: General requirements, frequency bands and electromagnetic disturbances, April 2011
- [4] Behera, T. M., Mohapatra S. K.: Improving Network Lifetime by Minimizing Energy Hole Problem in WSN for the Application of IoT, Facta Universitatis, Vol. 31, No. 2, June 2018, pp. 267-277, DOI: 10.2298/FUEE1802267B
- [5] Stanić, M.: A Novel Method for Improving Availability in Telephone Network of Electric Power Utility, IEEE Conference Publications, Telecommunications Forum (TELFOR), Belgrade, Serbia, November 2014., pp. 139-145
- [6] Mitić, D., Matić, V., Lebl, A., Stanić, M., Markov, Ž.: Centralized Detection of Pre-alarm State in Telephone Network of Electric Power Utility, Facta Universitatis, Vol. 29, No. 2, June 2016., pp. 297-308, DOI: 10.2298/FUEE1602297M
- [7] Stanić, M., Lebl, A., Mitić, D., Markov, Ž.: Detection of Pre-alarm State in Mixed Telephone Network of Electric Power Utility, Przegląd Elektrotechniczny (Electrical Review), Vol. 89, No 2a, February 2013, pp. 130-133
- [8] Sendin, A., Peña, I., Angueira, P.: Strategies for Power Line Communications Smart Metering Network Deployment, Energies, Vol. 7, No. 4, 2014, pp. 2377-2420, DOI: 10.3390/en7042377
- [9] Sarafi, A. M., Voulkidis, A. C., Livieratos, S., Cottis, P. G.: The Role of PLC Technology in Smart Grid Communication Networks in Smart Grids: Clouds, Communications, Open Source, and Automation. CRC Press, 2014, pp. 151-177
- [10] Wang, W., Xu, Y., Khanna, M.: A survey on the communication architectures in smart grid, Computer Networks: The International Journal of Computer and Telecommunications Networking, Vol. 55, No. 15, October 2011, pp. 3604-3629, DOI: 10.1016/j.comnet.2011.07.010
- [11] Bumiller, G., Lampe, L., Hrasnica, H.: Power line communications for large-scale control and automation systems, IEEE Commun. Mag., Vol 48, No. 4, April 2010, pp. 106-113, DOI: 10.1109/MCOM.2010.5439083

- [12] Stanić, M., Mitić, D., Lebl, A.: A Mobile Agents Framework for Integration of Legacy Telecommunications Network Management Systems, *Przegład Elektrotechniczny (Electrical Review)*, Vol 88, No. 6, January 2012, pp. 337-341
- [13] Solmaz, S. E., Gedik, B., Ferhatosmanođlu, H., Sözüer. S., Zeydan, E., Etemođlu, Ç. Ö.: ALACA: A Platform for Dynamic Alarm Collection and Alert Notification in Network Management Systems, *International Journal of Network Management*, Vol. 27, No. 4, July 2017, pp. 1-20, DOI: 10.1002/nem
- [14] Meng, Y., Qin, T., Liu, Y., He, C.: An Effective High Threating Alarm Mining Method for Cloud Security Management, *IEEE Access*, Vol. 6, April 2018, pp. 22634-22644, DOI: 10.1109/ACCESS.2018.2823724
- [15] Asres, M. W., Mengistu, M. A., Castrogiovanni, P., Bottacioli, L., Macii, E., Patti, E., Acquaviva, A.: Supporting Telecommunication Alarm Management System with Trouble Ticket Prediction, *IEEE Transactions on Industrial Informatics*, May 2020, pp. 1-10, ISSN 1551-3203, DOI: 10.1109/TII.2020.2996942
- [16] Iversen, W. B.: *Teletraffic Engineering and Network Planning*. Technical University of Denmark, 2015
- [17] Ma Q., Liu K., Xiao X., Cao Z., Liu Y.: Link Scanner: Faulty Link Detection for Wireless Sensor Networks, *Proceedings IEEE Infocom*, 2013, pp. 2688-2696
- [18] Aidarous. S., Plevyak, A.: *Telecommunications Network Management into 21 st century: Techniques, Standards, technologies and Applications*, Wiley - IEEE Press, December 1997, ISBN:978-0-780-31013-1
- [19] Krajnović, N.: The Design of a Highly Available Enterprise IP Telephony Network for the Power Utility of Serbia Company, *IEEE Communications Magazine*, Vol. 47, No. 4, April 2009, pp. 118-122
- [20] Madsen, L., Van Meggelen, J., Bryant, R.: *Asterisk: The Definite Guide*, [Online]: http://www.asteriskdocs.org/en/3rd_Edition/asterisk-book-html-chunk/asterisk-SysAdmin-SECT-1.html
- [21] Kamola, M.: Reconstruction of a social network graph from incomplete call detail records, *Proceedings of the International Conference on Computational Aspects of Social Networks (CASoN)*, Vol. 3, No. 3, 2011, pp. 136-140
- [22] Holleczeck, T., Yu, L., Lee, J. K., Senn, O., Ratti, C., Jaillet, P.: Detecting weak public transport connections from cellphone and public transport data, *Proceedings of the 2014 International Conference on Big Data Science and Computing*, 2014, pp. 299-304

-
- [23] Stanić, M.: An improvement of availability in mixed telephone network of electric power utility using pre-alarm states monitoring, PhD Dissertation, School of Electrical Engineering, University of Belgrade, Serbia, November 2013, <https://nardus.mpn.gov.rs/handle/123456789/6308>
- [24] Savović, T., Banjac, B., Maksić, D., Stanojević, M., Jovanović, D., Nedelicki, Z., Trenkić, B., Markov, Ž.: Telephone Exchange ETCE-D: Network Node Where Analog, Digital and Packet PLCs Meet, IEEE Conference Publications, Telecommunications Forum (TELFOR), Belgrade, Serbia, November 2003

A New Thermal Model of an Angular Contact Ball Bearings, in a Standard Arrangement, subjected to Radial Loads, based on State Variables and Control Volumes

Sebastian Cabezas¹, György Hegedűs² and Péter Bencs³

^{1,2} Institute of Machine Tools and Mechatronics, Faculty of Mechanical Engineering and Information Technology, University of Miskolc, 3515 Miskolc-Egyetemváros, Hungary
E-mails: szgtscab@uni-miskolc.hu, hegedus.gyorgy@uni-miskolc.hu

³ Institute of Energy Engineering and Chemical Machinery, Faculty of Mechanical Engineering and Information Technology, University of Miskolc, 3515 Miskolc-Egyetemváros, Hungary, E-mail: peter.bencs@uni-miskolc.hu

Abstract: Permanent or temporary failures in bearing systems are often caused by excessive or prolonged heat generation, within an angular contact ball bearing, during operations arising from external loads. Considering the complexity of getting experimental thermal measurements in an angular ball bearing arrangement, analytical techniques must be utilized in order to predict the thermal behavior thereof, taking into account variables such as rotational speed, the type of load and the operational conditions. The aim of this study is the development of a thermal model applying the state-space approach, able to predict thermal characteristics of an angular contact ball bearing in standard arrangement subjected to radial loads. For this purpose, an angular ball bearing, model 7203BEP, in standard arrangement, was treated as the representative model. The arrangement was divided into three independent control volumes, these are, the inner-race, the ball and the outer-race/housing. Thereafter, the energy equation and the theory of rolling contact heat transfer are utilized to determine heat fluxes and temperature variations between the contact regions. The thermal resistances developed between the ball/ inner-race, outer-race/ ball, inner-race/ shaft and outer-race/ housing were calculated as variables depending on the rotational speed, wherewith the thermal analysis is performed. Space variables including, temperature of the inner-race T_i , temperature of the balls T_b and temperature of the outer-race/ housing T_{oh} were calculated and the results were compared by Finite Element Analysis simulations using Ansys transient thermal software. The findings herein, show that the maximum value of mean deviation of temperature obtained with the proposed thermal model and the Finite Element Analysis (FEM) simulations was less than $sd < 3.50\%$, hence, indicating that the model is in good agreement with the numerical solutions. In this manner, the presented thermal model can be utilized, as an observer, to predict the thermal behavior, in different types of angular contact ball bearings, that undergo radial loads. Furthermore,

the thermal model provides relevant information for further studies, related to thermal distribution in machine components.

Keywords: Angular ball bearing; thermal model; thermal resistance; state-space approach; state variables

Nomenclature

a	Ellipse major axis (mm)	R_{is}	Thermal resistance between the inner-race and the shaft (K/W)
A_b	Surface area of the ball (m ²)	R_{ob}	Thermal resistance between the outer-race and the ball (K/W)
A_i	Surface area of the inner-race (m ²)	R_{oh}	Thermal resistance of the outer-race/ housing (K/W)
A_o	Surface area of the outer-race (m ²)	t	Time (s)
b	Ellipse minor axis (mm)	T_b	Temperature of the ball (°C)
c_p	Specific heat (J/kgK)	T_{bi}	Initial temperature of the ball (°C)
d_m	Mean diameter (mm)	T_h	Temperature of the housing (°C)
E	Young's modulus (N/mm ²)	T_i	Temperature of the inner-race (°C)
F	External load (kN)	T_{ii}	Initial temperature of the inner-race (°C)
F_t	Applied force (kN)	T_{is}	Initial temperature of the shaft (°C)
F_r	Radial force (kN)	T_l	Temperature of the lubricant (°C)
G_{rr}	Bearing type and load factor.	T_o	Temperature of the outer-race (°C)
h_l	Lubricant coefficient (W/m ² K)	T_{oh}	Initial temperature of the outer-race/ housing (°C)
k	Thermal conductivity (W/mK)	T_s	Temperature of the shaft (°C)
m_b	Mass of the ball (kg)	V	Tangential speed (m/s)
m_i	Mass of the inner-race (kg)		
m_{oh}	Mass of the outer-race/ housing (kg)		
M_{fr}	Rolling frictional moment (Nmm)		
n	Rotational speed (rpm)		
N	Number of balls		
\dot{Q}_{bi}	Heat generated from the ball to the inner-race (W)		

\dot{Q}_{bl}	Heat by convection between the ball and the lubricant (W)	α	Contact angle ($^{\circ}$)
\dot{Q}_f	Total friction heat generation (W)	α_d	Thermal diffusivity (m^2/s)
\dot{Q}_{fb}	Frictional heat into the ball (W)	γ	Poisson's ratio
\dot{Q}_{fi}	Frictional heat into the inner-race (W)	μ	Geometric factor 1. Ref.[10]
\dot{Q}_{fo}	Frictional heat into the outer-race (W)	ν	Lubricant kinematic viscosity (mm^2/s)
\dot{Q}_{il}	Heat by convection between the inner-race and lubricant (W)	ρ	Density (kg/m^3)
\dot{Q}_{oh}	Heat generated through the outer-race/housing (W)	ρ_c	Radii of curvature (mm)
\dot{Q}_{ol}	Heat by convection between the outer-race and lubricant (W)	ν	Geometric factor 2. Ref [10]
R	Thermal resistance (K/W)	Φ_{is}	Inlet shear heating reduction factor. Ref. [10]
R_{bi}	Thermal resistance between ball and the inner-race (K/W)	Φ_{rs}	Starvation reduction factor. Ref. [10]

Subscripts:

b	Ball
i	Inner-race
o	Outer-race
oh	Outer-race/ housing

1 Introduction

The performance of rotary machines leans on diverse factors, including the appropriate thermal conditions of rolling elements. The operational capability of the bearing might be affected by a sudden increase of temperature, mostly occasioned by friction among the elements comprising a rolling bearing. Although, rolling bearings have been called non-frictional elements [1], it is well known that rolling contact produces frictional moments, thereby generating the phenomena of heat transfer [2]. The thermal efficiency of a bearing arrangement will depend on its capacity to dissipate heat among the bearing components and the adjacent elements. Frictional moments depend on sundry variables, among them, the applied load, operating speeds, lubricant type, bearing arrangement, type of bearing, environmental conditions [1] and the determination of frictional moments is

substantiated by the Hertzian contact theory [3]. In order to enhance thermal analysis in bearings and knowledge thereof, for decades, a vast number of important investigations have been conducted, including the creation and utilization of computational tools to predict life and performance of bearings [4] and the development of mathematical expressions relating friction-power for specific types of bearings [5]. To mention some remarkable investigations regarding thermal behavior in bearings, J. L. Stein *et al.* [6] developed a dynamic mathematical model as the basis of an observer, so that bearing internal force can be on-line monitored based on easy to measure spindle system quantities, such as bearing temperature and spindle-speed. K. Mizuta *et al.* [7], studied heat transfer characteristics between the inner and outer ring measured experimentally, and the effect of balls as a heat carrier was calculated theoretically. T. Sibilli *et al.* [8], compared a thermal network model and a finite element model of an experimental high-pressure shaft ball bearing and housing in order to provide a template for predicting temperatures and heat transfer for a variety of bearing models. Z. De-xing *et al.*, estimated thermal performances with an optimized thermal grid model for a pair of front bearings mounted in a high-speed spindle. The results show that the deviation between the calculation and experimental measurements was 9%, which can be beneficial for operating accuracy and service life as bearing temperature rise can be forecasted [9]. The construction of experimental rigs presents various difficulties including, the location of temperature sensors in rotating elements, the accessibility to the inner parts of the bearing arrangement, the application of external radial, axial loads or a combination of both by external sources, the analysis of the lubrication regime wherewith the bearing is tested. Therefore, the utilization of the different computational, analytical and numerical techniques must be considered valid approaches to determine solutions, as long as these solutions have been tested or compared. At present, bearing manufacturers have developed equations and mathematical expressions to calculate frictional moments and are publicly issued in order to facilitate their utilization by engineers and researchers. Detailed information thereof, can be found in [10] [11].

Having said that, this paper presents a thermal model utilizing the state-space method and control volumes, capable of observing temperature differences in an angular contact ball bearing type SKF 7203 BEP mounted in a back-to-back (DB) arrangement, which is subjected to radial loads ranging from 0.75 – 7.5 kN

0 – 4000 rpm , taking into account the speed limits of conventional electric motor capabilities employed in bearing experimental testing rigs. The findings obtained with the proposed thermal model were compared with Finite Element Analysis (FEA) using Ansys transient thermal. The mean deviations between FEA simulations and the thermal model were calculated,

$sd = 1.40$ for the outer-race /housing temperature T_{oh} , $sd = 1.64$ for the ball temperature T_b and $sd = 1.40$ for the inner-race temperature T_i . Considering that the values of mean deviation are low, the thermal model is in accordance with numerical simulations. The present work aims to provide a practicable analytical tool wherewith the thermal behavior of the bearing components and adjacent elements thereof are observed, hence providing an intuitive and straightforward methodology that can be applied to bearings with similar geometries under mechanical forces alike.

2 Materials and Methods

Figure 1 illustrates the assembly model and a cross-sectional view of a DB back-to-back bearing arrangement subjected to radial loads exerted by an external source.

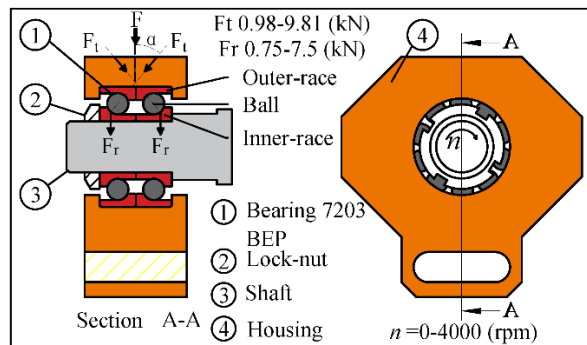


Figure 1

Scheme of an angular contact bearing in standard arrangement (Source: Author)

The assembly consists of four elements, the housing, in which the bearings are packed and the external load can be applied; the SKF 7203 angular contact ball bearing, in which heat is dissipated; the lock-nut, which fastens and supports the assembly; and the shaft. The development of the thermal model was divided into four stages, load model, frictional model, heat generation model and state-space variables model.

2.1 Load Model

Angular contact ball bearings are suitable for working under different types of loads, including axial loads, radial loads, combinations of axial and radial loads, preload in the axial direction, preload in radial direction, centrifugal forces [1, 6, 9], consequently, this type of bearing is widely used in high-speed machining

applications. It is important to consider that each type of load will produce different effects with regards to heat transfer and other phenomena such as vibrations. This research focuses on the thermal effects caused by pure radial loads, determining them depends on the applied force by the external source and the bearing contact angle, hence the radial force F_r is obtained using Equation (1) [1].

$$F_r = F_t \cdot \cos(\alpha) \quad (1)$$

2.2 Frictional Model

Heat transfer in angular contact ball bearings is associated not only with motion and the thermal physical properties of the bodies under rolling contact (inner-race and ball, outer-race and ball), but with the size and shape of the contact region [2]. Moreover, according to Hertzian contact theory, the pressure between two elastic bodies in contact will form an ellipse of major axis a and minor axis b as shown in Figure 2, which can be calculated using Equation (2) [2].

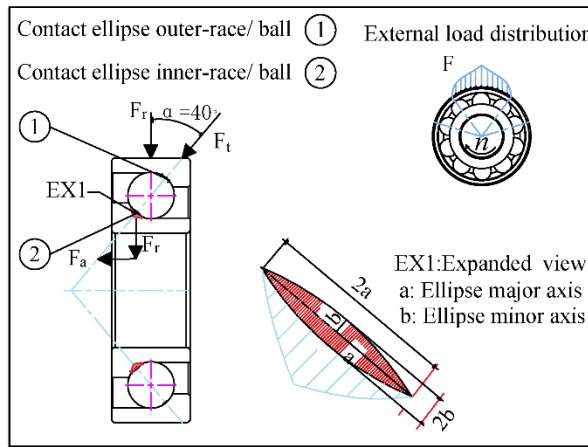


Figure 2

Force distribution and contact region (Source: Author)

$$a = \mu \cdot \left[\frac{3 \left(1 - \frac{1}{\gamma^2} \right) \frac{F_r}{\cos(\alpha)}}{E \sum \rho_c} \right]^{\frac{1}{3}} \quad (2)$$

$$b = \nu \cdot \left[\frac{3 \left(1 - \frac{1}{\gamma^2} \right) \frac{F_r}{\cos(\alpha)}}{E \sum \rho_c} \right]^{\frac{1}{3}}$$

As defined in the Introduction, nowadays bearing manufacturers provide mathematical models to determine frictional moments that follow real behavior of the bearings, considering the contact area and the internal and external factors. Inasmuch as in this paper a bearing model SKF 7203 BEP is being used, the rolling frictional moment was determined utilizing its proper mathematical model given by Equation (3) [10].

$$G_{rr} = 4.33 \cdot 10^{-7} \cdot d_m^{1.97} \left[F_r + 2.44 \cdot 10^{-12} d_m^4 n^2 + 2.02 F_t \cdot \sin(\alpha) \right]^{0.54} \quad (3)$$

$$M_{fr} = \Phi_{is} \Phi_{rs} G_{rr} (vn)^{0.6}$$

Equation (3), relates the effect of radial and axial forces, starvation factor, geometrical specifications of the angular bearing, rotational speed and the operating viscosity of the lubricant. For detailed information on the calculation method, revise reference [10]. The relation of the frictional moment and the rotational speed at different radial loads is presented in Figure 3.

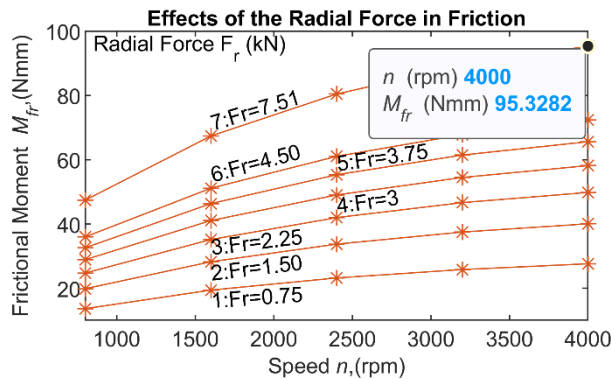


Figure 3
Frictional moment M_{fr} vs. rotational speed n

Figure 3 shows that the frictional moment M_{fr} increases in a non-linear behavior when the rotational speed n increases. This effect will directly influence the heat generation throughout the bearing and its adjacent components.

2.3 Heat Transfer Model

As in all phenomena of heat transfer, the dissipation of heat in angular bearings happens following the principles of distribution of thermal energy occurring due to spatial temperature differences [1] [12], and can be mathematically approached by heat transfer modes. Mostly, heat is generated by friction due to rolling contact (between the inner-race and balls, outer-race and balls). By conduction, heat is dissipated between the contact regions (inner-race, balls, outer-race, housing).

By convection, heat is dissipated between fluids or gases and solid bodies (oil-lubricant and balls, oil-lubricant and races). In some special bearing applications such as aerospace or high-temperature applications, might be useful to analyze heat transfer by radiation. Once the frictional moment is calculated, it is necessary to divide the structure arrangement shown in Figure 1 in a suitable way, thereby avoiding the presence of more unknown variables than equations to find solutions. This approach is achieved by selecting appropriate control volumes, it means, selecting a region of space bounded by a control surface through which heat is flowing [13]. On this application, the bearing arrangement was divided into three parts: the inner-race, which is a non-static part, exchanges heat with the balls, the lubricant and the shaft; the balls, which are a non-static part and exchange heat with the inner-race, lubricant, and outer-race; the outer-race/ housing which is a static part and exchanges heat with the balls, lubricant and the surroundings. Considering that the applied load is carried by the housing, the distribution of heat is conceived is illustrated in Figure 4.

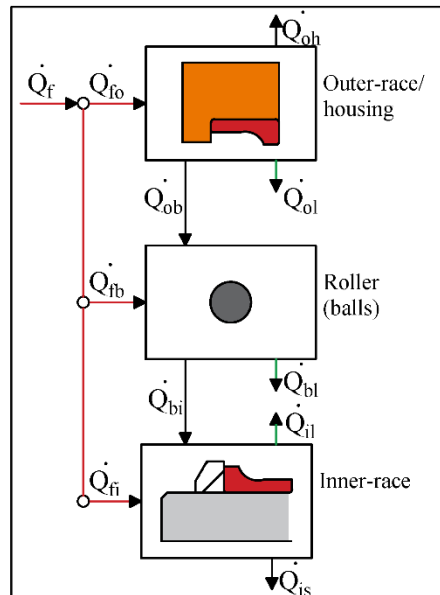


Figure 4

Heat transfer block diagram (Source: Author)

The total friction heat flow \dot{Q}_f [4] is obtained utilizing the power loss formula which relates the rotational speed n and the frictional moment M_{fr} [2].

$$\dot{Q}_f = 1.5 \cdot 10^{-4} \cdot M_{fr} \cdot n \quad (4)$$

A fully lubricant film between the rings and the balls is developed, hence separating the surfaces and allowing the functionality of the bearing under the manufacturer specifications. Heat by friction occurs at the contact surfaces and then is distributed to the inner-race \dot{Q}_{fi} , spheres \dot{Q}_{fb} and outer-race \dot{Q}_{fo} [6]. Since the rolling elements are designed to absorb most of the distributed load [1], it is established that 50% of the total power losses by friction is absorbed by the rolling elements (balls), the rest is divided between the inner-race 25% and outer-race 25% of the total power losses as stated in Equation (5) [6].

$$\begin{aligned}\dot{Q}_{fb} &= 0.5 \cdot \dot{Q}_f \\ \dot{Q}_{fi} &= 0.25 \cdot \dot{Q}_f \\ \dot{Q}_{fo} &= 0.25 \cdot \dot{Q}_f\end{aligned}\tag{5}$$

The relation between the power losses and the rotational speed for different radial loads is shown in Figure 5. The figure shows that the total heat \dot{Q}_t increases exponentially with regards to the rotational speed n and the radial load F_r .

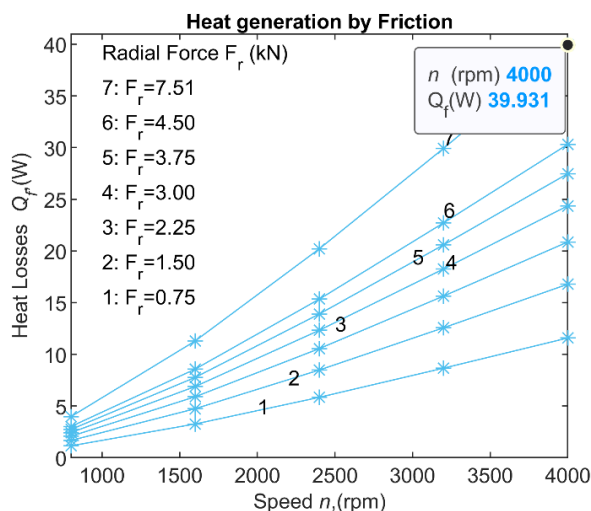


Figure 5

Heat losses \dot{Q}_f vs. rotational speed n

Heat by conduction is transferred between the spheres and inner-race \dot{Q}_{bi} , inner-race and the shaft \dot{Q}_{is} , outer-race and spheres \dot{Q}_{ob} and through the outer-race and housing \dot{Q}_{oh} [6].

The formulas are:

$$\begin{aligned}\dot{Q}_{bi} &= \frac{(T_b - T_i)}{R_{bi}} \\ \dot{Q}_{is} &= \frac{(T_i - T_{sh})}{R_{is}} \\ \dot{Q}_{ob} &= \frac{(T_o - T_b)}{R_{ob}} \\ \dot{Q}_{oh} &= \frac{(T_o - T_h)}{R_{oh}}\end{aligned}\quad (6)$$

The thermal resistances R_{bi} , R_{ob} for rotating elements, depend on the tangential speed, the Hertzian contact area, the thermal conductivity and the thermal diffusivity [5], and are obtained using Equation (7) [5].

$$R = \frac{0.8}{N \cdot b \cdot k} \left(\frac{\pi \cdot \alpha_d}{a \cdot V} \right)^{1/2} \quad (7)$$

Figure 6, illustrates the relation of the thermal resistances with respect to the rotational speed. It is noticeable that the thermal resistances between the contact regions R_{bi} and R_{ob} decrease with respect to the rotational speed n , hence heat dissipation by conduction between the contact regions will increase.

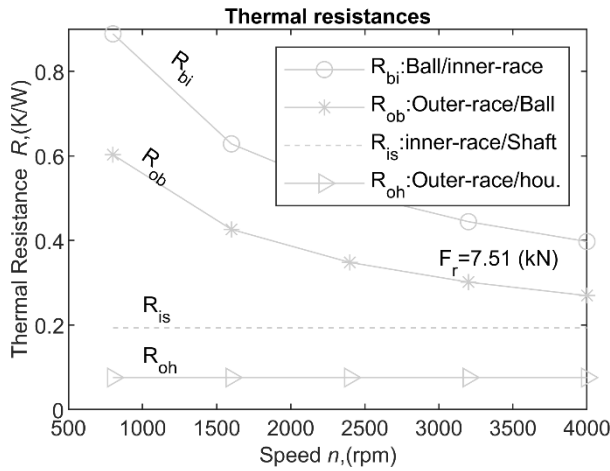


Figure 6
Thermal resistances R_i (K/W)

Heat by convection is dissipated between the inner-race and the lubricant \dot{Q}_{il} , balls and the lubricant \dot{Q}_{bl} , and outer-race and lubricant, \dot{Q}_{ol} , and are calculated using Equation (8) [6].

$$\begin{aligned}\dot{Q}_{il} &= h_l \cdot A_i \cdot (T_i - T_l) \\ \dot{Q}_{bl} &= h_l \cdot A_b \cdot (T_b - T_l) \\ \dot{Q}_{ol} &= h_l \cdot A_o \cdot (T_o - T_l)\end{aligned}\quad (8)$$

The temperature variations along the surfaces of the inner-race T_i , ball T_b and outer-race/ housing T_{oh} are calculated applying the energy equation to the three control volumes as follows:

$$\begin{aligned}m_i \cdot c_p \cdot \frac{\partial T_i}{\partial t} &= \dot{Q}_{fi} + \dot{Q}_{bi} - \dot{Q}_{il} - \dot{Q}_{is} \\ m_b \cdot c_p \cdot \frac{\partial T_b}{\partial t} &= \frac{1}{N} (\dot{Q}_{fb} + \dot{Q}_{ob} - \dot{Q}_{bi} - \dot{Q}_{bl}) \\ m_{oh} \cdot c_p \cdot \frac{\partial T_{oh}}{\partial t} &= \dot{Q}_{fo} - \dot{Q}_{ob} - \dot{Q}_{ol} - \dot{Q}_{oh}\end{aligned}\quad (9)$$

2.4 State-Space Model

Equation (9), cannot be solved by conventional algebraic methods since there will be more unknown variables than equations. On that account, this paper presents a steady-space approach wherewith modelling and observing a system can be done selecting appropriate state-variables and input-variables sufficient to describe the complete behavior of the system. The state-variables are the temperature of the inner-race T_i , the temperature of the balls T_b and the temperature of the outer-race/ housing T_{oh} . The input variables have been selected meticulously in order to obtain appropriate results. The input variables must be easily measurable by external sensors or calculated by mathematical expressions, and can be selected to suit the problem [14]. Therefore, the power losses by friction \dot{Q}_f which depends on the applied load, rotational speed, lubrication-regime together with temperature of the outer-race T_o were chosen as input-variables. Hence, the description of the system using state-space approach is given by Equation (10).

$$\begin{aligned}
 \begin{bmatrix} m_i \cdot c_p \dot{T}_i \\ m_b \cdot c_p \dot{T}_b \\ m_{oh} \cdot c_p \dot{T}_{oh} \end{bmatrix} &= \begin{bmatrix} -\left(\frac{1}{R_{bi}} + \frac{1}{R_{is}} + h_i A_i\right) & \frac{1}{R_{bi}} & 0 \\ \frac{1}{N \cdot R_{bi}} & -\frac{1}{N} \left(\frac{1}{R_{ob}} + \frac{1}{R_{bi}} + h_i A_b\right) & 0 \\ 0 & \frac{1}{R_{ob}} & -\frac{1}{R_{oh}} \end{bmatrix} \cdot \begin{bmatrix} T_i \\ T_b \\ T_{oh} \end{bmatrix} + \begin{bmatrix} 0.25 & 0 \\ 0.5 & \frac{1}{N \cdot R_{ob}} \\ 0.25 & \left(\frac{1}{R_{bi}} + h_i A_o\right) \end{bmatrix} \cdot \begin{bmatrix} \dot{Q}_f \\ T_o \end{bmatrix} \\
 y &= \begin{bmatrix} 1 & 0 & 0 \\ 0 & 1 & 0 \\ 0 & 0 & 1 \end{bmatrix} \cdot \begin{bmatrix} T_i \\ T_b \\ T_{oh} \end{bmatrix} \tag{10}
 \end{aligned}$$

Although the system mathematically is controllable, it is important to remark that the proposed model only serves as an observer, it means that the state-variables at $t = t_0$ can be exactly determined from observation of the output over a finite time interval. Further details about controllability and observability are described in reference [14].

3 Results

In this section, the determination of the temperature fields of the three control volumes (inner-race T_i , ball T_b , outer-race/ housing T_{oh}), is presented. The solutions were analyzed utilizing the proposed thermal model given in Equation (9), and finite element analysis simulations.

3.1 State-Space Model Solution

The state-space system wherein the state variables T_i , T_b and T_{oh} are analyzed, was determined using MATLAB. The thermal properties of the materials comprising the angular bearing, the initial temperatures of the shaft T_{ish} , oil-mist T_l , inner-race T_{ii} , balls T_{bii} and outer-race/ housing T_{ohi} , are given in Table 1. The geometric specifications of the angular ball bearing necessary to find numerical solutions can be found in the manufacturer's reference [10].

The interval time t is set up until reaching steady-state conditions. The interval time of the thermal analysis for the inner-race and the balls was set up at $t = 30 s$. For the outer-race/housing was set-up at $t = 300 s$. The responses of the state-space thermal model are shown in Figure 7 for the inner-race; Figure 8, for the balls and Figure 9 for the outer-race/housing.

Table 1
Thermal properties and initial conditions

Thermal Property	Initial Condition
Thermal conductivity	$k = 46.6$ (W/mK)
Poisson's ratio	$\gamma = 0.27$
Specific heat	$c_p = 460$ (J/kgK)
Density	$\rho = 7810$ (kg/m ³)
Oil mist convection coefficient	$h_l = 409$ (W/m ² K)
Initial temperatures	$T_{ish} = 25$ (°C), $T_{ii} = 26.5$ (°C), $T_{ohi} = 25$ (°C) $T_{bii} = 25$ (°C), $T_l = 25$ (°C)
Applied radial force	$F_r = 7.5$ (kN)
Rotational speed	$n = 0 - 4000$ (rpm)

Due to radial loads, frictional moments are developed between the inner-race and the ball. Part of the heat energy is absorbed in the inner-race and part is dissipated to the lubricant film. During the interval time $t = 30$ s, applying the operational conditions for the radial force and rotational speed given in Table 1, a temperature increment $\Delta T_i = 5.24$ °C occurs in the inner-race as shown in Figure 7.

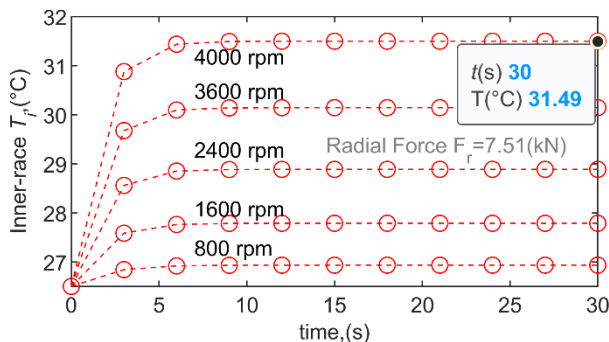


Figure 7
Temperature distribution of the inner-race T_i

An important function of the balls is to distribute the loads uniformly through the bearing components. Considering that most of the frictional moment is absorbed by the balls, it is noteworthy that a high temperature increment $\Delta T_b = 27.50$ °C during $t = 30$ s occurs, as shown in Figure 8.

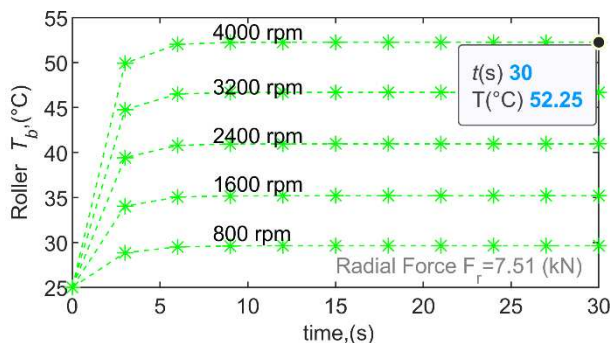


Figure 8
 Temperature distribution of the balls T_b

Since the volume comprising in the outer-race/ housing arrangement is bigger compared to the balls and inner-race, very low temperature increments occur at $t = 30\text{ s}$. Consequently, more time is required to reach steady-state conditions. A temperature increment $\Delta T_{oh} = 21.23\text{ }^\circ\text{C}$ occurs at $t = 300\text{ s}$ as depicted in Fig. 9.

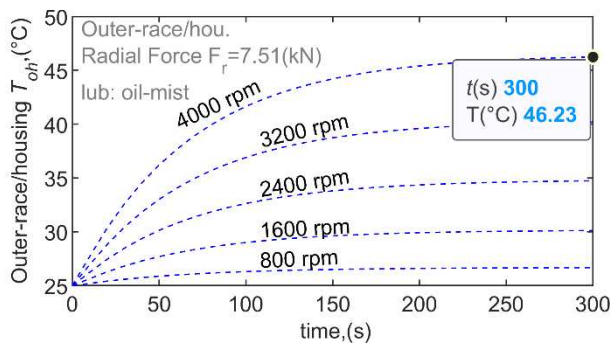


Figure 9
 Temperature distribution of the outer-race/ housing T_{oh}

3.2 Finite Element Analysis

To demonstrate the applicability of the proposed thermal model, FEA simulations were performed using ANSYS transient thermal software, for each of the control volumes. The initial conditions for the temperatures are given in Table 1, the time set up for the analysis is the same applied in the previous section. With the aim to obtain more accurate values, the mesh elements were selected as **tetrahedrons of 0.0001 mm size for the inner-race and spheres** as shown in Figure 10 and Figure 11, and **tetrahedrons of 0.01 mm size for the outer-race/housing** as

shown in Figure 12. In the case of the outer-race/ housing, the mesh can be smaller considering that it is a fixed assembly and using small size elements as in the two other control volumes is not relevant.

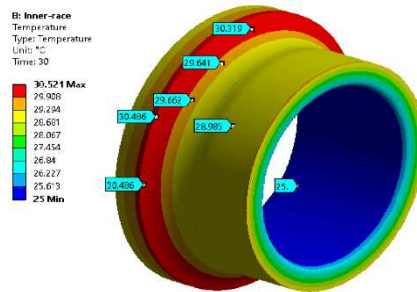


Figure 10

FEA thermal simulation of the inner-race T_i

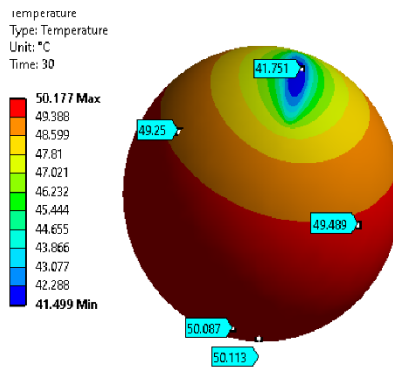


Figure 11

FEA thermal simulation of the ball T_b

Figure 11 illustrates a clear temperature distribution in the rolling elements, starting from the heat dissipation in the Hertzian contact region and distributing the heat through the ball.

Figure 12 illustrates that the most heated part of the outer-race/housing assembly is the region of contact between the balls and the outer-race. Furthermore, this figure also depicts that the housing is the least heated part of the assembly.

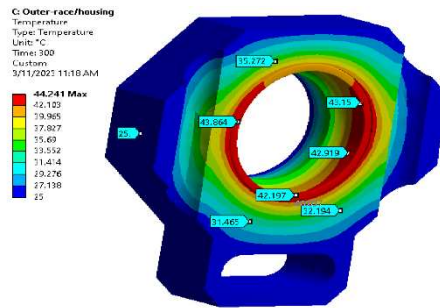


Figure 12

FEA thermal simulation of the outer-race/ housing T_{oh}

The temperature distribution using the proposed thermal and the finite element analysis simulations is presented in Figure 13.

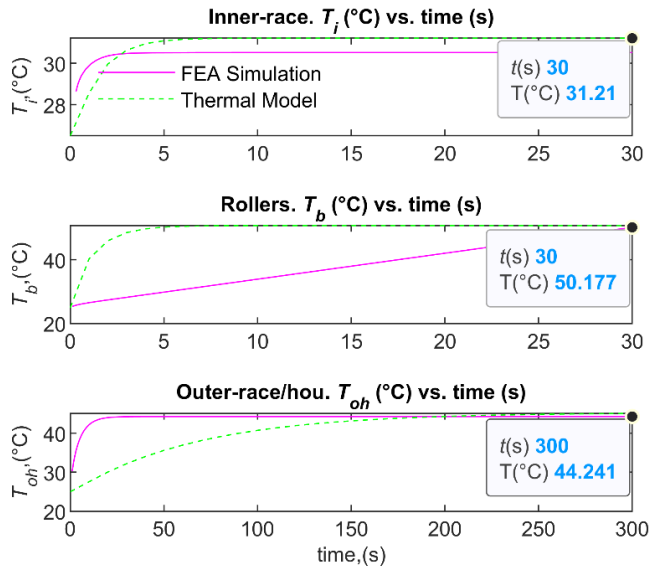


Figure 13

Temperature distribution. Thermal model and FEA simulations

As depicted in Figure 13, the thermal behavior for the inner-race T_i and outer-race/housing T_{oh} regarding the FEA simulations and the thermal model, present similar thermal behavior and it is clearly seen that during the established period of time, the final mean values do not differ prominently. In the case of the balls, the thermal behavior T_b for the FEA simulation exhibit a linear behavior as compared to the behavior obtained for the thermal model. However, the final values at the end of the specified time, do not differ prominently.

Table 2 presents the results of the thermal model and FEA simulations, including the percentage of deviation between both results and the average temperature and the temperature increment from the initial temperatures.

Table 2
Thermal Model and FEA Analysis comparison at $n = 4000$ (rpm) $F_r = 7.51$ (kN)

Control Volume	t , (s)	Thermal Model (°C)	FEA sim. (°C)	Temp. difference (°C)	Temp. increment ΔT (°C)	Dev. sd
Inner-race	30	31.49	30.52	0.97	5.24	0.68
Balls	30	52.50	50.17	2.30	27.50	1.64
Outer-race/housing	300	46.23	44.24	1.9	21.23	1.40

Conclusions

A thermal model to predict temperature variations for an angular contact ball bearing, in back-to-back arrangement, subjected to radial loads, using a state-space approach was presented in this paper. The assembly was divided into three control volumes, inner-race, balls and outer-race/ housing. Two best suited input-variables for the state-space model were selected, as the frictional heat \dot{Q}_f (which depends on the applied load, rotational speed, lubrication regime, geometry of the bearing) and the temperature of the outer-race T_o . It could be seen that the thermal resistances between the ball and the inner-race R_{bi} and between the outer-race and the ball R_{ob} decrease, when the rotational speed n increases, in this sense, the heat dissipation rates increase. The thermal resistances of the outer-race/ housing R_{oh} , inner-race and shaft remain constant R_{is} . The output-variables T_i , T_b , T_{oh} which represent the temperature of three control volumes were solved analytically by finding temperature responses with initial conditions at $t = t_0$. The temperature distribution of the inner-race T_i , balls T_b and outer-race/ housing T_{oh} , were determined by the proposed thermal model and were compared by FEA simulations.

The maximum mean deviation between the thermal model and the Finite Element Analysis simulations was found in the balls and was $sd = 1.64$. For the case of the inner-race and outer-race/housing, they were $sd = 0.68$ and $sd = 1.40$ respectively. Since the values of the mean deviation are low, it is said that the thermal model is in good agreement with numerical models and can be used to predict thermal behavior in angular bearings.

The presented model is controllable and observable; however, in this research, the model's importance lies in its observability, as temperature behavior can be predicted analytically. The presented methodology is conceived, aiming to be used in the academic and industrial fields related to machine-tools and other types of machinery, wherein the thermal effects are of enormous importance and need continuous analysis.

References

- [1] T. A. Harris and M. N. Kotzalas, *Rolling Bearing Analysis*. Advanced Concepts of Bearing Technology, Taylor and Francis Group, 5th Edition, 2006
- [2] A. Bejan, Theory of rolling contact heat transfer, *Journal of Heat Transfer*, Vol. 111, No. 2, pp. 257-263, 1989, <https://doi.org/10.1115/1.3250672>
- [3] L. Houpert, An Engineering Approach to Hertzian Contact Elasticity - Part I, *Journal of Tribology*, Vol. 123, No. 3, pp. 582-588, 2001, <https://doi.org/10.1115/1.1308043>
- [4] R. J. Parker, Comparison of Predicted and Experimental Thermal Performance of Angular Contact Ball Bearings, NASA Technical Paper, No. 2225, 1984
- [5] R. A. Burton and H. E. Staph, Thermally Activated Seizure of Angular Contact Bearings, *Tribology Transactions*, Vol. 10, No. 4, pp. 408-417, 2008, 10.1080/05698196708972200
- [6] J. L. Stein and J. F. Tu, A State-Space Model for Monitoring Thermally Induced Preload in Anti-Friction Spindle Bearings of High-Speed Machine Tools, *Journal of Dynamic Systems, Measurement and Control*, Vol. 116, No. 3, pp. 372-386, 1994, <https://doi.org/10.1115/1.2899232>
- [7] K. Mizuta, T. Inoue, Y. Takahashi, S. Huang, K. Ueda and H. Omokawa, Heat Transfer Characteristics Between Inner and Outer Rings of an Angular Ball Bearing, *Journal of Dynamic Systems, Measurement and Control*, Vol. 32, No. 1, pp. 42-57, 2003, 10.1002/htj.10070
- [8] T. Sibilli and U. Igie, Transient Thermal Modeling of Ball Bearing Using Finite Element Method, *Journal of Engineering for Gas Turbines and Power*, Vol. 140, No. 3, 2018, <https://doi.org/10.1115/1.4037861>
- [9] Z. De-xing C. Weifang and L. Miaomiao, An optimized thermal network model to estimate thermal performances on a pair of angular contact ball bearings under oil-air lubrication, *Applied Thermal Engineering*, Vol. 131, pp. 328-339, 2018, <https://doi.org/10.1016/j.applthermaleng.2017.12.019>
- [10] SKF, SKF Catalogue, 2018, skf.com
- [11] TIMKEN Company, Angular Contact Ball Bearing Catalogue, 2019, www.timkencatalogues.com
- [12] H. Herwig and A. Moschallski, *Wärmeübertragung (Heat Transfer)*, Springer Vieweg, 3rd Edition, 2014
- [13] T. L. Bergman and A. S. Lavine, *Fundamentals of Heat and Mass Transfer*, John Wiley and Sons, 8th Edition, 2017
- [14] R. S. Burns, *Advanced Control Engineering*, Butterworth Heinemann, 1st Edition, 2001

Waste Elimination in the Assembly Process using Lean Tools

Peter Szabó¹, Samuel Janík¹, Miroslava Mlkva¹, György Czifra²

¹ Faculty of Materials Science and Technology in Trnava, Slovak University of Technology in Bratislava, ul. J. Bottu č. 2781/ 25, 917 24 Trnava, Slovak Republic, E-mail: peter.szabo@stuba.sk, samuel.janik@stuba.sk, miroslava.mlkva@stuba.sk

² Óbuda University, Bánki Donát Faculty of Mechanical and Safety Engineering Népszínház u. 8, 1081 Budapest, E-mail: czifra.gyorgy@bkg.uni-obuda.hu

Abstract: A highly dynamic competitive environment leads industrial companies to constantly re-evaluate their processes and strategies. Globalization, strong competition, as well as ever-evolving trends are putting pressure on businesses to increase their flexibility to respond immediately to these trends and to develop the ability to produce products based on consumer demands. Continued efforts for greater flexibility are supported by the Lean concept, which is considered one of the most efficient production concepts. Lean methods are a recognized traditional approach to eliminating waste and streamlining production processes. In recent years, a new Industry 4.0 paradigm has been defined. As a counterpoint to the usual methods, it brings new technological approaches. By integrating these two philosophies, it is possible to achieve strategic goals, reduce costs, increase competition, etc. The aim of the paper is to point out the possibilities of applying lean tools to eliminate waste in the assembly process. With the help of lean tools, the identified shortcomings and waste are eliminated, bottlenecks and inefficient flows in the production process are identified. In this paper, we point out the importance and need for the application of lean methods in industrial enterprises, in order to identify the causes of unnecessary waste of resources (e.g. material, human resources, financial resources, etc.).

Keywords: Assembly; Waste Elimination; Lean Tools; Values Stream Mapping

1 Introduction

In recent years, a new paradigm of Industry 4.0 has been defined, the so-called fourth industrial revolution with the potential to take production processes to the next level [1]. Industry 4.0, as a counterpoint to the usual methods, brings new technological approaches for companies. By integrating these two philosophies, especially into manufacturing companies, it is possible to achieve strategic goals,

reduce costs and increase competitiveness [2]. One of all possibilities is the lean manufacturing strategy. Lean manufacturing aims to reduce costs by removing value-added activities. Based on the Toyota manufacturing system, many lean manufacturing tools (e.g. Just in Time, Value Stream Mapping – VSM, etc.) are widely used in industrial manufacturing, including the automotive industry [3].

Industry 4.0 is characterized by a "blending of technology that blurs the boundaries between digital, physical and biological spheres" Industry 4.0 marks a shift in the manufacturing industry for digitization and decentralization of premises from production halls to office spaces and across enterprise networks [4]. The digital transformation of manufacturing is also affected by such trends as IoT, Industry 4.0, data and analytics, artificial intelligence and machine learning [5]. It also enables the creation of a smart network of machines, products, components, properties and systems throughout the value chain, thus forming a smart factory. Both of these approaches aim to increase productivity and flexibility [1]. Industry 5.0 is a new concept that focuses on collaborative collaboration between humans and machines. The goal is to create sustainable products and services [6].

2 Theoretical Review – Lean Tools and Waste Elimination

Lean manufacturing is currently a manufacturing paradigm. The goal of lean manufacturing is to improve/optimize production processes in various areas, including reducing production costs [7], improving the quality of production processes [8], improving/shortening delivery times [8, 9], increasing flexibility [10], avoiding waste in processes [11], etc. Lean manufacturing emphasises visual control and transparency, which makes it easier to identify problems in the process [12].

The paper focuses on the elimination of waste in the production process by identifying unnecessary activities, streamlining the process using lean tools and techniques in accordance with the requirements of Industry 4.0.

2.1 Waste – Characteristics, Types of Waste

Waste (loss) is any activity (process, cost) that is performed in the production of products or in the implementation of a service, and which does not add value to the product and increases its costs [13]. Wastage is very wide and can occur in a variety of activities. Seven main types of waste are most frequently mentioned in the literature, under the acronym TIMWOOD [14]. A more detailed description of each type of waste can be found in Table 1.

Table 1
Description of individual types of waste [based on: 15, 16, 17]

Types of waste	Description
<i>Transportation</i>	It includes any movement of materials that does not add any value to the product. Transportation between processing stage results in prolonging production cycle times, the inefficient use of labour and space.
<i>Inventory</i>	It means having unnecessarily high levels of raw materials, works-in-process and finished products. Extra inventory leads to higher inventory financing costs, higher storage costs and higher defect rates.
<i>Motion</i>	It includes any unnecessary physical motions or walking by workers which divert them from actual processing work. This might include walking around the factory floor to look for a tool, or even unnecessary or difficult physical movements, due to poorly designed ergonomics, which slow down the workers.
<i>Waiting</i>	It is idle time for workers or machines due to bottlenecks or inefficient production flow on the factory floor. It includes small delays between processing of units. This waste occurs whenever goods are not moving or being worked on.
<i>Overproduction</i>	It is unnecessary to produce more than the customer demands, or producing it too early before it is needed. This increases the risk of obsolescence and the risk of producing the wrong thing.
<i>Overprocessing</i>	It is unintentionally doing more processing work than the customer requires in terms of product quality or features such as polishing or applying finishing in some areas of product that will not be seen by the customer.
<i>Defects</i>	In addition to physical defects which directly add to the costs of goods sold, this may include late delivery, production according to incorrect specifications, use of too much raw materials or generation of unnecessary scrap.

In addition to these types of waste, waste also includes untapped human potential. This waste occurs when organizations separate the role of management from employees [18]. It follows from the above that the cause of waste can be, e.g. clutter, insufficient communication, poor planning, etc. This problem can be avoided by using various tools and methods such as VSM, Spaghetti diagram, or process analysis.

2.2 Selected Lean Methods

Lean manufacturing methods are a widely accepted traditional approach to eliminating waste and streamlining production processes [2]. The methods that have been selected for the purposes of research and publication form an active part of the everyday life of the researched industrial enterprises (see the sample of research). Industry 4.0, as a counterpoint to the usual methods, brings new technological approaches for companies. To realize the full potential of Industry

4.0, companies need to understand new technologies and their opportunities. To take advantage of all the opportunities offered by Industry 4.0, it is essential that the various systems are fully integrated with each other, otherwise it is possible that only 40-60% of their potential value will be captured [19]. Preliminary research shows that Industry 4.0 technologies can be integrated into selected lean manufacturing methods in order to make them more efficient.

2.2.1 Spaghetti Diagram

Spaghetti diagrams are Lean tools that can be used to identify wasted motion. A Spaghetti diagram is a visual tool that shows the physical movement of a “work object” such as a product, an employee or document, through the processes in a value stream [20]. Fig. 1 shows an example of Spaghetti diagram. Lean Enterprise Institute defines Spaghetti diagram as diagram of the path taken by a product as it travels through the steps along a value stream. So-called because in a mass production organization the product’s route often looks like a plate of spaghetti [21].

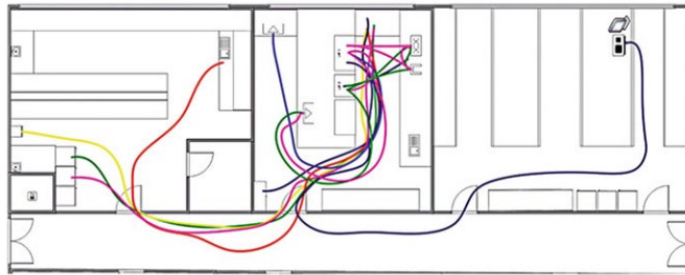


Figure 1
Example of Spaghetti diagram [21]

This type of diagram allows to use different colours for various products, workers or technical means and track the movement at different times. After the analysis we can identify the movement lengths, number of movements, overlapping and crossing movements and their characteristics according to the chosen classification [22]. It is a quick and easy way to track distances of parts and people on the shop floor. Please note that the spaghetti diagram is, by itself, not an optimization method. It only gives you the current state data of the distances [23]. Applying the result of the Spaghetti diagram, we can identify inefficient movements and ineffective areas, eliminate the number of staff, and make changes in the work organisation or workstation layout [22].

2.2.2 VSM – Value Stream Mapping

Value Stream Mapping (VSM) or Value Stream Analysis is an analytical technique that is one of the basic methods of lean manufacturing philosophy. Based on Abdulmalek and Rajgopal [24] this map is used to identify sources of waste and to identify lean tools for reducing the waste. Value stream mapping is a Lean management method that allows you to visualize, analyze and improve all the steps in a product delivery process. A value stream map displays all the important steps of your work process necessary to deliver value from start to finish. It allows you to visualize every task that your team works on and provides single glance status reports about each assignment's progress [25].

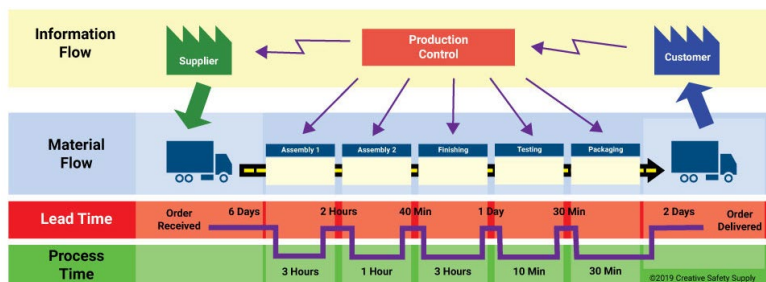


Figure 2
Example of Value Stream Mapping [26]

Value stream mapping is an analytical tool that is considered one of the most effective in optimizing production. It monitors all activities that add and do not add value for the customer. When creating a map of the flow of values, it is essential to state the parameters characterizing the individual processes. These parameters serve as performance indicators, based on which we can determine whether the process is in the desired state [27].

Industry 4.0 leads to an interconnected production environment where it is possible to monitor and share data in real time. By applying Auto-ID technology it is possible to immediately identify an object, with the help of Big Data it is possible to analyze a large amount of data, which facilitates their consolidation [28]. VSM, which constantly receives new data and information from the receipt of the order through the production process to the sending of the order, can effectively guide the entire flow and constantly identify waste. Such intelligent process control lays the foundation for optimizing production processes, thus enabling the flow of values of several possible alternatives to be mapped [2].

VSM, which is based on the support of Industry 4.0 technologies, has better transparency thanks to constant monitoring of the value chain in real-time, which leads to greater flexibility in the decision making process [28].

Value stream mapping helps identify possible instead of losses, bottlenecks, weaknesses and reasons for inefficient flows anywhere in the enterprise [3].

The benefits of value stream mapping are [22]:

- With the help of VSM, you can identify wasteful activities.
- VSM provides a clear view of the work process - where value-adding and non-value-adding stages form. A good practice is also to visualize how long it takes for work items to go through them.
- VSM highlights the current workflow and brings the focus on future improvement.

2.2.3 Yamazumi Chart

To achieve a customer driven value stream it is important to design the production or manufacturing system to be consistent with the pace at which the customer is demanding a part or product. This pace is often referred to as the “Takt time” [3, 27]. Takt time or clock time is the basic indicator of lean manufacturing. *Takt Time* may be defined based on the market demand and the time available for production, that is, it is about the pace of production necessary to answer the demand. It is the result of the ratio of work time available by slot and the number of units for production [29]. Yamazumi chart is a Japanese method designed to visualize the time data of activities identified in the analyzed process. The data is displayed in the form of a bar graph with a color resolution of activities based on their inclusion in the identified categories [3]. According to Semjon & Evin [30], the Yamazumi chart is: *“a folded column graph showing the balance of the load cycle time between several operators on the assembly line. It may be made for one or more assembly line products.”* Sabadka et al, [31] characterizes the Yamazumi chart as a bar chart that shows the total cycle time for each operator when performing their process in the production flow.

3 Data and Research Methodology

In the previous chapters, selected methods of lean manufacturing used in automotive companies operating in the Slovak Republic were presented (since they are multinational corporations with representation in several countries around the world). The presented results are based on research tasks performed in industrial companies belonging to the automotive segment and their supply chains. The survey was conducted on a sample of 13 companies selected at random. The aim of the survey was to determine the level of application of lean methods in order to eliminate waste in the production process in order to increase the efficiency of the investigated processes. The results are shown in Figure 4, the findings were obtained during long-term analysis and cooperation within the frame of cooperation with these companies in research projects.

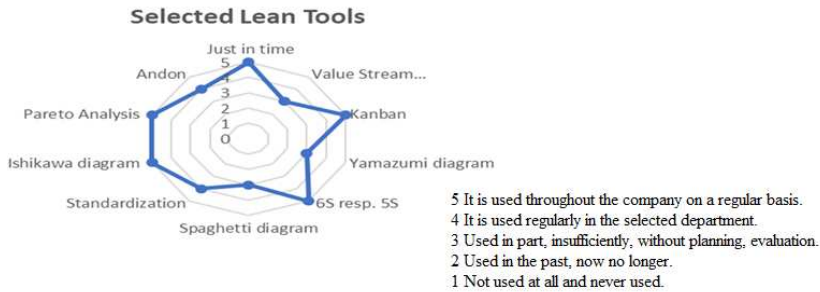


Figure 4

Lean manufacturing methods usage in Automotive (source: own processing based on several surveys)

From the graph (Figure 4) we have shown that methods such as Ishikawa Diagram, Pareto Analysis, JIT, 6S and Kanban are used in the automotive industry sufficiently, which may either be their simplicity of application, or relation to the requirements of standards that are obligatory on the automotive industry. Method Andon and Standardization is used in enterprises, but in some cases only in selected workplaces. The VSM method as well as the Yamazumi and Spaghetti diagrams are poorly utilized in the enterprises surveyed. Based on an extensive review of the existing literature and authors' evaluations, Table 2 shows a matrix to illustrate which I4.0 tools can be used to support the lean methods and tools analyzed. The tools were selected based on a review of academic and corporate publications [28].

Table 2
Lean methods and Industry 4.0 tools linking matrix [based on: 28]

Lean methods I4.0 tools	JIT / JIS	Kanban	VS M	VM	
				5 S	Andon
Human-computer interaction (HCI)		x	x	x	x
Digital object memory	x				
Digital twin/simulation	x	x	x	x	
Cloud computing	x		x		
Real-time computing	x	x	x	x	x
Big data & data analytics	x	x	x		

In the case study, we point out the importance and need for the application of the examined methods in companies, because they make it possible to identify the causes of unnecessary waste of resources. The VSM, Yamazumi chart and Spaghetti chart helps identify losses, bottlenecks and inefficient flows in the production process.

4 Lean Tools Application for Waste Elimination – Company Case Study

This part of the paper will deal with the systematic identification and elimination of waste and inefficiency by the application of selected lean manufacturing methods in the context of Industry 4.0 technologies. In order to meet the requirements of lean manufacturing and to be able to produce efficiently and at the lowest cost, we chose to use lean manufacturing methods in the analysis of the selected assembly process and based on the results of the analysis propose solutions to eliminate waste and streamline the process of assembly. The selected assembly process is characterized as manual, no machines are used in the assembly process. The analysis was performed using the method of predefined times MOST, from which we gathered the necessary data. The collected data were interpreted using the YAMZUMI graph, the lean production methods: VSM, and the spaghetti diagram.

The analysis was executed on the project of the assembly line, which consists of lines A and B. Figure 5 shows a map of the value flow (VSM) of the selected assembly line (B). The VSM map will allow us to identify wastes in the process, monitor VA activities (with added value) and NVA activities (without added value), and identify opportunities for improvement (kaizen). VSM represents the assembly process of line B, which consists of 2 parts (Bx, By), where 2 products are assembled separately, which form the finished product with the product from line A. The complete product, which is created by combining products from lines A and B is paired at the marriage station. In the value stream map, a data box is assigned to each assembly station. This box contains information:

- CT – Cycle Time,
- TT – Takt Time,
- CTT – Company Takt Time,
- Utilization – Operator utilization (%),
- WIP – Work in Progress.

CT represents the time within which it is possible to complete all process steps at the workplace and is calculated using predefined time methods – MOST. TT is a manufacturing term to describe the required product assembly duration that is needed to match the demand, in order to meet customer requirements. The selected assembly line does not work with 100% efficiency, but only with 95%. This (measured) parameter is reflected in the time at which the assembly line must produce. This time is called the Company Takt Time (CTT). The goal of lean manufacturing is to synchronize CT and CTT as much as possible by balancing, greatly reducing the waste caused by waiting. Utilization reflects the percentage utilization of individual operators at the respective assembly stations. WIP records inventory expectations in the process. WIP is the minimum number of materials in stock of process which an employee needs to complete the process without undue waiting. However, the aim is to minimize these stocks so there won't be unnecessary material (waste) in inventory.

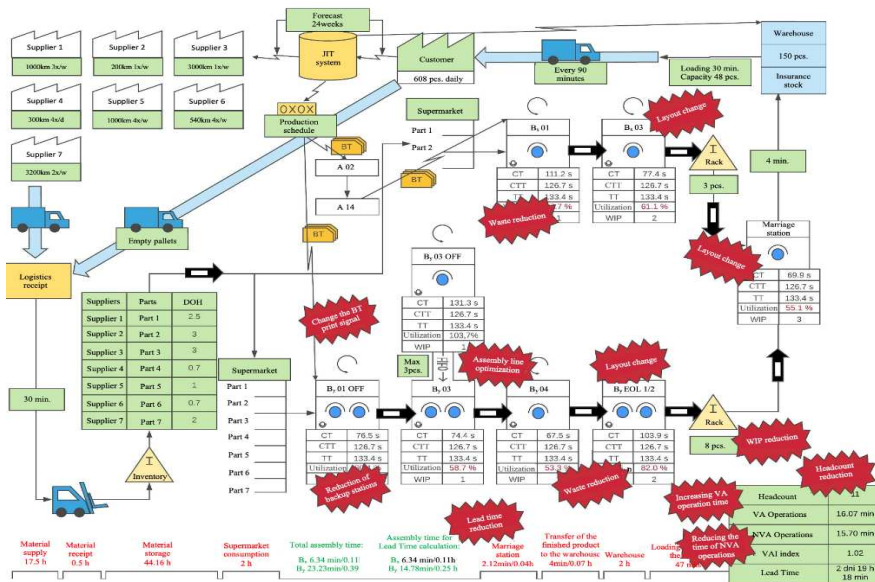


Figure 5

Identified kaizens in the VSM of the current state of the B line

The lower part of the VSM (Figure 5) shows the time axis. The beginning of the timeline contains 4 times - material deliveries, material receipt, material storage, and material consumption in supermarkets. The timeline further contains the assembly times for the B_x and B_y line, individually. The total assembly time of the B_x line is equal to the assembly time used to calculate the total lead time. Operators work at stations either directly on the line (online) or at stations near the assembly line (offline). This line does not contain offline stations and each station is served by only one operator. On B_y, these 2 times are different, since the B_y 03 off station operates in parallel, at the same time as the B_y 03 station. Each station B_y 01 off, B_y 03 and B_y EOL 1/2 is operated by two operators, which we also took into account when calculating the total assembly time. In the calculation, we also took into account the backup stations on the B_y line 03. The timeline also displays:

- CTT time at Marriage station (station where products from line A and B are paired),
- the time required to move the finished set to the warehouse of the finished products,
- the time of holding inventory in the warehouse of finished products (in case of problems in production, these stocks provide time to eliminate errors without endangering deliveries for the customer),
- loading of finished products into the truck for dispatch,
- the time required to transport the finished products to the customer.

At the end of the timeline is a data sheet illustrating:

- total number of operators on the line B - 11 ($B_x - 2$, $B_y - 8$, Marriage 1)
- VA operations (16,07 min.),
- NVA operations (15,70 min.),
- VAI index of operations (1,02),
- Lead Time (2 days 19h 18 min.).

By adding the CT of station Marriage, the stations on both lines B_x , B_y (stations where two operators work are added twice), we obtained the sum value for value-added (VA) processes.

The value for NVA operations is obtained as the difference of the total assembly time with VA operations. NVA is caused by the waste within the processes. The VAI value-added index is obtained with use of the formula: $VAI = \Sigma VA / \Sigma NVA$.

Lead time is the result of adding the times defined on the timeline, except for the assembly time of the B_x line. Since both assembly lines produce the same product reference in parallel, the assembly time of line B_y is used to calculate the Lead Time.

The output of VSM is a graphical representation of the value stream and the main indicator is the value-added index (VAI), which we obtain as a proportion of activities that add value to the customer with those that have no added value for them.

The VSM of line B provided us with a comprehensive view of how the project works from the order, across production to the final shipment. Through VSM, we received a comprehensive analysis of the entire project, and we did not approach the processes individually, but as a set of all processes that are interconnected.

The Yamazumi graf is a visual tool that helps in finding an effective employee cycle in the process. By interpreting the data obtained using the MOST method and their subsequent application to the VSM method for the purpose of a more detailed analysis, we compiled a Yamazumi graph (Figure 6). In addition to VA (value added - green) and NVA (non value added - red) operations, the Yamazumi chart also takes into account BVA (business value added - yellow) operations and untapped potential (waste caused by waiting - gray). Although these operations (BVA) have no value for the customer, they are necessary in the assembly process. The Yamazumi graph clearly shows the current utilization of operators in relation to the takt time and shows in detail the process operations and their distribution with respect to VA, NVA, BVA and untapped potential. The most common waste is the waste caused by scanning, for this reason it is specifically marked in the graph (NVA scanning - pink).

The graph of Figure 6 shows the utilization of operators at individual stations of line B. It is clear from the graph that at several stations the operators are not

utilized effectively, mostly at the station B_y 03, 04 and Marriage station, where there is a waste caused by waiting more than 50 seconds. Significant waste caused by waiting is also at the B_y 01 off station, but these stations are ergonomically very demanding for operators. At the offline station B_y 03 off A / B, the operator is utilized above the Company Takt Time, and therefore there is a risk of slowing down the entire production process of the B line. At present, this anomaly is covered by employees who are best trained and able to work more efficiently than the time result of the MOST analysis. By compiling a value stream map and interpreting the predefined time data using a Yamazumi graph, we were able to identify the wastes that occur in the assembly process on line B.

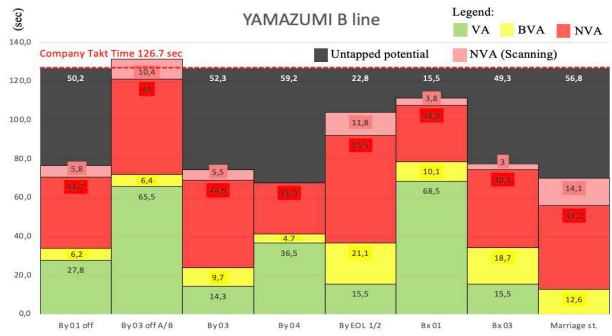


Figure 6 Yamazumi chart showing waste including scanning on the B line

The spaghetti diagram identifies and highlights waste caused by the excessive motion of operators and, compared to VSM, is only created for a specific section of the layout. Organizations tend to ignore the importance of workplace layout and operators movements within the layout. The biggest waste of motion we identified using VSM analysis and Yamazumi graph regarding CTT occurs on the backline at B_x 01, B_x 03, and B_y EOL 1/2. To visually illustrate the waste caused by motion, we created a spaghetti diagram by observing the assembly process and the operators (Figure 7).

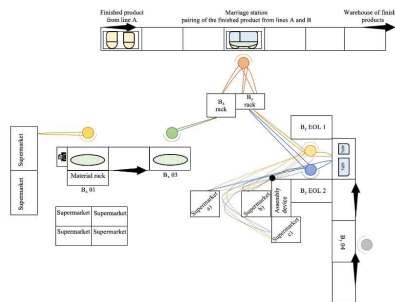


Figure 7 Spaghetti diagram applied on a selected part of the B line layout

5 Results and Discussion

The most frequently identified wastes based on the analysis (waiting, motion, overprocessing, WIP), opportunities for improvement are also marked on the value stream map (Figure 5) using the “Kaizen” symbol. The most significant opportunities to eliminate the identified waste are:

- assembly line optimization, reduction of stocks in the process,
- reduction of waste in assembly processes by optimizing, reducing overprocessing,
- changing the layout of workplaces to reduce waste caused by excessive motion of operators.

After adding up the waste that occurs when scanning on line B, we reached a value of 54,4 seconds. The barcode scanning process itself is not included in this calculation. At present, organizations mostly use a wireless barcode scanner for scanning purposes (see Figure 8). Scanner holders, which also serve as chargers, are located at operators' distances at all assembly stations.



Figure 8
ZEBRA wireless scanner [32]



Figure 9
Gloves MARK 2 standard [33]

The German company ProGlove is a relatively young company that has been present on the European market since September 2016. They strive to improve, streamline work processes with regard to ergonomics through the application of digitization and the fourth industrial revolution (Industry 4.0). The company manufactures and distributes gloves that include a detachable scanner holder. There are several variants of gloves to choose from. The best choice for the selected analyzed assembly process according to the authors of the paper is the variant of gloves "MARK 2 standard" shown in Figure 9.

The advantages of the "MARK 2 STANDARD" gloves include:

- higher safety of operators due to the adhesion of gloves which allows a firmer grip of the material,
- simple process documentation (digitization of collected data from scanning),
- increased efficiency of processes and reduction of errors due to verification of parts,
- elimination of motion waste caused by retrieving and returning the scanner to the holder, improved ergonomic conditions of employees.

By implementing this technology across Line B, it is possible to eliminate the waste caused by picking up and returning the scanner during the scanning process. The expected streamlining of assembly processes at individual stations where scanning is used is shown in the updated Yamazumi charts (Figure 10).

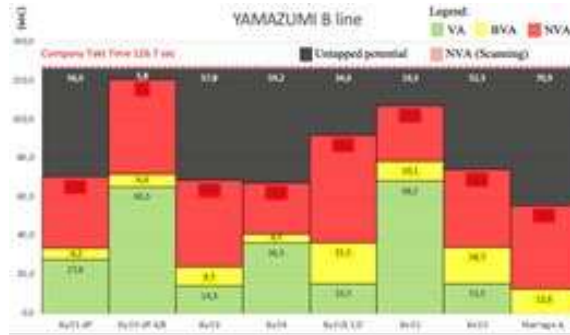


Figure 10

Yamazumi chart after implementation of a new scanning technology

Figure 11 shows the current layout of a selected part of the B_y line, stations B_y 03, B_y 04 off, and B_y 04. At stations B_y 03 and B_y 04, we used the Yamazumi graph (Figure 6) to identify high wastes caused by waiting:

- B_y 03 – 57,8 seconds,
- B_y 04 – 59,2 seconds per operator.

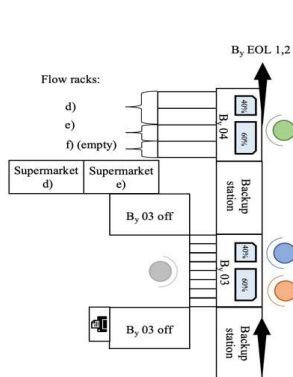


Figure 11

Current layout of the selected part selected of the B line – station B_y 03 and B_y 04

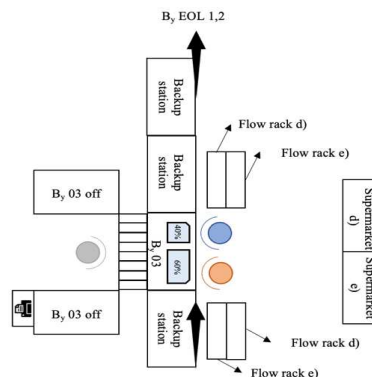


Figure 12

Proposed layout of the selected part of the B line – station B_y 03 and B_y 04

Figure 12 shows the new proposed layout, which was designed based on rebalancing the original one (Figure 11). By moving the flow racks, which are necessary for assembly, and relocating the supermarkets to the other side of the

assembly line so that they are in direct access to the flow racks, it is possible to merge the B_y 03 station with the B_y 04 station. The Yamazumi graphs (Figures 13 and 14) represent the time required to perform all station assembly processes with relation to the CTT before and after the optimization design. With the new layout proposal, it is possible to increase the percentage utilization of B_y 03 station operators from the original 54,38% to 81,14% and at the same time reduce the required number of Line B employees by one operator.

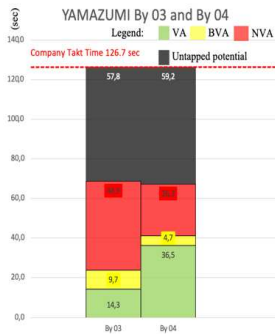


Figure 13

Yamazumi graph before proposal on station By 03 and By 04

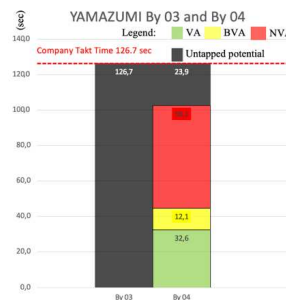


Figure 14

Yamazumi graph after proposal on station By 03 and By 04

Based on the analysis using the spaghetti diagram (Figure 7), we identified waste caused by excessive motion. By interpreting the data using the Yamazumi graph (Figure 10), we identified the waste caused by waiting at stations:

- B_x 01 – 19,3 seconds,
- B_y EOL 1/2 – 35,6 seconds,
- B_x 03 – 52,3 seconds,
- Marriage station – 70,9 seconds

Based on these findings, we can streamline assembly stations by changing the layout and balancing assembly processes between stations. We suggest changing the layout according to Figure 15.

Most important step is to move the B_x assembly line closer to the Marriage station, and therefore also to the B_x rack. This layout change, can reduce the excessive motion of the B_x 03 station operator when inserting the product into the rack by 3,6 seconds. By relocating the B_x assembly line, a new free space will be created behind the line. This space can be used to create a new supermarket zone that would be at a more acceptable distance from the B_y EOL 1/2 stations. By relocating supermarkets, we can reduce the waste caused by the motion of B_y EOL 1/2 station operators by an average of 3,4 seconds.

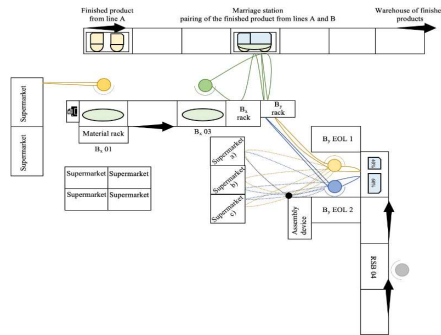


Figure 15

Proposed layout of the selected part of the B line supplemented by a spaghetti diagram

Due to high waste of waiting, it is possible to rebalance the assembly processes between the stations B_x 01, B_x 03, and Marriage station by moving selected parts of the assembly process activities of the B_x 03 station (in the duration of 7,9 sec of a total 13,7 sec) to the B_x 01 station. The next balancing step is to remove the Marriage station operator and move all his assembly processes out to the B_x 03 station.

Yamazumi graphs (Figures 16 and 17) represent the outcome of process rebalancing even though the graphs also take into account the streamlining of the scanning process by implementing the new Industry 4.0 technology.

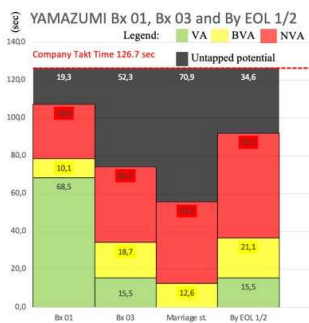


Figure 16

Yamazumi graph before proposal on station Bx 01, Bx 03, Marriage station and By EOL 1/2 and By 04.

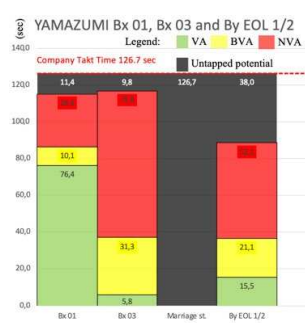


Figure 17

Yamazumi graph proposal on station Bx 01, Bx 03, Marriage station and By EOL 1/2 and By 04

The utilization of operators on the B_x line would increase after balancing. The utilization of the operator of B_x 01 station would change from the original 84,77% to 91% and of the B_x 03 station from 58,72% to 92,27%. The utilization of the operators of the B_y EOL 1/2 station would decrease from 72,69% to 71,01% due to the streamlining of the layout and the reduction of motion waste.

By implementing the proposal, we would be able to remove the operator of the Marriage station.

As a result of Value Stream Mapping (Figure 5), we identified waste of overproduction. Work in progress (WIP) is located on the racks for finished products of the B_x and B_y lines. The minimum stock (3 pcs defined as a standard of organization) is necessary in case of errors in the assembly process. However, there is a maximum stock of 3 pcs in the rack of B_x products and maximum stock of up to 8 pcs in the rack of B_y line products, which creates a disparity between them. The creation of excess stock is caused by different assembly times of the assembly lines: A – 27,45 minutes, B_x – 6,34 minutes, B_y – 14,78 minutes.

The reduction of stocks in the B_x rack is ensured by changing the BT printing (orders). BT is not printed at station B_x 01 at the time of receipt of orders, but only after scanning BT at station A 14. This change provides space to assemble the required product (B_x) only when it's needed due to shorter line assembly time. It also contributes to reducing work in progress.

BT is printed at the moment of receiving the order on the B_y line (B_y 1 off). The same reference of the main product is mounted in parallel on line A and line B_y in spite of different assembly times of the lines. By proposing to use the same principle of BT printing on the B_y line, and B_x line, it would be possible to reduce WIP. Whereas there is a longer time of B_y line compared to B_x line, authors of the paper propose to print BT on station B_y 01 off at the moment of scanning BT on station A 07. By proposing a change of BT printing on the RSB line, we would be able to reduce stocks in the B_y racks from 8 pcs. to 3pcs.

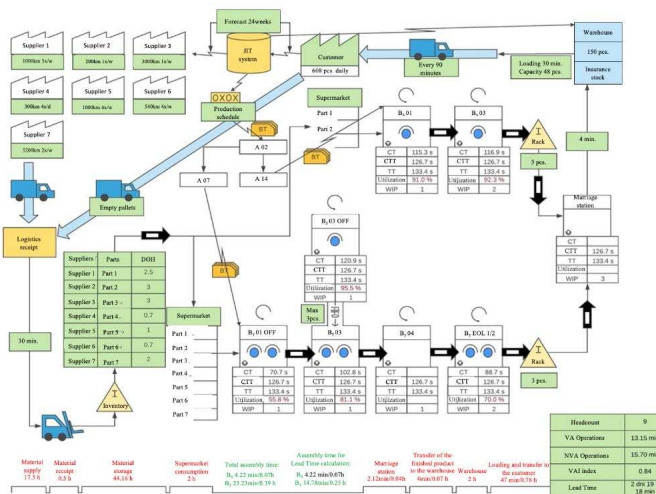


Figure 18
VSM map of B line after implementing proposals

Figure 18 shows the future Value Stream Map for line B after the implementation of each proposal.

By implementing proposals - balancing assembly stations, changing layouts, and implementing selected Industry 4.0 technologies, the organization would be able to:

- reduce the number of operators on line B from 11 to 9, reduce labor costs,
- reduce the time of VA operations from 16,07 minutes to 13,15 minutes,
- reduce the value of the VAI index from 1,02 to 0,84,
- eliminate identified wastes, streamline assembly processes,
- improve the ergonomic conditions of employees,
- reduce WIP, optimize the percentage utilization of operators.

Conclusion

The link between Lean production and Industry 4.0 implementation can be identified at a glance. Lean production is considered an important building block of digitalization of organisations. Comparing obtained mean values of lean production utilisation with results of surveys using same scale and instrument for examining management tools utilisation, reveals that lean production is not amongtop ten used management tools in Central Europe, implying a relative low readiness for Industry 4.0 implementation [34]. It is necessary to realize that the implementation of lean manufacturing as well as the principles and methods of Industry 4.0 into business is a strategic decision of the company's top management. Based on the findings, it is possible to declare that Industry 4.0 technologies and Lean Manufacturing methods can be integrated. This integration can multiply the effect of their use - streamlining production, improving processes, working conditions and all activities that lead to a leaner production.

Acknowledgement

The paper is a part of project VEGA No. 1/0721/20 „*Identification of priorities for sustainable human resources management with respect to disadvantaged employees in the context of Industry 4.0*“.

This publication has been published with the support of the Operational Program Integrated Infrastructure within project “*Research in the SANET network and possibilities of its further use and development*”, code ITMS 313011W988, co-financed by the ERDF.

References

- [1] Pavlovic, D., Milosavljevic, P., Miladenovic, S.: Synergy between Industry 4.0 and lean methodology. *J. Mechatron. Autom. Identif. Technol.* 5(4), 17-20 (2020)

- [2] Valamede, L. S., Akkari, A. C. S., & Cristina, A. (2020) Lean 4.0: A new holistic approach for the integration of lean manufacturing tools and digital technologies. *International Journal of Mathematical, Engineering and Management Sciences*, 5(5), 851-868, <https://doi.org/10.33889/IJMEMS.2020.5.5.066>
- [3] Czifra, G., Szabó, P., Míkva, M., & Vaňová, J. (2019) Lean principles application in the automotive industry. *Acta Polytechnica Hungarica*, 16(5), 43-62. DOI: 10.12700/APH.16.5.2019.5.3
- [4] Johanesová, V., Stupavská, L., Vanova, J., & Cambal, M. (2019) Linking Industry 4.0 and Slovak Republic. *DAAAM Proceedings; Katalinic, B., Ed.; DAAAM International Vienna: Vienna, Austria, 1*, 1122-1130
- [5] Azemi, F., Šimunović, G., Lujčić, R., Tokody, D., & Rajnai, Z. (2019) The use of advanced manufacturing technology to reduce product cost. *Acta Polytechnica Hungarica*, 16(7), 115-131, DOI: 10.12700/APH.16.7.2019.7.7
- [6] The path from Industry 4.0 to Industry 5.0 [online] [cit. 2023-11-03] Available on: <https://www.atoss.com/en/insights/blog/from-industry-4-0-to-industry-5-0>
- [7] Cabrita, M. D. R., Domingues, J. P., & Requeijo, J. (2016) Application of Lean Six-Sigma methodology to reducing production costs: case study of a Portuguese bolts manufacturer. *International Journal of Management Science and Engineering Management*, 11(4), 222-230, <https://doi.org/10.1080/17509653.2015.1094755>
- [8] Sarkar, B., & Moon, I. (2014) Improved quality, setup cost reduction, and variable backorder costs in an imperfect production process. *International journal of production economics*, 155, 204-213, <https://doi.org/10.1016/j.ijpe.2013.11.014>
- [9] Ouyang, L. Y., Chen, C. K., & Chang, H. C. (2002) Quality improvement, setup cost and lead-time reductions in lot size reorder point models with an imperfect production process. *Computers & Operations Research*, 29(12), 1701-1717, [https://doi.org/10.1016/S0305-0548\(01\)00051-X](https://doi.org/10.1016/S0305-0548(01)00051-X)
- [10] Dey, S., Sharma, R. R. K., & Pandey, B. K. (2019) Relationship of manufacturing flexibility with organizational strategy. *Global Journal of Flexible Systems Management*, 20(3), 237-256, <https://doi.org/10.1007%2Fs40171-019-00212-x>
- [11] Santosa, W. A., & Sugarindra, M. (2018) Implementation of lean manufacturing to reduce waste in production line with value stream mapping approach and Kaizen in division sanding upright piano, case study in: PT. X. In *MATEC Web of Conferences* (Vol. 154, p. 01095) EDP Sciences. <https://doi.org/10.1051/matecconf/201815401095>

- [12] Buer, S. V., Strandhagen, J. O., & Chan, F. T. (2018) The link between Industry 4.0 and lean manufacturing: mapping current research and establishing a research agenda. *International journal of production research*, 56(8), 2924-2940
- [13] Křivánek, D. (2009) *The way to lean*. (Guide to obstacles and rules) Žilina: IPA Slovakia
- [14] Mašín, I. (2003) *Value stream mapping in production processes*. 1st Edition. Liberec: Institute of Industrial Engineering. ISBN 80-902235-9-1
- [15] Capital, M. (2004) Introduction to lean manufacturing for Vietnam. Published Article by Mekong Capital Ltd.
- [16] Elnamrouty, K., & Abushaaban, M. S. (2013) Seven wastes elimination targeted by lean manufacturing case study “gaza strip manufacturing firms”. *International Journal of Economics, Finance and Management Sciences*, Vol. 1, No. 2, 2013, pp. 68-80, doi: 10.11648/j.ijefm.20130102.12
- [17] Shah, D., & Patel, P. (2018) Productivity improvement by implementing lean manufacturing tools in manufacturing industry. *International Research Journal of Engineering and Technology*, 5(3), 3-7
- [18] The 8 Wasted of Lean [online] [cit. 2021-08-20] Available on: <https://theleanway.net/The-8-Wastes-of-Lean>
- [19] Manyika, J., Chui, M., Bisson, P., Woetzel, J., Dobbs, R., Bughin, J., & Aharon, D. (2015) *The Internet of Things: Mapping the value beyond the hype*. Publisher: Mckinsey Global Institute
- [20] Pyzdek, T. (2021) Spaghetti Diagrams. In *The Lean Healthcare Handbook* (pp. 25-28) Springer, Cham. [online] [cit. 2021-08-20] Available on: <https://link.springer.com/content/pdf/10.1007%2F978-3-030-69901-7.pdf>
- [21] Spaghetti chart [online] [cit. 2021-09-25] Available on: <https://www.lean.org/lexicon/spaghetti-chart>
- [22] Senderská, K., Mareš, A., & Václav, Š. (2017) Spaghetti diagram application for workers’ movement analysis. *UPB Scientific Bulletin, Series D: Mechanical Engineering*, 79(1), 139-150, https://www.scientificbulletin.upb.ro/rev_docs_arhiva/full5a2_608068.pdf
- [23] All About Spaghetti Diagrams [online] [cit. 2021-09-25] Available on: <https://www.allaboutlean.com/spaghetti-diagrams/>
- [24] Abdulmalek, F. A.; Rajgopal, J. (2007) Analyzing the benefits of lean manufacturing and value stream mapping via simulation: A process sector case study. *International Journal of production economics*, 2007, 107.1: 223-236, <https://doi.org/10.1016/j.ijpe.2006.09.009>

- [25] What is Value Stream mapping? Benefits and Implementation [online] [cit. 2021-09-25] Available on: <https://kanbanize.com/lean-management/value-waste/value-stream-mapping>
- [16] Value Stream Mapping (VSM) [online] [cit. 2021-09-25] Available on: <https://www.creativesafetysupply.com/articles/value-stream-mapping-vsm/>
- [27] Fekete, M. & Hulvej, J. (2013) „Humanizing“ Takt Time and Productivity in the Labor – Intensive Manufacturing Systems [online]. Zadar, Croatia – *International Conference 2013* [cit. 2018-05-16] ISBN 978-961-6914-02-4. Dostupné na internete: <http://www.toknowpress.net/ISBN/978-961-6914-02-4/papers/ML13-245.pdf>
- [28] Mayr, A., Weigelt, M., Kühn, A., Grimm, S., Erll, A., Potzel, M., & Franke, J. (2018) Lean 4.0-A conceptual conjunction of lean management and Industry 4.0. *Procedia Cirp*, 72, 622-628, <https://doi.org/10.1016/j.procir.2018.03.292>
- [29] Santos, D. M. C., Santos, B. K., & Santos, C. G. (2021) Implementation of a standard work routine using Lean Manufacturing tools: A case Study. *Gestão & Produção*, 28(1), e4823, <https://doi.org/10.1590/0104-530X4823-20>
- [30] Semjon V. & Evin E., (2009) Increasing the productivity of the assembly line by balancing of assembly stations using the Yamazumi method. *Transfer Inovácií* 13, 2009, 73-77
- [31] Sabadka, D., Molnár, V., Fedorko, G., & Jachowicz, T. (2017) Optimization of production processes using the Yamazumi method. *Advances in Science and Technology. Research Journal*, 11(4), 175-182, DOI: <https://doi.org/10.12913/22998624/80921>
- [32] ZEBRA wireless scanner [online] [cit. 2021-05-25] Available on: www.zebra.com, 2020
- [33] Gloves MARK 2 standard [online] [cit. 2021-05-25] Available on: www.proglove.com, 2020
- [34] Rashad, W., Lazanyi, K., Potocan, V., & Nedelko, Z. (2019) How does Business Orientation of Manufacturing Enterprises Define the Utilisation of Lean Production. *Acta Polytech. Hung*, 17, 257-276, DOI: 10.12700/APH.17.9.2020.9.1

The Effect of the Ball-Track Connection on the Energy Behavior of the Roller Gearing Gearbox

Polák József László

Széchenyi István University of Győr, Department of Road and Rail Vehicles
Egyetem tér 1, 9026 Győr, Hungary; e-mail: polakj@ga.sze.hu

Abstract: In this paper, I present an energetic study of the roller gearing gearbox by investigating the friction phenomena at the ball-track contact. The novelty of the subject is that the gearbox under investigation is a Hungarian invention, the energetic investigation of which has not been dealt with before. The study was carried out using a mathematical model based on analytical principles, in the course of which the principles and models used for ball bearings and ball screw drives were adapted and applied accordingly. It is important to mention that the study does not cover the complete gearbox, so losses outside the ball-race contact, e.g. bearing friction, seal friction, oil friction, air friction, etc., have not been considered in this paper.

Keywords: roller gearing gearbox; ball-track connection; rolling friction; coefficient of friction

1 Introduction

In this paper, I present an energetic study of the roller gearing gearbox by investigating the friction phenomena at the ball-track contact. The energetic behaviour of gearbox used in engineering, and in particular in the automotive industry, is of great importance, and typically involves the identification of the sources of engine losses and their magnitude. This is particularly important in the case of electrically powered vehicles, as these losses have a significant impact on the vehicle's range, hence the importance of whether or not a gearbox is used in the design of an electrically powered vehicle and, if so, what its parameters are.

The novelty of the topic lies in the fact that the engine under investigation is a Hungarian invention, the energetic investigation of which has not been dealt with before. The roller gearing gearbox was invented by a Hungarian physicist [1] who wanted to use this type of action to transmit and modify rotary motion, since ball bearings only function as orienting, bedding components and are therefore not capable of modifying the rotary motion that passes through them, while spindle-

ball drives typically convert rotary motion into rectilinear motion, but none of them is directly suitable for transmitting and modifying rotary motion.

Figure 1 shows the physical model of the roller gearing gearbox under test. The gear can be defined as a dynamic system with three degrees of freedom since the balls in the connection are assumed to be elastic. The figure shows the general coordinates (q_1 - q_4) that can be used to define the physical model of the gear.

The essence of the operation of the roller gearing gearbox is that ball(s) are used as transmission elements to transfer the movement and torque between the driving and driven wheels.

The ball enters the drive at a specific point and rolls into the converging grooves on the surface of the two discs. The groove transfers the drive from the driven wheel to the drive wheel through the wall. As the two discs rotate together, the ball travels along the grooves at their intersection point, and at the end of the grooves, the ball leaves the connection. Balls that are out of contact are guided back to the entry point on a leading path.

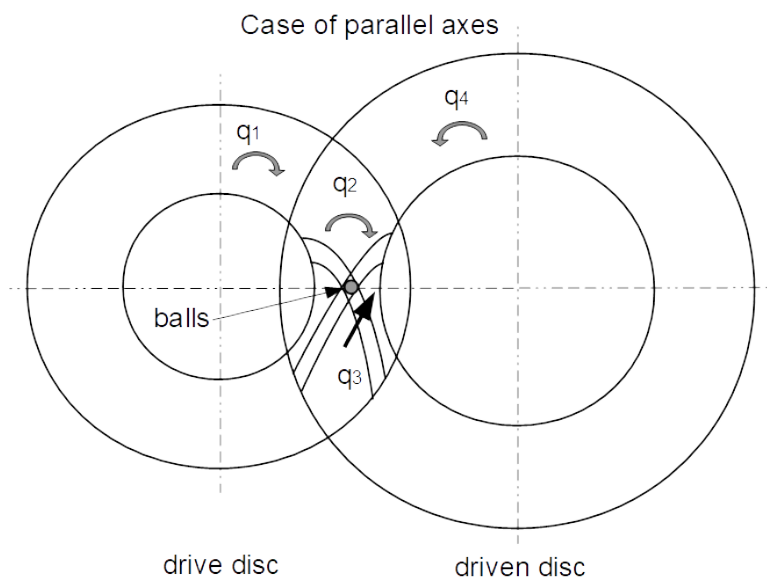


Figure 1

Physical model of the gearbox focused on the position and movement of the ball

The study was carried out using a mathematical model based on analytical principles, in the course of which the principles and models used for ball bearings and ball screw drives were appropriately adapted and applied. For these two machine elements, a very large literature has been produced on their motion, energetic behaviour and sizing, and this area is, therefore, highly researched.

However, it is important to note here that the working, loading and motion relations of the two machine elements are very similar, so that their mathematical modelling is broadly the same, while in the case of the roller gearing gearbox the ball-track relation is very similar to the previous one, but their motion characteristics with respect to each other are significantly different, which requires a modification of the relations applied to the previous cases.

In any case, it should be mentioned that the study does not cover the complete gearbox, so losses outside the ball-track relationship, e.g. bearing friction, seal friction, oil friction, air friction, etc., have not been considered in this paper.

In the case of an gearbox these losses are of great importance and play a key role in determining the total losses of the gearbox, but since in this article the ball-race contact is investigated, these losses have been neglected.

The total friction loss in a roller gearing gearbox includes the sliding and rolling friction loss in the ball-track contact and the friction loss in the return track, which is created between the balls and the return track. The friction loss in the system can be well described by some empirical relationships. These relations take into account the important parameters that are generated during the drive, such as load, rotation speed, lubricant, surface roughness, friction coefficient, etc. The relations describing this phenomenon require an accurate estimation of the friction forces and torques acting on the drive and driven rollers at the different working points.

In recent years, Hupert has developed simple and efficient computational procedures in the field of rolling bearings [2, 3]. And Olaru et al. have developed analytical models to determine the frictional forces generated during the operation of ball screw [4, 5]. The author has attempted to develop a new analytical model to determine the friction losses of roller gearing gearbox based on friction models of rolling element bearings and ball screw systems.

In the first part of the paper, the forces acting on the ball-track contact are presented, followed by the tangential forces and the geometric characteristics of the roller gearing gearbox that determine the friction losses of these gearbox. In the light of these, an analytical mathematical model is created to study the energetic behaviour of this gearbox through a specific concrete case.

2 Determination of the Forces Acting on the Ball

2.1 Determination of the Forces Acting on the Ball at the Contact Surface of the Ball Track

Figures 2, 3 show the forces acting on the balls in the x-z and x-y planes. By looking at the forces acting on the ball at the i-th point of the trajectory, it can be seen that between the groove wall of the driving disc and the ball, a force in the normal direction (F_{ni}), perpendicular to the trajectory wall, and a force in the tangential direction (F_{ti}), pointing in the direction tangential to the trajectory, are generated due to the driving force of the disc (F_{hi}). As shown in the Figure 2, the normal directional force can be further decomposed into planar forces (F_{nixz} , F_{nixy}). The driving force on the groove wall can be determined from the torque of the driving motor (M_{mot}) and the distance of the ball from the axis of rotation (r_i) this force can be computed by relationship:

$$F_{hi} = \frac{M_{mot}}{r_i} \quad (1)$$

Knowing the driving force, the normal force between the ball and track can be determined on the basis of Figure 4 with the following relation:

$$F_{ni} = \frac{F_{hi}}{\cos \alpha \cdot \cos \beta} \quad (2)$$

Indexing i along the trajectory is necessary because the radius of the gear in the x-y plane, the radius of gyration (r_i) and the radius of curvature of the trajectory depend on the position of the ball, and therefore vary continuously, unlike the case of rolling bearings or ball bearings, where the radius is the same along the entire trajectory of the motion.

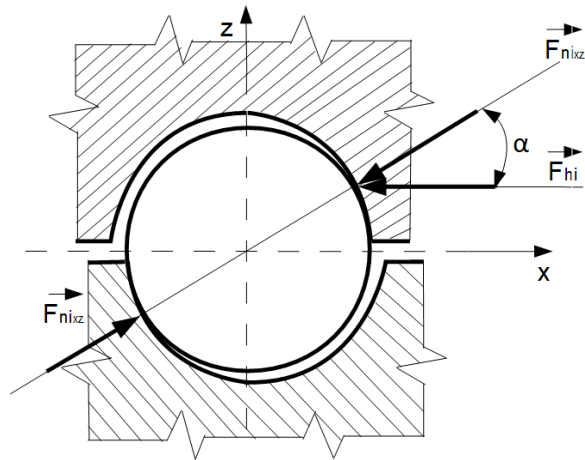


Figure 2
Forces acting on a ball moving in track in the x-z

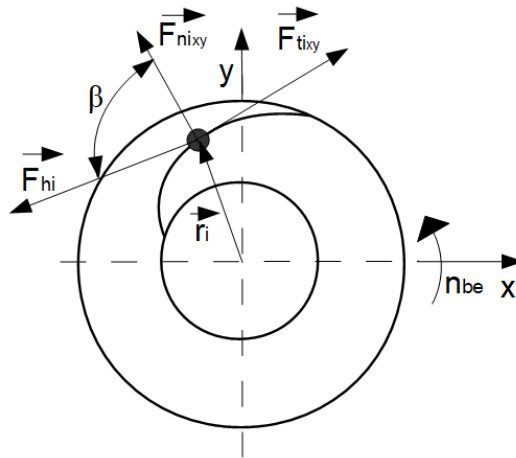


Figure 3
Forces acting on a ball moving in track in the x-y

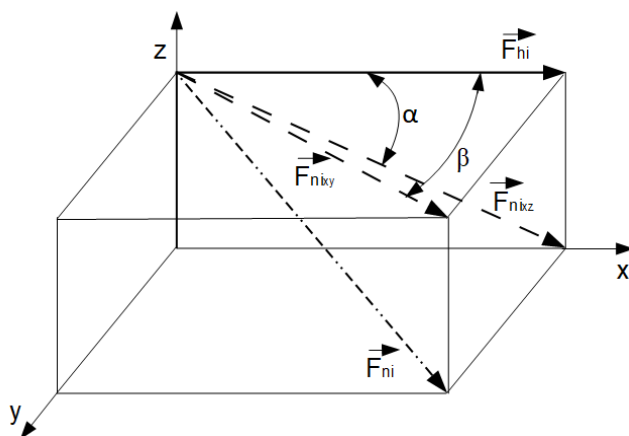


Figure 4

Determination of the spatial normal force (F_{ni}) acting on the ball

2.2 Determination of Tangential Force at the Contact Surface of the Ball Track

The forces acting at the ball-track contact are: hydrodynamic rolling resistance force (F_r), the force of pressure at the ball-track contact (F_{ni}), the force of sliding (F_f), the force of pressure between the balls (F_g).

The hydrodynamic rolling force generates an EHD (elastohydrodynamic lubricating regime) lubrication condition at the contact surface by means of Poiseuille flow through the lubricant, which can be defined by the following relation [2, 4]:

$$F_r = 2,86 \cdot E \cdot Rx^2 \cdot k^{0,348} \cdot G^{0,022} \cdot U^{0,66} \cdot W^{0,47} \quad (3)$$

“where E [GPa] is the equivalent modulus of elasticity determined from the modulus of elasticity of the related materials, Rx [m] is the equivalent radius in the direction of rolling, k [-] is the ratio of the rolling radii, G , U , W [-] dimensionless material parameters, speed parameters and load parameters”.

In the case of a drive disk-ball connection:

$$\frac{1}{Rx1} = \frac{2}{d_w} - \frac{2 \cdot \cos \alpha}{d_m + d_w \cdot \cos \alpha} \quad (4)$$

In the case of a ball-driven disk:

$$\frac{1}{Rx2} = \frac{2}{d_w} + \frac{2 \cdot \cos \alpha}{d_m - d_w \cdot \cos \alpha} \quad (5)$$

Determination of the ratio (k) of the rolling radii:

$$k = \frac{Ry}{Rx} \quad (6)$$

Determination of the transverse equivalent radius (Ry):

$$Ry1 = \frac{f_1 \cdot d_w}{2 \cdot f_1 - 1} \quad \text{and the} \quad Ry1 = \frac{f_2 \cdot d_w}{2 \cdot f_2 - 1} \quad (7)$$

“where f_1 and f_2 are the curvature parameters for the drive disk and the driven disk, respectively, and d_w is the diameter of the ball”. Based on practical experience, the value of f generally varies between 0.515... 0.54 [5].

Definition of the material parameter (G):

$$G = E \cdot \alpha_p \quad (8)$$

“where α_p [GPa] is the piezoviscosity coefficient”.

Determination of the speed parameter (U):

$$U = \frac{v \cdot \eta_0}{Rx \cdot E} \quad (9)$$

To determine the speed difference between the ball and the track, a new parameter, which is nothing but the internal gear ratio (i_{1b}) must be introduced [6]. The internal gear shows how many turns the transfer ball makes per turns of the drive disk. The determination of the internal gear ratio can be determined as the quotient of the speed of the drive disc (n_1) and the speed of the ball (n_b):

$$i_{1b} = \frac{n_1}{n_b} \quad (10)$$

The speed of the drive disc can be clearly specified, while the speed of the ball must be determined. To determine the speed of the ball, the diameter of the ball (d_b), the length of the path travelled by the ball, which can be determined by extracting from the geometric model the length of a path segment (l_1) and the angular rotation of the drive disc (α_1) associated with the path segment Figure 5.

Using the parameters extracted from the model, you must first determine the number of turns of a ball (n_{b11}) required to make a section of track with the following relation [6]:

$$n_{b11} = \frac{l_1}{d_w \cdot \pi} \quad (11)$$

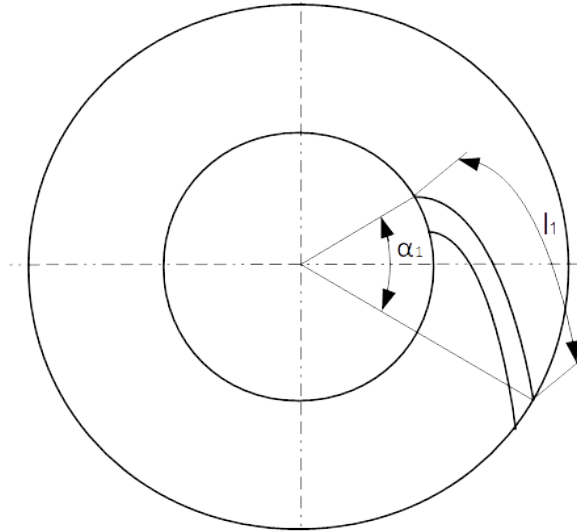


Figure 5

Length of a ball-track and associated rotation angle of the disc [6]

Once the ball speed required to complete a section of track has been determined, the ball speed per speed of the drive disk can be determined by dividing the 360° corresponding to one section by the angular rotation of the disk required to complete one section (α_l [°]) and thus the value obtained shall be multiplied by the number of turns of the ball required to make a section of track [6]:

$$n_b = \frac{360^\circ}{\alpha_{l1}} \cdot n_{bt1} \quad (12)$$

If the ball speed (n_g) is projected on one turn of the drive disk, the internal gear ratio is equal to the speed of the ball. Knowing the internal transmission ratio, the rotation of the ball can be determined by the following relation:

$$n_b = n_{mot} \cdot i_b \quad (13)$$

n_{mot} is the speed of the drive motor, i.e. the speed of the drive disk. Using the parameters defined above, the speed difference between the ball and the track can already be determined:

$$v = n_b \cdot d_w \cdot \frac{\pi}{60000} \left[\frac{m}{s} \right] \quad (14)$$

The load parameter (W) can be determined by the following relation:

$$W = \frac{F_n}{E \cdot R x^2} \quad (15)$$

3 Torques at the Ball-Track Connection

The moment at the contact ellipse can be divided into two parts, the torque due to elastic deformation (T_{er}) at the contact surface of the ball track and the frictional moment (T_f) between the ball track and the ball.

The friction torque (T_f) is due to the local shear stress (τ) between the contact surfaces, which can be determined by the following relation [2, 4]

$$T_f = \int \tau \cdot z \cdot dA = \int \mu \cdot p \cdot z \cdot dA \quad (16)$$

“where (z) is the distance between the line of clean rolling and the position of the shear stress, (μ) is the local coefficient of friction, and (p) is the local contact pressure”.

Assuming a Hertz pressure distribution and a constant coefficient of friction (μ_m), equation (16) can be approximated by the following equation [2, 4]:

$$T_f = 0,1 \cdot \mu_m \cdot \frac{F_n \cdot a^2}{Rd} \cdot (1 - 5 \cdot Y^3 + 3 \cdot Y^5) \quad (17)$$

“where Rd is the radius of deformation in relation to the ball-track;” and can be determined as follows:

$$R_d = \frac{2 \cdot d_w \cdot f}{2 \cdot f + 1} \quad (18)$$

in context (17), Y is a relative parameter that can be interpreted between the clean rolling point and the center of the contact ellipse.

To determine the major axis (a) and minor axis (b) of the contact ellipse, the length of the half-axes must be determined with the following approximations [2, 3]:

$$a \approx 1,552 \cdot R_x \cdot k^{0,4676} \cdot \left(\frac{F_n}{E \cdot R_x^2} \right)^{1/3} \quad (19)$$

$$b \approx 1,502 \cdot R_x \cdot k^{-0,1876} \cdot \left(\frac{F_n}{E \cdot R_x^2} \right)^{1/3} \quad (20)$$

“where T_{er} is the moment of elastic resistance in the case of clean rolling”; which can be determined by the relation of Snare [2, 3, 4]:

$$T_{er} = 7,48 \cdot 10^{-7} \cdot \left(\frac{d_w}{2} \right)^{1/3} \cdot F_n^{1,33} \cdot (1 - 3,519 \cdot 10^{-3} \cdot (k - 1)^{0,806}) \quad (21)$$

4 Friction Forces and Moments in Ball Track Contact

The total tangential force is the algebraic sum of the tangential contact forces in the rolling direction in the ball-track contact of the drive disc

$$F1 = \frac{T_{c1} + T_{c2} + T_{er1} + T_{er2} + T_b}{d_w} + F_{r1} + F_{r2} + \frac{(F_{r1} + F_{r2}) \cdot d_w \cdot \cos \alpha}{d_m} + \frac{F_i}{2} \quad (22)$$

Frictional torque generated at the ball-track contact of the drive disc:

$$Ts_1 = F1 \cdot R1 \quad (23)$$

“where $R1$ is the rolling radius of the ball-to-track connection”:

$$R1 = \frac{d_{m1}}{2} + \frac{d_w \cdot \cos \alpha}{2} \quad (24)$$

“where d_{m1} is the mean value of the radius of the track of the drive disk in the x-y plane”.

The total friction moment for n balls is defined as the sum of the friction torques of the balls underload:

$$Ts_1 = \sum_1^n Ts_i \quad (25)$$

The total tangential force in relation to the ball track of the driven disk can be determined by vector algebraic summation of forces in the rolling direction:

$$F2 = \frac{T_{c1} + T_{c2} + T_{er1} + T_{er2} + T_b}{d_w} + F_{r1} + F_{r2} - \frac{(F_{r1} + F_{r2}) \cdot d_w \cdot \cos \alpha}{d_m} + \frac{F_b}{2} \quad (26)$$

Friction torque generated in relation to the ball-track of the driven disk:

$$Ts_2 = F2 \cdot R2 \quad (27)$$

“where $R2$ is the rolling radius of the ball-to-track connection”:

$$R2 = \frac{d_{m2}}{2} + \frac{d_w \cdot \cos \alpha}{2} \quad (28)$$

“where d_{m2} is the mean value of the radius of the track of the driven disk in the x-y plane”.

The total friction torque on the driven disk tracks for n pieces balls can be determined as the sum of the friction torques of the balls under load:

$$Ts_2 = \sum_1^n Ts_{2i} \quad (29)$$

5 Estimation of Efficiency in the Tested Gearbox

When estimating the efficiency, sliding friction is neglected since pure rolling is assumed, and the efficiency can be described by the following relation:

$$\eta = \frac{T_{mot} - Ts_1 - Ts_2}{T_{mot}}. \quad (30)$$

6 The Results of the Study

A numerical program has been developed to analyse the variation of transmission friction torque and efficiency with drive motor torque.

The geometrical parameters used for testing the gearbox are given in the table 1.

Table 1
The geometrical parameters used for testing the gearbox

No.	Parameters	Values
1.	ball diameter	$dw = 6 \text{ mm}$
2.	average radius of the tracks of drive disk in the x-y plane	$dm1 = 47.5 \text{ mm}$
3.	average radius of the tracks of driven disk in the x-y plane:	$dm2 = 65 \text{ mm}$
4.	total number of balls:	$Z = 86 \text{ pcs}$
5.	number of connected balls:	$z = 5 \text{ pcs}$
6.	contact angle:	$\alpha = 20^\circ$
7.	surface roughness of the ball:	$Rg = 0.6 \text{ }\mu\text{m}$,
8.	Surface roughness of the track of the drive and driven disk:	$Rt = 1.6 \text{ }\mu\text{m}$,
9.	coefficient of friction between balls:	$\mu b = 0.1$
10.	lubricant viscosity:	$\eta_0 = 0.1 \text{ Pas}$
11.	For the parameter Y , it is assumed to be 0.34 for both the drive disc and the driven disc [7].	$Y=0,34$,
12.	the curvature parameters $f1$ and $f2$ for the drive disk and the driven disk are 0,53 [7].	$f1, f2=0,53$
13.	The drive motor torque was varied between 0... 100 Nm.	$T_{mot}=0\dots 100 \text{ Nm}$

Figure 6 shows that there is a small increase in efficiency in the initial stage ($dM \approx 2 \text{ Nm} \rightarrow d\eta \approx 0.2\%$), which shows a monotonic decrease after tipping over ($dM \approx 97 \text{ Nm} \rightarrow d\eta \approx 1.5\%$). Figure 7 shows that the friction torque increases slightly exponentially.

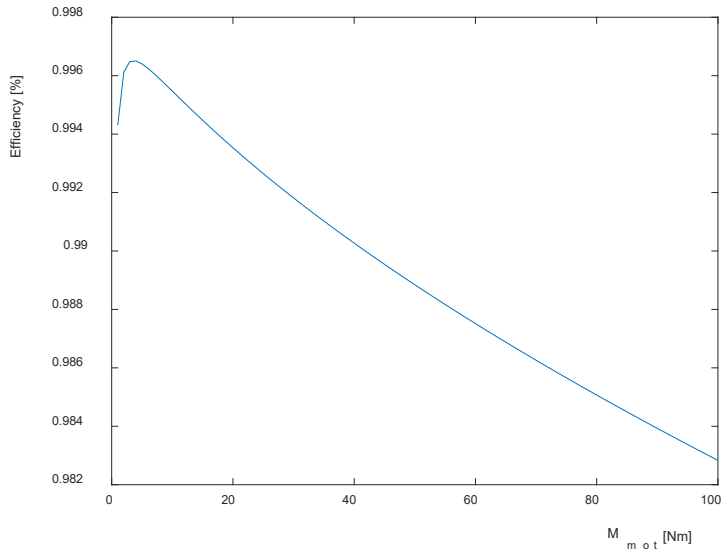


Figure 6

Variation in gearbox efficiency as a function of drive motor torque over the full operating range ($M_{mot}=0 \dots 100$ Nm)

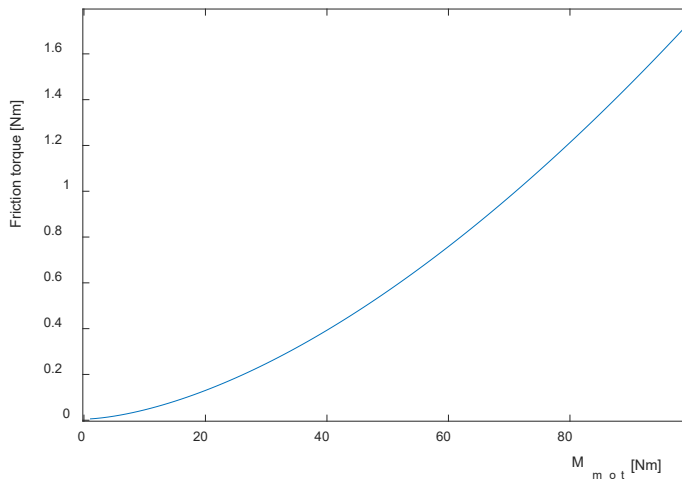


Figure 7

Variation of friction torque as a function of drive motor torque over the full operating range ($M_{mot}=0 \dots 100$ Nm)

7 Investigation of Some Geometrical Parameters of the Roller Gearing Gearbox

In the case of a roller gearing gearbox, it is worthwhile to define the geometric parameters that affect the energetic behaviour of the gearbox over the full operating range, just as has been done for geared gearboxes.

When considering the geometric parameters of the gearbox, two geometric parameters seem to be of interest and importance, one is the ball diameter (d_w) and the other is the average groove radius in the x-y plane (r_x), as these are the parameters that typically determine the motion and loading conditions of the associated components. In addition to the two geometrical parameters, the viscosity of the lubricating oil (η) used may also be of interest, as it has a significant effect on the friction generated during component contact, which is not negligible from an energy point of view, therefore, it is also worth investigating the lubricating oil viscosity.

Thus, the parameter vector of the roller gearing gearbox can be written as shown in the following figure:

$$\mathbf{p} = [d_w, r_x, \eta] \quad (1)$$

With the engine model and the selected parameters, a parameter sensitivity analysis can be performed.

In the first test, the ball diameter was varied by using four different ball diameters to investigate the variation in engine efficiency over the full operating range. The ball diameters were 1 mm, 3 mm, 6 mm, 9 mm.

The result of the run is shown in the Figure 8. From the obtained efficiency curves it is clear that the optimum ball size is not easy to determine, as the gearbox with small diameter balls ($d_w=1\text{mm}$, 3 mm) has a good efficiency in the initial stage but it deteriorates steadily with increasing load, probably due to the small surface area load transfer and the resulting overload.

As the ball size increases ($d_w=6\text{ mm}$), the efficiency of the gearbox is worse in the initial low-load stage, but improves significantly in the higher load ranges, so this means that the energetically optimal behaviour (deformation, lubrication film) is obtained in the higher load ranges.

With a further increase of the ball size ($d_w=9\text{ mm}$), the maximum efficiency does not increase, but the losses in the initial phase increase, so the tendency of the optimal ball size, i.e. to be smaller or larger, cannot be determined, but must always be determined according to the specific load conditions.

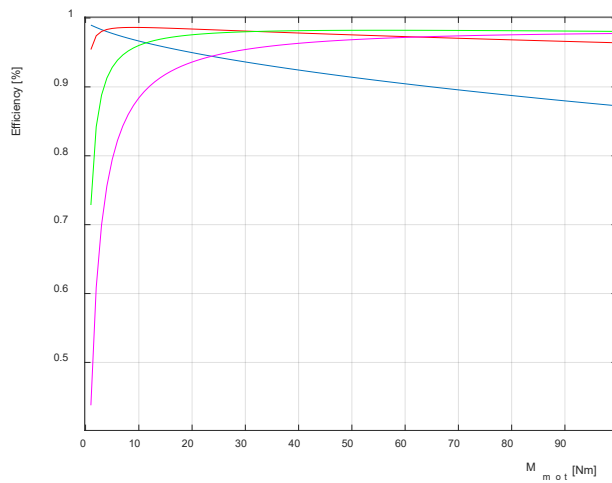


Figure 8

The effect of ball size variation on engine efficiency: $n_{\text{mot}} = 1000$ rpm, $M_{\text{mot}} = 1 \dots 100$ Nm
 (blue line: $d_w = 1$ mm, red line: $d_w = 3$ mm, green line: $d_w = 6$ mm, purple line: $d_w = 9$ mm)

In the second test, the size of the radius in the x-y plane of the ball trajectory was varied by examining the variation of the engine efficiency over the full operating range for four different trajectory radii. The orbit radii were 10 mm, 50 mm, 100 mm, 150 mm.

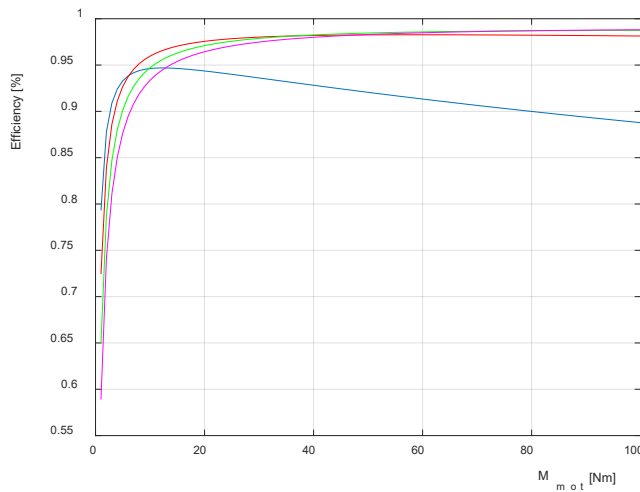


Figure 9

Effect of variation in the radius of the ball orbit in the x-y plane on the efficiency of the gearbox: $n_{\text{mot}} = 1000$ rpm, $M_{\text{mot}} = 1 \dots 100$ Nm (blue line: $r_x = 10$ mm, red line: $r_x = 50$ mm, green line: $r_x = 100$ mm, purple line: $r_x = 150$ mm)

The result of the run is shown in the Figure 9. From the efficiency curves obtained, it is clear that the optimum orbit radius cannot be determined in general since apart from the smallest radius ($r_x=10$ mm) orbit, there is no significant variation in the efficiency of the gearbox for the other three orbits over the whole operating range, so the optimum size can be determined according to the load conditions.

In the third test, the dynamic viscosity of the lubricating oil used was varied by testing the change in engine efficiency over the full operating range with four different viscosities of oil. The selected oil viscosities were as follows: 0,1 Pas; 0,3 Pas; 0,6 Pas; 1,0 Pas.

The result of the run is shown in the following figures (Figure 10, Figure 11). Examining the first diagram, it appears as if there is a single efficiency curve on the diagram, so it was necessary to draw the second diagram, which zooms in on the near-horizontal section of the diagram, from which it can be seen that the change in lubricating oil viscosity has a very minimal effect on engine losses, and therefore further investigation is negligible from this point of view.

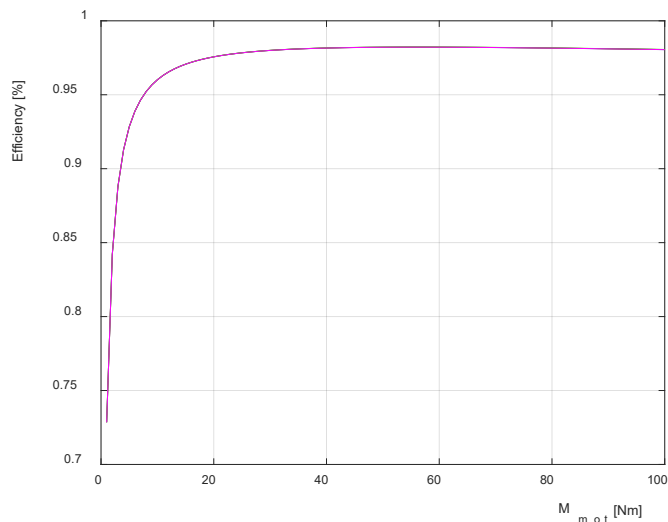


Figure 10

Effect of lubricating oil dynamic viscosity variation on engine efficiency: $n_{mot} = 1000$ rpm, $M_{mot} = 1 \dots 100$ Nm (blue line: $\eta = 0,1$ Pas, red line: $\eta = 0,3$ Pas, green line $\eta = 0,6$ Pas, purple line: $\eta = 1,0$ Pas)

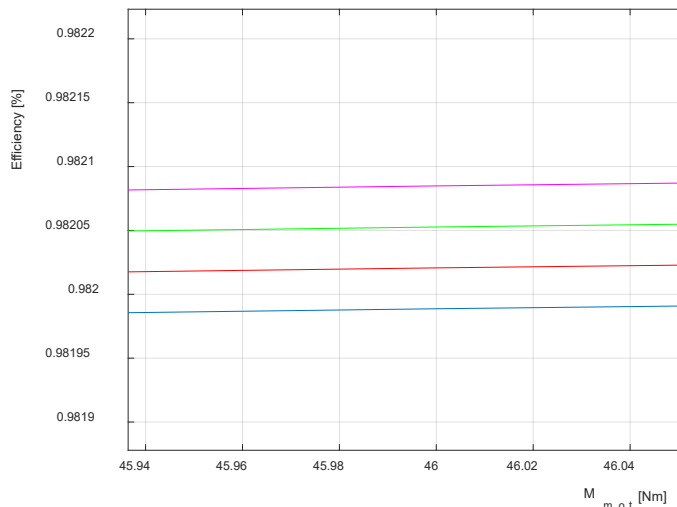


Figure 11

Effect of lubricating oil dynamic viscosity variation on engine efficiency: $n_{mot}=1000$ rpm, $M_{mot}=1 \dots 100$ Nm (blue line: $\eta=0,1$ Pas, red line: $\eta=0,3$ Pas, green line $\eta=0,6$ Pas, purple line: $\eta=1,0$ Pas)

Conclusion

Based on the balance of forces and torques acting on the ball, the rolling friction forces between the discs and the balls are determined by the shear stress at the contact surfaces. The frictional force includes the rolling friction force, which was determined by considering two components, the moment due to elastic deformation and the frictional moment between the ball and the track.

By summing the sliding and rolling resistance of the contact ellipse, we obtain the force and torque acting on the discs for the case of a contact ball. Extending the contact of one ball to all balls in contact gives the total frictional torque on the discs.

The results obtained by the model are realistic based on the results presented in the literature on systems operating on similar principles.

Several simplifications have been made in the construction of the mathematical model created, these simplifications were mainly made in the definition of some geometric parameters, such as the average radius of the trajectories of the driving and driven discs in the x-y plane, which negatively affects the accuracy of the model, therefore, the model needs further refinement, which will be carried out in the near future.

The analytical procedure used in this paper is an improvement of the modelling procedure used by our department in previous papers [8, 9, 10, 11, 12, 13].

Acknowledgment

The research was supported by the Ministry of Innovation and Technology NRDI Office within the framework of the Autonomous Systems National Laboratory Program.

References

- [1] Dr. Pál Bogár, Bearings for Gearings presentation, International Conference on Gears, 2015 october5-7, pp. 115-126, 11p.
- [2] HOUPERT, L., “Numerical and Analytical Calculations in Ball Bearings”, Proc. of Congres Roulements, Toulouse, 5-7 Mai (1999), pp. 1-15
- [3] HOUPERT, L., “Ball Bearing and Tapered Roller Bearing Torque: Analytical, Numerical and Experimental Results”, Proc of STLE Annual Meeting, Houston, May 19 – 23, 2002
- [4] OLARU, D.N., LORENZ, P., RUDY, D., CRETU, SP., PRISACARU, GH., “Tribology Improving the Quality in the Linear Rolling Guidance Systems”, Part 1- “Friction in Two Contact Points Systems”, Proc. of the 13th International Colloquium on Tribology, Esslingen (Germany), 15-17 January, 2002
- [5] OLARU, D. N., P.LORENZ, D. RUDY, “Friction in the Circular – Arc Grooves Linear Rolling Guidance System”, Tribologie und Schmierungstechnik, 2 (2004), pp. 9 –14
- [6] Péter Öri, József Polák, The research of the static and dynamic characteristics of the components of the roller gearing gearbox in order to determine the strength dimensioning, XIII. IFFK 2019, Budapest, 2019. August 26- 29, Paper 29
- [7] Dumitru Olaru, George C. Puiu, Liviu C. Balan, Vasile Puiu, A New Model to Estimate Friction Torque in a Ball Screw System, in book: Product Engineering, January 2005
- [8] Dr. István Lakatos, Valve timing of vehicle engines, Győr, Hungary: Jaurinum Bt. (1994) , 132 p.
- [9] Lakatos, István, Engine power measurement in stationary operating condition on a roller vehicle brake pad, MicroCAD 2010: XXIV. microCad International Scientific Conference: Section E: Materials Science and Technology, Miskolc, Hungary: University of Miskolc (2010) pp. 33-38, 6 p.
- [10] Dániel, Pup; Ádám, Titrik; Ferenc, Szauter; László, Bisits, Fitting and optimizing an intelligent electric powertrain into an existing city vehicle, OGÉT 2013 XXI International Mechanical Engineering Meeting, Cluj-Napoca, Romania: Hungarian Technical Scientific Society of Transylvania (EMT) (2013) pp. 330-333., 4 p.

- [11] István, Lakatos, Ádám, Titrik, DETERMINATION OF POWER AND TORQUE CURVES OF VEHICLES BASED ON DIAGNOSTIC METHODS, Proceedings of the 12th International Conference on Heat Engines and Environmental Protection, Budapest, Magyarország : Budapest University of Technology and Economics, Department of Energy Engineering (2015), pp. 43-49, 7 p
- [12] Tamás Péter; István Lakatos; Ferenc Szauter, Analysis of the Complex Environmental Impact on Urban Trajectories, ASME 2015 International Design Engineering Technical Conferences and Computers and Information in Engineering Conference: Mechatronics for Electrical Vehicular Systems, New York (NY), Amerikai Egyesült Államok: American Society of Mechanical Engineers (ASME) (2016) Paper: DETC2015-47077; V009T07A071, 7 p.
- [13] Hegyi, N., & Jósvai, J., Hazardous Situations and Accidents Caused by Light and Medium Unmanned Free Balloon Flights. *Acta Technica Jaurinensis*, 2020, pp. 295-308, 13p.

Review of Methods for Determining the Moment of Inertia and Friction Torque of Electric Motors

Gusztáv Áron Sziki, Attila Szántó, Éva Ádámkó

University of Debrecen, Faculty of Engineering

Ótemető u. 2-4, 4028 Debrecen, Hungary

szikig@eng.unideb.hu; szanto.attila@eng.unideb.hu; adamko.eva@eng.unideb.hu

Abstract: Our research group, at the Faculty of Engineering of the University of Debrecen, has extensively studied the dynamic modelling and simulation of electric motor's over the past ten years. Many simulation programs have been developed for various motor types. The technical parameters and characteristics of the motors are used as input data for the above-mentioned programs. Among these data, important dynamic characteristics are the moment of inertia and friction torque of the rotor. The friction torque includes windage, ventilation, bearing and brush friction losses. In many cases, however, the manufacturer does not provide these data in the datasheet, so they must be determined experimentally. Several methods exist in the scientific literature for the above purpose. Our research group has also developed and applied such methods in recent years. This publication reviews these methods by presenting the applied experimental setups and procedures. In addition, considering the available literature data and our previous experience, we give the accuracies that can be achieved by the methods and any difficulties that may arise during the experiments and the related computational procedures.

Keywords: electric motor; dynamic characteristics; moment of inertia; friction torque

1 Introduction

At the Faculty of Engineering of the University of Debrecen, our research group has dedicated its efforts to studying electric vehicle drives in the last ten years. The main topic of the research is the modelling, simulation, and optimization of different electric vehicle drives with the original aim to help the more conscious design of the prototype race cars made by student teams at our faculty. To achieve this goal, a vehicle dynamics simulation program has been developed in MATLAB/Simulink environment [1] [2], which can compute the dynamics functions of a vehicle from its technical characteristics and data. With the help of the above program and an optimizing procedure, the most advantageous technical data and characteristics of a vehicle can be determined for a given competition task.

This program includes the simulation of the drive system, including the electric motor [3] [4]. The inputs of the motor simulation module are the electromagnetic and dynamic characteristics of the motor. The dynamic characteristics are the moment of inertia and friction torque of the rotor. These dynamic characteristics serve as inputs also for other simulation programs developed in NI LabVIEW Control Design and Simulation Module [3] [5] and other widely used programs such as Ansys-Maxwell RMXprt [6, 7, 8]. Additionally, they are also important for the accurate dynamic modelling and testing of various high-performance motor control strategies [9].

This paper reviews and classifies the available experimental-based methods in scientific literature to identify the above-mentioned dynamic characteristics as precisely as possible.

2 Review and Classification of Methods for Identifying the Dynamic Characteristics

The methods for identifying the above-mentioned dynamic characteristics can be classified into three groups. These groups are:

- 1) The direct measurement of the friction torque, and after that, the identification of the moment of inertia.
- 2) The direct measurement of the moment of inertia and, after that, the identification of the friction torque.
- 3) The simultaneous identification of the moment of inertia and friction torque.

Methods belonging to the three groups mentioned above are described in Sections 2.1, 2.2 and 2.3, respectively.

2.1 Methods based on the Direct Measurement of the Friction Torque

In these methods, the friction torque of the rotor is directly measured as a function of the angular speed. Figure 1 shows a typical experimental setup for this purpose.

During the experiment, the analyzed motor is driven by an induction motor supplied by a 3-phase AC voltage through a frequency converter. Varying the supply voltage frequency, the angular speed of the induction motor, therefore that of the analyzed motor is varied. Measuring the torque on the shaft of the analyzed motor by a rotary torque meter at different angular speeds, its friction torque-angular speed characteristic ($M_{brake}(\omega)$) is determined. The accurate value of the angular speed is measured by an optical LED sensor.

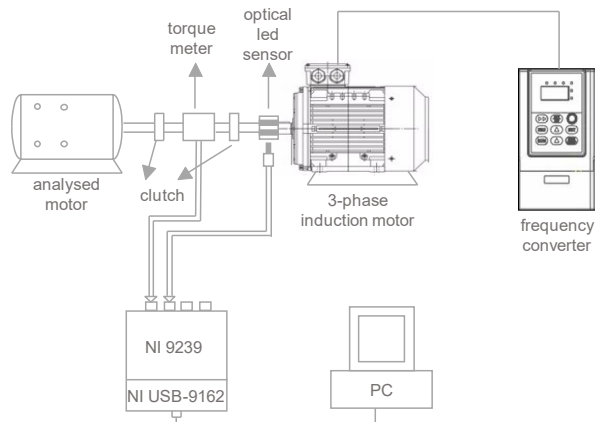


Figure 1

Typical experimental setup for the direct measurement of friction torque, as the function of angular speed

After the measurement of friction torque, the rotor's moment of inertia is identified. For the identification, different methods can be applied (see Section 2.2), but the simplest way is to perform a retardation test on the motor. During the retardation test, the analyzed motor is freely run out until it stops, while its angular speed is measured vs time. From the angular speed vs time curve – obtained from the retardation test – the angular acceleration vs angular speed curve of the rotor can be given. From the angular acceleration vs angular speed ($\varepsilon(\omega)$) and friction torque vs angular speed ($M_{brake}(\omega)$) curves, the moment of inertia of the rotor can be calculated at different angular speeds as:

$$J_r = \frac{M_{brake}(\omega)}{\varepsilon(\omega)} \quad (1)$$

In reference [10], this method is applied for a series-wound DC (SWDC) motor, and the friction torque vs angular speed characteristic of its rotor, together with the result of a retardation test on it, are presented (Figure 2).

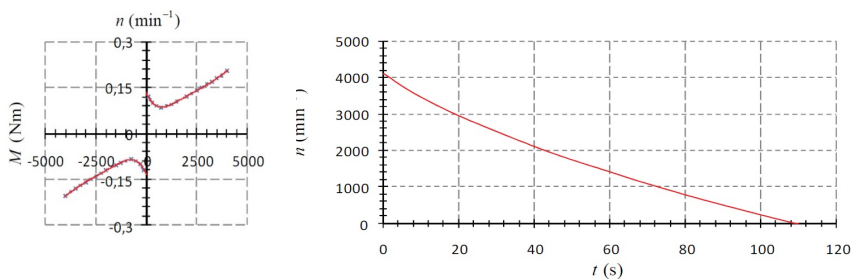


Figure 2

The friction torque vs angular speed characteristic of the analyzed SWDC motor, together with the result of a retardation test performed on it [10]

However, in [10], the obtained value for the moment of inertia and the uncertainties of the measured friction torques are not presented; furthermore, the method's accuracy is not reported. It is crucial to note that the accurate measurement of the friction torque can only be achieved by utilizing a torque meter with low nominal torque and high accuracy class. (Typical values for a commercially available device that can be applied for this purpose are: 0.5 Nm and 0.5%, respectively). Since the friction torque of electric motors, in some instances, can be less than 0.1 Nm, the relative error of torque measurement can be 2.5% or a higher value just because of the inaccuracy of the torque meter. Considering other experimental factors, the above error can be a significantly higher value. Since the relative error of the moment of inertia obtained for the rotor is further increased by the uncertainties of the angular accelerations coming from the retardation test, the approximated relative error of the moment of inertia determination is 4% or a higher value applying this method.

2.2 Methods based on the Direct Measurement of the Moment of Inertia

In this method, the moment of inertia of the rotor is directly measured; after that, the friction torque is identified as a function of angular speed. Knowing the moment of inertia, different methods can be applied to identify the friction torque, but the simplest way is to perform a retardation test on the motor. From the angular speed vs time curve – obtained from the retardation test – the angular acceleration vs angular speed curve of the rotor can be given. Multiplying this curve with the previously measured moment of inertia, the friction torque vs angular speed curve of the rotor can be obtained.

In [11], different experimental techniques for directly measuring the moment of inertia of a rigid body are described and critically analyzed. The torsional and multifilar torsional pendulum methods are usually considered the most accurate among the oscillatory methods. In [11] [12], a relative error of less than 1% is reported for a trifilar torsional pendulum. It has to be emphasized, that the main source of error during the measurements with a multifilar pendulum comes from the inaccurate positioning of the center of gravity of the rotor. In [13], the relative error of the physical pendulum method for the determination of the moment of inertia of rigid bodies is presented as the function of the suspension distance. The reported values vary between 2.5 and 5%. According to the conclusion of the article, the optimal distance corresponding to the minimum value of 2.5% is somewhat smaller than the distance at which the total mass of the pendulum, concentrated in one point, must be placed, that the resulting mathematical pendulum's moment of inertia be the same, as the one of the original pendulum [13]. That is, the relative error of the physical pendulum method cannot be less than 2.5%.

Oscillatory methods similar to the physical pendulum method can also be used to determine the moment of inertia of electric motor rotors. The simplest way to do

this is to eccentrically attach a point-like body of weight G_1 to the rotor at a given distance (a) from the axis of rotation (Figure 3), and then swing the resulting physical pendulum.

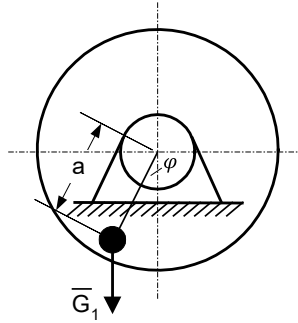


Figure 3

Experimental determination of the moment of inertia using the physical pendulum method

After that, the moment of inertia of the rotor can be calculated with the following formula [14]:

$$J_r = G_1 \cdot a \cdot \left(\frac{T^2}{4 \cdot \pi^2} - \frac{a}{g} \right) \quad (2)$$

In Equation (2), T is the period of the oscillation and g is the magnitude of the gravitational acceleration. It should be noted, that the error caused using the linearized equation of motion when deriving Equations (2) is negligible if, and only if the oscillation amplitude (φ) is less than ~ 0.1 rad, and it causes less than 1% relative error if the oscillation amplitude is below 0.4 rad.

In addition, the larger the friction torque acting on the rotor, the more imprecisely the oscillation time can be measured. Besides, applying the method can lead to considerable inaccuracies if the rotor is not well-balanced, and it is usually challenging to find its center of gravity or suspension center. Consequently, the value of the relative error of the method is significantly higher than the reported minimum value in [13].

Figure 4 shows the measurement arrangement of a modified, more accurate version of the previously presented oscillatory method. In this method, the rotor is placed on two ideal, horizontal, and parallel edges.

By displacing the system from its equilibrium position, it will be swinging. The moment of inertia of the rotor can be calculated as follows [14]:

$$J_r = G_1 \cdot a \cdot \left(\frac{T^2}{4 \cdot \pi^2} - \left(\frac{a}{g} + \frac{r^2}{a \cdot g} \right) \right) \quad (3)$$

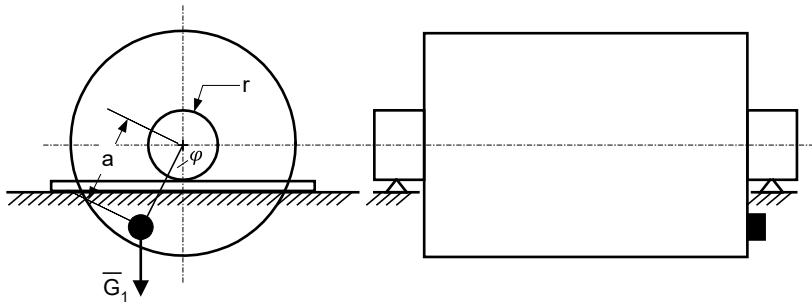


Figure 4

Experimental setup for the modified oscillatory method to measure the moment of inertia of the rotor

In Equation (3), a is the distance between the point-like body and the center line of the rotor, r is the radius of its shaft, T is the period of the oscillation, and g is the magnitude of gravitational acceleration. It has to be emphasized, that the error caused using the linearized equation of motion when deriving Equations (3) is negligible if, and only if, the oscillation amplitude (φ) is less than ~ 0.1 rad, and it causes less than 1% relative error if, the oscillation amplitude is below 0.4 rad. It has to be also mentioned, that we can get accurate results only, if the rotor is well-balanced, and the edges and the shaft are ideally rigid and smooth surfaced.

Furthermore, the values of parameters a and G_1 have to be chosen optimally to a given rotor with the moment of inertia J_r and rolling radius r . And, of course, all the quantities in the formula must be measured precisely.

In another method [15], the rotor of mass m with rolling radius r rolls down on an incline with an angle α (Figure 5).

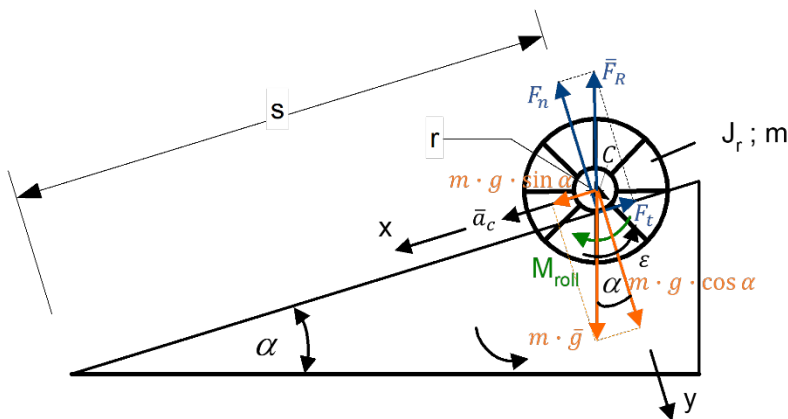


Figure 5

Experimental setup for the measurement of the moment of inertia of the rotor

From a video record – captured by a high-resolution camera – the position-time function of the rotor's center of mass $s(t)$ can be given. From the $s(t)$ function, the velocity-time function, and finally, the acceleration of the rotor's centre of mass (a_c) can be calculated [15]. Because the rolling friction between the rotor and the incline is not negligible, two individual roll-down experiments must be performed using different incline angles (α_1 and α_2). The value of both α_1 and α_2 are typically below 2° , thus rolling without slipping can be assumed. For the two roll-down experiments the following six dynamics equations can be written:

$$m \cdot g \cdot \sin \alpha_1 - F_{t1} = m \cdot a_{c1} \quad (4)$$

$$m \cdot g \cdot \cos \alpha_1 - F_{n1} = 0 \quad (5)$$

$$F_{t1} \cdot r - M_{roll1} = J_r \cdot \varepsilon_1 \quad (6)$$

$$m \cdot g \cdot \sin \alpha_2 - F_{t2} = m \cdot a_{c2} \quad (7)$$

$$m \cdot g \cdot \cos \alpha_2 - F_{n2} = 0 \quad (8)$$

$$F_{t2} \cdot r - M_{roll2} = J_r \cdot \varepsilon_2 \quad (9)$$

In the above equations F_t is the friction force, a_c and ε are the acceleration of the center of mass and angular acceleration of the rotor, M_{roll} is the rolling friction torque, which is calculated as:

$$M_{roll1} = f \cdot F_{n1}, M_{roll2} = f \cdot F_{n2} \quad (10)$$

In the above equation f is the arm of the rolling friction, which can be also expressed with the rolling friction coefficient (c) as $f = c \cdot r$.

Since the rotor is rolling without slipping:

$$\varepsilon_1 = \frac{a_{c1}}{r}, \varepsilon_2 = \frac{a_{c2}}{r} \quad (11)$$

From Equations (4-11) the moment of inertia of the rotor can be calculated as [15]:

$$J_r = mr^2 \left(g \frac{\frac{\tan \alpha_2 - \tan \alpha_1}{a_{c2}} - \frac{a_{c1}}{\cos \alpha_2}}{\cos \alpha_1} - 1 \right) \quad (12)$$

It has to be mentioned, that during a usual experiment, the velocity of the center of mass of the rotor is always below 1 km/h [15]. Thus, in case of a rotor with a rolling radius of 1.5 cm [15], the angular velocity of the rotor is always below 19 rad s^{-1} . The normal load on the shaft of the same rotor is about 120 N. Under the above conditions, based on the related scientific literature [16-19], the arm of rolling resistance is constant with a good approximation.

It must be also emphasized, that Formula 12 gives accurate result if, and only if, all the quantities are measured very precisely. If it is fulfilled, calculation with Gauss' Law of Error Propagation and validation measurements prove, the relative error of the method is about 2.5% [15].

In general, it can be concluded that directly measuring the moment of inertia of the rotor with sufficient accuracy is only possible if the rotor is demounted from the motor. Demounting the rotor can be destructive to the motor and laborious; therefore, it is not recommended.

2.3 Simultaneous Identification of the Moment of Inertia and Friction Torque

This section presents methods for simultaneously identifying the moment of inertia and friction torque without demounting the rotor from the motor. Several methods exist for simultaneous identification [9, 16, 20-22]. Section 2.3.1 gives examples for the identification by direct measurement, while Section 2.3.2 by offline methods.

2.3.1 Identification by Direct Measurement

In [20], a procedure for simultaneously and directly measuring the friction torque and moment of inertia of electric motors is given. The procedure is based on retardation tests on the motor applying additional loads – steel discs (1, 2) – on its rotor with different moments of inertia and equal masses (Figure 6). The discs are attached to the steel shafts (8) by applying four clamping rings (9) of the same type.

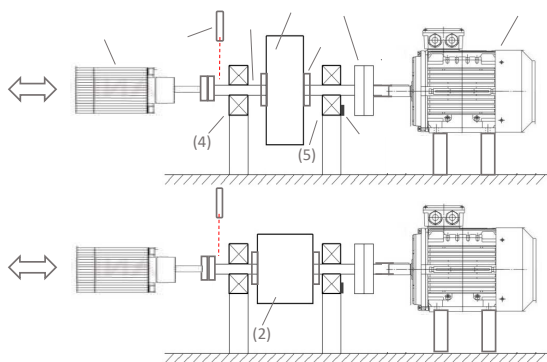


Figure 6

Experimental setup for the simultaneous direct measurement of the moment of inertia and friction torque of the rotor [20]

The equal masses produce equal friction torques in the supporting bearings (4, 5). During the experiments, a drive motor (11) is attached to the system's shaft through a clutch. When voltage is applied to the drive motor, the system starts to rotate from a standstill until it reaches its top speed. Then, the drive motor (11) and the shaft are disconnected, causing the rotating masses to slow gradually until they come to a halt. While the system slows down, its angular speed is monitored by an optical LED sensor (12). Simultaneously, the surface temperature of the outer ring of the

bearing (5) is observed using a Resistance Temperature Detector (14). The entire experiment involves four measurements: First with only disc (1), second with disc (1) and the analyzed motor, third with disc (2) and the analyzed motor, and lastly with only disc (2) connected to the drive motor (11). Figure 7 shows the system's angular speed vs time function gained from the second measurement. The connection is released at the moment 1.8 s.

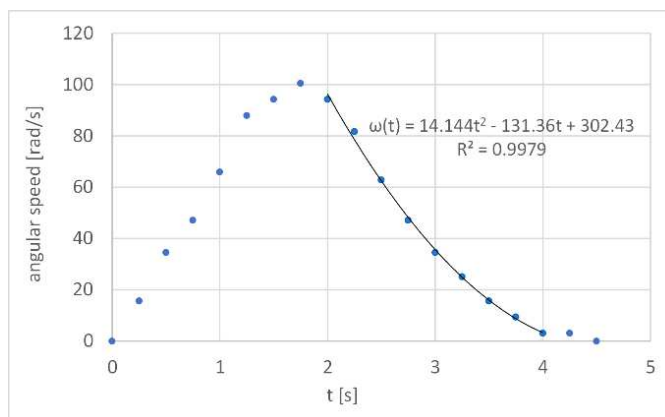


Figure 7

Angular speed vs time function of the system when disc (1) and the analyzed motor are connected to the drive motor. The connection is released at the moment 1.8 s

The rotating systems' angular acceleration vs time functions are calculated by derivation from the fitted angular speed vs time functions. After that, the angular acceleration is given as a function of angular speed. Thus, the results of the four experiments are four angular acceleration vs angular speed functions. For the four experiments, we can write the following four equations:

$$M_{brake}^* = (J_1 + J_{add1}) \cdot \varepsilon_1 \quad (13)$$

$$M_{brake}^* + M_{brake} = (J_1 + J_r + J_{add2}) \cdot \varepsilon_{1m} \quad (14)$$

$$M_{brake}^* = (J_2 + J_{add1}) \cdot \varepsilon_2 \quad (15)$$

$$M_{brake}^* + M_{brake} = (J_2 + J_r + J_{add2}) \cdot \varepsilon_{2m} \quad (16)$$

In Equations (13), (14), (15) and (16):

$$J_{add1} = J_{shaft} + 2 \cdot J_{clpr} + 2 \cdot J_{ring} \quad (17)$$

$$J_{add2} = J_{shaft} + 2 \cdot J_{clpr} + 2 \cdot J_{ring} + J_{clutch} \quad (18)$$

In the equations above M_{brake} and J_r are the friction torque and moment of inertia of the rotor of the analyzed motor, M_{brake}^* is the summed friction torque of supporting bearings 4 and 5, J_1 , J_2 , J_{shaft} , J_{clpr} , J_{clutch} , J_{ring} are the moments of inertia of disc (1), disc (2), one shaft, one clamping ring, the clutch and the inner

ring of a supporting bearing, which were calculated from their measured geometric data and masses, and ε_1 , ε_{1m} , ε_{2m} , ε_2 , are the angular accelerations of the four rotating systems during the retardation tests. From Equations (13-16) the following equations can be derived for the moment of inertia and friction torque of the analyzed motor:

$$J_r = \frac{J_2 \cdot \varepsilon_{2m} - J_1 \cdot \varepsilon_{1m}}{(\varepsilon_{1m} - \varepsilon_{2m})} - J_{add2} \quad (19)$$

$$M_{brake} = (J_2 - J_1) \cdot \frac{\varepsilon_{1m} \cdot \varepsilon_{2m}}{(\varepsilon_{1m} - \varepsilon_{2m})} - (J_1 + J_{add1}) \cdot \varepsilon_1 \quad (20)$$

Instead of Equation (20) the friction torque can be also expressed as the function of the moment of inertia of the rotor (J_r) and other parameters. Using the previously determined constant value of the moment of inertia in the whole angular speed range in this formula, the errors of the experimentally determined friction torques can be further reduced, mainly below 30 rad s^{-1} . It has to be noted, that the main advantage of the direct measurement of the friction torque (see in Section 2.1) against this method, that it is more accurate in the low angular speed range.

The accuracy of the presented method strongly depends on the measurement conditions and procedure. In the case of the optimal selection and implementation of the measurement conditions and procedure, the errors of the determined moment of inertia and friction torque can be minimized. To minimize the error, the following should be done:

- 1) Moments of inertia J_1 and J_2 have to be chosen optimally.
- 2) The measurement times, thus the heating of the bearings, have to be minimized.

The determination of the optimal values of J_1 and J_2 , at which the error of the experimentally determined moment of inertia is minimum, together with the effect of the heating of the bearings on the accuracy of the method are discussed in detail in Section 4 in Reference [20]. Under optimal measurement conditions, the certified relative error of the method for the measurement of the moment of inertia is 4.3-5.3%, while for the measurement of the friction torque is 3-6% in the $[30; 120] \text{ rad s}^{-1}$ angular speed range. Under 30 rad s^{-1} angular speed, the experimental errors are significantly higher, because of the higher standard deviations of the angular accelerations determined from the measured angular speeds. Thus, only the $[30; 120] \text{ rad s}^{-1}$ angular speed range in Figure 8, where the moment of inertia is approximately constant, can be used for evaluation. The average value of the moment of inertia in the above range, is considered as its experimentally determined value. Figures 8 and 9 show the experimentally determined moment of inertia and breaking torque of a squirrel cage induction motor.

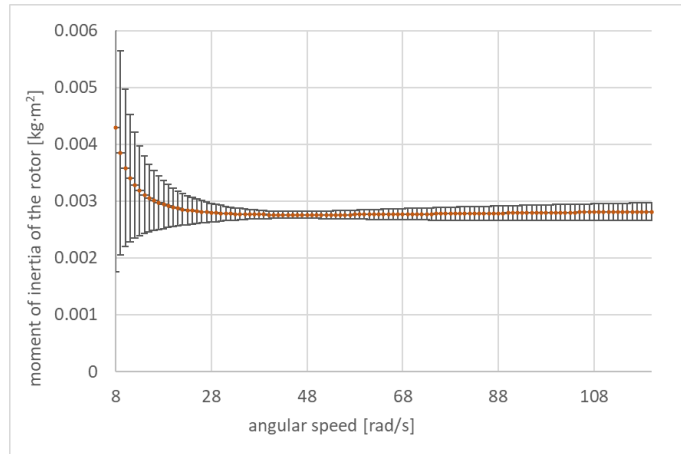


Figure 8

The experimentally determined values of the moment of inertia of the rotor of a squirrel cage induction motor [20]

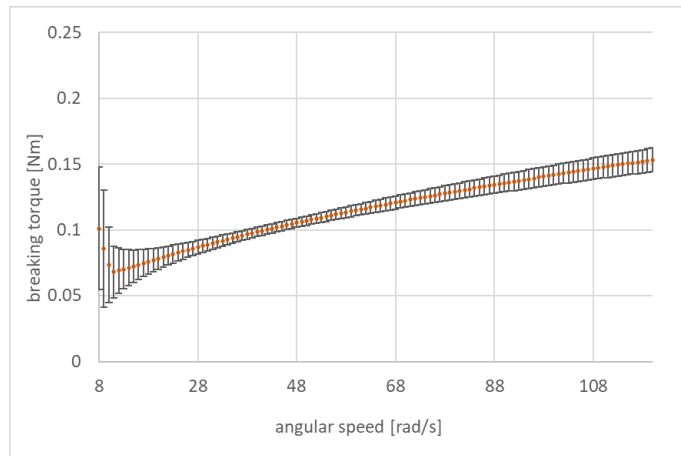


Figure 9

The experimentally determined friction torque of the rotor of a squirrel cage induction motor [20]

2.3.2 Identification by Offline Methods

The goal of offline parameter identification is to accurately estimate various motor parameters, which can include electrical, mechanical, and thermal characteristics. These parameters are essential for motor control, performance analysis, and design optimization. To carry out offline parameter identification, specific tests and measurements are performed on the motor, and the acquired data is then analyzed and processed to estimate the desired parameters. Here are a few commonly used offline parameter identification methods for electric motors:

- 1) Locked Rotor Test: In this test, the rotor of the motor is mechanically prevented from rotating while an electrical voltage is applied to the stator windings. By measuring the resulting current and voltage, parameters such as winding resistance, leakage inductance, and core losses can be estimated. [23]
- 2) No-Load Test: This test involves running the motor without any mechanical load applied to the output shaft. By measuring the no-load current, no-load voltage, and rotational speed, parameters like core losses, friction, and windage losses can be determined. [24]
- 3) Load Test: Load tests are conducted by subjecting the motor to various mechanical loads while measuring the input voltage, input current, and rotational speed. By analyzing these measurements, parameters such as torque constant, motor efficiency, and mechanical losses can be identified. [25]
- 4) Thermal Analysis: Thermal analysis involves monitoring the temperature rise of the motor during operation under different load conditions. By measuring and analyzing the temperature data, parameters related to thermal resistance, heat transfer coefficients, and thermal time constants can be estimated. [26]

Sometimes, Direct Parameter Measurements are also classified here, in which certain motor parameters are measured directly using specialized equipment. [4]

The acquired data from these tests are typically processed using mathematical modelling, curve fitting techniques, or advanced data analysis methods and algorithms – e.g., genetic algorithm [9] [21] – to estimate the motor parameters accurately. The accuracy and reliability of the estimation depend on the test setup, data quality, and the mathematical models and algorithms used for analysis. Offline parameter identification methods are valuable for obtaining crucial motor information without the need for real-time operation or control. They provide insights into motor characteristics and enable better motor control, system design, and performance optimization.

In [9, 21, 22], experimental offline methods for the parameter identification of an induction motor drive are presented. In [21], the method uses speed-time curves obtained during the retardation test on the drive, with an appropriate model for the mechanical losses and the mean squared error performance function based on a genetic algorithm approach, to obtain the unknown mechanical parameters of the tested drive. Theoretically estimated and experimentally determined speed-time curves, obtained from retardation tests, are compared, but the accuracies of the identified parameters are not given. In [22], a new step-by-step approach to identifying the parameters of an induction machine combining free acceleration and deceleration transient data is presented. When the machine is in standstill without mechanical load, the three-phase ac power is applied to the stator terminals. During the free acceleration transient, the measurement of the stator line voltage and current

is required only. The free acceleration torque characteristic is used to identify the moment of inertia of the rotor, and a new algorithm is proposed to perform it with higher accuracy. The identification results are compared with motor parameters determined from locked-rotor and no-load tests, and the obtained relative difference is about 3%. The parameters of the different mechanical losses were not identified. In [9], a method is described for the offline identification of the electromagnetic and mechanical parameters of a mathematical model of an induction motor using genetic algorithms. Identification is performed using data acquired during a test consisting of a transient from standing still to a certain speed and successive free motion to standing still.

Conclusions

Methods for identifying the moment of inertia and friction torque of rotors in electric motors, have been reviewed here, in detail. The following conclusions can be drawn:

- The direct measurement of the moment of inertia, with sufficient accuracy, is usually only possible if the rotor is removed from the motor. In this case, several methods exist, the error of which strongly depends on the selection of the value of the measurement parameters and their measurement uncertainties. The least error can be achieved by using a trifilar torsion pendulum, which is approximately 1%.
- Removing the rotor is laborious and can lead to damage to the motor, so it is usually not recommended.
- If the rotor is not removed from the motor, one of the following procedures is recommended:
 - Direct measurement of the friction torque using a rotary torque meter, then determining the moment of inertia from a retardation test. Applying a commercially available torque meter with a nominal torque of 0.5 Nm and accuracy class 0.5%, the estimated attainable relative error of friction torque and moment of inertia determination is 3% and 5%, respectively.
 - Direct simultaneous measurement of the friction torque and moment of inertia. The attainable relative error with the method presented in this publication is 3-6% and 4-5%, respectively.
 - Applying an offline parameter identification method. The main advantage of these methods is that a lot of, or all the unknown parameters of an electric motor can be identified simultaneously. Their drawbacks are their complexity and the inaccuracy of the applied models and algorithm can result in significant errors in the identified parameters. In addition, a unique model has to be developed for each motor type.

Acknowledgement

"SUPPORTED BY THE ÚNKP-22-3 NEW NATIONAL EXCELLENCE PROGRAM OF THE MINISTRY FOR INNOVATION AND TECHNOLOGY FROM THE SOURCE OF THE NATIONAL RESEARCH, DEVELOPMENT AND INNOVATION FUND."



"THE RESEARCH WAS SUPPORTED BY THE THEMATIC EXCELLENCE PROGRAMME (TKP2020-NKA-04) OF THE MINISTRY FOR INNOVATION AND TECHNOLOGY IN HUNGARY."

References

- [1] Szántó, A., Hajdu, S., & Sziki, G. Á. (2020) Dynamic simulation of a prototype race car driven by series wound DC motor in Matlab-Simulink. *Acta Polytech. Hung.* 17(4), 103-22
- [2] Sziki, G. Á., Szántó, A., & Mankovits, T. (2021) Dynamic modelling and simulation of a prototype race car in MATLAB/Simulink applying different types of electric motors. *International Review of Applied Sciences and Engineering*, 12(1), 57-63
- [3] Sziki, G. Á., Sarvajcz, K., Szántó, A., & Mankovits, T. (2020) Series wound DC motor simulation applying MATLAB Simulink and LabVIEW control design and simulation module. *Periodica Polytechnica Transportation Engineering*, 48(1), 65-69
- [4] Sziki, G. Á., Sarvajcz, K., Kiss, J., Gál, T., Szántó, A., Gábora, A., & Husi, G. (2017) Experimental investigation of a series wound dc motor for modeling purpose in electric vehicles and mechatronics systems. *Measurement*, 109, 111-118
- [5] Abbas, A. N. (2014) Design and implementation of close loop DC motor speed control based on Labview. *Int. J. Enhanc. Res. Eng. Sci. Technol.*, 3(7), 354-361
- [6] Aishwarya, M., & Brisilla, R. M. (2022) Design of Energy-Efficient Induction motor using ANSYS software. *Results in Engineering*, 16, 100616
- [7] Gecer, B., Tosun, O., Apaydin, H., & Serteller, N. F. O. (2021, October) Comparative analysis of SRM, BLDC and induction motor using ANSYS/maxwell. In *2021 International Conference on Electrical, Computer, Communications and Mechatronics Engineering (ICECCME)* (pp. 1-6). IEEE
- [8] Allirani, S., Vidhya, H., Aishwarya, T., Kiruthika, T., & Kowsalya, V. (2018, May) Design and performance analysis of switched reluctance motor using ANSYS Maxwell. In *2018 2nd International Conference on Trends in Electronics and Informatics (ICOEI)* (pp. 1427-1432) IEEE

- [9] Alonge, F., D'Ippolito, F., Ferrante, G., & Raimondi, F. M. (1998) Parameter identification of induction motor model using genetic algorithms. IEE Proceedings-Control Theory and Applications, 145(6), 587-593
- [10] Hadžiselimović, M., Blaznik, M., Štumberger, B., & Zagradišnik, I. (2011) Magnetically nonlinear dynamic model of a series wound DC motor. Przegład Elektrotechniczny, 87(12b), 60-64
- [11] Genta, G., & Delprete, C. (1994) Some considerations on the experimental determination of moments of inertia. Meccanica, 29(2), 125-141
- [12] Tang, L., & Shangguan, W. B. (2011) An improved pendulum method for the determination of the center of gravity and inertia tensor for irregular-shaped bodies. Measurement, 44(10), 1849-1859
- [13] Dowling, J. J., Durkin, J. L., & Andrews, D. M. (2006) The uncertainty of the pendulum method for the determination of the moment of inertia. Medical engineering & physics, 28(8), 837-841
- [14] Ludvig, Gy. (1983) Gépek dinamikája. Műszaki könyvkiadó
- [15] Szántó, A., Kiss, J., Mankovits, T., & Sziki, G. Á. (2021) Dynamic Test Measurements and Simulation on a Series Wound DC Motor. Applied Sciences, 11(10), 4542
- [16] The Engineering ToolBox : Dynamics : Rolling Friction
www.engineeringtoolbox.com/rolling-friction-resistance-d_1303.html
- [17] LaClair, T. J. (2006). Rolling resistance. The pneumatic tire, 475
- [18] Reimpell, J., Stoll, H., & Betzler, J. (2001) The automotive chassis: engineering principles. Elsevier
- [19] Dr. ILOSVAI Lajos Prof. Emeritus (2013) Járműdinamika
- [20] Szántó, A., Ádámkó, É., Juhász, G., & Sziki, G. Á. (2022) Simultaneous measurement of the moment of inertia and braking torque of electric motors applying additional inertia. Measurement, 204, 112135
- [21] Reljić, D. D., & Jerkan, D. G. (2014) Experimental identification of the mechanical parameters of an induction motor drive. In Proceedings of the X international symposium on industrial electronics (INDEL 2014) (pp. 106-114)
- [22] Despalatović, M., Jadrić, M., & Terzić, B. (2005) Identification of induction motor parameters from free acceleration and deceleration tests. Automatika: časopis za automatiku, mjerenje, elektroniku, računarstvo i komunikacije, 46(3-4), 123-128
- [23] Maraaba, L. S., Al-Hamouz, Z. M., Milhem, A. S., & Twaha, S. (2019) Comprehensive parameters identification and dynamic model validation of interior-mount line-start permanent magnet synchronous motors. Machines, 7(1), 4

- [24] Ayasun, S., & Nwankpa, C. O. (2005) Induction motor tests using MATLAB/Simulink and their integration into undergraduate electric machinery courses. *IEEE Transactions on education*, 48(1), 37-46
- [25] A. Cavagnino, M. Lazzari, F. Profumo and A. Tenconi, "Axial flux interior PM synchronous motor: parameters identification and steady-state performance measurements," *Conference Record of the 1999 IEEE Industry Applications Conference. Thirty-Forth IAS Annual Meeting (Cat. No.99CH36370)*, Phoenix, AZ, USA, 1999, pp. 2552-2559, Vol. 4, doi: 10.1109/IAS.1999.799199
- [26] Rehman, Z., & Seong, K. (2018) Three-D numerical thermal analysis of electric motor with cooling jacket. *Energies*, 11(1), 92

Pre-Calculation of the Implementation of a Warehouse Management System, for a Specific Company

Brigitta Zsótér

Department of Engineering Management and Economics,
Faculty of Engineering, University of Szeged
Mars tér 7, 6724 Szeged, Hungary, zsoterb@mk.u-szeged.hu

Katalin Végh

Independent researcher, Slovakia
mmoi@mk.u-szeged.hu

Abstract: Companies constantly seek solutions for complex technical and economic tasks and this is especially difficult for small and medium-sized enterprises. For this, we provide an example in the barcode processing area. By looking at several versions at one company, we will show how much it costs to introduce a barcode-based warehouse management system. Our specific task was to pre-calculate the expansion of the existing ERP (Enterprise Resource Planning) system with a barcode warehouse management system. To this end, we have looked at good practices in recent years, as part of various field surveys, with several companies, across Hungary. The cost of building a barcode warehouse management system is HUF 25837559. It can be implemented on its own or with support. The barcode warehouse management system can be extended to all employees, but a version that is only extended to office employees, can also be analyzed. Accordingly, four cases were examined. In one of these cases, we set-up the theory, that in the structure of the barcode system, we extend the project management module in the expansion of the ERP system only among office employees, and thus, the investment pays off in 5 years, from existing resources. The NPV is HUF 13220000, the IRR is 43.24%, the profitability index is 1.71, DPB is 2.92 years. The logic of the calculations can be used in many other areas.

Keywords: warehouse management system; ERP; barcode; pre-calculation; NPV; DPB; IRR

1 Introduction

Providing adequate and accurate information is increasingly valued by companies. Developing the information system requires specific efforts considering local characteristics, the available technology and the business environment. Due to the large number of companies and their various activities, case studies are appropriate to explore the best practices in the field. European trends count on the increasing importance of medium-sized companies in the case of small, open economies like Hungary [1]. In the course of our work, a Hungarian company in the area of the city Szeged, was selected to present how to implement a new barcode warehouse management system, which will facilitate the day-to-day operation of the business.

Enterprise Resource Planning (ERP) systems are state-of-the-art enterprise management technologies that integrate and encompass the company's internal operational functions with high efficiency. In this way, they facilitate the support of managerial decisions and the provision of information, and at the same time lay the foundations for the development of business intelligence [2].

When asked what ERP is, the following text gives a nuanced overview: "What is the simplest ERP definition? Think about all the core processes needed to run a company: finance, HR, manufacturing, supply chain, services, procurement, and others. At its most basic level, ERP integrates these processes into a single system. But new ERP systems are anything but basic. They provide visibility, analytics, and efficiency across every aspect of a business. Using the recent technologies, ERP systems facilitate the flow of real-time information across departments, so businesses can make data-driven decisions and manage performance – live." [3].

According to this, based on the text, let's think under the definition of the simplest ERP for all the basic processes required to run a company, such as finance, HR, manufacturing, supply chain, services, procurement and others. At the simplest level, ERP integrates these processes into a single system. But new ERP systems are anything but basic. In all aspects of the company provides transparency, analysis and efficiency. The most modern technologies ERP systems facilitate the real-time flow of information between certain departments, so businesses are able to make data-centric decisions and to perform. The maturity of a company's management system is determined by how well the company can implement and use information technology in its management system. A mature company that continuously applies information technologies can use them much faster to achieve its goals and thereby increase its competitiveness [4]. Information and time become the decisive factors of production. A company can be considered successful if its business (management, executive and administrative) activities and processes are supported by information technologies, e. g., management and execution procedures and methods that require computer support at the given time level [5]. The quality information system should therefore be part of the logistics management system [6].

Nowadays, a critical competency for the successful work managers is the ability to work with large amounts of data, to know them, to draw relevant conclusions from them and to make further decisions based on them [7]. Information systems help them in this activity, which fundamentally influence the way of working with data and information, as well as the ways of decision-making and communication [8]. The information system is a set of information, people, used information technologies, work organization, business management, as well as technical tools and methods for the collection, transmission, storage and further processing of data for the purpose of creating and providing information. The method tells us what we have to do in a certain stage of development or operation [9].

Information systems are currently an essential part of successful business management. When we talk about information systems for business process support and decision support, we mean business applications that are collectively known as enterprise resource planning systems – ERP.

An ERP category information system can be defined as an effective tool that can cover the planning and management of the main internal business processes at all levels, from operative to strategic [10]. ERP is a packaged business software system that enables the automation and integration of most business processes and the sharing of business data within the entire company. The most important internal processes covered by ERP systems are production, internal logistics, HR and economics. The main purpose of these systems is the integration of individual business functions at the level of the entire company, i.e., the integration of various applications used in the company that ensure the information needs of individual departments and divisions into a unit working on a unified database, and thus reduces the risk [11].

The expectations of ERP systems cover flexibility, expandability and modularity. Flexibility means that the system must be able to work in harmony even when installed on different platforms, and communicate with personal computers as well as other electronic devices, such as robotic arms on production lines or automated material handling equipment in warehouses. Within extensibility, we can distinguish between vertical and horizontal growth, in both cases the expectation is that the system is able to continue to function even in the event of increasing product volume or widening product range, and to be able to perform its tasks even during the introduction of new processes [12].

As a result of integration, the efficiency of the internal operating system of companies is improved, the time spent on work processes is reduced, thus their costs and risks are reduced and customer satisfaction is significantly improved.

The concept of lean management has been in focus for recent years. It aims to learn the sources of various losses inherent in operational processes and eliminate them [13]. Undoubtedly, the benefits are available if related data is adequately managed. An advantage of standard corporate management information systems

over custom-designed integrated corporate management systems is that they are ready to purchase and a much more cost-effective solution [14].

The lean approach is based on the triple unity of purpose, process and respect for people. Its main question is how to produce the highest value for the customer using the least possible resources, time, energy and effort [15]. A lean organization recognizes what value means to its customers and strives to constantly increase it in key processes [16]. The ultimate goal is to provide perfect value to the customer through a perfect value-creating process, in which the rate of loss is zero. In order to achieve this, the lean approach shifts the focus of management from the optimization of isolated technologies, devices and departments to the optimization of the flow of products and services, whose value processes flow through technologies, devices and departments all the way to customers. The power inherent in people is one of the driving forces behind lean. It builds on the employees and their ideas, which is why this is also its critical point [17]. How do we get them to do it in a society where it is not natural to “idea” at the level of operators [18] [19]?

Beyond the great opportunities of developing a corporate information system, some limitations must be considered. A remarkable issue is that standard systems are built according to a general corporate structure, and as a result, they cannot be adapted to each company so easily. In this case, we need to rethink whether we are adapting the system itself to the business or the business to the system. In both cases, these appear as a cost factor in the company’s budget.

Another disadvantageous issue may be the burden placed on the employees to learn the new system. Initially, employees may be afraid to use the new system. As the learning phase can take many months, this is also a cost in the budget. Moreover, the data migration from a predecessor system to the new architecture can be difficult or impossible. As a result, a source of error arises during the transfer of data, and in some cases functional achievements and outages may occur between the two structures.

2 The Case of a Specific Corporate Management Information System

2.1 The Corporate and the Corporate Management Information System of company called “P@rtner”

The company was founded 30 years ago in the Szeged area. Currently, 14 people work at the company. They are produced special vehicles and machines based on individual customer requirements. For example, “smart” fertilizer spreader with

GPS communication, snow plow, special trailers. The purpose of our research is to plan a financial pre-calculation for the company regarding the purchase of the new barcode warehouse management system. After that, the company's managers decide whether to buy it or not. If they bought the warehouse management system, what would be the payback period for the investment? We are looking for answers to these questions.

We present the most important information related to product identification after the presentation of the specific corporate management system. We present the barcode identification method most suitable for the company. We are also described the parameters of the selected barcode data collector and barcode printer. Then we will make the economic calculation of these. The process of our research can be seen in the Figure 1.

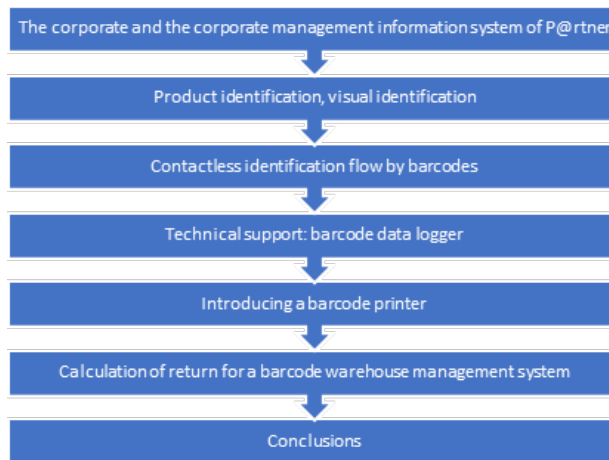


Figure 1
The process of our research

The corporate management information system of P@rtner. ERP is the standard corporate management system designed by Rose Software Kft., The predecessor system of which is the Helix corporate management information system is still operating at the examined company. The standard corporate management information system is a modular architecture built around a framework. Table 1 shows the modules of the P@rtner corporate management system.

Table 1
P@rtner. ERP corporate management information system modules

Framework	
Trading module	Tangible asset
Manufacture	Wages and labor
CRM	Stock registry

Project management	Controlling, Business intelligence
Document management	Vehicle and implement registration module
Process management	EKÁER module
Web portal, ERP on the web	mobile.P@RTNER
Web shop	mobile.sales (PDA)
Banking relationship	Additional features

2.2 Product Identification, Visual Identification

We present the important things about product identification and visual identification, as we alluded to in the previous chapter. Most industrial companies, including tourism [20] [21] and food supply companies [22], have realized that it is essential to use product identification and tracking systems, but at the same time, the implementation of the system requires joint work of technical, business and legal expertise. Beyond a logistic approach, management researchers and economists also are dealing with the problem [23]. The inclusion of information from customers and clients in the system is becoming more and more important in order to improve logistics processes. Competitiveness requires cost-effective production and services from businesses, the key to which can be the proper identification and tracking of products [24].

A highlighted task within the supply chain is product identification and tracking [25]. Visual identification, which requires a person, does not meet today's logistical requirements, due to its excessive slowness and high error rate [26].

By using product identification systems, products can be tracked, process control and inventory management can be improved. In the long run, this allows for automatic product identification and traceability, thus improving supply chain strategies. It increases the overall redesignability of the entire supply chain by removing a number of barriers that limit the structure of the supply chain [27].

Today, science and technology have become very dominant, with human knowledge and skills as the primary resource [10]. Within this, project management [28] is of increasing importance, including the inclusion of information in the system, which may come from customers and clients, possibly in the field of logistics [29].

Several categories of identification are known, the best known of which is automatic identification. This identification includes the procedures and technologies that make it possible to obtain information about an object without human intervention and transform it for further use [30]. Automatic product identification systems can provide companies with a lot of information about different operations in the supply chain. However, it is important to collect reliable information continuously. The ultimate goal is to find the appropriate data collection technology [31].

In the increasing corporate competition, the cost-effective production of products and the provision of services, warehousing [32], special storage and transport are important, the key to which may be the appropriate identification. In practical life, we can encounter two types of product identification. These are the two types of tactile and non-tactile identification. One identifies the product using tactile (mechanical) holes and cams. Unlike contactless forms of identification, there is a physical contact here. For non-contact identification systems, four types can be distinguished. The chip card or RFID chip the electronic one uses to carry the data. In the optical solution, products are identified using a barcode. In the case of magnetic identification, you can track the products with the help of a magnetic stripe, while on a satellite-based GPS, you can track the products using an on-board computer.

2.3 Contactless Identification Flow by Barcodes

A simple but widely effective optical solution for product identification and checking product flow is a barcode system. A barcode is a square or rectangular shape that contains analog black lines with white spaces of various sizes. The black lines and spaces in a barcode represent a machine-readable code in the form of numbers and characters. It follows that a barcode is the way to encode information into a pictographic pattern, that can then be read, by a machine [33].

A barcode is an identifier consisting of a combination of numbers and letters, which is a coded form that can be read without any touch by machines. A barcode is just an identifier, a reference number that points to a specific element in a database. All other information is stored in the current database.

There are two main types: one-dimensional and two-dimensional barcodes. A one-dimensional barcode is a defined alternation of vertical dark lines and light gaps of different thicknesses that provide information to the reader. In contrast, two-dimensional barcodes can carry much more information than their 1D counterparts. Two-dimensional identifiers use different geometric shapes for identification.

The most common barcode is EAN13 (GTIN-13), but in the database of the examined company, the corporate management information system generates a barcode from the item numbers, although in some cases this has to be overwritten, but it is very useful. Article numbers consist of numeric and alphanumeric characters. Therefore, the most appropriate encoding is Code 128.

Code 128 is a rapidly expanding barcode system. The Code 128 barcode has 11 module-wide characters, each consisting of three lines and three spaces. This barcode system includes 2 types of verification codes for increased security. The main features of this barcode type are: it can display high information densities and alphanumeric character sets, it can be continuous and self-checking, and it can be of variable length and its various uses are standardized.

The scanning itself is done by barcode scanners. Sensors must be able to read black and white lines on products quickly and efficiently. At the same time, they must transmit the acquired information to a computer or terminal, which can immediately identify them with the help of the built-in product database [34].

2.4 Technical Support: Barcode Data Logger

The company needs to purchase data loggers and a barcode printer for barcode product identification. We will calculate the return on these. We describe the properties of the specific barcode data logger. The acquisition of 4 barcode data loggers is required during the investment. In the selection process, we aimed to provide the company with a data collector that is very powerful and, last but not least, industrial.

For this purpose, we proposed two types of terminals, the first of which is a Honeywell EDA61K mobile barcode data acquisition terminal, and the second is the newest member of the MC3000 series made by Zebra Symbol. In terms of value for money, the two products fall into almost the same category.

During the selection, the Zebra MC3300 was chosen by the investor. The Zebra MC3300 barcode mobile handheld data collection terminal is part of Zebra's highly successful MC3000 series, which dates back 15 years. The Zebra MC3300 barcode data logger runs on the Android operating system and is also equipped with a huge 4-inch color touch screen. Developed for warehousing and manufacturing environments with the following parameters (Table 2).

Table 2

Developed for warehousing and manufacturing environments with the following parameters

Component	Parameters
CPU type	Qualcomm 8056 1.8 Ghz hexa-core 64 bit
RAM	2GB, 16GB Flash (Standard)
Operating system	Android 7.0 Nougat AOSP GMS operating system
Keyboard	29-key keyboard
Screen	WVGA 4-inch color touch screen (480 × 800 pixels)
Roaming, Bluetooth	IEEE 802.11 a / b / g / n / ac / d / h / i / k / r / w fast roaming, Bluetooth 4.1, 2.1 + EDR
IP	IP54, -20 ° C to + 50 ° C, can be dropped from 1.5 meters
Barcode scanner	1D laser imager barcode scanner, normal distance

2.5 Introducing a Barcode Printer

The third pillar of the system is the barcode printer, with which the barcodes generated by the ERP system can be converted into physical form. The label

printer is also a device designed and manufactured by Zebra Symbol that listens to the ZD220. Its predecessor is the Zebra GC420 label printer.

The Zebra ZD220 is an entry-level model among 4” printers. More specific parameters are (Table 3):

Table 3
More specific parameters

Component	Specific parameters
Type of printing	Direct thermal or thermal transfer printing
Resolution	203 dpi / 8 dots per mm
Print speed	102mm / sec
Memory	256 MB Flash; 128 MB SDRAM
Program language support	EPL, ZPL
Maximum print width	4.09 in. / 104 mm
Firmware (basic software)	ZPL II; EPL 2; XML

3 Calculation of Return for a Barcode Warehouse Management System

Besides the technical and technological evaluation, the implementation of the idea requires financial approval. The return on the investment may influence the selected solution or the services added to the system. The cost of setting up a barcode warehouse management system is HUF 25837559 (data based on 2023). It can be implemented only on its own or with the help of support. The barcode warehouse management system can be extended to all employees, but a version that is only extended to office employees can also be analyzed. Accordingly, four cases were examined. In case of A, we make the cost calculation for a barcode warehouse system paid for with our own capital, in which the project management module is built for the entire workforce.

In case of B, in addition to our own capital, we pay the costs from refundable state support, in which we want to expand the project management module to the full number of employees.

In case C, we pay with own capital, in which the project management module is extended only to office workers. In case of D, we are combined C and B.

A summary of our results is shown in Table 4. The economic evaluation of the investment is checked by some indicators [35], including:

NPV: Net Present Value [36]

IRR: Internal Rate of Return [37]

PI: Profitability Index

DPB: Discounted Payback Period [38] [39]

Table 4
Summary of our calculation results

	Case A	Case B	Case C	Case D
NPV (HUF)	5991000	2886000	13220000	10115000
IRR (%)	18.05	11.49	43.24	32.56
PI	1.23	1.11	1.71	1.54
DPB (year)	4.06	4.50	2.92	3.24

Based on the results obtained:

Case A, with the introduction of the barcode warehouse management information system, will show a return within 5 years, using only the company's own resources. The net present value (NPV) received is HUF 5991000, which is higher than HUF 0, so the investment is expected to increase the value of the company [40] and result in a positive net income in the 5-year period under review. The calculated internal rate of return is 18.05%, which is higher than the expected return of 6%. The profitability index was 1.23 in the calculation, which is greater than 1. The discounted payback period is 4.06 years, based on which the project will pay for itself in year 5. As the calculated and expected values are the same, this indicator also meets the expectations. Overall, Alternative A can be accepted.

Case B assumes that the introduction of the barcode warehouse management information system would return within 5 years by involving equity and repayable state support. The net present value obtained during the investigation was positive, 2886 HUF; therefore, an investment is expected to increase the value of the company. As a second indicator, we examined the internal rate of return, which was 11.49%. As this value is higher than the expected return of 6%, this indicator is also considered acceptable. Next, we examined the profitability index, which is 1.11. As greater than 1, it is considered acceptable. Finally, we calculated the discounted payback period, resulting in 4.50 years. The return on investment is also expected within the expected 5 years. In summary, option B is also acceptable for all indicators.

Case C assumed that we will extend the project management module in the expansion of the ERP system only among office employees in the structure of the barcode system, and thus the investment will return in 5 years. NPV for the case is HUF 13220000. This value is greater than zero and is therefore considered acceptable. The internal rate of return was 43.24%. The present result shows a higher return than the expected 6%. The profitability index was 1.71, which is higher than 1. The last time the discounted payback period was calculated, and the result was 2.92 years, which means that the investment pays off in the third year. The project must therefore be approved. In the case of C, all the calculated values

deviated in the positive direction compared to the set one, so we can accept this alternative as well.

Case D assumed that with the extended project management for office staff, the barcode warehouse management system would return in 5 years, financed from its own and repayable state support. The first indicator was the net present value (NPV), for which we received HUF 10115000. We then examined the internal rate of return, which gave a value of 32.56%. This result is higher than the expected 6% yield, so we also accept this final result. The profitability index is calculated at 1.54, which is greater than 1. The discounted payback period is 3.24 years. In summary, in the case of D as well, all indicators showed a corresponding value.

Conclusions

The case example showed that the problem must be dealt with in a complex manner. We know that there exist more modern technologies and there are many possibilities within them, but integration into the system is more important than the device. That is why we chose the tool described above. We made economic calculations for four investment alternatives. As the four investment alternatives met the exam requirements. However, one needs to choose the one that is best for ones' company.

Comparing all the indicators, we can see that Case C, provides the highest net present value, profitability index and internal rate of return. In addition, the return on the investment is the best in this case compared to the others. So, this alternative is best suited for a business that consists of nothing more than the introduction of a barcode warehouse management system with an extended project management module for office employees involving only equity.

But if we also take into account the subjective factor, that this system does not yet fully cover the possibilities of an integrated corporate management information system, e.g., a record of the working time associated with the bar code system to be introduced at a later date. Then, in that case, the best solution would be the first, Case A, which does not bring as much revenue to the business as Case C, but provides a more promising opportunity for further development for the company.

According to the research question, as to whether it is worth implementing the warehouse management system, the case studies of this paper provides confirmation. The return on the investment is within four years, which can be considered positive. This case study can serve as a sample for similar projects, including any evaluation methods.

References

- [1] Hetyei J. and Salgóné Sziklai K.: ERP systems in Hungary in the 21st Century (in Hungarian), Computer Books Kiadó Kft. Budapest, 2009
- [2] Csipkés M.: The importance of product identification and tracking in supply chain processes (in Hungarian), *Logisztika*, 2018, Vol. 4, No. 2, pp.

41-46

- [3] Kis K.: Quality improvement and development with the involvement of corporate partners at the University of Szeged Faculty of Engineering (in Hungarian), *Jelenkori társadalmi és gazdasági folyamatok*, 2020, Vol. 15, No. 3-4, pp. 25-53
- [4] Berényi L.: Project management: Integration of projects into an organization (in Hungarian), Miskolc, Hungary, Bibor Kiadó, 2015
- [5] Hampel Gy.: Support for solving logistics problems in Excel 2016 (in Hungarian), *Jelenkori társadalmi és gazdasági folyamatok*, 2017, Vol. 12, No. 3, pp. 219-229
- [6] Prezenszki J.: Warehousing-Logistics (technique, technology, organization, service) (in Hungarian), Ameropa Publishing House, Budapest, 2010
- [7] Pamlényi K. and Gál J.: Specialties and difficulties of storing and transporting biosimilar medicines, In: Bodnár K.; Privóczki Z. (ed.): 7. Logistics in the Southern Great Plain: Peer-reviewed scientific conference publication (in Hungarian), Csongrád, Hungary, Agro-Assistance Kft., 2021
- [8] Kovács Sz., Lux G. and Páger B.: The role of medium-sized companies in the manufacturing industry: the first results of a Hungarian research (in Hungarian), *Területi Statisztika*, 2017, Vol. 57, No. 1, pp. 52-75, doi:10.15196/TS570103
- [9] Sayer N. J. and Williams B.: *Lean for Dummies*, 2nd Edition. Wiley Publishing, NJ, 2012
- [10] Košovská I. and Váryová I. and Ferenczi Vaňová A.: ERP systems and their contribution to the accounting and financial department of the company (in Slovakian), Available online: <https://docplayer.net/23169663-Erp-systemy-a-ich-prinos-pre-uctovne-a-financne-oddelenie-podniku.html> (accessed on 6 Februar 2023)
- [11] Hammer M. and Leonard D. and Davenport T.: Why don't we know more about knowledge, *MIT Sloan Management Review*, 2004, Vol. 45, No. 4, pp. 14-18
- [12] Kučera M. and Látečková A.: *Business Information Systems* (in Slovakian), Slovak University of Agriculture in Nitra, 2004
- [13] Berényi L.: Lean development: creating value or eliminating losses (in Hungarian) *Marketing és menedzsment*, 2015, Vol. 49, No. 2, pp. 47-60, p. 14
- [14] Sárkány Zs.: The role of integrated corporate management information systems in increasing the efficiency of corporate management, Thesis, (in Hungarian) Faculty of Informatics, University of Debrecen, Debrecen, 2009

- [15] Gabriel E.: The lean approach to project management, *International Journal of Project Management*, 1997, Vol. 15, No. 4, pp. 205-209
- [16] Csontos B. and Gál J.: Planning of installation of production capacity and aspects of selection are sustainability for your interest (in Hungarian), *Jelenkori társadalmi és gazdasági folyamatok*, 2019, Vol. 14, No. 3, pp. 153-161
- [17] Illés S.: International elderly migration in Hungary, *Migrációske i Etničke Teme*, 2006, Vol. 22, No. 1-2, pp. 53-77
- [18] Nagy J.: Supply chain management techniques, Workshop (in Hungarian), Budapest Corvinus University, Budapest, 2008, pp. 3-12
- [19] Némón Z.: Warehousing skills (Production and wholesale warehousing) (in Hungarian), Trade and Tourism Further Education Kft., Budapest, 2016, pp. 7-105
- [20] Michalkó G., Illés S. and Vizi I.: Territorial differences in the presumed niches of new tourists in Hungary (in Hungarian), *Földrajzi Értesítő*, 2007, Vol. 55, No. 3-4, pp. 271-289
- [21] Illés S.: Tourism and migration from a mayor's perspective (in Hungarian), *Comitatus*, 2007, Vol. 17, No. 10, pp. 50-66
- [22] Végh K. and Illés S.: Hypothetical models of food consumption behaviour by the elderly, Lambert Academic Publishing, Saarbrücken, 2011
- [23] Dobos I. and Michalkó G. and Sasvári P.: The publication performance of Hungarian economics and management researchers: a comparison with the Visegrád 4 countries and Romania, *Regional Statistics*, 2021, Vol. 11, No. 2, pp. 165-182
- [24] Harausová H.: Process approaches in quality management (in Slovakian), University of Prešov in Prešov, 2012
- [25] Kučera M. and Štefánek J. and Cvečko J.: Information systems in agriculture (in Slovakian), Slovak University of Agriculture in Nitra, 2002
- [26] Bruckner T. and Kol.: Creation of information systems (in Slovakian), Grada Publishing, 2012
- [27] Molnár Z.: Effectiveness of information systems (in Slovakian), Grada Publishing, 2001
- [28] Rábová I. and Drlík M.: Business information systems, their architecture and development (in Slovakian), University of Konstantin Filozof in Nitra, 2013
- [29] Hencz Cs. I. and Czigány A. and Gényi T.: Identification systems in the entire product life cycle, In: *Logistics systems and theories: Berkesné H. O. et al.* (in Hungarian), UNIVERSITAS-Győr Nonprofit Kft., Győr, 2011, pp. 69-87

-
- [30] Darlington C. and Urban B.: Adoption of automatic identification systems by grocery retailers in the Johannesburg area, *Journal of Transport and Supply Chain Management*, 2011, Vol. 5, No. 1, pp. 88-107
- [31] Körmendi L. and Pucsek J.: Theory and practice of logistics (in Hungarian), SALDO Financial Consulting and Informatics Zrt., Budapest, 2008
- [32] Anupam Ch.: Barcode Technology and its Application in Libraries, University of Nebraska - Lincoln (2019). *Library Philosophy and Practice*, Available online: <https://digitalcommons.unl.edu/cgi/viewcontent.cgi?article=6896&context=libphilprac> (accessed on 5 Februar 2023)
- [33] SAP AG Available online: <https://www.sap.com/corporate/en/company/history.html> (accessed on 5 Februar 2023)
- [34] Kováč M.: Trends in the development of ERP systems (in Slovakian), Available online: <http://www.sjf.tuke.sk/transferinovacii/pages/archiv/transfer/14-2009/pdf/234-236.pdf> (accessed on 4 Februar 2023)
- [35] Fabulya Z.: Cost optimizing of autoclaving in Excel environment, *Analecta Technica Szegedinensia*, 2008, Vol. 2, pp. 19-25
- [36] Shank J. K.: Analysing technology investments—from NPV to Strategic Cost Management (SCM), *Management Accounting Research*, 1996, Vol. 7, No. 2, pp. 185-197
- [37] Hartman J. C. and Schafrick I. C.: The relevant internal rate of return, *The Engineering Economist, A Journal Devoted to the Problems of Capital Investment*, 2004, Vol. 49, No. 2, pp. 139-158
- [38] Horváth J. and Benkő-Kiss Á.: Estimation principles of investment value for Individual Agricultural Investors, *Lucrari Stiintifice Management Agricol*, 2011, Vol. 13, No. 1, pp. 67-74
- [39] Nagy S.: Discounting models and a possible application of the results of hyperbolic discounting (in Hungarian), *Jelenkori társadalmi és gazdasági folyamatok*, 2014, Vol. 9, No. 1-2, pp. 85-93
- [40] Molnár Z.: Business information systems (in Slovakian), Available online: <broucek.chytrak.cz/download/fsi/PIS/PIS1.ppt> (accessed on 31 July 2022)

Improving Multiagent Actor-Critic Architectures, with Opponent Approximation and Dropout for Control

Gabor Paczolay, Istvan Harmati

Department of Control Engineering, Budapest University of Technology and Economics, Magyar tudósok krt. 2, H-1117 Budapest, Hungary
paczolay@iit.bme.hu; harmati@iit.bme.hu

Abstract: In the domain of reinforcement learning, solution proposals to multiagent problems are evolving. We propose a new algorithm, MADDPGX, to handle the problem of higher uncertainty created by other agents' actions by an enemy actor approximator, and we investigate the most efficient techniques of estimations. This approximation works using a neural network, which has the input of the state and the output as the action (probably preferred by the enemy agent). We also experimented with dropout, a tool commonly used for neural networks, but has not been used efficiently for reinforcement learning until now. We have also found that in multiagent actor-critic scenarios, it can improve overall performance. Generally, our contribution is the use of action approximation of adversaries and the dropout usage in actor-critic systems, with a conclusion that the newly proposed methods will perform better in zero-sum multi-agent robot system scenarios. The experiments were conducted in a multiagent predator-prey environment.

Keywords: reinforcement learning; multiagent learning; dropout; MADDPG; MADDPGX

1 Introduction

Reinforcement learning is a fast emerging field in the domain of artificial intelligence. Due to the increase of the computing powers, it is becoming a reality to solve more complex control problems efficiently, which would otherwise require a very fragile and precise mathematical model. However, having multiple agents in the environment makes it much harder to solve the task as each agent introduces a high uncertainty related to their specific policy, because as each agent performs their own action, the learning algorithms generally rely on that specific choice, and it is harder to deal with the fact that those agents will later perform another action in the same situation due to their learning having advanced. This problem is addressed by the sub-domain of multiagent reinforcement learning, which considers the multitude of the agents and either tries to pay attention to the opponents' actions

(this branch is called as a competitive multi-agent scenario) or tries to figure out an action ensemble which leads to the most reward (this is called as a cooperative multi-agent scenario). Our proposed algorithm, that is presented in this paper was tested on both the cooperative and the competitive elements of the environment that we use, and as it will later be clear due to the results, it behaves the best when it is used on the competitive domain due to the lower uncertainties in this scenario.

Whenever we, humans, try to figure out the best action that would contradict our opponent's hostile behavior, we can ask ourselves: "What would my opponent do in this situation?" Then, we take this estimation and form our next action, based on it, deciding the action which yields us the best returns. This method is what we use in our proposed algorithm: We estimate the opponents' state-action assignment (in actor-critic algorithms, it is the actor) and train our actor such that it takes this estimation as part of its input. The critic is also trained based on the assumptions made by the approximating model.

Later in this paper we examine the effects of applying dropout in the field of reinforcement learning. It is actively used in general deep learning due to its effect of decreasing the possibility of overfitting, but up until now, its usage was opposed for reinforcement learning, especially because higher variance is not required in single-agent reinforcement learning. The dropout effects were not tested in the domain of multiagent reinforcement learning, we address this problem in our paper. Our results show that dropout has its certain place in this field as well, and we try to give as precise information on its possible applications.

Littman [12] was the first to use Minimax-Q, a zero-sum multiagent reinforcement learning algorithm and he applied it to a simple robotics soccer game environment, later Hu and Wellmann [11] brought the Nash-Q algorithm to the world and they utilized in a small grid-world environment to show the algorithm's achievements. Bowling [4] sped up the training process while ensuring convergence by varying the learning rate. Later, he applied his proposal, the Win or Learn Fast methodology to an algorithm based on an actor-critic system to have better multiagent performance [5].

Reinforcement learning's huge leap forward happened when convergence of deep neural networks was improved and one could use them in these scenarios. Mnih *et al.* [15] invented the Deep Q-Network (DQN) algorithm and its invention was made to play Atari games with success by multiple frame feeds and using experience replay for better chance for convergence. Then, researchers combined deep reinforcement learning and multi-agent systems, its most simple form is called independent multi-agent reinforcement learning. Foerster *et al.* [8] experimented with stabilizing experience replay, a buffer of states, actions, rewards and next states to improve convergence, for independent Q-learning (IQL) by utilizing so-called fingerprints. Researchers have also made multiple advancements in the field of centralized learning and decentralized execution as well, for example, when Foerster *et al.* [7] created Counterfactual Multi-Agent Policy Gradients, where the

problem of multi-agent credit assignment was solved by training agent policies by comparing its actions to other actions it could have taken. Sunehag et al. [21] used Value Decomposition Networks with a common reward and Q function decomposition. Lowe et al. [14] made improvements to the Deep Deterministic Policy Gradient algorithm by a changing the critic to contain all actions of all of the agents, this change, thus the algorithm would be able to learn multi-agent environments with better efficiency. Shihui et al. [19] made advancements to the previously described MADDPG algorithm by altering it to achieve better performance in environments with zero-sum payoff by using a method based on the Minimax-Q learning algorithm. Davies [6] applied a Model Opponent Learning algorithm to the previously mentioned MADDPG method. Casgrain et al. [3] modified Mnih's Deep Q-network algorithm by using methods based on Nash equilibria, which made it able to solve multi-agent environments.

To inspect the performance of their algorithms, researchers have also made several benchmarks, even for multiagent environments. Vinyals et al. [24] took the game of Starcraft II and made it to be a learning environment for multi-agent scenarios. Samvelyan et al. [18] also utilized Starcraft as a multiagent benchmark environment, but in this case, the aim was micromanagement, controlling each unit separately. Liu et al. [13] created a multiagent, continuous simulated physics-based soccer environment. Bard et al. [2] made huge advancements of multi-agent learning with the Hanabi game benchmark, where the agents have to cooperate with each other in partially observable scenarios.

Other kinds of control and learning algorithms may also be considered, too. Babqi et al. [1] compared MPC and PI control for power electronic devices. Hakan et al. [9] created a test platform for vertical drones. Preitl et al. [17] utilized quadratic programming in fuzzy systems. Precup et al. [16] used generic 2DOF linear and fuzzy controllers for integral processes. Hemza et al. [10] utilized fixed point iteration in single variable second order systems, while Zamfirache et al. [25] used an actor-critic RL solution for servo systems. Our method is more robust than the methods listed in the paragraph.

Our work also builds upon the MADDPG algorithm and takes a similar route to the Model Opponent Learning algorithm, but relies more upon the action approximation of the actors using a neural network where the inputs are the states and the outputs are the agent's most probable preferred actions. This is our main contribution in this paper, and it can improve the performance of agents in competitive environments. Also, we dive deeper into the possible architectures and algorithm realizations of the action approximation. In addition, we approach the usage of dropout in ways that were not used before with as precise information on its usage as we can. This contribution utilizes a method previously, solely, used in other domains of deep learning and proves to be useful in deep reinforcement learning as well.

Our new methodologies have their certain positions in engineering applications as well. The opponent approximator method is usable for zero-sum multi-agent robot systems, such as collision avoidance in aircraft control, where the other planes can be considered as “enemies”, and the objective is to minimize the time of arrival. It is also in Unmanned Aerial Vehicles of other types, for guarding an area against intruders. Our dropout contribution is also utile under these conditions, but it can also be useful in any multi-agent scenarios, control problems included. The new ideas of this paper are the MADDPGX algorithm and the dropout utilization.

In this work, first we take a look at the theoretical background. Later, we show the used benchmarks for our tests, then we explain our experiments and the results obtained by them. At the end, we conclude our work and give suggestions for future research possibilities.

2 Theoretical Background

2.1 Markov Decision Processes

Markov Decision Process is a discrete-time process for decision making modeling. Figure 2 shows the basics of this mathematical framework. It has the following elements: states of the whole environment, selectable actions by the agent, transition probabilities between the states with respect to the actions and rewards given to the agents. [1]. Every timestep the process has the same method: starting at a specific state (s), it has an available action space. From that, the agent selects an action (a), and based on the state-action pair, it will receive a reward (r), then it arrives in a new state (s'). A stochastic process is called Markovian if:

$$P(\mathbf{a}^t = \mathbf{a} | \mathbf{s}^t, \mathbf{a}^{t-1}, \dots, \mathbf{s}^0, \mathbf{a}^0) = P(\mathbf{a}^t = \mathbf{a} | \mathbf{s}^t) \quad (1)$$

which can be described such as state transitions depend only on the last state and the currently selected action. Due to this, only these two are important in the decision of the following state.

The policy, a state-action assignment, is very important in Markov Decision Processes. Agents are trying to seek for an optimal one which can maximize the return, the sum of discounted expected rewards. Discount in this case means that agents prefer an immediate reward against one in the future, thus, a coefficient determines how better a reward is with respect to the same amount of reward in the next state. To find a general solution for the policy, one has to seek for a fixed point of the Bellman equation via iterative search. The Bellman equation has the following form:

$$v(\mathbf{s}, \pi^*) = \max_a (r(\mathbf{s}, \mathbf{a}) + \gamma \sum_{s'} p(\mathbf{s}' | \mathbf{s}, \mathbf{a}) v(\mathbf{s}', \pi^*)) \quad (2)$$

where $r(s, a)$ is the reward gained from selecting action a in state s , γ is the coefficient deciding how much more important are rewards of the present in comparison with the future rewards, and $p(s'|s, a)$ is the transition probability function. It is concluded from this equation that if the agent is familiar with the dynamics of the environment, it can find the optimal values.

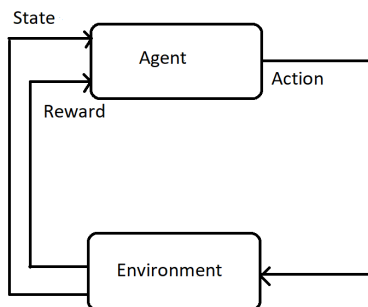


Figure 1
Markov Decision Process

2.2 Reinforcement Learning

Reinforcement learning is a subproblem of Markov Decision Process whenever the either rewards or the state transition probabilities are not known. In this case, one has to seek to create a proper model of the environment by trying specific actions and learning from the rewards and the errors.

There are two main kinds of reinforcement learning: **value-based** and **policy-based** reinforcement learning.

In the scenario of value-based reinforcement learning, agents are rendering values to the states or to the actions that are selectable from specific states. The aforementioned values coincide with the expected reward whenever the agent selects a certain action in a specific state.

The most generally utilized kind of value-based reinforcement learning is called **Q-learning**. It is an algorithm based on action-values, so these values are rendered to all of the state-action pairs of the environment. These values, called Q-values, correspond to the value equal to the amount of reward one could get by taking a certain action in a certain state. The equation for the update of the Q-values is the following:

$$Q(s', a) \leftarrow (1 - \alpha) \cdot Q(s, a) + \alpha \cdot (r + \gamma \cdot \max_{a'} Q(s', a')) \quad (3)$$

where α corresponds to the learning rate and γ corresponds to the discount for the reward [17]. is an off-policy TD (temporal difference) control algorithm. The policy

is to choose the action that would currently maximize the Q-function in the present state.

In policy-based reinforcement learning, the actions are a parametric function of the state. Of this type, the most common technique is **policy gradient** [18], when the policy is given by the parameters θ , and the agent tries to reach the maximum expected reward for a specific trajectory $r(\tau)$. This gives us that the cost function based on the parameters is this equation:

$$J(\theta) = E_{\pi_{\theta}}[r(\tau)] \quad (4)$$

The tuning of the parameters is performed with respect to the gradient of the cost function:

$$\theta_{k+1} = \theta_t + \alpha \Delta J(\theta_t) \quad (5)$$

Policy-based methods have their own advantages and disadvantages. They are able to map environments with great or continuous action spaces efficiently. Value-based methods cannot map huge action spaces due to the increasing value-table size. Policy-based methods are also efficient for scenarios with randomness. On the other hand, they are more prone to get stuck in a local maximum instead of finding the optimal policy.

2.3 Multi-Agent Systems, Markov Games

To fully understand the Markov games, one has to talk about the stochastic framework of matrix games. In that, first each agent takes an action, then they get their current reward. This reward is based on all of the agents' action. These scenarios can be described in a matrix form, where one agent selects the row based on its action, and the other selects the column, and the intersection contains the reward for each agent. These games can only contain a single state.

A multi-state augmentation of matrix games is called Markov game, or with another wording, Stochastic game. Another approach can be that Markov games are a multi-agent extension of Markov Decision Processes. In these games, all of the states contain a specific matrix called payoff matrix, which has the same form as the matrix in Matrix games. Thus, the reward is decided by the mutual action of the agents, and this can be also said about the next state. A game is said to be Markovian if it adheres to the following:

$$P(a_i^t = a_i | s^t, a_i^{t-1}, \dots, s^0, a_i^0) = P(a_i^t = a_i | s^t) \quad (6)$$

which means that the upcoming state is solely dependent on the previous state and the present actions selected by all of the agents.

2.4 Deep Reinforcement Learning

Deep reinforcement learning is a subclass of reinforcement learning which is aided by a neural network.

An artificial neural network is a subset of machine learning. In this case, the function approximation is performed by a network of (even huge amounts of) artificial neurons. Artificial neurons resemble biological neurons, and their behavior is determined by the following equation:

$$y = \text{Act}(\sum w\mathbf{x} + b) \quad (7)$$

In this equation, x corresponds to the input vector. w is the weight vector, which is taken with a by-element product of the previously mentioned input vector. b is called bias, as it is a variable constant added to the other inputs. This can also be described as a regular weight connected to the input of the constant 1. $\text{Act}()$ corresponds to the activation function, which ensures that the system becomes nonlinear by introducing nonlinearity, thus letting otherwise linear systems predict nonlinear relations. The tuning of the parameters, w and b , are performed by backpropagation, where the partial derivative errors with respect to the inputs are calculated starting from the final error, and then this error is propagated backwards through previous layers up until the input vector.

One must talk about the difference between traditional reinforcement learning and deep reinforcement learning. The latter has a considerable number of advantages, such as abandoning the state table by approximating the states with neural networks, which is more robust than general linear approximators. This allows us to map scenarios with huge or even continuous state spaces without worrying about the memory need of the whole state space. On the other hand, deep reinforcement learning converges in less situations, thus a multitude of improvements have been made to ensure convergence of the learning in more scenarios.

2.5 Actor-Critic

An amalgamation of value-based and policy-based reinforcement learning is called an actor-critic algorithm. This algorithm contains two distinct neural networks: The first is called Critic, which resembles value-based reinforcement learning, by approximating a value function, and the second is called the Actor, which, as in policy-based reinforcement learning, renders an action to the present state. The latter network is tuned, based on the direction suggested by the Critic. The actor follows an approximate policy gradient as:

$$\begin{aligned} \nabla_{\theta} J(\theta) &\approx \mathbb{E}_{\pi_{\theta}} [\nabla_{\theta} \log \pi_{\theta}(s, a) Q_w(\mathbf{s}, \mathbf{a})] \\ \Delta \theta &= \alpha \nabla_{\theta} \log \pi_{\theta}(s, a) Q_w(\mathbf{s}, \mathbf{a}) \end{aligned} \quad (8)$$

The latter equation is the more critical from a practical point of view, as it gives us the direction of the parameter updates. In that equation, α corresponds to the learning rate, a scalar which determines the amount of parameter change. The other parts show that the direction is given by the gradient of the log-policy times the value function.

The policy gradient approximation reduces efficiency in one part due to the bias introduced, and this bias can make our learning fail. The value function approximation has to be chosen with great care to avoid this bias.

In comparison with regular deep reinforcement algorithms, actor-critic algorithms achieve better performance. By the utilization of the critic network, the system can avoid being stuck in a local extremum, and by the usage of the actor network, better convergence can be achieved in addition to mapping systems with huge or even continuous action spaces.

2.6 MADDPG Algorithm

MADDPG, Multiagent Deep Deterministic Policy Gradients is a multiagent extension to the DDPG (Deep Deterministic Policy Gradients) algorithm, which is an actor-critic algorithm for continuous action spaces.

First of all, both MADDPG and DDPG use an experience replay buffer to recall previous state-action-reward-next state tuples. It stores and recalls the tuples (x^j, a^j, r^j, x'^j) . By its utilization, the system will utilize previous experience more efficiently as it will learn the experience multiple times, as well as it will converge with a higher success rate due to access not only to the latest experiences.

Let's take a closer look at the training of the actor and critic networks. The critic is updated by minimizing the loss as here:

$$\mathcal{L}(\theta_i) = \frac{1}{S} \sum_j (y^j - Q_i^\mu(x^j, a_1^j, \dots, a_N^j))^2 \quad (9)$$

Where,

$$y^j = r_i^j + \gamma Q_i^\mu(x'^j, a_1^j, \dots, a_N^j) \Big|_{a_{k'} = \mu_{k'}(o_k^j)} \quad (10)$$

This latter equation shows that for the next actions, we use the target actors to compute them. Meanwhile, the actor is updated using the following sampled policy gradient:

$$\nabla_{\theta_i} J \approx \frac{1}{S} \sum_j \nabla_{\theta_i} \mu_i(o_i^j) \nabla_{a_i} Q_i^\mu(x^j, a_1^j, \dots, a_i, \dots, a_N^j) \Big|_{a_i = \mu_i(o_i^j)} \quad (11)$$

In this equation, we see that we take the gradient with respect to the Actor's parameters with the help of a central critic.

2.7 Dropout

Dropout is mostly used to reduce overfitting in deep neural networks. Overfitting is a case when the function approximator (in this case, the neural network) renders the parameters to the training data well, but misses generalization, thus the approximator cannot be utilized for any useful task (apart from the occasions where input values are a subset of the training values). [19] [21] If it is applied to a neural network (or rather, to a layer), then the network's (or layer's) neurons are only present with a p probability during the training process. In other words, at each training stage, individual neurons are either eliminated from the net with a probability $1 - p$ or kept with a probability p , such that only a reduced network is left. In the testing/inference process, however, all neurons are present. This training method makes the training process noisy, forcing nodes to probabilistically take on more or less responsibility for the inputs. As the network is not used fully during the training process, instead, a subset of the layers is used, a wider network is required for layers with dropout that for ones without, for the same level of representation. The most used, and usually the most efficient probability rate for the dropout is 0.5.

3 Experiments

As a benchmark, we used the Multiagent Particle Environments (MPE) library. It is a multiagent environment ensemble with several environments, which are either communication-based or are about circle-shaped agents moving in a continuous 2D world, trying to accomplish specific tasks. It is written in Python, and its interface resembles (and is built upon) the quasi-standard interface of OpenAI's Gym environments, which makes connecting agents easier. The differences between its interface and Gym's are due to the fact that Gym does not support multiagent environments up until the writing of the paper, thus the multitude of observations and actions are listed in a unique but easily comprehensible way. From this environment ensemble of MPE, we used the "simple-tag" environment. This is a predator-prey (or pursuit-evasion) environment with 3 predators and one prey, and the latter is faster (and also has better acceleration). There are also obstacles on the plane that cannot be crossed. The agent movement behavior is described as follows:

$$F_i = m_i \cdot a_i * u + z \quad (12)$$

where m_i is the agent mass, a_i is the agent acceleration (if it exists in the scenario, otherwise it is strictly 1), u is the agent action and z is the noise (if exists). Then, from the forces, a velocity is calculated:

$$v_i = v_i + \frac{F_i(1-d)}{m_i} \cdot dt \quad (13)$$

where d is the damping. The here unnecessary product and division by the mass is applied due to the possible addition of environmental forces in other scenarios. Finally, the position is calculated such as:

$$x_i = x_i + v_i \cdot dt \quad (14)$$

The predators have to catch the prey agent, and they get a positive reward for catching the agent, while being caught, the prey gets a negative reward. For evading the problem of sparse rewards, which means that the received rewards are present only on a small subset of the environment steps, reward shaping was turned on. In this case, the prey gets bigger rewards for being as distant from the predators as possible, and the predators get negative reward based on the minimum distance to the prey agent (thus the reward is relatively bigger if one agent is closer to the prey). The exact reward function for the prey is as follows:

$$r = c \cdot (-10) + 0.1 \sqrt{\sum (x_{prey} - x_{pred})^2} \quad (15)$$

where r is the reward, c is the collision boolean, and x are the positions. The reward function for the predator is the following:

$$r = c \cdot 10 - 0.1 \cdot \min_{a \in prey} \sqrt{\sum (x_a - x_{pred})^2} \quad (16)$$

In our environment settings, as there is only one prey, the minimizing part disappears and the latter parts of both equations become the same. The only difference between the two-reward function is the c part: while for the preys it means a boolean (0 or 1), for the predators it counts all collision between the predators and the prey, thus reaching the prey with multiple agents yields more reward.

The episodes are terminated after 25 steps, this number seemed to be well balanced regarding the training being meaningful and the episode length not being too long for the training process and other calculations. With this length we also evaded that the episodes would stall, with the prey agent getting stuck caught by predators for long times, modifying the rewards by a big amount. A sample picture of the environment can be seen on Figure 3, where the red circles are the predators, the green one is the prey, and the bigger black circles are the obstacles that cannot be traversed. The goal of the environment for the predator is to minimize the time in which it arrives the closest to the prey, and for the prey the goal is to maximize the distance between itself and the predators.

First, we tried to improve the training by approximating other agents' behavior. In this case, the agent observations are augmented by the most probable action that some other agents (the enemies or all other agents) would take. The most probable action for each opponent is approximated by a neural network, which takes the observation as input and outputs a value (the action) with a dimension equal to its action space. The training of this neural network consists of applying the agents' selected action to the present observation.

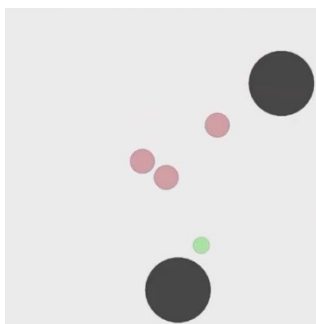


Figure 3

Predator-Prey environment of the Multiagent Particle Environments library

This training can happen online, at each timestep, or from the experience replay in conjunction with the training of the actors and critics. As the actor now requires the most probable actions as well, these have to be computed for the training process. The critic training was not modified from the MADDPG training for this algorithm.

Algorithm 1 shows the MADDPGX algorithm. As it can be seen, it is mostly based on the MADDPG algorithm, with some differences. The most important difference is that the selected actions are not calculated as $a = \mu_i(x)$ but $a = \mu_i(x, m)$, where m is the ensemble of the approximated actions and is calculated for all i as $m_i = N_{e_i}(x)$. The other difference between our algorithm and the original is also related to the former, it is that the actor is updated with the calculation of the previous $N_{e_i}(x)$ values. Inbetween, the N_{e_i} networks are also updated such that they would approximate the enemy actions based on the corresponding states. The training of the neural networks happens independently. The control law is given just as in MADDPG, but with the opponents added:

$$\nabla_{\theta_i} J \approx \frac{1}{S} \sum_j \nabla_{\theta_i} \mu_i(o_i^j, N_{e_i}(o_i^j)) \nabla_{a_i} Q_i^\mu(x^j, a_1^j, \dots, a_i, \dots, a_N^j) \Big|_{a_i = \mu_i(o_i^j, N_{e_i}(o_i^j))} \quad (31)$$

The computational complexity of our algorithm is:

$$O(4n^4)$$

Where, n is the number of neurons in the network. The stability of the controller is the same as the stability of MADDPG, so it can be described as stable but not in all situations. The system converges, but the optimality is not guaranteed for MARL situations, as in all other similar scenarios.

The algorithm was created with Python and PyTorch, and the experiments were run on a Google Colab instance (due to the varying speed of the instances, the average running times could not be usefully extracted for the experiments, thus this information is rather omitted). The networks consisted of three layers: two hidden layers and one output layer. The hidden layers' dimension was 64 neurons. This level of network complexity seemed to be enough for learning the environments for

all of the algorithms. The activation function of the inner neurons was ReLU (Rectified Linear Unit), while for the output, a tanh activation function was applied. As noted, the actors' dimension was equal to the observation space dimension plus the tracked agents' action space dimension, and the output dimension was equal to the agent's action space dimension. The action approximators' input dimension is equal to the tracked agent's observation space and its output is the tracked agent's action space. The critics were the same as in the MADDPG algorithm, with the input dimension being equal to the sum of all agents' action and observation space dimension, and the output is 1 (the Q value). An Adam optimizer was used as all of the neural network optimizers. The critic loss was a mean squared error loss and the actor loss was the same as in the base MADDPG algorithm, with the exception that for the actor loss, the approximations are needed to be made. The action approximator loss was dependent on the type of the action space: for discrete action spaces, cross-entropy loss was used, while for continuous action spaces, a mean squared error was used. In both cases, the losses consider the difference between the approximated and the taken action. Throughout all experiments, the learning rate as 0.01, the batch size was 1024 and τ (the target network coefficient) was 0.01. γ was set to be 0.95. These values are selected to provide a good balance between convergence and learning speed.

In a later experiment, we checked how applying dropout would affect the performance of the agents. As it applies more variance, the basic idea to check it was the expectation of finding more rewarding Nash equilibria. We experimented with the application of dropout on the actor and the critic network separately, and have seen which one is capable of improving the performance score. For the experiments, the dropout layers of 0.5 probability were applied after the first and second fully connected layers of the networks.

Initialize Models: μ_i, C_i, N_{e_i}

for episode = 1 to M **do**

 Initialize a random process \mathcal{N} for action exploration

 Receive initial state \mathbf{x}

for $t = 1$ to $max - episode - length$ **do**

 For each agent i , take the subset of opponent agents e_i

 calculate $m_i = N_{e_i}(o_i)$

m_i is the most probable action of the enemies

$N_{e_i}(o_i)$ is the actor approximator with the observation as input and most probable action as output

 for each agent i , select action $a_i = \mu_{\theta_i}(o_i, m_i) + \mathcal{N}_t$ w.r.t. the current policy and exploration

 Execute actions $a = (a_1, \dots, a_N)$ and observe reward r and new state \mathbf{x}'

 Store $(\mathbf{x}, a, r, \mathbf{x}')$ in replay buffer \mathcal{D}

$\mathbf{x} \leftarrow \mathbf{x}'$

for agent $i = 1$ to N **do**

 Sample a random minibatch of S samples $(\mathbf{x}^j, a^j, r^j, \mathbf{x}^j)$ from \mathcal{D}

 Set $y^j = r_i^j + \gamma Q_i^{\mu'}(\mathbf{x}^j, a_1, \dots, a_N) |_{a_{k'} = \mu_{k'}(o_k^j)}$

 Update N_{e_i} networks:

 Loss is MSE for continuous actions, Cross-Entropy for discrete

 For all e_i , training input is \mathbf{x}^j , training output is a^j

Update critic by minimizing the loss $\mathcal{L}(\theta_i) = \frac{1}{S} \sum_j (y^j - Q_i^\mu(\mathbf{x}^j, a_1^j, \dots, a_N^j))^2$
 Update actor using the sampled policy gradient:

$$\nabla_{\theta_i} J \approx \frac{1}{S} \sum_j \nabla_{\theta_i} \mu_i(o_i^j, N_{e_i}(o_i^j)) \nabla_{a_i} Q_i^\mu(x^j, a_1^j, \dots, a_i, \dots, a_N^j) |_{a_i = \mu_i(o_i^j, N_{e_i}(o_i^j))}$$

end for
 Update target network parameters for each agent i :
 $\theta_i \leftarrow \tau \theta_i + (1 - \tau) \theta_i$
end for
end for

Algorithm 1
 MADDPGX

Figures 4 and 5 show some examples of the environment working. In all of them, we can see the fleeing agent (blue) is trying to maneuver away from the red agents. The examples were taken after the 23000th episode to give the agents enough time to learn the environment.

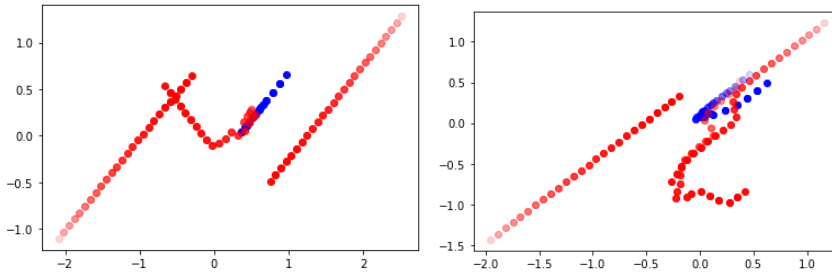


Figure 4

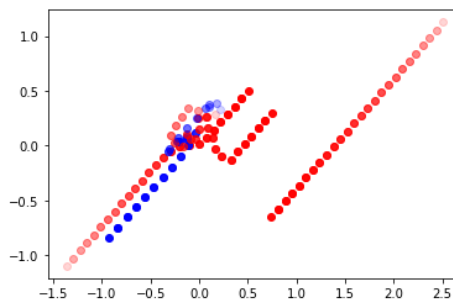


Figure 5

In all of the three examples, we see that both the predator and the prey agents have successfully learned the environment, as the predators are chasing the prey, and the prey is trying to flee from the predators. Figure 5 shows that two predators are trying to surround the prey, and a third one is chasing it directly. After the latter being close, the prey finds a way to free from the agents. Figure 6 shows that now two agents are chasing the prey directly, and the prey had to change its direction towards its starting point to evade the agents. In the third example, Figure 7, the prey and the two predator agents are "fighting", but then the prey agent successfully escapes.

4 Results

All experiments were run for 25000 episodes, this seemed to be enough for learning the environment and the opponent and the results did not change significantly by further increasing the episode number. Then, we extracted the mean rewards for all agents and episodes. For the easier digestion of the huge dataset (or in other words, to extract useful data out of the mean episode rewards), we introduced two baselines to be compared: One is the number of episodes where the prey agent's mean reward was above zero, and the other is the number of episodes where the prey agent's mean reward is higher than the sum of the other three agents' mean reward. These baselines were chosen arbitrarily, but they still represent the performance of the algorithms adequately.

Table 0 shows how many times the prey agent got a mean reward above zero of the 25000 episodes. Table 1 shows the number of occurrences when the prey mean reward was higher than the reward sum of the three predators.

First, let's check how the action approximation performs compared to the MADDPG vs MADDPG contests. Out of 8 different situations, 3 ended with univocal dominance for our algorithm, 4 was contested (in a sense that either the predator or the prey side was better with our algorithm, but the other side was worse after that) and one ended with definitely worse results than the original algorithms. This result clearly shows that our addition to the MADDPG algorithm improved the performance of the agents.

Now, let's check the different versions of the action approximator algorithm. For these experiments, the results can be seen in Table 4 and 5, where the former expresses the number of episodes where the prey's reward was greater than zero, and in the latter table, the predator sum is compared, just as in Table 1. It can be seen that from all the 6 comparisons, at 4 times the one where the approximator is updated online, right after the reception of the opponents' selected actions, supersedes the performance of the agent where the action approximator is updated from the experience replay, together with the learning of the actor and the critic in the general MADDPG algorithm. It can also be seen that for some reason, when the

action approximator is used not only for enemies, but for friendly agents as well, the performance of the system severely drops. Thus, our algorithm is better to be used only for modeling the enemies, not for modeling all other agents and trying to find a friendly Nash equilibrium using the approximators. This can be a result of divergence due to the higher variance of the system caused by the approximators, as it is much harder to find an equilibrium when all of the models are approximating each other.

The effect of the dropout can also be examined. First, let's look at the case when dropout is added to the Actor network, its results can be seen in Table 0 and 1. Of all the 16 comparisons, according to Table 0, in 14 cases the network with dropout superseded the one without it, meanwhile according to Table 1, 13 cases were better with dropout than without it. This shows that applying dropout to the actor network can generally yield better performance in multi-agent scenarios.

Table 1

Number of episodes where the prey's mean reward was above zero. The first line shows in which agent(s) our algorithms were used, and which subtype was implemented. Pred means predator, and A means Actor.

No.	Pred Dropout A	Pred	Normal	Prey	Prey Dropout A
1	31	43	70	11502	12854
2	11	11	20	2426	3352
3	5590	21685	49	26	27
4	15690	17882	21	27	23
5	18052	20519	20575	20	33
6	38	44	2314	22	40
7	86	17	436	45	51
8	28	39	1646	7039	9959

Table 2

Number of episodes where the prey's mean reward was above the sum of the predators' mean reward. The first line shows in which agent(s) our algorithms were used, and which subtype was implemented. Pred means predator, and A means Actor.

No.	Pred Dropout A	Pred	Normal	Prey	Prey Dropout A
1	2276	2792	3405	12729	14463
2	1652	1651	1675	4128	4415
3	8307	22458	2903	1871	1820
4	17582	19461	1928	1545	1039
5	19024	21368	20827	1356	2298
6	2198	2567	4444	1894	2580
7	2939	1569	5003	2298	2299
8	2196	2603	2861	10600	11082

We applied dropout to the critic network as well, and the results can be seen in Tables 2 and 3. Of the 16 cases, only in 7 cases this method happened to be better than the system without it. Also, when the network with critic dropout was better, usually the score did not improve much. However, in one case (No. 3 while our algorithm is on the predator side) the score improved significantly, so there can be some cases when applying dropout to the critic can be beneficial. The utility of the dropout possibilities in the critic network could be further examined.

The results show that our contributions are an improvement upon the previously available methods.

Table 3

Number of episodes where the prey's mean reward was above zero. The first line shows in which agent(s) our algorithms were used, and which subtype was implemented. Pred means predator, and C means Critic.

No.	Pred Dropout C	Pred	Normal	Prey	Prey Dropout C
1	4088	43	70	11502	60
2	32	11	20	2426	14
3	46	21685	49	26	35
4	20065	17882	21	27	43
5	21036	20519	20575	20	34
6	38	44	2314	22	39
7	18920	17	436	45	47
8	4285	39	1646	7039	32

Table 4

Number of episodes where the prey's mean reward was above the sum of the predators' reward. The first line shows in which agent(s) our algorithms were used, and which subtype was implemented. Pred means predator, and C means Critic

No.	Pred Dropout C	Pred	Normal	Prey	Prey Dropout C
1	7639	2792	3405	12729	1602
2	2661	1651	1675	4128	1142
3	2267	22458	2903	1871	1918
4	21040	19461	1928	1545	1971
5	21812	21368	20827	1356	2221
6	2542	2567	4444	1894	2406
7	19913	1569	5003	2298	2344
8	7684	2603	2861	10600	1380

Table 5

Number of episodes where the prey's mean reward was above zero. The first line shows in which agent(s) our algorithms were used, and which subtype was implemented. Pred means predator, V means that the version where the update is done in each step is implemented, and all means that the approximation for cooperative agents is also implemented

No.	Pred V All	Pred V	Pred	Normal	Prey	Prey V
1	17936	46	43	70	11502	19441
2	18858	11	32	20	2426	38
3		18799	21685	49	26	27

Table 6

Number of episodes where the prey's mean reward was above the sum of the predators' mean reward. The first line shows in which agent(s) our algorithms were used, and which subtype was implemented. Pred means predator, V means that the version where the update is done in each step is implemented, and all means that the approximation for cooperative agents is also implemented.

No.	Pred V All	Pred V	Pred	Normal	Prey	Prey V
1	19606	2614	2792	3405	12729	20741
2	20594	1652	2661	1675	4128	2775
3		19878	22458	2903	1871	1907

Conclusions and Future Work

According to our results, our proposals have clear benefits compared to the systems without it. Approximation of the actors of other agents visibly improves the performance, however, it is only beneficial in the system when it is used for competitive elements of the environments. Instead, it is rather advised to be omitted when using it for cooperative elements, or in other words, it is better to only approximate the enemies' behavior rather than using it for the approximation of the friendly agents' actors. Dropout also has clear benefits, but only when it is used for the actor, for the critic it is only really beneficial in some rare cases.

Regarding the actor approximation, the proposed idea is favorable to other algorithms due to the fact that with an insignificant loss on data efficiency, one can receive much better performance on the long run. As a comparison of the proposed systems and other types of control algorithms, actor-critic reinforcement learning algorithms are more versatile and robust than hand-made and other data-driven solutions.

There are still some challenges to explore in the future that we leave for upcoming researches. Further testing of dropout in the world of multi-agent reinforcement learning still awaits us to do. It is surely worth more effort to check whether the dropout on the critic is unusable for all of the possible situations, or as our results stated, which are the situations where the critic dropout is also utile. In addition, further testing of the dropout rates can be interesting. Also, the efficiency of the algorithm can be examined when the enemies' observations are not available, even

in a Partially Observable Markov Decision Process. This could be done, for example, with the help of Long Short-Term Memory (LSTM) systems, where the neural network preserves a state between timesteps, thus it is able to have a memory. Also, a variable learning rate could be utilized for further improvement of the learning systems, such as Bowling's Win or Learn Fast (WoLF) [3] method. Its usage for deep reinforcement learning could be investigated.

Acknowledgements

The research reported in this paper is part of project no. BME-NVA-02, implemented with the support provided by the Ministry of Innovation and Technology of Hungary from the National Research, Development and Innovation Fund, financed under the TKP2021 funding scheme. Support by the European Union project RRF-2.3.1-21-2022-00004 within the framework of the Artificial Intelligence National Laboratory.

References

- [1] A. J. Babqi, B. Alamri: A comprehensive comparison between finite control set model predictive control and classical proportional-integral control for grid-tied power electronics devices. *Acta Polytechnica Hungarica*, Volume 18, Issue 7, 07-2021
- [2] N. Bard, J. N. Foerster, S. Chandar, N. Burch, M. Lanctot, H. F. Song, E. Parisotto, V. Dumoulin, S. Moitra, E. Hughes, I. Dunning, S. Mourad, H. Larochelle, M. G. Bellemare, M. Bowling: The hanabi challenge: A new frontier for ai research, *Artificial Intelligence*, 2019
- [3] P. Casgrain, B. Ning, S. Jaimungal: Deep q-learning for nash equilibria: Nash-dqn, arXiv preprint arXiv:1904.10554, 2019
- [4] M. Bowling and M. Veloso: Multiagent learning using a variable learning rate, *Artificial Intelligence*, (136):215-250, 2002
- [5] M. H. Bowling, M. M. Veloso: Simultaneous adversarial multi-robot learning, In *IJCAI*, pp. 699-704, 2003
- [6] I. Davies, Z. Tian, J. Wang: Learning to model opponent learning, arXiv preprint arXiv:2006.03923, 2020
- [7] J. Foerster, G. Farquhar, T. Afouras, N. Nardelli, S. Whiteson: Counterfactual multi-agent policy gradients, *Proceedings of the AAAI Conference on Artificial Intelligence*, 32(1), 2017
- [8] J. Foerster, N. Nardelli, G. Farquhar, T. Afouras, P. H. S. Torr, P. Kohli, S. Whiteson: Stabilising experience replay for deep multi-agent reinforcement learning, *International conference on machine learning*, pp. 1146-1155, 2017
- [9] Ü. Hakan, Ö. Irfan, Y. Uğur, K. Metin: Test Platform and Graphical User Interface Design for Vertical Take-Off and Landing Drones. *Romanian Journal of Information Science and Technology*, 25, pp. 350-367, 2022

-
- [10] R. Hemza, J. Tar.: Multiple Components Fixed Point Iteration in the Adaptive Control of Single Variable 2nd Order Systems. *Acta Polytechnica Hungarica*, Volume 18, pp. 69-86, 09-2021
- [11] J. Hu, M. Wellman. Nash q-learning for general-sum stochastic games. *Journal of Machine Learning Research*, 4:1039-1069, 01 2003
- [12] M. L. Littman. Markov games as a framework for multi-agent reinforcement learning. In *Proceedings of the Eleventh International Conference on Machine Learning*, pp. 157-163, 1994
- [13] S. Liu, G. Lever, J. Merel, S. Tunyasuvunakool, N. Heess, T. Graepel: Emergent coordination through competition, *arXiv preprint arXiv:1902.07151*, 2019
- [14] R. Lowe, Y. Wu, A. Tamar, J. Harb, P. Abbeel, I. Mordatch: Multi-agent actor-critic for mixed cooperative-competitive environments, In I. Guyon, U. V. Luxburg, S. Bengio, H. Wallach, R. Fergus, S. Vishwanathan, and R. Garnett, editors, *Advances in Neural Information Processing Systems 30*, pp. 6379-6390, Curran Associates, Inc., 2017
- [15] V. Mnih, K. Kavukcuoglu, D. Silver, A. Graves, I. Antonoglou, D. Wierstra, M. Riedmiller: Playing atari with deep reinforcement learning, *arXiv preprint arXiv:1312.5602*, 2013
- [16] R-E Precup, S. Preitl, E. M. Petriu, J. K. Tar, M. L. Tomescu, C. Pozna: Generic two-degree-of-freedom linear and fuzzy controllers for integral processes, *Journal of the Franklin Institute*, Volume 346, Issue 10, pp. 980-1003, 2009
- [17] Z. Preitl, R. E. Precup, J. Tar, M. Takács: Use of Multi-parametric Quadratic Programming in Fuzzy Control Systems. *Acta Polytechnica Hungarica*, Volume 3, 2006
- [18] M. Samvelyan, T. Rashid, C. Schroeder de Witt, G. Farquhar, N. Nardelli, T. G. J. Rudner, C. Hung, P. H. S. Torr, J. Foerster, S. Whiteson: The starcraft multi-agent challenge, *arXiv preprint arXiv:1902.04043*, 2019
- [19] Shihui, Y. Wu, X. Cui, H. Dong, Fang, Fei, S. Russell: Robust multi-agent reinforcement learning via minimax deep deterministic policy gradient, In *Proceedings of the AAAI Conference on Artificial Intelligence*, Volume 33, pp. 4213-4220, 2019
- [20] N. Srivastava, G. Hinton, A. Krizhevsky, I. Sutskever, R. Salakhutdinov: Dropout: a simple way to prevent neural networks from overfitting, *The journal of machine learning research*, 15(1):1929-1958, 2014
- [21] P. Sunehag, G. Lever, A. Gruslys, W. M. Czarnecki, V. Zambaldi, M. Jaderberg, M. Lanctot, N. Sonnerat, J. Z. Leibo, K. Tuyls, T. Graepel: Value-decomposition networks for cooperative multi-agent learning, *arXiv preprint arXiv:1706.05296*, 2017

- [22] R. S. Sutton, D. McAllester, Singh: Policy gradient methods for reinforcement learning with function approximation, In Proceedings of the 12th International Conference on Neural Information Processing Systems, page 1057-1063, Cambridge, MA, USA, 1999. MIT Press
- [23] R. S. Sutton and A. G. Barto: Reinforcement Learning: An Introduction, Volume 9, 1998
- [24] O. Vinyals, T. Ewalds, S. Bartunov, P. Georgiev, A. S. Vezhnevets, M. Yeo, A. Makhzani, H. Kättler, J. Agapiou, J. Schrittwieser, J. Quan, S. Gaffney, S. Petersen, K. Simonyan, T. Schaul, H. van Hasselt, D. Silver, T. Lillicrap, K. Calderone, P. Keet, A. Brunasso, D. Lawrence, A. Ekermo, J. Repp, R. Tsing: Starcraft ii: A new challenge for reinforcement learning, arXiv preprint arXiv:1708.04782, 2017
- [25] I. A. Zamfirache, R.-E. Precup, R. C. Roman, E. M. Petriu: Neural Network-based control using Actor-Critic Reinforcement Learning and Grey Wolf Optimizer with experimental servo system validation, Expert Systems with Applications, Volume 225, 2023

Mass Reduction of Upright of a Racing Car with Innovative Methods

Csányi Mihály, Molnár Ildikó

Óbuda University Bánki Donát, Faculty of Mechanical and Safty Engineering,
Népszínház utca 8, 1081 Budapest, Hungary, cbk7dz@stud.uni-obuda.hu,
molnar.ildiko@uni-obuda.hu

This article deals with the team's examination of a suspension component of their Formula race car, the upright, using various development methods. The original component was made of 6061 aluminum alloy and weighed 530 grams. In addition to weight reduction, we examined the resistance and structural strength optimization of the upright using various methods. The redesigns were done using FUSION 360 and ANSYS programs." The vehicle's performance characteristics are influenced by the material, the load capacity. To ensure competitiveness, several studies and publications have been carried out in terms of compliance with mass and fatigue strength criteria.

Keywords: generative design; topology optimization; shape optimization; mass reduction; Formula Student; upright; suspension development

1 Introduction

The tasks of the upright include transmitting the forces between the road and the vehicle, thus creating sufficient grip. Another task is to reduce the dynamic stresses of the vehicle's components, increasing their life cycle. It is important for the system to operate in the appropriate vibration range, thus avoiding self-excitation phenomenon and ensuring comfortable traveling for passengers. A well assembled suspension can actively contribute to the car's driving stability.

Taking into consideration the competition regulations, the O.U.R. Team has built a double-wishbone suspension, which is easy to install and provides very wide adjustment options. This construction consists of a lower and an upper control arm pair (so-called A-Arm), and another two - one is responsible for suspension and one for steering. On the non-steered rear axis, the steering bar is replaced by a fixed bar [Figure 1]. The bars are connected to the upright at three different points, using different ball joints. The upright is the part of the suspension where the components are mounted. The wheel shaft is fixed with a double bearing center of the upright. On the outer side, the wheel rim is attached to the wheel hub, which is held by the

upright. On the side of the upright, the caliper is attached in two points. On the inner side, the suspension elements, control arms, and steering bars are connected to the upright with ball joints. If we want to measure the angular velocity, temperature, and forces at the wheels, various sensors can be mounted on extra consoles.

The suspension elements converge at the upright, so when designing the upright, we can have an effect on how to adjust the driving dynamic properties. Changing the length of the suspension bars can affect the wheel alignment. We can make changes on the camber, caster angles and kingpin angles. There are several possible mounting points for the steering bar in order to have better steering option. [1, 2, 3]

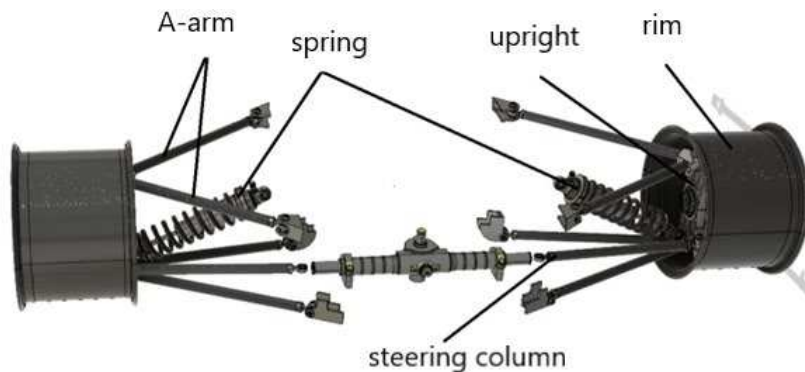


Figure 1

Geometric arrangement

The cars designed and assembled by the teams need to meet some serious requirements just like in Formula 1. The uprights were designed based on the rules created by the organization Formula SAE International.

- V.3.1.1.: „The vehicle must have a fully operational suspension system with shock absorbers, front and rear, with usable minimum wheel travel of 50 mm, with a driver seated.”

- V.3.1.3.: „All suspension mounting points must be visible at Technical Inspection by direct view or by removing any covers.”

- V.3.1.5.: „All spherical rod ends and spherical bearings on the suspension and steering must be one of:

- Mounted in double shear
- Captured by having a screw/bolt head or washer with an outside diameter that is larger than spherical bearing housing inside diameter.”

-V.3.2.4.: „The steering system must have positive steering stops that prevent the steering linkages from locking up (the inversion of a four bar linkage at one of the pivots). The stops may be placed on the uprights or on the rack and must prevent the wheels and tires from contacting suspension, bodywork, or Chassis during the track events.” [4]

2 Forces Acting on the Upright

During racing, there are consecutive accelerations with full load, quick direction changes, and strong braking due to cornering. Table 1 summarizes the maximum critical forces that can affect the vehicle while cornering at high-speed in one direction. The values shown on Table 1 are based on preliminary simulations. The calculations take into account that the front-rear distribution of the mass is expected to be 40-60% influenced by the rear-mounted engine.

Table 1
Maximum forces occurring during a right-hand turn [1]

OUTER PART OF THE LEFT FRONT WHEEL						
	Static	Braking	Turning	Acceleration	Braking+Turning	Acceleration+Turning
F _x [N]	0	-2450	0	802	-3508	1859
F _y [N]	0	0	-2158	0	-2821	-1496
F _z [N]	613	1065	1167	349	1525	808
INNER PART OF THE RIGHT FRONT WHEEL						
	Static	Braking	Turning	Acceleration	Braking+Turning	Acceleration+Turning
F _x [N]	0	-2450	0	802	-1392	-256
F _y [N]	0	0	-457	0	-1120	206
F _z [N]	613	1065	247	349	605	-111
INNER PART OF THE REAR WHEEL						
	Static	Braking	Turning	Acceleration	Braking+Turning	Acceleration+Turning
F _x [N]	0	-802	0	2450	-1859	3508
F _y [N]	0	0	-2158	0	-1496	-2821
F _z [N]	613	349	1167	1065	808	1525
OUTER PART OF THE RIGHT REAR WHEEL						
	Static	Braking	Turning	Acceleration	Braking+Turning	Acceleration+Turning
F _x [N]	0	-802	0	2450	256	1392
F _y [N]	0	0	-457	0	206	-1120
F _z [N]	613	349	247	1065	-111	605

The critical forces that were taken into account during the examination were defined with a 250 kg racing car in the case of a 7.625 m radius turn at a speed of 11 m/s during acceleration and braking. The maximum acceleration and deceleration for the race tires selected by the team can be 1.8 g. Exceeding this acceleration, grip (adhesion) cannot be guaranteed, and the tire may slip. During our examinations, we used the maximum forces that could occur on the wheel, so in the case of a right turn, (forces on) the outer side of the left wheel of the front axle, the inner side of the right wheel, and the outer side of the left wheel and the inner side of the right wheel of the rear axle (Figure 2).

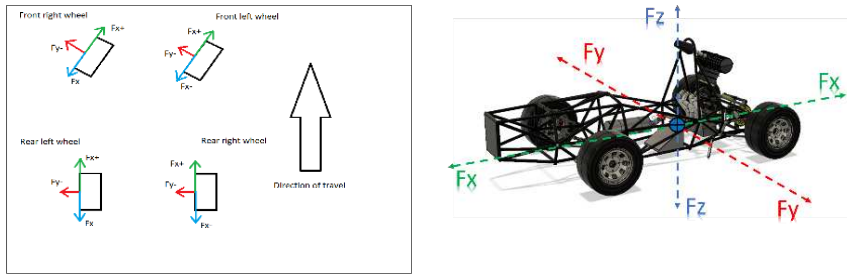


Figure 2

Presentation of the maximum forces between the wheels and the road

During braking, the brake caliper presses the brake pads against the brake disc, slowing the vehicle down. Forces and torques are generated during the friction, which must be endured by the upright. We needed the force that struck at the brake caliper attachment points. To determine that, first we had to give the necessary braking torque. The braking torque can be used to determine the force at the attachment points, if we know the force of the arm/lever.

3 Simulation of the Initial Upright

With the knowledge of the forces, we created a finite element simulation of the current geometry. The maximum forces acting differently per wheel had to be examined in separate simulations. If we had done it in the same simulation, the forces in opposite directions would not have shown realistic solutions. The upright was not designed in this program, so first we had to export the geometry from another program. The material of the upright, which was selected as AISi7(LM25) aluminum alloy during the design, was replaced with 6061 aluminum alloy desired to be used by the team. This material is more easily available and can be found in the optimization programs used.

The preparation of an appropriate mesh grid is a basic requirement for acceptable and usable computational results. After creating the grid, we defined the forces, torques, and points of application. When specifying forces, there was an option to choose between distributed, gravitational, and point forces. [5, 6]

The forces between the tire and the road are transmitted through the bearings to the upright, but only in radial directions (on the x and y axes). In the 2022 version of the program, it was possible to separately select a bearing force effect. The program had not operated the lateral transfer of forces through the bearings yet, so the cross-directional forces had to be specified as distributed forces on the surface in contact with the bearing side wall. Afterwards, we placed an external force of 85 mm radius on the brake caliper attachment points. To define the steering force, we exerted force on the steering link attachment point as shown in Figure 3.

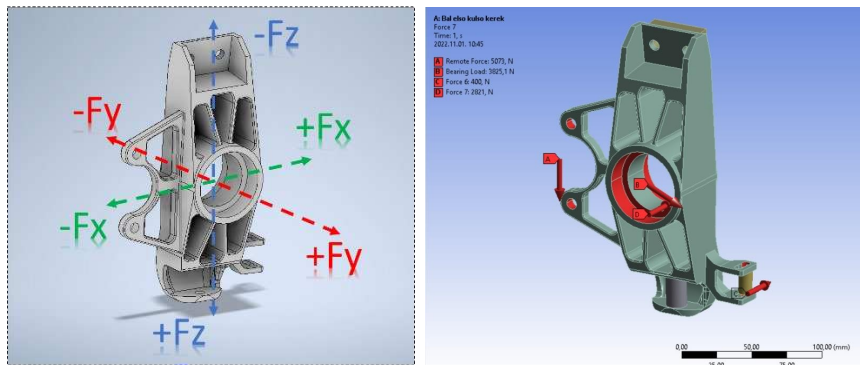
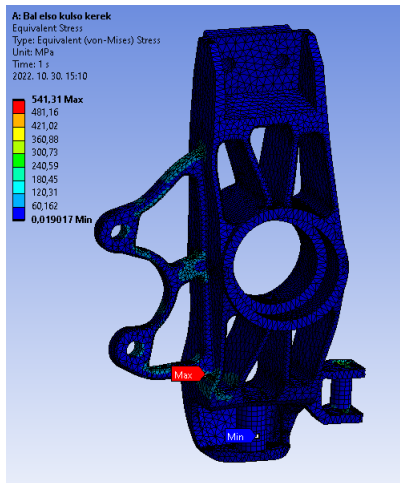


Figure 3

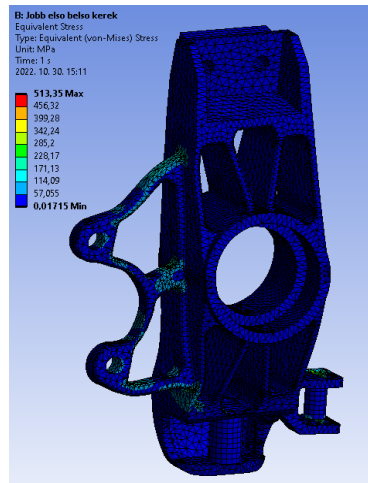
Defining the force effects in ANSYS

During the meshing procedure of the uprights, we used tetrahedral elements. The maximum of 128,000 nodes provided by the Ansys Mechanical Student version proved to be sufficient for the detailed meshing of the upright's structure. To ensure accurate representation of the results, local mesh refinement was applied at necessary locations. Quadratic element order was used in the mesh construction.

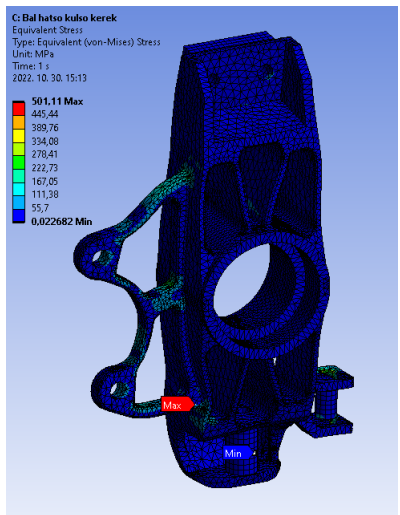
The suspension arms were connected with the help of shafts, which were attached to the pre-shaped parts of the upright with a screw-nut combination. With this type of fastening, we applied pre-tension, which the structure also had to withstand. The magnitude of the pre-tensioning force was approximately 4000 N based on the experience of other teams. The maximum geometric deformation (Total Deformation) and the stresses acting on the body (Equivalent Stress) were examined as a result of the specified forces and constraints. As can be seen from Figure 3 and Table 2, the starting upright and the selected material do not meet our expectations. Although our deformation values are in the appropriate range, the stress values and the safety factors derived from them are not. The desired strength properties can be achieved in two ways: by using a stronger material selection, which generally leads to an increase in mass, or by creating a more favorable structural design.



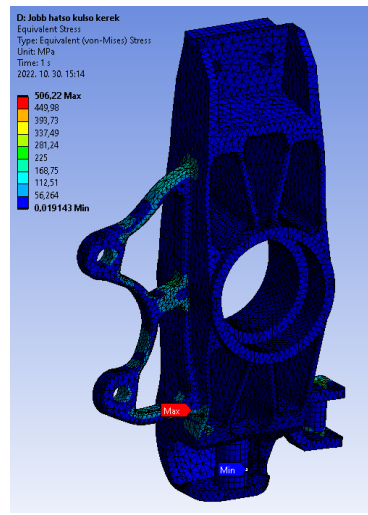
Upright for the left front wheel



Upright for the right front wheel



Upright for the left rear wheel



Upright for the right rear wheel

Figure 3

The Von Mises stress distribution of an initial upright designed ANSYS

Table 2
Simulation results of starting upright in ANSYS

ANSYS	Category	Mass [g]	Material	Max. stress [Mpa]	Min. safety factor	Deformation [mm]
Initial upright	Left front wheel outer	530	6061 Aluminium	541	0,51	0,22
Initial upright	Right front wheel inner	530	6061 Aluminium	513	0,54	0,22
Initial upright	Left rear wheel outer	530	6061 Aluminium	501	0,55	0,24
Initial upright	Right rear wheel inner	530	6061 Aluminium	506	0,54	0,22

3.1 Mass and Structural Optimization

During the optimization, we strive to achieve the best possible state or result based on a pre-determined criterion. In technical life, we know several types of optimizations. While the optimization of a production process may be more common, the optimization of a component's mass, structure and resistance to external effects is the most well-known during the development of a component. Mass reduction can be achieved by reducing volume or using a more favorable density material. We performed several studies although I will not go into in detail now. [7]

One of the optimizations we carried out was executed with generative design. Firstly, we ranked the obtained bodies by mass. This was important because our goal was to reduce mass and optimize the structure. In addition to the mass, we also had to take into account the production method and safety factors. The choice was made with 5-axis machining, made of titanium 6Al-4V material, with a safety factor of 2 and a total weight of 327g.

This type of alloy is a much denser material than aluminum, yet less quantity was used so that it can be considered successful in terms of weight reduction. This is partly due to the mechanical strength of the material. The resistance of the external effects on the body and the structural strength of the upright can be evaluated with the help of simulation programs.

During the second optimization method, the shape optimization, we wanted to lay emphasis on the presentation of the differences between the construction of the old and the new bodies, so we chose aluminium 6061 as the examination material. Compared the initial upright, we managed to achieve here nearly 20% (19,2%) mass reduction.

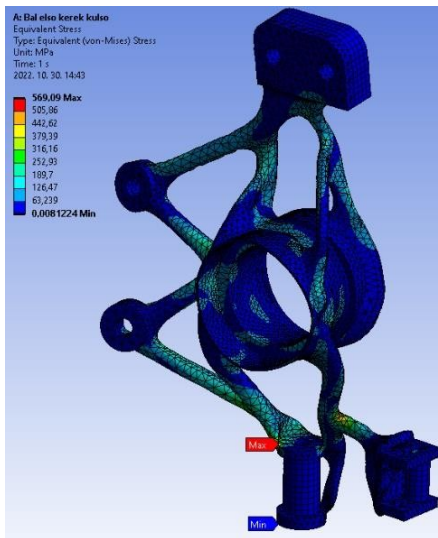
With design methods supported by AI, a lot of time can be saved, and such results can be achieved, which would be impossible with traditional design methods. Not

surprisingly, it is used more frequently when the aim is to reduce mass. In Hungary, more racing teams have used it for working processes. AI helped design a suspension part by the BME Formula Racing Team, an upright and a rim by the Arrabona Racing Team. We can find more examples of the achievements of AI internationally.

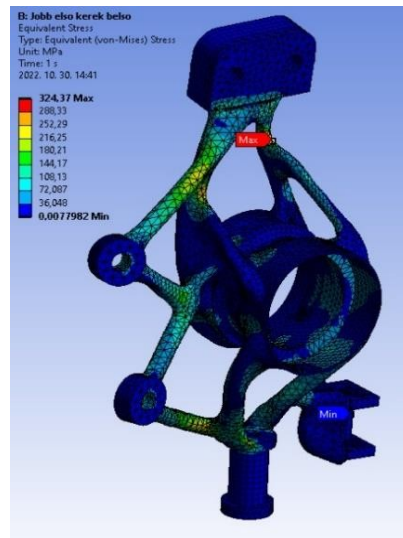
Besides the public sector, artificial intelligence-design is on the rise in the industry. One notable example is the Czinger 21C hypercar, which was created with generative design and additive manufacturing methods in 2020. The production of the vehicle started in 2021 and the first cars will be ready by 2023. [8, 9, 10,11]

3.2 Static Finite Element Simulation Results of the Designed Uprights

The optimized bodies were examined from a strength point of view, with constant/static and transient simulations. Dynamic effects were ignored because the regulations for the race track are strict. These various unevenness and dynamic loads are not allowed. During the examinations, we took into account that the initial geometries had to be in the same plane in order to be comparable. The simulation runs were checked and compared to the results of the initial body. Specifically, we made sure that the connecting parts of the initial geometry that needed to be left free for simulation purposes were in contact with prohibited zones. This way, the vehicle's internal coordinate points of the connection points did not change, so the same forced and constraints were placed on the new body like on the initial body. After the simulations had been run, we examined and compared the results with results of the initial body.



Upright for the left front wheel



Upright for the right front wheel

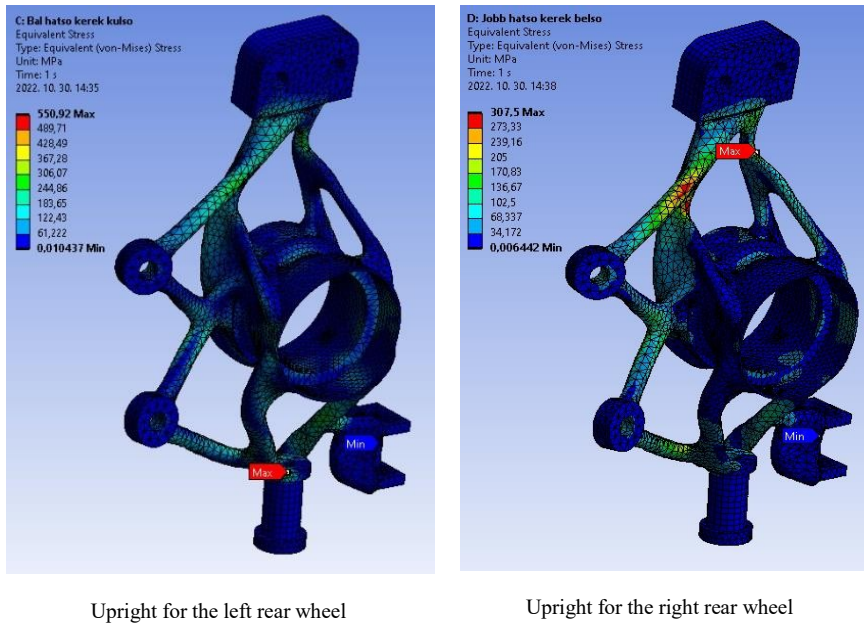


Figure 4

The Von Mises stress distribution of an upright designed with shape optimization while presenting deformation

Table 3

The results of the simulations of the initial upright in the ANSYS program

ANSYS	Category	Mass [g]	Material	Max. stress [Mpa]	Min. safety factor	Deformation [mm]
Generative design	Left front wheel outer part	327	Titan Al6-V4	569	1,55	1,1
Generative design	Right front wheel inner part	327	Titan Al6-V4	324	2,7	0,78
Generative design	Left rear wheel outer part	327	Titan Al6-V4	551	1,6	1,31
Generative design	Right rear wheel outer part	327	Titan Al6-V4	308	2,87	0,73

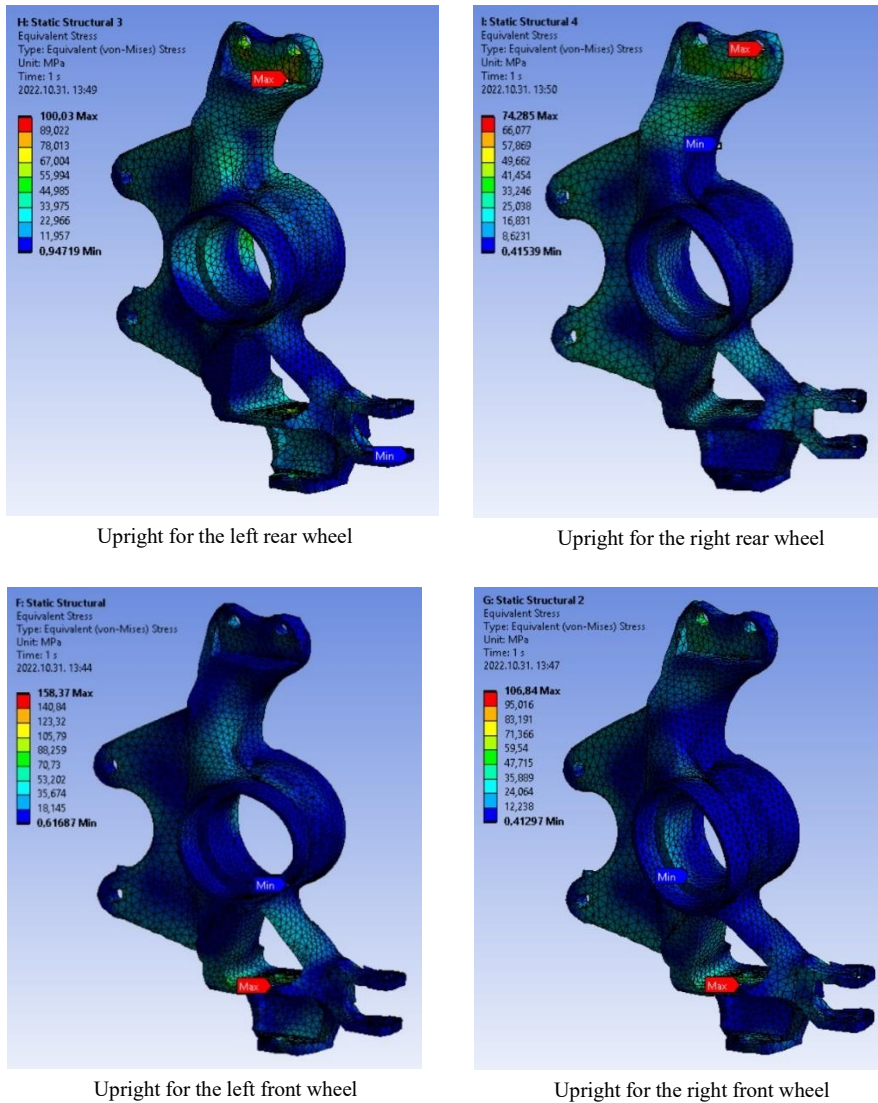


Figure 5

The Von Mises stress distribution of an upright designed with shape optimization while presenting deformation

In order to get more information about the construction of the upright, we did transient simulations too. During the transient simulation, we examined the acceleration process followed by braking in a curve, with the highest possible acceleration due to tire adhesion. We examined during transient finite element simulation. The boundary conditions of forces can be seen in Table 1.

Table 4

The results of the simulations of the initial upright in the ANSYS program

ANSYS	Category	Mass [g]	Material	Max. stress [Mpa]	Min. safety factor	Defromation [mm]
Shape optimization	Left front wheel outerpart	428	6061 Aluminium	158	1,74	0,21
Shape optimization	Right front wheel innerpart	428	6061 Aluminium	107	2,57	0,11
Shape optimization	Left rear wheel outer part	428	6061 Aluminium	100	2,75	0,19
Shape optimization	Right rear wheel innerpart	428	6061 Aluminium	74	3,71	0,11

4 Results

Overall, we can say that there was an improvement in terms of the mass of the bodies in the case of both redesigned uprights. With generative design, the value was reduced to 327 grams, and with the help of topological optimization, it was possible to reduce it to 428 grams. If we managed to achieve nearly 20% or more mass reduction in all parts of the vehicles, we could see improvement in fuel consumption and in the characteristics of driving dynamics as well.

During the optimization, we were also able to achieve the goal of maintaining or even increasing the structural strength of the construction of the upright, despite the mass reduction, thus preserving or even increasing the safety of use.

According to Fusion 360, a part can be made with five-axis machining, but the result from generative design would be 3D printed due to the thin geometries.

Conclusions

The best choice of the upright optimization is the one with topological optimization. The generative design is not perfected although it can draw the attention to ours. One benefit of the topological optimization is that the geometry created with this method has better deformation values than the geometry made by the generative design. We managed to keep the deformation value at nearly 0.2 mm. In the case of the generative design controlled by AI, this value exceeded 1 mm. We can say that we did not succeed in making such a breakthrough in the field of mass reduction with the topological design as with the generative design. However, as we need a reliable construction for the first racing car of the team, overall, the shape optimization method is the ideal choice.

The research can be continued with other parts of vehicles as well. This technology can be used in a number of other industries where the efficiency of processes can be increased by mass reduction. Despite the results in the private sector, the parts manufactured in piece production in a similar way do not usually end up in mass production. If there was a technology enabling the fast and precise production of these bodies/shapes, the design methods that I showed would have more importance.

In the future, we aim to conduct more thermodynamics and fluid dynamics simulations in order to get more important information about parts.

References

- [1] Das A. Virtual Prototype of Upright Assembly of A Race Car for SUPRA SAEINDIA Competition. *International Journal of Mechanical and Industrial Technology*. 2015;2(2):79-86
- [2] Óskar Kúld Pétursson: Uprights, wheel hubs and brake system for a new Formula Student race car, School of Science and Engineering, 2016
- [3] Anshul Dhakar, Rishav Ranjan: Force Calculation in Upright of a FSA Race Car, *International Journal of Mechanical Engineering and Technology (IJMET)* Volume 7, Issue 2, March-April 2016, pp. 168-176
- [4] Formula SAE Rules 2022, <https://www.fsaeonline.com/cdsweb/app/NewsItem.aspxNewsItemID=1ddb17e7-00fc-4716-829a-09413f519eba>
- [5] Stephen Srchoff: *Finite Element Simulations with ANSYS Workbench 2023*, SDC Publications, 2023
- [6] Yogesh Kumar, Rehan Abad Siddiqui, Yogesh Upadhyay, Shivam Prajapati: Kinematic and Structural Analysis of Independent type suspensionsystem with Anti-Roll bar for Formula Student Vehicle Conference: 3rd International Conference on Contemporary Advances in Mechanical Engineering [accessed Oct 10 2023]
- [7] Gersborg-Hansen, A., Bendsoe, M. P. & Sigmund, O.: Topology optimizationof heat conduction problems using the finite volume method. *Structual Multidisc Optim* 31, 251-259 (2006)
- [8] Jørgen Eliassen, *Simuleringsbasert-design for full utnyttelse av additiv tilvirkning*, 2017 2
- [9] William Kinkead, Adrian Pickering, James Waldo, Connor Morette, Zachary Sears: *Design and Optimization of a Formula SAE Vehicle*, 2016
- [10] Dr. Lévai Zoltán, *Gépjárművek szerkezetana (Construction of motor vehicles)*, Egyetemi Tankönyv (university book), ISBN 963 17 25189
- [11] https://www.researchgate.net/figure/FSAE-Germany-Endurance-track_fig2_320102772, 2022.09.21.